

Són molts els noms que ara em venen al cap. Molta gent que ha fet possible que aquesta Tesi arribés a la seva fi. Tot i que no veig possible expressar el meu agraïment en poques frases, voldria almenys intertar-ho.

Un agraïment molt especial a les meves directores, la Dra. Virginia Cádiz i la Dra. Ana Mantecón, per la seva confiança, així com per la seva dedicació, suport i ajuda que m'han mostrat al llarg d'aquests anys.

També agrair als professors del grup de Polímers: la Dra. Àngels Serra, la Dra. Marina Galià, el Dr. Toni Reina i el Dr. Joan Carles Ronda i la resta de professors de l'àrea de Química Orgànica: el Dr. Sergio Castellón, la Dra. Maribel Matheu i la Dra. Yolanda Díaz per la vostra disponibilitat i els vostres valuosos consells sempre que els he necessitat.

I would like to thank Dr. Barry Hunt, from the University of Sheffield, not only for accepting me in his group, but also for his scientific advice and encouragement.

I would also like to thank Dr. Andrew Cook for his helpful advices, suggestions and friendship. My thanks to Chou, Richy, Adam, Gabin and Arturo for the great time that I had in Sheffield.

També voldria donar les gràcies als meus companys del laboratori per la vostra ajuda sempre que l'he necessitat i en especial a la Lúdia per compartir amb mi les alegries i les penes. Gràcies per la teva valuosa amistat. Sense tu aquests quatre anys haurien estat molt diferents.

Finalment, voldria agrair el recolzament dels meus pares que sempre m'han fet costat en totes les decisions de la meva vida. Gràcies per interessar-vos al llarg d'aquests anys per l'evolució d'aquest projecte i animar-me i encoratjar-me quan més ho he necessitat.

Cèsar, moltes hores invertides en aquesta Tesi te les he robat a tu. Gràcies per la teva comprensió i recolzar-me en tot moment. T'estimo.



# A P P E N D I X

## LIST OF ABBREVIATIONS

<b>ADPPO</b>	Allyl diphenyl phosphine oxide
<b>AIBN</b>	2,2'-Azobisisobutyronitrile
<b><math>\gamma</math>-BL</b>	$\gamma$ -Butirolactone
<b>BOE</b>	Bycicloorthoester
<b>BTMA</b>	Benzyl trimethylammonium chloride
<b>COSY</b>	Correlation spectroscopy
<b>DBU</b>	1,8-diazabicyclo[5.4.0]-undec-7-ene
<b>DCC</b>	Dicyclohexylcarbodiimide
<b>DEMMP</b>	Diethyl(methacryloyloxymethyl)phosphonate
<b>DEPT</b>	Distortionless enhanced polarization transfer
<b>DEVP</b>	Diethyl vinyl phosphonate
<b>DGEBA</b>	Diglycidyl ether of bisphenol A
<b>DMAP</b>	4-(N,N-dimethylamino)pyridine
<b>DMTA</b>	Dynamic thermomechanical analysis
<b>DOPO</b>	9,10-dihydro-9-oxa-10-phosphaphenantrene-10-oxide
<b>DOPO-BQ-Gly</b>	10-(2',5'-Bis(glycidyoxy)phenyl)-9,10-dihydro-9-oxa-10-phosphaphenantrene-10-oxide
<b>DOPO-Gly</b>	9-(9,10-dihydro-9-oxa-10-phosphaphenantrene-10-oxide)

	oxide)-2,3-epoxy propyl
<b>DOPOMA</b>	2-[10-(9,10-dihydro-9-oxa-10-phosphaphenantrene-10-oxide-10-yl)] maleic acid
<b>DSC</b>	Differential scanning calorimetry
<b>EDC</b>	N-(3-Dimethylaminopropyl)-N'-ethyl-carbodiimide
<b>EPC</b>	Epichlorohydrin
<b>FTIR</b>	Fourier transform infrared spectroscopy
<b>GPC</b>	Gel permeation chromatography
<b>HSQC</b>	Heteronuclear single quantum correlation
<b>IHPO</b>	Isobutyl bis(hydroxypropyl) phosphine oxide
<b>IHPO-Gly</b>	Isobutyl bis(glycidyl propyl ether) phosphine oxide
<b>LOI</b>	Limiting oxygen index
<b>MASS</b>	Magic angle sample spinning
<b>MCPBA</b>	m-Chloroperbenzoic acid
<b>Mw</b>	Molecular weight
<b>NMR</b>	Nuclear magnetic resonance
<b>PGE</b>	Phenyl glycidyl ether
<b>SEM</b>	Scanning electron microscopy
<b>SOC</b>	Spiroorthocarbonate
<b>SOE</b>	Spiroorthoester
<b>SOE-Ac</b>	1,4,6-Trioxaspiro [4,4]-2-nonylmethyl acetate
<b>SOE-AC</b>	1,4,6-Trioxaspiro [4,4]-2-nonylmethyl acrylate
<b>SOE-AChom</b>	Poly[(1,4,6-trioxaspiro [4,4]-2-nonylmethyl acrylate
<b>SOE-Br</b>	2-Bromomethyl-1,4,6-trioxaspiro [4,4] nonane
<b>SOE-DOPOMA</b>	Bis[(1,4,6-trioxaspiro [4,4] nonan-2-yl)-methyl] 2-[10-(9,10-dihydro-9-oxa-10-phosphaphenantrene-10-oxide-10-yl)] maleate
<b>SOE-OH</b>	2-Hydroxymethyl-1,4,6-trioxaspiro [4,4] nonane
<b>SOE-OSi</b>	1,4,6-Trioxaspiro[4,4]-2-nonylmethyl trimethylsilyl ether
<b>SOE-P</b>	(1,4,6-Trioxaspiro [4,4] nonan-2-yl)-methyl 3-[10-(9,10-dihydro-9-oxa-9-phosphaphenantrene-10-oxide
<b>SOE-PGE</b>	2-Phenoxymethyl-1,4,6-trioxaspiro [4,4] nonane

Appendix

<b>SOE-Si</b>	1,4,6-Trioxaspiro [4,4]-2-nonylmethyl 3-trimethylsilyl propionate
<b>ST</b>	Styrene
<b>TGA</b>	Thermogravimetric analysis
<b>TMS</b>	Tetramethylsilane
<b>Tg</b>	Glass transition temperature
<b>XRD</b>	X-Ray diffraction



## C H A P T E R 2

# SYNTHESIS AND POLYMERIZATION OF PHOSPHORUS OR SILICON-CONTAINING SPIROORTHOESTERS

*Spiroorthoesters based materials are promising systems to avoid undesirable shrinkage during polymerization and polymer curing. In particular, the development of phosphorus or silicon-containing spiroorthoesters show great promise in the design of new materials, which improve their flame retardance properties and reduce the shrinkage upon polymerization or crosslinking.*

*This chapter describes the synthesis and polymerization of three new phosphorus or silicon based spiroorthoesters, and their application to modify epoxy resins of these new spiroorthoesters*

- 
- 2.1.** Introduction
  - 2.2.** Objectives
  - 2.3.** Experimental Procedures and Results
    - 2.3.1.** Microwave-Assisted Synthesis of a Novel Phosphorus-Containing Spiroorthoester, Characterization and Cationic Polymerization

**2.3.2.** Synthesis of a Novel Bis-Spiroorthoester Containing 9,10-dihidro-9-oxa-10-phosphaphenantrene-10-oxide as a Substituent: Homopolyme-rization and Copolymerization with Diglycidyl Ether of Bisphenol A

**2.3.3.** Novel Silicon-Containing Spiroorthoester with Combined Flame Retardancy and Low Shrinkage Properties to Modify Epoxy Resins

**2.3.4.** Copolymerization of a Silicon-Containing Spiroorthoester with a Phosphorus-Containing Diglycidyl Compound. Influence in Flame Retardance and Shrinkage

## 2.1 INTRODUCTION

---

Spiroorthoesters (SOEs) are bicyclic monomers that can be prepared from the reaction of oxiranes with lactones in the presence of Lewis acids.<sup>1-5</sup> Bodenbenner, in 1959 synthesized the first spiroorthoester, the 1,4,6-trioxaspiro [4,4] nonane, from the reaction of ethylene oxide with  $\gamma$ -butirolactone in the presence of boron trifluoride ( $\text{BF}_3$ ) in 33% yield (Figure 2.1).

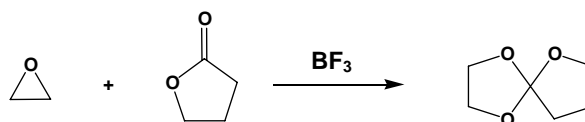


Figure 2.1. Synthesis of 1,4,6-trioxaspiro [4,4] nonane.

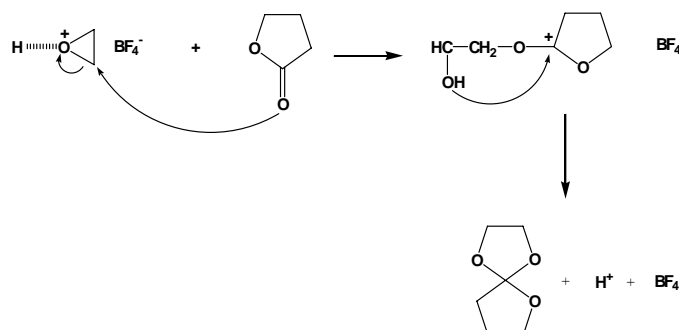


Figure 2.2. Mechanism of spiroorthoester formation.

<sup>1</sup> Bodenbenner, K.; *Justus Liebigs Ann* 1959, 625, 183.

<sup>2</sup> Igarashi, M.; Takata, T.; Endo, T. *Macromolecules* 1994, 27, 2628.

<sup>3</sup> Matejka, L.; Dusek, K.; Chabanne, P.; Pascault, J. P. *J Polym Sci Part A: Polym Chem* 1997, 35, 665.


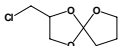
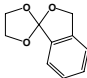
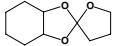
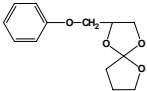
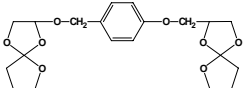
<sup>4</sup> Nishida, H.; Sanda, F.; Endo, T.; Nakahara, T.; Ogata, T.; Kusumoto, K. *J Polym Sci Part A: Polym Chem* 2000, 38, 68.

<sup>5</sup> Nishida, H.; Morikawa, H.; Nakahara, T.; Ogata, T.; Kusumoto, K.; Endo, T. *Polymer* 2005, 46, 2531.

Figure 2.2 illustrates the mechanism proposed in the literature<sup>1,6</sup> for the synthesis of SOEs, where the initiation is the activation of the epoxide group with a Lewis acid, followed by a nucleophilic attack of the carbonylic oxygen of the lactone on the carbon of the epoxide, to yield a carbocation stabilized by the two adjacent oxygen atoms. This intermediate, through a cyclization reaction, gives the SOE.

Many other SOEs have been synthesized in the last decades. Some of them are listed in table 2.1 and also included in the same table is the percentage of volume change (expansion) during homopolymerization.

**Table 2.1.** Spiroorthoesters and volume change during homopolymerization.

Ref.	Structure	Volume Change (%)
		+ 0.1 (25 °C)
		—
		decomposed
		0.0 (25 °C)
		+ 12 (30 °C)
		—

<sup>6</sup> Chabanne, P.; Tighzert, L.; Pascault, J. P. *J Polym Sci Part A: Polym Chem* 1994, 33, 787.

<sup>7</sup> Bailey, W. J.; *Elastoplast* 1973, 5, 142.

<sup>8</sup> Sun, R. L. J. *Synthesis of Monomers which Expand on Polymerization*, Ph. D. thesis, University of Maryland, College Park, 1975.

<sup>9</sup> Bailey, W. J.; Iwama, H.; Tsushima, R.; *J Polym Sci. Symp* 1976, 56, 117.

+ 0.4 (25° C)

9

Another way to obtain SOEs is through the modification of a previously synthesized SOE which has an additional functional group as a substituent. Two different methods have been reported to modify the 2-bromomethyl-1,4,6-trioxaspiro [4,4] nonane (SOE-Br). Firstly, by treating this SOE with a strong base, an unsaturated SOE, 2-methylene-1,4,6-trioxaspiro [4,4] nonane,<sup>10,11</sup> [Figure 2.3 (a)] was obtained through an elimination reaction. Secondly, an esterification reaction was also described to modify the SOE-Br with the reaction of carboxylic acid in the presence of DBU,<sup>12-14</sup> to obtain an ester-containing SOE [Figure 2.3 (b)].

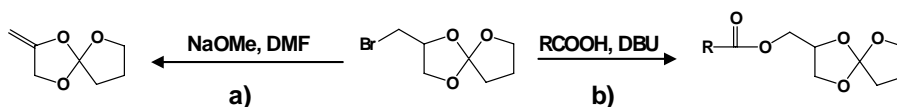


Figure 2.3. Modification reactions of SOE-Br.

The spiroorthoesters polymerize with cationic initiators such as protonic and Lewis acids. Matyjaszewski<sup>15</sup> studied the cationic polymerization of 1,4,6-trioxaspiro [4,4] nonane by NMR spectroscopy and proposed the mechanism evolved during the polymerization, which consist of a rapid reversible opening of one of the rings in the SOE, followed by the slower opening of the second ring with formation of the ester linkage. Meanwhile, Matyjaszewski suggested two

<sup>10</sup> Endo, T.; Bailey, W. J. *J Polym Sci Part C: Polym Lett* 1980, 18, 25.

<sup>11</sup> Endo, T.; Okawara, M.; Yakazaki, N.; Bailey, W. J. *J Polym Sci Part A: Polym Chem* 1981, 19, 1283.

<sup>12</sup> Endo, T.; Kitamura, N.; Takata, T.; Nishikubo, T. *J Polym Sci Part C: Polym Lett* 1988, 26, 517.

<sup>13</sup> Kitamura, N.; Takata, T.; Endo, T.; Nishikubo, T. *J Polym Sci Part A: Polym Chem* 1991, 29, 1151.

<sup>14</sup> Nishikubo, T.; Kameyama, A.; Kudo, H.; Tsutsui, K. *J Polym Sci Part A: Polym Chem* 2002, 40, 1293.

<sup>15</sup> Matyjaszewski, K. *J Polym Sci Part A: Polym Chem* 1984, 22, 29

steps during the polymerization of SOEs, the mode for the opening was not determined. Bailey<sup>9,16</sup> reported a more detailed mechanism, shown in Figure 2.4, where the initiation reaction is an attack of an electrophile (Lewis acid;  $R^+$ ) to the acetal (way A) or ether oxygen (way B) of the SOE to form an oxonium cation, followed by isomerization into a carbocation stabilized by the two adjacent oxygen atoms. The propagation reaction is an attack by another monomer to form an oxonium cation, accompanying the isomerization of the acetal moiety into an ester moiety.

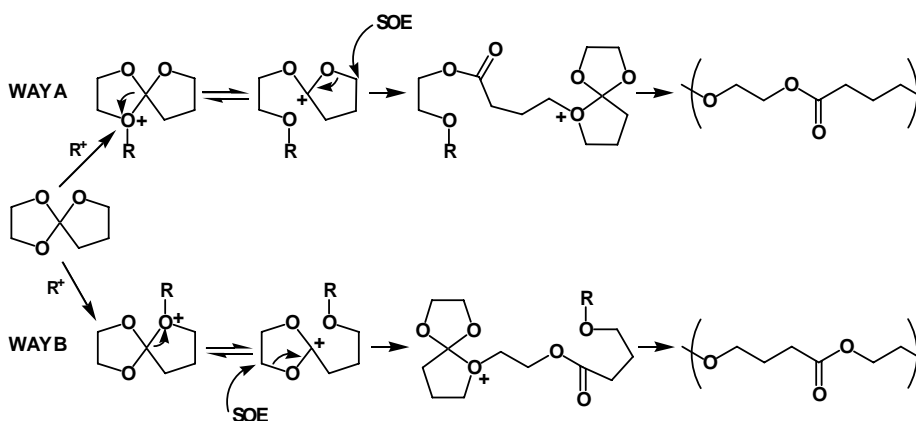


Figure 2.4. Double ring-opening polymerization mechanism of SOEs.

Latter studies demonstrate that temperature is one of the most important factors during the SOE polymerization,<sup>17,18</sup> because in depending on the temperature it is possible to obtain two different polymers (Figure 2.5). At low temperatures (<40 °C) a poly(cyclic orthoester) is obtained by the single ring-opening. This reaction is reversible,<sup>19</sup> and with treatment of acids it is possible to recover the initial SOE monomer. On the other hand, the polymerization of

<sup>16</sup> Bailey, W. J.; Sun, R. L. *Am Chem Soc, Div Polym Chem: Polymer Prepr* 1972, 13(1), 281

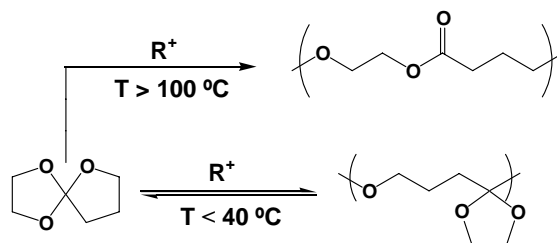
<sup>17</sup> Chikaoka, S.; Takata, T.; Endo, T. *J Polym Sci Part A: Polym Chem* 1990, 28, 3101.

<sup>18</sup> Chikaoka, S.; Takata, T.; Endo, T. *Macromolecules* 1991, 24, 6557.

<sup>19</sup> Chikaoka, S.; Takata, T.; Endo, T. *Macromolecules* 1991, 24, 331.

SOEs at high temperatures ( $>100\text{ }^{\circ}\text{C}$ ) generates irreversibly a poly(ether-ester) by the double ring-opening process.

As has been mentioned previously, SOEs are one kind of so-called “expanding monomers”, which are monomers that lead to zero shrinkage or even positive expansion during the double ring-opening polymerization.<sup>20</sup> From table 2.1, slight to moderate expansion can be seen for the majority of presented SOEs during polymerization.

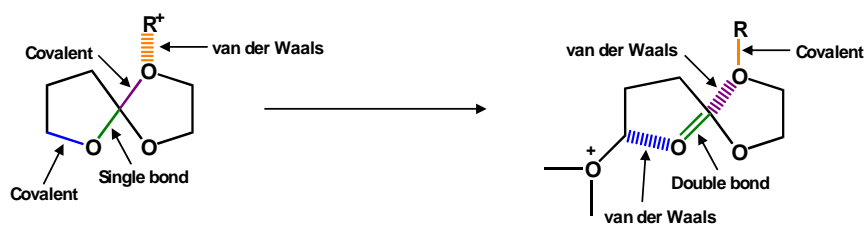


**Figure 2.5.** Spiroorthoesters polymerization in dependence of the temperature.

The reason for the expansion during polymerization can be rationalized by comparing the bond changes between the monomer and polymer forms (Figure 2.6).<sup>9,20</sup> There are two processes which lead to some contraction; one bond shifts from a van der Waals distance to a covalent distance, and one bond goes from a single covalent bond to a double covalent bond. This shrinkage is counteracted by the two bonds that move from a covalent distance to a near van der Waals distance in the polymer form. The overall effect of these bond changes is near zero shrinkage or even a slight expansion.

<sup>20</sup> Sathir, R. K.; Luck, R. M. Ed.; *Expanding Monomers. Synthesis, Characterization and Applications*. CRC Press, Boca Raton, 1992.

24 | Synthesis of Spiroorthoesters



**Figure 2.6.** Bond transitions during the homopolymerization of a SOE.

The main markets which require materials that exhibit low shrinkage during polymerization and polymer curing and flame retardant properties are the electronic industry. Epoxy resins are widely used in these industries as advanced composite matrices for manufacturing printed circuit boards, encapsulants for semiconductors and insulating materials. They are used because they present moisture, solvent and chemical resistance, toughness, superior electrical and mechanical properties, and good adhesion to many substrates.<sup>21</sup> However, the shrinkage upon crosslinking and flame retardant properties of epoxy resins should be improved.

Several different approaches have been used to reduce the shrinkage of the resin systems, such as the use of high molecular weight starting materials, the processing at low temperatures, and the use of fillers. However, these methods are not totally efficient as the shrinkage is due to the crosslinking reaction rather than as a consequence of the production methods. The most effective method of solving this problem is to copolymerize an expanding monomer with epoxy resins. Several systems have been studied until now and have shown reduced shrinkage versus the system with the pure epoxy resin.<sup>22,23</sup>

The other problem of the epoxy resins, above mentioned, is their high flammability. Traditionally, halogen-containing monomers such as diglycidylether of tetrabispheol A have been used to render effective flame retardant

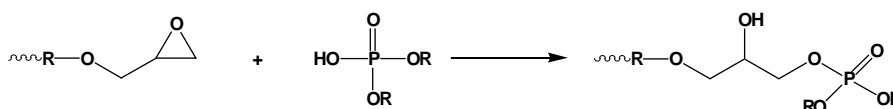
<sup>21</sup> Epoxy resins. Chemistry and Technology. C. A. May editor. New York: Marcel Dekker; 1988.

<sup>22</sup> Bailey, W. J. Am Chem Soc 1986, 54, 23

<sup>23</sup> Watanabe, M.; Taguchi, H.; Gitsmatsu, T. Ind Mater 1989, 37, 85.

properties, although their uses are limited because of their productions of toxic and corrosive gases as well as carcinogenic chemicals during combustion. Many efforts have been made in the last years to develop environmentally flame retardant epoxy resins by the introduction of phosphorus<sup>24-27</sup> or silicon.<sup>24,28,29</sup>

Organophosphorus compounds can be directly introduced into a thermosetting epoxy resin with the reaction of P-OH groups of dialkyl (or diaryl) phosphates with the oxirane rings (Figure 2.7).<sup>30</sup> However, the greatest degree of flame retardancy has been achieved through the use of phosphorus-containing glycidyls or phosphorus-containing curing agents, because normally they contain a higher weight fraction of phosphorus. There is an extremely wide range of phosphorus-containing flame retardants, since the element exists in several oxidation states. Several phosphine oxide, phosphate, and phosphonate-based epoxides and curing agents described in the literature are shown in Figure 2.8.<sup>31-42</sup>

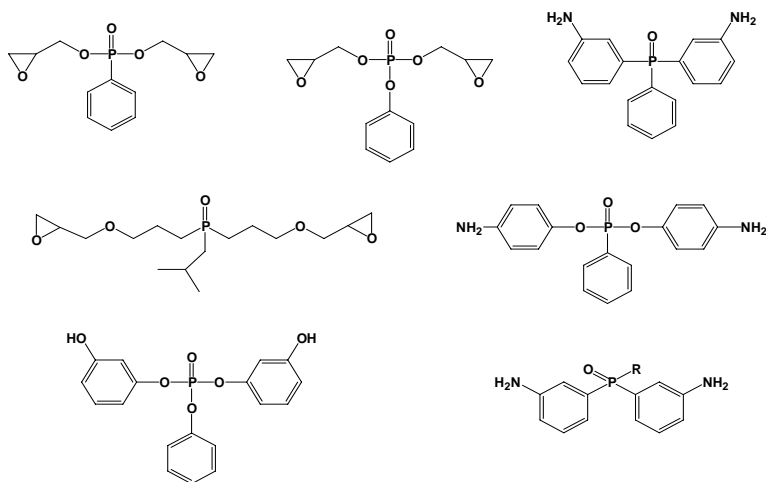


- <sup>24</sup> Lu, S. Y.; Hamerton, I. *Prog Polym Sci* 2002, 27, 1661.  
<sup>25</sup> Levchik, S. V.; Weil, E. D. *Polym Int* 2004, 53, 1901.  
<sup>26</sup> Jain, P.; Choudhary, V.; Varma, I. K. *J Macromol Sci. Polym Rev* 2002, C42(2), 139.  
<sup>27</sup> Weil, E. D.; Levchik, S. *J Fire Sci* 2004, 22, 25.  
<sup>28</sup> Mercado, L. A.; Reina, J. A.; Galià, M. *J Polym Sci Part A: Polym Chem* 2006, 44, 5580.  
<sup>29</sup> Mercado, L. A.; Reina, J. A.; Galià, M. *Polym Degrad Stab* 2006, 91, 2588.  
<sup>30</sup> Derouet, D.; Morvan, F.; Brosse, J. C. *J Appl Polym Sci* 1996, 62(11), 1855.  
<sup>31</sup> Chin, W. K.; Shau, M. D.; Tsai, W. C. *J Polym Sci Part A: Polym Chem* 1995, 33, 373.  
<sup>32</sup> Bucknigham, M. R.; Lindsay, A. J.; Stevenson, D. E.; Muller, G.; Morel, E.; Costes, B.; Henry, Y. *Polym Degrad Stab* 1996, 54, 311.  
<sup>33</sup> Liu, Y. L.; Hsiue, G. H.; Chiu, Y. S.; Jeng, R. J.; Perno, L. H. *J Appl Polym Sci* 1996, 61, 613.  
<sup>34</sup> Liu, Y. L.; Hsiue, G. H.; Chiu, Y. S.; Jeng, R. J. *J Appl Polym Sci* 1996, 61, 1789.  
<sup>35</sup> Liu, Y. L.; Hsiue, G. H.; Lee, R. H.; Chiu, Y. S. *J Appl Polym Sci* 1997, 63, 859.  
<sup>36</sup> Liu, Y. L.; Hsiue, G. H.; Chiu, Y. S. *J Polym Sci Part A: Polym Chem* 1997, 35, 565.  
<sup>37</sup> Alcón, M. J.; Ribera, G.; Galià, M.; Cádiz, V. *Polymer* 2003, 44, 7291.  
<sup>38</sup> Levchik, S. V.; Camino, G.; Luda, M. P.; Costa, L.; Muller, G.; Coates, B. *Polym Degrad Stab* 1998, 60, 169.  
<sup>39</sup> Wang, C. S.; Shieh, J. Y. *Eur Polym J* 2000, 36, 443.  
<sup>40</sup> La Rosa, A. D.; Failla, S.; Finocchiaro, P.; Recca, A.; Siracusa, V.; Carter, J. T.; McGrail, P. T. *J Polym Eng* 1999, 19, 151.  
<sup>41</sup> Cho, C. S.; Chen, L. W.; Fu, S. C.; Wu, T. R. *J Polym Res* 1998, 5, 59.  
<sup>42</sup> Li, J. Z.; Chen, S. Y.; Xu, X. M. *J Appl Polym Sci* 1990, 40, 417.

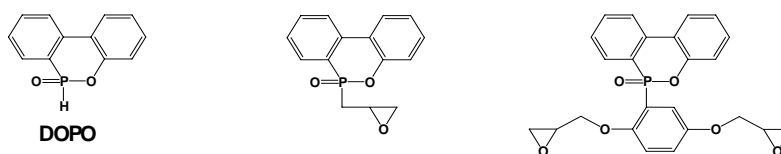
There are many reports of the use of a rigid and bulky phosphonate derivative, 9,10-dihydro-9-oxa-10-phosphaphenanthrene-10-oxide (DOPO) and its derivatives in the formulation of epoxy resins. This compound contains a P-O-

**Figure 2.7.** Dialkyl (or aryl) phosphate modified epoxy resins.

C bond whose thermal stability is unusually high, and which can be attributed to the O=P-O group being protected by phenylene groups. Several DOPO based glycidyls and curing agents have been described in the literature and are shown in Figure 2.9.<sup>43-50</sup>



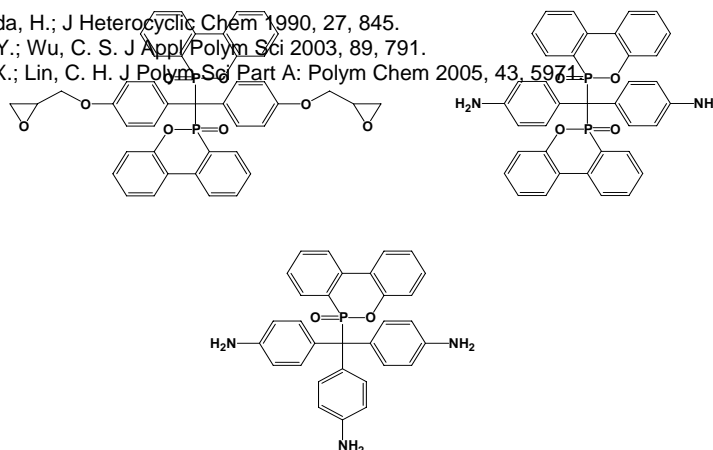
**Figure 2.8.** Chemical structures of several phosphorus-containing epoxy resins and curing agents.



<sup>43</sup> Yamada, Y.; Yasuda, H.; *J Heterocyclic Chem* 1990, 27, 845.

<sup>44</sup> Liu, Y. L.; Hsu, C. Y.; Wu, C. S. *J Appl Polym Sci* 2003, 89, 791.

<sup>45</sup> Lin, C. H.; Cai, S. X.; Lin, C. H. *J Polym Sci Part A: Polym Chem* 2005, 43, 5974.



**Figure 2.9.** DOPO based epoxy resins and curing agents.

Organosilicon compounds have demonstrated efficiency in improving the flame retardancy of various polymeric materials. Different approaches have been developed in the last few years to introduce silicon into the epoxy resins, mainly by the modification of commercial epoxy resins with hydroxyl-terminated siloxanes and silandiols<sup>51,52</sup> or by the synthesis of silicon-containing glycidyls<sup>28,29,53,54</sup> and curing agents. Several of those structures are shown in

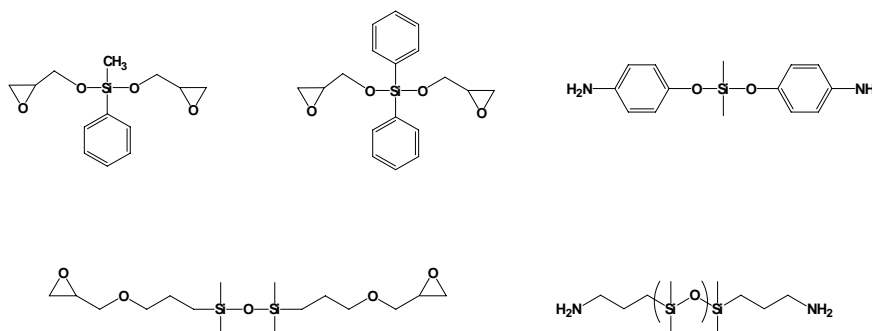


Figure 2.10.

## 2.2 OBJECTIVES

---

Until now a large amount of SOEs have been synthesized to solve the shrinkage associated to the polymerization, but no attention has been paid to improve their flame retardancy.

Figure 2.10. Silicon-containing epoxides and curing agents.

<sup>46</sup> Liu, Y. L.; Tsai, S. H. *Polymer* 2002, 43, 5757.

<sup>47</sup> Alcón, M. J.; Espinosa, M. A.; Galià, M.; Cádiz, V. *Macromol Rapid Commun* 2001, 22, 1265.

<sup>48</sup> Wang, C. S.; Shieh, J. Y. *J Appl Polym Sci* 1999, 73, 353.

<sup>49</sup> Liu, Y. L. *J Polym Sci Part A: Polym Chem* 2002, 40, 359.

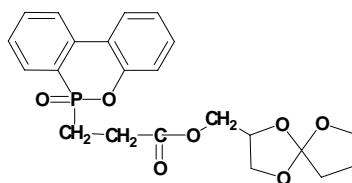
<sup>50</sup> Cho, C. S.; Chen, L. W.; Chiu, Y. S. *Polym Bull* 1998, 41, 45.

<sup>51</sup> Wu, C. S.; Liu, Y. L.; Chiu, Y. S. *Polymer* 2002, 43, 4277.

<sup>52</sup> Lin, S. T.; Huang, S. K. *Eur Polym J* 1997, 33, 365.

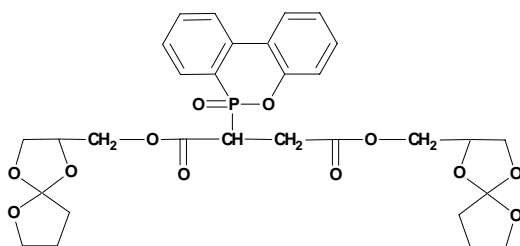
The main objective of the work described in this chapter was to develop new spiroorthoesters which contain in their structure a flame-retardant heteroelement, such as phosphorus or silicon. This objective can be divided into four sub objectives:

**1.** To synthesize and homopolymerize a new phosphorus-containing spiroorthoester, (1,4,6-trioxaspiro[4,4] nonan-2-yl)-methyl 3-[10-(9,10-dihydro-9-oxa-9-phosphapentanthrene-10-oxide-10-yl)] propanoate (SOE-P, Scheme 2.1) and to study its copolymerization with phenylglycidyl ether.



**Scheme 2.1.** Chemical Structure of SOE-P monomer.

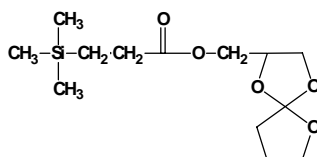
**2.** To synthesize a new phosphorus-containing spiroorthoester, bis[(1,4,6-trioxaspiro[4,4] nonan-2-yl)-methyl] 2-[10-(9,10-dihydro-9-oxa-10-phosphapentanthrene-10-oxide-10-yl)] maleate (SOE-DOPOMA, Scheme 2.2) and evaluate the properties of the materials obtained from its homopolymerization and copolymerization with diglycidyl ether of bisphenol A.



**Scheme 2.2.** Chemical Structure of SOE-DOPOMA monomer.

<sup>53</sup> Hsiue, G. H.; Liu, Y. L.; Tsiao, J. J Appl Polym Sci 2000, 78, 1.

**3.** To synthesize and evaluate the properties of the materials obtained from the homopolymerization of a new silicon-containing spiroorthoester, 1,4,6-trioxaspiro[4,4]-2-nonylmethyl 3-trimethylsilyl propanoate (SOE-Si, Scheme 2.3) and its copolymerization with diglycidyl ether of bisphenol A.



**Scheme 2.3.** Chemical Structure of SOE-Si monomer.

**4.** To evaluate the effects on thermal, mechanical, flame-retardant properties, and volume change during crosslinking of a silicon-containing spiroorthoester (SOE-Si) with mixtures of diglycidyl ether of bisphenol A and a phosphorus-containing glycidyl derivative, 10-(2',5'-bis(glycidyoxy)phenyl)-9,10-dihydro-9-oxa-10-phospha-phenanthrene-10-oxide (DOPO-BQ-Gly). Also, the aim of this study is to investigate the synergistic effect of phosphorus and silicon on flame retardancy.

## 2.3 EXPERIMENTAL PROCEDURES AND RESULTS

---

The following four studies including experimental procedures and results performed in this chapter have been published in scientific journals or submitted for publication.

The work described in Section 2.3.1 has been published in the Journal of Polymer Science Part A: Polymer Chemistry 2006, 44, 4722 and deals with the

---

<sup>54</sup> Crivello, J. V.; Bi, D. J Polym Sci Part A: Polym Chem 1993, 31, 3121.

synthesis and characterization of a novel phosphorus-containing spiroorthoester (SOE-P) prepared by a Michael addition between  $\alpha,\beta$ -unsaturated SOE-acrylate and DOPO under microwave irradiation. The SOE-P was homopolymerized and copolymerized with phenylglycidyl ether with ytterbium triflate as a cationic initiator.

The work described in Section 2.3.2 will be published in the Journal of Polymer Science Part A: Polymer Chemistry (in press) and describes the synthesis and characterization of a novel phosphorus-containing spiroorthoester (SOE-DOPOMA) prepared by an esterification reaction with a hydroxylated spiroorthoester and a phosphorus-containing diacid. This new spiroorthoester was crosslinked alone and with the diglycidyl ether of Bisphenol A with ytterbium triflate as a cationic initiator. The properties of the obtained materials were evaluated by differential scanning calorimetry, thermogravimetric analysis, and thermodynamomechanical analysis. The shrinkage effect on crosslinking and the flame retardant properties were also determined.

The work described in Section 2.3.3 has been submitted for publication in the Journal of Polymer Science Part A: Polymer Chemistry and describes the synthesis and characterization of a novel silicon-containing spiroorthoester (SOE-Si) prepared by an esterification reaction with a hydroxylated spiroorthoester and a silicon-containing acid. Their homopolymerization and its copolymerization with the diglycidyl ether of Bisphenol A were made with ytterbium triflate as a cationic initiator.

And finally, the work of Section 2.3.4 has been submitted for publication in Polymer Degradation and Stability and includes the cationic copolymerization of spiroorthoesters with diglycidyl compounds with ytterbium triflate as an initiator. The flame retardant heteroelements were introduced by a silicon-containing spiroorthoester (SOE-Si) and a phosphorus-containing diglycidyl compound (DOPO-BQ-Gly). The effect in the flame retardance properties of a combination of both heteroelements was studied. The shrinkage upon crosslinking for all the materials was also evaluated.



# C H A P T E R 1

## INTRODUCTION AND SCOPE

---

---

*Nowadays the polymeric materials are used in a lot of applications due to their interesting properties. However, they present some limitations, such as their high flammability and the shrinkage upon polymerization and polymer curing.*

*This chapter discusses the contribution in the recent years to improve the two limitations above mentioned, and explains the aims of this thesis.*

---

- 1.1.** Introduction
- 1.2.** Scope and Purpose of this thesis

## 1.1 INTRODUCTION

---

Over the last few decades the replacement of conventional materials by synthetic polymeric materials has increased dramatically owing to the versatility, low density, and sometimes novel properties of the latter. Although the polymers have become widely accepted in a lot of applications, many of them are extremely flammable and, in presence of sufficient heat and oxygen, burn easily and rapidly. The problem is not only the destruction of the material but the smoke and toxic gases generated which are the main causes of hazards in a fire. This has led to the introduction of stricter legislation and safety standards concerning flammability in the plastics industry and on the fire resistant materials market.

To find methods to minimise polymer flammability it is important to understand the thermal decomposition processes of polymeric materials. The combustion of a polymer is a complex process involving a series of interrelated and/or independent stages which take place in the condensed phase and the vapour phase, and at the interface between these two phases. The most important step in the burning of a polymer is the fuel production stage, in which an external heat source causes an increase in temperature, resulting in the dissociation of chemical bonds and the evolution of volatile fragments. These volatiles diffuse into the air to create a flammable mixture, which starts the combustion when this mixture reaches the ignition temperature. Flaming combustion is exothermic and generates energy, in the form of heat transferred back to the material, to decompose the polymer further thus producing more fuel and so maintaining the combustion cycle (Figure 1.1).<sup>1</sup>

Successful strategies to reduce the flammability of a material involve breaking one or more stages of the combustion cycle to reduce the rate or change the mechanism of combustion. All flame retardants act in the vapour

---

<sup>1</sup> Ebdon, J. R.; Jones, M. S. Flame Retardants. Polymeric Materials Encyclopedia; J.C. Salomone, Ed., CRC Press, Boca Raton, 1996, Vol 3, p. 2397.

phase and/or the condensed phase through a physical or chemical mechanism<sup>2</sup>, which are described below:

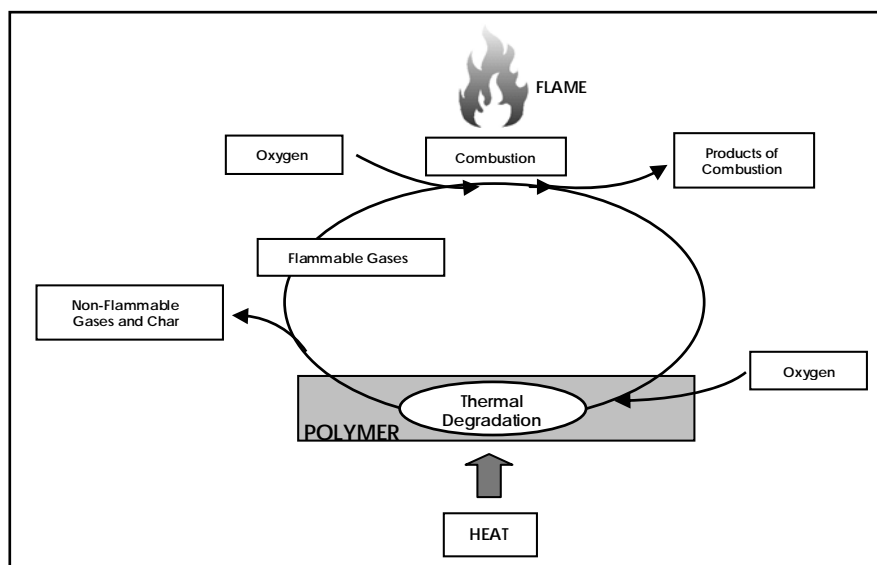


Figure 1.1. Combustion cycle of a polymer.

(a) Char formation: Some flame retardants act in the condensed phase promoting char formation on the surface, which acts as a barrier to inhibit gaseous products from diffusing to the flame and to shield the polymer surface from heat and air.

(b) Intumescent layer: In this case, the flame retardants swell when exposed to fire or heat to form a porous foamed mass, which acts as a barrier to heat, air and pyrolysis products.<sup>3,4</sup>

<sup>2</sup> Lu, S.-Y.; Hamerton, I. *Prog Polym Sci* 2002, 27, 1661.

<sup>3</sup> Camino, G.; Costa, L.; Luda, M. P. *Macromol Symp* 1993, 74, 71.

<sup>4</sup> Le Bras, M.; Bourbigot, S.; Revel, B. *J Mater Sci* 1999, 34, 5777.

(c) Reactions in the vapour phase: Vapour-phase retardants act interfering with the free radical reactions involved in flame propagation.<sup>5-7</sup>

(d) Cooling: The cooling happens when the flame retardant decomposes endothermically to cool the pyrolysis zone at the combustion surface.<sup>8,9</sup>

(e) Dilution: The dilution could take place in the solid or vapour phase. In the former, the flame retardant acts to dilute the polymer and reduce the concentration of decomposition gases. In the latter, the flame retardant decomposes to inert gases, which act to dilute the flammable gases.

There exist two different approaches to achieve flame retardancy in polymeric materials; these are known as the additive type and reactive type. Additive type flame retardants are incorporated into the polymer by physical means, generally during processing. This obviously provides the most economical way to achieve flame retardancy. Nevertheless, they have several disadvantages, such as poor compatibility, leaching from the polymer, particularly if used for external applications and they may even volatilize during use. They also have to be used in significantly high concentrations in order to be effective, which may in turn affect the physical and mechanical properties of the polymer.<sup>2,10</sup> On the other hand, the reactive flame retardants involve a covalently bond with the flame-retardant unit and the polymer. The reactive strategy may be achieved in two ways: by simple copolymerization of monomers containing flame-retardant groups and by modification of the existing polymers.<sup>11,12</sup> The relatively low loadings required to achieve sufficient flame retardancy to a large extent maintain the original physical and

<sup>5</sup> Camino, G.; Costa, L. *Polym Degrad Stab* 1988, 20, 271.

<sup>6</sup> Gann, R. G.; Dipert, R. A.; Drews, M. J. *Encyclopedia of Polymer Science and Engineering* 2<sup>nd</sup> ed.; Wiley-Interscience: New York, 1987, Vol. 7, p. 154.

<sup>7</sup> Rosser, W. A.; Inami, S. H.; Wise, H. *Combust Flame* 1966, 10, 287.

<sup>8</sup> Vandersall, H. L. *J Fire Flamm* 1971, 2, 97.

<sup>9</sup> Papa, A. J. *Flame Retardancy of Polymeric Materials*. Kuryla, W. C.; Papa A. J. Eds., Marcel Deker: New York, 1975, Vol 3.

<sup>10</sup> Cullis, C. F.; Hirschler, M. M. *The Combustion of Organic Polymers*. Clarendon Press, Oxford, 1981.

<sup>11</sup> Price, D.; Pyrah, K.; Hull, R.; Milnes, G. J.; Ebon, J. R.; Hunt, B. J.; Joseph, P.; Konkel, C. S. *Polym Degrad Stab* 2001, 74, 441.

<sup>12</sup> Ebdon, J. R.; Hunt, B. J.; Jones, M. S.; Thorpe, F. G. *Polym Degrad Stab* 1996, 54, 395.

mechanical properties of the polymer. Furthermore, the flame retardant is thus not easily lost from the polymer, eliminating one of the major problems associated with the additive approach.<sup>13,14</sup>

Although in the last few years there has been an increase of heteroelements used in flame retardants, the commercial market is still dominated by compounds based on halogens, notably bromine and chlorine. They present exceptional efficiency, acting basically in the vapour-phase by reacting with HO<sup>•</sup> and H<sup>•</sup> radicals<sup>5-7</sup>, which are responsible for propagation of combustion via chain branching. However, they have some negative aspects, particularly their potential for releasing toxic and corrosive gases as well as carcinogenic chemicals during combustion.<sup>15</sup> A growing demand for ecological and safe flame retardant systems, with the growing number of restrictions and recommendations from the European Community and the United States government, has promoted the development of nonhalogen-containing flame retardants.

Phosphorus-containing polymers are considered environmentally friendly flame retardants because they generate less toxic gas and smoke than halogen-containing compounds.<sup>16-19</sup> Phosphorus-based flame retardants are mainly active in the condensed phase and arise as a consequence of thermal generation of phosphorus acids (Figure 1.2). These acids change the thermal degradation mechanism of the polymer, promoting esterification and dehydration of the polymer to give a carbonaceous char layer, which insulates the material from the flame and also acts as a barrier to fuel transfer.<sup>1,20</sup>

---

<sup>13</sup> Matheu, D.; Nair, C. P. R.; Ninan, K. N. *Polym Int* 2000, 49, 48.

<sup>14</sup> Liu, Y. L.; Hsiue, G. H.; Chiu, Y. S.; Jeng, R. J.; Ma, C. *J Appl Polym Sci* 1996, 59, 1619.

<sup>15</sup> Nelson, G. L. *The future of fire retarded materials: applications and regulations*. FRCA; 1994, p. 135.

<sup>16</sup> Kishore, K.; Annakutty, K. S.; Mallick, M. *Polymer*, 1988, 29, 762.

<sup>17</sup> Horrocks, A. R.; Zhang, J.; Hall, M. E. *Polym Int* 1994, 33, 3470.

<sup>18</sup> Liou, G. S.; Hsiao, S. H. *J Polym Sci Part A: Polym Chem* 2001, 39, 1786.

<sup>19</sup> Sato, M.; Yokohama, M. *J Polym Sci Part A: Polym Chem* 1980, 18, 2751.

<sup>20</sup> Camino, G.; Costa, L.; Luda, M. P. *Polym Degrad Stab* 1991, 33, 131.

8 | Introduction and Scope

As an alternative to the use of phosphorus compounds as environmentally friendly flame retardants, silicon compounds can also be used. The flame retardancy arises partly from the property that such compounds have in diluting the combustible organic gases and partly from the barrier that siliceous residues can form to an advancing flame.<sup>21-23</sup>

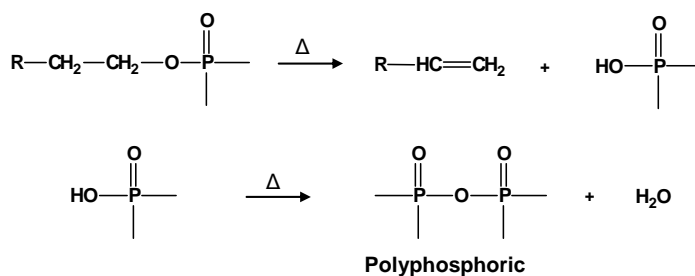


Figure 1.2. Thermal degradation of a phosphorus-containing polymer.

As mentioned above, phosphorus or silicon compounds can be used alone as environmentally friendly flame-retardant elements, and moreover, it has been described a synergistic effect when both elements are present in the material.<sup>24-28</sup> This means that the resulting flame retardance effect is greater than the predicted on the basis of the additivity effect of the individual elements. The reason for the synergistic effect is that phosphorus offers the tendency of char formation, and silicon provides the thermal stability of the forming char during fire.<sup>28-30</sup>

<sup>21</sup> Lomakin, S. M.; Artois, M. I.; Zaikov, G. E. *Flamability of polymeric materials*. New York: Nova Science, 1996, p. 139.

<sup>22</sup> Wu, C. S.; Liu, Y. L.; Shun, Y. *Polymer* 2002, 43, 4277.

<sup>23</sup> Ebdon, J. R.; Hunt, J. B.; Joseph, P. *Polym Degrad Stab* 2003, 83, 181.

<sup>24</sup> Liu, Y. L.; Chou, C. I. *Polym Degrad Stab* 2005, 90, 515.

<sup>25</sup> Chiang, C. L.; Ma C. C. M. *Polym Degrad Stab* 2004, 83, 207.

<sup>26</sup> Liu, Y. L.; Chiu, Y. C.; Wu, C. S. *J Appl Polym Sci* 2003, 87, 404.

<sup>27</sup> Hsiue, G. H.; Liu, Y. L.; Tsiao, J. *J Polym Sci Part A: Polym Chem* 2001, 39, 986.

<sup>28</sup> Hsiue, G. H.; Liu, Y. L.; Tsiao, J. *J Appl Polym Sci* 2000, 78, 1.

<sup>29</sup> Li, Q.; Jiang, P.; Su, Z.; Wei, P.; Wang, G.; Tang, X. *J Appl Polym Sci* 2005, 96, 854.

<sup>30</sup> Liu, Y. L.; Wu, C. S.; Chiu, Y. S.; Ho, W. H. *J Polym Sci Part A: Polym Chem* 2003, 41, 2354.

Another problem, often overlooked, that affects the polymeric materials is the shrinkage during polymerization and polymer curing, and the consequences can be presented in many different forms (Figure 1.3). For example, in cast electrical insulators, polymerization shrinkage can produce internal stress in the polymer, which can reduce the durability of the material as a consequence of the appearance of microvoids and microcracks. In molding applications, polymer shrinkage results in incomplete filling of the mold and poor replication of the mold surface. In polymeric coatings poor adhesion of the coating to the substrate can be observed.<sup>31</sup>



Figure 1.3. Typical polymer shrinkage problems.

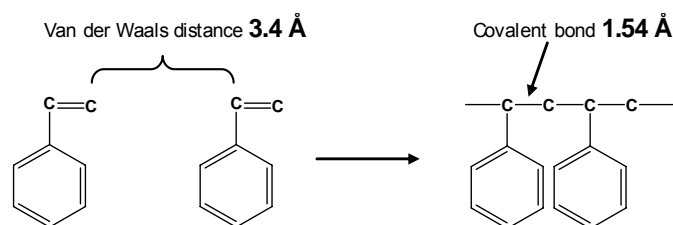
The most common way in the industry of reducing the shrinkage during polymerization and polymer curing is through a physical approach, using inert fillers such as silica, mica, quartz, etc., and passive fillers such as polyvinylchloride powders, polystyrene beads, etc.<sup>31,32</sup> It does mean that the dimensionally unstable polymer is replaced by fillers, which exhibit no dimensional change during the polymerization and cure processes. However, this method is not applicable in many encapsulating, potting, and impregnating applications due to the significant increase of the viscosity, which restricts

<sup>31</sup> Sadhir, R. K.; Luck, R. M. Ed. Expanding Monomers. Synthesis, Characterization and Applications. CRC Press, Boca Raton, 1992.

<sup>32</sup> Lee, H.; Neville, K. Handbook of Epoxy Resins. McGraw-Hill, New York, 1982, Chap. 14.

material flow, and mold fill. Another problem in the use of fillers is their tendency to settle out, and this leads to inhomogeneous systems.

To find new methods to intrinsically solve the shrinkage problem, it is essential to discover what causes it. One of the main causes is the fact that the monomer molecules are located at a van der Waals distance from one another, whereas in the polymer the monomeric units move to within a covalent distance of each other<sup>31-35</sup> (Figure 1.4). Therefore, the atoms are much closer to one another in the polymer than they were in the original monomer.



**Figure 1.4.** Bond changes which produce shrinkage during polymerization of styrene.

Another important factor that we have to take into consideration is the mechanism of the polymerization.<sup>33,34</sup> In condensation polymerization, the shrinkage is also partially related to the small molecule which is eliminated during the formation of the new bond. Obviously, the shrinkage depends on the size and the amount of the eliminated molecules. During addition polymerization, even though there is no small molecule eliminated, there is still large shrinkage in many cases, because of the change in distance between atoms. In ring-opening polymerization, the shrinkage is less than in the other two cases just discussed. Not only is a small molecule not eliminated during the polymerization, but for every bond that undergoes a change from a van der

<sup>33</sup> Bailey, W. J.; *J Macromol Sci-Chem* 1975, A9(5), 849.

<sup>34</sup> Bailey, W. J.; Iwama, H.; Tsushima, R. *J Polym Sci. Polym Symp* 1976, 56, 117.

<sup>35</sup> Fukuda, F.; Hirota, M.; Endo, T.; Okawa, W.; Bailey, W. J. *J Polym Sci Part A: Polym Chem* 1982, 20, 2935.

Waals distance to a covalent distance, another bond goes from a covalent distance to a van der Waals distance.

In tables 1.1 to 1.3 some typical calculated shrinkages during polymerization of different monomers are listed. These are grouped under polymerization mechanism.

**Table 1.1.** Calculated shrinkage during condensation polymerization.

<b>Monomer A</b>	<b>Monomer B</b>	<b>Shrinkage (%)</b>
Diethyl adipate	Hexamethylenediamine	66
Dimethyl adipate	Hexamethylenediamine	31
Adipic acid	Hexamethylenediamine	22

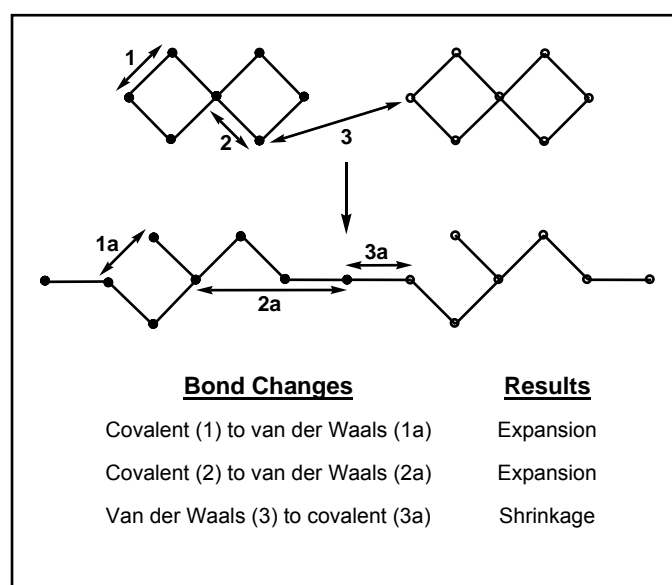
**Table 1.2.** Calculated shrinkage for addition polymerization.

<b>Monomer</b>	<b>Shrinkage (%)</b>
Ethylene	66
Vinyl chloride	34.4
Styrene	14.5

**Table 1.3.** Calculated shrinkage during ring-opening polymerization.

<b>Monomer</b>	<b>Shrinkage (%)</b>
Ethylene oxide	23
Styrene oxide	9
Diglycidyl ether of Bisphenol A	5

To find monomers which would give near zero shrinkage or even expansion on polymerization, the most viable approach would be monomers which could polymerize under ring-opening polymerization. Above it was rationalized that the single ring-opening polymerization produces less shrinkage than any of the other forms of polymerization. Therefore, if monomers could polymerize under double ring-opening polymerization, less shrinkage or even some expansion could be expected. In 1973, William J. Bailey proposed that the compounds which fulfil this requirement are bicyclic compounds with fused rings. In the bicyclic monomer, for every bond that undergoes a shift from a van der Waals distance to a covalent distance, at least two other bonds shift from a covalent distance to a near van der Waals distance.<sup>31,36-38</sup> These bond changes produce expansion as illustrated in Figure 1.5.



**Figure 1.5.** Bond transitions during the polymerization of a bicyclic compound.

<sup>36</sup> Bailey, W. J. *Elastoplast* 1973, 5, 142.

<sup>37</sup> Sanda, F.; Hitomi, M.; Endo, T. *J Polym Sci Part A: Polym Chem* 2001, 39, 3159.

<sup>38</sup> Nishida, H.; Sanda, F.; Endo, T.; Nakahara, T.; Ogata, K.; Kusumoto, K. *J Polym Sci Part A: Polym Chem* 1999, 37, 4502.

Furthermore, Bailey proposed two other requirements to get “expanding monomers”: (1) that each ring contain at least one heteroatom, so that the catalyst can be available for the polymerization (2) that the rings do not open in a symmetrical manner. For example, an oxygen atom in one ring may form a carbonyl group while the corresponding oxygen in the other ring would form an ether group.

There are several classes of compounds that fulfil all of the requirements. These include the spiroorthoesters (SOEs), the spiroorthocarbonates (SOCs) and the bicyclic orthoesters (BOEs).<sup>31,39-42</sup> Their structure shown in Figure 1.6.

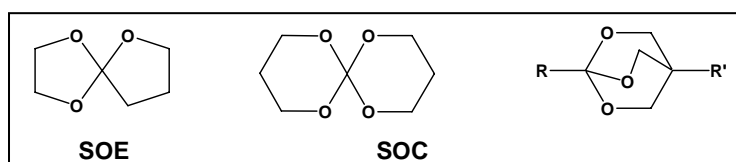


Figure 1.6. Expanding monomers.

Among them, SOEs are useful expanding monomers because they can be easily formed from epoxides and lactones. Thus, they have been chosen in this work to reduce the shrinkage.

## 1.2 SCOPE AND PURPOSE OF THIS THESIS

---

Until now there are not any approaches described in the literature that improve both the flame retardance and the shrinkage associated with the polymerization process. In some applications, like in the electronic industry, it is desirable to obtain materials that present these two properties. Thus, the purpose of the work reported in this thesis was to develop new materials which

<sup>39</sup> Takata, T.; Endo, T. *Prog Polym Sci* 1993, 18, 839.

<sup>40</sup> Cheng, K.; Takata, T.; Endo, T. *Macromolecules* 1995, 28, 3048.

<sup>41</sup> Bailey, W. J.; Katsuki, H.; Endo, T. *J Am Chem Soc, Div Polym Chem* 1974, 155, 445.

<sup>42</sup> Endo, T.; Okawara, M.; Saigo, K.; Bailey, W. J. *J Polym Sci Part C: Polym Lett* 1980, 18, 771.

combine flame retardancy properties and low shrinkage during polymerization and/or polymer curing. Several approaches have been developed to achieve these desired properties and are grouped in different chapters as follows:

Chapter 2 describes the synthesis and polymerization of novel phosphorus- and silicon-containing spiroorthoesters. Their application to modify epoxy resins, through the cationic copolymerization of these new spiroorthoesters with epoxy resins, and their properties were also evaluated. Moreover, the effect of combining phosphorus and silicon was also studied with the purpose of investigating the synergistic effect.

Chapter 3 describes the synthesis of new linear polymers that contain a spiroorthoester and phosphorus moieties in the side chain, obtained through a radical copolymerization of a spiroorthoester-containing acrylate with several phosphorus polymerizable monomers. In subsequent cationic ring-opening polymerization of the spiroorthoester moiety, the polymers were crosslinked with no accompanying volume shrinkage. Moreover, the application of the linear polymer containing SOE moieties in the side chain to modify epoxy resins was studied.

Finally, chapter 4 describes a new method of copolymerization of a spiroorthoester with epoxy resins using microwave irradiation and this system was then compared with conventional heating.

## C O N C L U S I O N S

- 1.** Phosphorus- and silicon-containing spiroorthoesters were synthesized by two different approaches: esterification reaction or Michael addition from spiroorthoester precursors. The spiroorthoester moiety was obtained from  $\gamma$ -butirolactone and an epoxide.
- 2.** Linear polymers which contain phosphorus and spiroorthoester moieties in the side chain were obtained by radical polymerization from an acrylate-containing spiroorthoester and different radically polymerizable phosphorus-containing comonomers. The polymers were crosslinked by a cationic double ring-opening of the spiroorthoester moieties with ytterbium triflate as an initiator.
- 3.** Linear polymers which contain a spiroorthoester moiety in the side chain were successfully crosslinked with phosphorus-containing glycidyl derivatives.
- 4.** Microwave irradiation showed to be useful method to synthesize one of the phosphorus-containing spiroorthoesters, which could not be obtained by conventional heating. These conditions allowed the crosslinking of a SOE with DGEBA with lanthanide triflates as initiators in reaction times significantly shorter than in conventional heating conditions.
- 5.** All the above synthetic approaches led to materials with phosphorus or silicon heteroatoms and linear ester-ether moieties, introduced by double ring-opening of SOEs, which showed enhanced flame retardance and low shrinkage or even expansion upon curing.

# CONTENTS

---

## CHAPTER 1 - INTRODUCTION AND SCOPE

---

- 1.1 Introduction 3
- 1.2 Scope and Purpose of this thesis 12

## CHAPTER 2 - SYNTHESIS OF PHOSPHORUS OR SILICON-CONTAINING SPIROORTHOESTERS

---

- 2.1 Introduction 17
- 2.2 Objectives 25
- 2.3 Experimental procedures and results 27
  - 2.3.1 Microwave-Assisted Synthesis of a Novel Phosphorus-Containing Spiroorthoester, Characterization and Cationic Polymerization. 31
  - 2.3.2 Synthesis of a Novel Bis-Spiroorthoester Containing 9,10-dihydro-9-oxa-10-phosphaphenantrene-10-oxide as a Substituent: Homopolymerization and Copolymerization with Diglycidyl Ether of Bisphenol A. 47
  - 2.3.3 Novel Silicon-Containing Spiroorthoester with Combined Flame Retardancy and Low Shrinkage Properties to Modify Epoxy Resins. 69
  - 2.3.4 Copolymerization of a Silicon-Containing Spiroorthoester with a Phosphorus-Containing Diglycidyl Compound. Influence in Flame Retardance and Shrinkage 89

## **CHAPTER 3 - CROSSLINKING THROUGH SPIROORTHOESTERS AS PENDANT GROUPS**

---

**3.1 Introduction 105**

**3.2 Objectives 109**

**3.3 Experimental Procedures and Results 110**

**3.3.1 Phosphorylated Copolymers Containing Pendant, Crosslinkable Spiroorthoester Moieties. 115**

**3.3.2 Flame Retardance and Shrinkage Reduction of Polystyrene Modified with Acrylate Containing-Phosphorus and Crosslinkable Spiroorthoester Moieties. 133**

**3.3.3 Crosslinking of a Polyacrylate Bearing a Spiroorthoester Pendant Group with Mixtures of Diglycidyl Ether of Bisphenol A and Phosphorus-Containing Glycidyl Derivatives. 151**

## **CHAPTER 4 - MICROWAVE CURING OF A SPIROORTHOESTER-EPOXY SYSTEM**

---

**4.1 Introduction 169**

**4.2 Objectives 172**

**4.3 Experimental Procedures and Results 173**

**4.3.1 Microwave Accelerate Polymerization of 2-Phenoxymethyl-1,4,6-trioxaspiro [4,4] nonane with Diglycidyl Ether of Bisphenol A 177**

## **CHAPTER 5 – CONCLUSIONS 191**

---

## **CHAPTER 6 – APPENDIX: LIST OF ABBREVIATIONS 193**

---

# C H A P T E R 4

## MICROWAVE CURING OF A --- SPIROORTHOESTER-EPOXY SYSTEM ---

*Increasing production demand of thermoset polymers have promoted the development of alternative curing methods. Microwave irradiation is a promising alternative to conventional heating for the curing of thermosets, with a significant increase in the reaction rate.*

*This chapter describes the copolymerization of a spiroorthoester with diglycidyl ether of bisphenol A under microwave irradiation and its comparison with conventional heating.*

- 
- 4.1.** Introduction
  - 4.2.** Objectives
  - 4.3.** Experimental Procedures and Results
    - 4.3.1.** Microwave Accelerate Polymerization of 2-Phenoxymethyl-1,4,6-trioxaspiro [4,4] nonane with Diglycidyl Ether of Bisphenol A

## 4.1 INTRODUCTION

---

Increasing production demand of epoxy resins, due their application in the growing aerospace and microelectronics industries, has promoted the development of alternative curing methods that accelerate this process, which is the bottleneck in the production process of these materials.

Whilst thermal curing increases the cure rate and thus lowers the cure time, this is limited by the fact that the maximum rate of reaction for any given curing system already has an optimum temperature. Heating it to a temperature higher than this optimum would not increase its rate of reaction, but instead lead to thermal degradation of the material.

The incentive for using alternative non thermal curing methods is typically to accelerate the curing process and thus reduce the time of cure. These include the use of ultraviolet light, gamma rays and electron beams. Ultraviolet light has limited application due to its poor penetration ability. Gamma rays are from naturally radiating sources such as Cobalt-60, with enormous radiation hazards and environmental issues. Electron Beam curing has proved to be an accelerated and efficient curing method, but requires often unacceptably high capital outlay. In many systems, the use of microwave irradiation has shown to be a viable alternative for the curing of thermosets polymers, with a significant increase in the rate of reaction.<sup>1 - 8</sup>

The use of microwave irradiation as an alternative heat source is becoming more and more popular in chemistry. Its good acceptance in inorganic and organic synthesis arises from the immense increase in reaction speed, which

---

<sup>1</sup> Bogdal, D.; Penczek, P.; Pielichowski, J.; Prociak, A. *Adv Polym Sci* 2003, 163, 193.

<sup>2</sup> Clark, D. E.; Sutton, W. H. *Ann Rev Mater Sci* 1996, 26, 299.

<sup>3</sup> Marand, E.; Baker, K. R.; Graybeal, J. D. *Macromolecules* 1992, 2243.

<sup>4</sup> Tanrattanakul, V.; SaeTiaw, K.; *J Appl Polym Sci* 2005, 97, 1442.

<sup>5</sup> Jacob, J.; Chia, L. H. L.; Boey, F. Y. C. *J Mater Sci* 1995, 30, 5321.

<sup>6</sup> Jayanthi, J.; Boey, F. Y. C.; Chia, L. H. L. *Am Ceram Soc. Ceram Trans* 1997, 57.

<sup>7</sup> Boey, F. Y. C.; Yap, B. H.; Chia, L. *Polym Testing* 1999, 18, 93.

<sup>8</sup> Boey, F. Y. C.; Yap, B. H. *Polym Testing* 2001, 20, 837.

compares favorably with conventional heating for a large number of reactions. Apart from this main advantage, significant improvements in yield, reduction of side reactions and cleaner products have been observed.<sup>9-11</sup>

A simple explanation of the above phenomena is the different mechanism of heating. Traditionally, chemical synthesis has been achieved through conductive heating with an external heat source. Heat is driven into the substance, passing first through the walls of the vessel in order to reach the solvent and reactants. This is a slow and inefficient method for transferring energy into the system because it depends on the thermal conductivity of the various materials that must be penetrated. The thermal equilibrium between the temperature of the vessel and the reaction mixture can take hours.

Microwave heating, on the other hand, is a very different process and it is based on dielectric heating, where the polar molecules, that have a permanent dipole moment, try to align to the applied electromagnetic field resulting in rotation, friction, and collision of molecules, and thus, in heat generation. As a result, the heating rate and efficiency of microwave heating strongly depends on the dielectric properties and the relaxation times of the reaction mixture.<sup>10,12,13</sup>

The use of microwave irradiation in polymer chemistry is an emerging field of research.<sup>14,15</sup> As a result, the number of publications on microwave-assisted polymerizations per year has been growing rapidly (Figure 4.1). Also, in the last few years special attention has been given to microwave curing of thermoset materials.

---

<sup>9</sup> *Microwaves in Organic Synthesis*; Loupy, A. Ed.; John, Wiley & Sons, NY 2006.

<sup>10</sup> Lidström, P.; Tierney, J.; Wathey, B.; Westman, J. *Tetrahedron* 2001, 57, 9225.

<sup>11</sup> Deshayes, S.; Liagre, M.; Loupy, A.; Luche, J. P.; Petit, A. *Tetrahedron* 1999, 55, 10851.

<sup>12</sup> *Microwave Synthesis: Chemistry at the Speed of Light*; Hayes, B. L. CEM Publishing, Matthews 2002.

<sup>13</sup> Gabriel, C.; Gabriel, S.; Grant, E. H.; Halstead, B. S. J.; Mingos, D. M. P. *Chem Soc Rev* 1998, 27, 213.

<sup>14</sup> Wiesbrock, F.; Hoogenboom, R.; Schubert, U. S. *Macromol Rapid Commun* 2004, 25, 1739.

<sup>15</sup> Hoogenboom, R.; Schubert, U. S.; *Macromol Rapid Commun* 2007, 25, 1739.

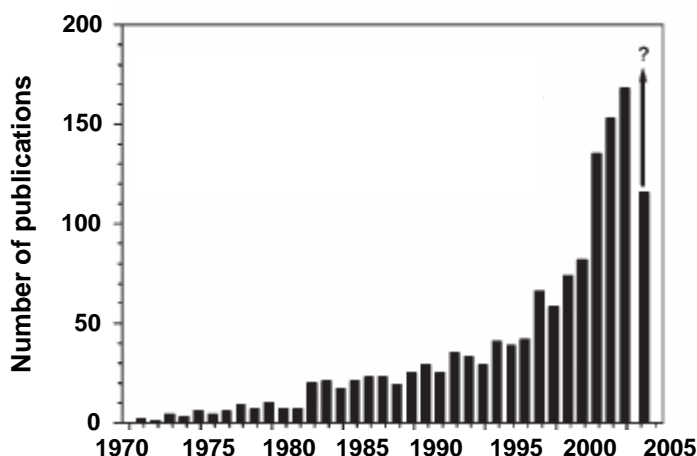


Figure 4.1. Number of publications on microwave-assisted polymerization per year.

Microwave curing of epoxy resins has been investigated by many scientists in terms of structure, dielectric properties, mechanical properties, degradation, percentage of cure, and glass transition temperatures. Thullier<sup>16</sup> studied the influence of continuous and pulsed microwave radiation in the curing of a mixture of diglycidyl ether of bisphenol A (DGEBA) with 4,4'-diaminodiphenylsulfone (DDS) as a curing agent, showing that a low pulse repetition induced the homopolymerization of DGEBA together with the reaction of DGEBA with DDS, while a continuous pulse only promotes the reaction with amines. Other authors<sup>17,18</sup> studied the same reactive curing system and observed that when it is exposed under microwave irradiation, the power absorbed by the sample first increased to a maximum and then decreased before reaching a constant value. Moreover, a significant increase in the reaction rate for the microwave curing of DGEBA/DDS system has been observed by different authors.<sup>19,20</sup> However, other authors<sup>21,22</sup> observed a lower degree of cure and

<sup>16</sup> Thullier, F. M.; Jullien, H.; Loustalot, M. F. G. *Polym Commun* 1986, 27, 206.

<sup>17</sup> Teffal, M.; Gourdenne, A. *Eur Polym J* 1983, 19, 543.

<sup>18</sup> Beldjoudi, N.; Gourdenne, A. *Eur Polym J* 1988, 24, 53.

<sup>19</sup> Lewis, D. A.; Hedrick, J. C.; McGrath, J. E.; Ward, T. C. *Polym Prep* 1987, 28, 330.

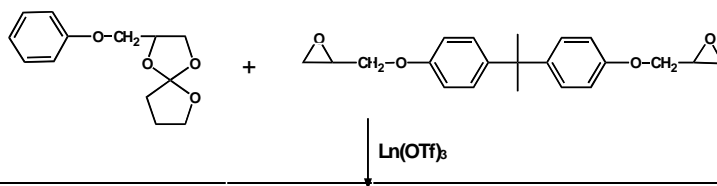
proposed that the microwave irradiation accelerated the curing reaction during the first stages of the process, inducing a rapid crosslinking, which created a rigid network that can trap unreacted functional groups, thus actually causing a lower degree of cure which affects the final properties of the material.

Other epoxy resins<sup>23,24</sup> and curing agents<sup>7,8,25</sup> have also been studied, showing that microwave irradiation is a promising and versatile method to achieve the curing of epoxy materials with considerable reduction in the curing time.

## 4.2 OBJECTIVES

Although in recent years microwave irradiation has won popularity in the curing of epoxy resins because of the reduction in curing times, no spiroorthoester has been copolymerized with epoxy resins under microwave conditions.

Thus the main objective of the work described in this chapter was to develop new thermosetting materials based on the copolymerization of a spiroorthoester, 2-phenoxyethyl-1,4,6-trioxaspiro [4,4] nonane (SOE-PGE) with the diglycidyl ether of bisphenol A (Scheme 4.1) under microwave conditions and the comparison of the analogous materials obtained under conventional thermal conditions. Moreover, two lanthanide catalysts were used and their behaviour compared.



<sup>20</sup> Wei, J.; Hawley, M. C.; DeMeuse, M. T. *Polym Eng Sci* 1993, 33, 1132.

<sup>21</sup> Jow, J.; Hawley, M. C.; Fingel, M.; Kemp, E. *Polym Eng Sci* 1988, 28, 1450.

<sup>22</sup> Tanrattanakul, V.; Jaroendee, D. *J Appl Polym Sci* 2006, 102, 1059.

<sup>23</sup> Zhang, D.; Crivello, J. V.; Stoffer, J. O. *J Polym Sci Part B: Polym Phys* 2004, 42, 4230.

<sup>24</sup> Wallace, M.; Attwood, D.; Day, R. J.; Frank, H. *J Mater Sci* 2006, 41, 5862.

<sup>25</sup> Fu, Bao.; Hawley, M. C. *Polym Eng Sci* 2000, 40, 2133.



Scheme 4.1

## 4.3 EXPERIMENTAL PROCEDURES AND RESULTS

---

The following work includes the experimental procedures and the results of the study performed in this chapter has been submitted for publication in Macromolecular Chemistry Physics and describes the first copolymerization of a spiroorthoester, the 2-phenoxyethyl-1,4,6-trioxaspiro [4,4] nonane (SOE-PGE), with diglycidyl ether of bisphenol A under microwave conditions and its comparison with conventional heating.

## MICROWAVE-ASSISTED SYNTHESIS OF A NOVEL PHOSPHORUS-CONTAINING SPIROORTHOESTER, CHARACTERIZATION AND CATIONIC POLYMERIZATION

J. Canadell, A. Mantecón, V. Cádiz

Departament de Química Analítica i Química Orgànica. Universitat Rovira i Virgili.  
Marcel·lí Domingo s/n, 43007 Tarragona, Spain

---

### Abstract

A new phosphorus-containing spiroorthoester, (1,4,6-trioxaspiro [4,4] nonan-2-yl)-methyl 3-[10-(9,10-dihydro-9-oxa-9-phosphaphenanthrene-10-oxide-10-yl)]-propa-noate (SOE-P), was synthesized under microwave irradiation with a short reaction time (1h), because classical thermal heating did not lead to the desired product. The structure of the new monomer was confirmed by  $^1\text{H}$ ,  $^{13}\text{C}$ , and  $^{31}\text{P}$ . SOE-P was homopolymerized and copolymerized with phenyl glycidyl ether with ytterbium triflate as a cationic initiator in DSC experiments. These reactions were monitored by FTIR/ATR, and the formation of poly(ether-ester)s with a pendant bulky phosphorylated group was shown.

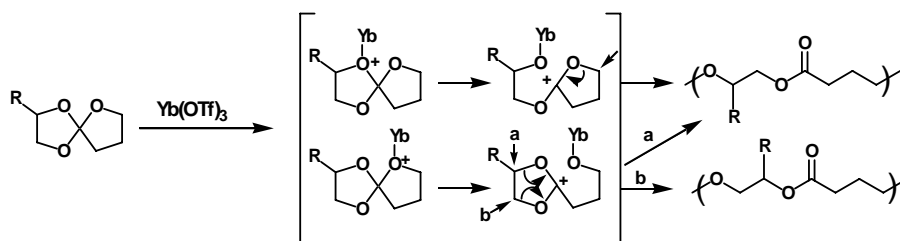
**Keywords:** cationic polymerization; flame retardance; heteroatom-containing polymers; microwave synthesis; spiroorthoester; ytterbium triflate

---

### INTRODUCTION

Epoxy resins have a good combination of attractive properties such as moisture, solvent and chemical resistance, toughness, superior electrical and mechanical

properties, and good adhesion to many substrates.<sup>1</sup> However, one of their disadvantages is that they are more flammable than similar thermosets, because they have a



**Scheme 1.** Cationic polymerization of SOE.

reduced tendency to carbonize. In recent years, the modification of epoxy resins has received increasing attention in an attempt to improve their flame resistance, particularly through halogen-free flame-retardant intumescent-based technology, which is an alternative to both halogenated and inorganic flame retardants.<sup>2-4</sup> One way of retarding polymer combustion is to block the source of fuel by covering the outer layer of the material with a nonflammable coating, such as a phosphorous containing compound. Reactive organic phosphorous compounds are powerful flame retardants, and thus attract more attention.<sup>3</sup>

Another disadvantage of epoxy resins is that they shrink during curing, which leads to a significant change in volume. This shrinkage is a major problem in such industrial applications as industrial castings,

coatings, mold replication, and microelectronics, because it leads to poor adhesion to the substrate, delamination, and microvoids and microcracks, which reduce the durability of the materials. One way of solving this problem is to copolymerize the epoxy resins with the so-called "expanding monomers",<sup>5</sup> which are monomers that lead to zero shrinkage or even positive expansion during polymerization. Some kinds of cyclic monomers such as spiroorthoesters (SOEs), spiroortho-carbonates (SOCs), and bicycloortho-esters (BOEs) have been reported to maintain their volume or actually expand during the double ring-opening polymerization.<sup>5-8</sup> SOEs can be readily synthesized from epoxides and lactones<sup>9,10</sup> and undergo cationic ring-opening polymerization by Lewis acid catalysts.

In this study, we synthesized a new phosphorus-containing spiroorthoester, (1,4,6-trioxaspiro[4,4] nonan-2-yl)-methyl 3-[10-(9,10-dihydro-9-oxa-9-phosphaphenanthrene-10-oxide-10-yl)] propanoate (SOE-P), derived from 9,10-dihydro-9-oxa-10-phosphaphenanthrene-10-oxide (DOPO), in an attempt to combine both their flame retardance and expanding properties. The incorporation of this rigid and bulky phosphorus-containing moiety confers good flame retardant properties on epoxy resins.<sup>11</sup> SOEs polymerize with cationic initiators to afford linear poly(ether-ester)s<sup>12-14</sup> (Scheme 1). They can also be used to modify epoxy resins.<sup>15,16</sup> Thus, we tested the ability of this phosphorus-containing spiroorthoester to homopolymerize and to copolymerize with epoxide, in this case with phenyl glycidyl ether as a model compound.

In the polymerization reactions of SOE-P, we used ytterbium triflate as the cationic initiator. In previous studies, our research group demonstrated that lanthanide triflates are Lewis acids that can cure epoxy resins.<sup>17,18</sup> Lanthanide triflates are commercially available and have many advantages over  $\text{BF}_3$  derivatives and alkylating agents, because they maintain their catalytic activity even in the presence of water.<sup>19</sup> The strong electron-withdrawing capacity of the trifluoromethanesulfonate anion enhances the Lewis acid character of the initiator. Moreover, lanthanide

cations have low electronegativities, strong oxophilicities, and large ionic radii, and they coordinate to the oxygen atoms of monomers to create the active species.<sup>20</sup>

## EXPERIMENTAL

### Materials

Commercial DOPO was kindly supplied by Aismalibar and it was purified before use by heating at 130 °C under vacuum for 2 h and then gradually heated to 150 °C. The purified product was cooled to room temperature under argon atmosphere. Phenylglycidyl ether (PGE; Aldrich), epibromohydrin (Fluka),  $\gamma$ -butyrolactone ( $\gamma$ -BL; Aldrich), boron trifluoride diethyl etherate ( $\text{BF}_3 \cdot \text{OEt}_2$ ; Aldrich), triethylamine (Fluka), acrylic acid (Aldrich), 1,8-diazabicyclo[5.4.0]undec-7-en (DBU; Aldrich), 3-*tert*-butyl-4-hydroxy-5-methylphenyl sulfide (Aldrich), hydrogen hexachloroplatine (IV) ( $\text{H}_2\text{PtCl}_6$ , Aldrich) were used as received. All solvents were purified by standard procedures. The polymerization catalyst, ytterbium (III) trifluoromethanesulfonate [ $\text{Yb}(\text{OTf})_3$ ], was purchased from Aldrich and used without purification.

### Instrumentation

The microwave irradiated reaction was carried out in a 10-mL reactor vial, using a CEM Discover mono-

modal microwave reactor and an IR temperature sensor and operating at a maximum power of 300 W.

NMR spectra ( $^1\text{H}$ , 400 MHz;  $^{13}\text{C}$ , 100.6 MHz; and  $^{31}\text{P}$ , 161.9 MHz) were obtained using a Varian Gemini 400 spectrometer with Fourier transform,  $\text{CDCl}_3$  as the solvent, and tetra-methylsilane (TMS) or phosphoric acid as internal standards.

Calorimetric studies (DSC) were carried out on a Mettler DSC-821e thermal analyzer in covered Al pans under  $\text{N}_2$  at scan rates of 10  $^\circ\text{C}/\text{min}$  for the first scan and 20  $^\circ\text{C}/\text{min}$  for the second scan.

The isothermal polymerization process at 180  $^\circ\text{C}$  was monitored with a FTIR-680PLUS spectrophotometer at a resolution of 4  $\text{cm}^{-1}$  in the absorbance mode. An attenuated-total-reflection accessory with thermal control and a diamond crystal was used to determine FTIR/ATR spectra.

Thermal stability studies were carried out on a Mettler TGA/SDTA851e/LF/1100 with  $\text{N}_2$  and air as a purge gas at scan rates of 10  $^\circ\text{C}/\text{min}$ .

Modified UL-94 Burn Test: three sample bars (30 x 20 x 0.5  $\text{mm}^3$ ) were used for this test. The height of the Bunsen burner flame was 25 mm and the height from the top of the Bunsen burner to the bottom of the test bar was 10 mm. All test bars underwent two trials and each

trial consisted of ignition for 10 s, after which the flame was removed and the time for self-extinguishing and dripping characteristics were recorded.

### Synthesis of 2-bromomethyl-1,4,6-trioxaspiro [4,4] nonane (SOE-Br)

A total of 50 g (0.36 mol) of epibromohydrin was added dropwise for 15 min at a temperature below 10  $^\circ\text{C}$  in argon atmosphere to a mixture of 180 g of (2.09 mol) of  $\gamma$ -BL and 1.5 mL (11.8 mmol) of  $\text{BF}_3 \cdot \text{OEt}_2$  as a catalyst. After the addition was complete, the mixture was stirred for 60 min at the same temperature. The reaction was quenched by the addition of 1.9 mL (13.5 mmol) of triethylamine. After the solvent had been removed under reduced pressure, the residue was distilled fractionally to yield 60.4 g (74 %) of transparent liquid.

$^1\text{H}$  NMR ( $\text{CDCl}_3$ , two diastereomers):  $\delta(\text{ppm}) = 4.54\text{-}4.48$  (m, 1H, -O-CH-), 4.43-4.37 (m, 1H, -O-CH-), 4.21-4.17 (dd, 2H, -O-CH<sub>2</sub>-), 3.98-3.87 (m, 6H, -O-CH<sub>2</sub>-), 3.91-3.31 (m, 4H, Br-CH<sub>2</sub>-), 2.20-2.11 (m, 4H, -CH<sub>2</sub>-), 2.05-1.98 (m, 4H, -CH<sub>2</sub>-).

$^{13}\text{C}$  NMR ( $\text{CDCl}_3$ , two diastereomers):  $\delta(\text{ppm}) = 129.98$  (s, spiranic C), 129.88 (s, spiranic C), 75.48 (s, -O-CH-), 74.74 (s, -O-CH-), 68.72 (s, -O-CH<sub>2</sub>-), 67.68 (s, -O-CH<sub>2</sub>-), 67.40 (s, -O-CH<sub>2</sub>-), 67.38 (s, -O-CH<sub>2</sub>-), 32.87 (s, -CH<sub>2</sub>-), 32.81 (s,

-CH<sub>2</sub>-), 32.74 (s, Br-CH<sub>2</sub>-), 32.28 (s, Br-CH<sub>2</sub>-), 24.20 (s, -CH<sub>2</sub>-), 24.05 (s, -CH<sub>2</sub>-).

### Synthesis of SOE-acrylate

A total of 10 g (45.0 mmol) of SOE-Br with 10 mL of anhydrous DMSO was added slowly to a mixture of 3.24 g (45.0 mmol) of acrylic acid and 6.84 g (45.0 mmol) of DBU in 20 mL of anhydrous DMSO, stored under argon atmosphere in a three-necked flask in a bath at 65 °C. This mixture was stirred vigorously for a period of 30 min during the addition. After the addition was complete, the mixture was stirred for an additional 5 h at the same temperature. When the reaction had finished, 8 mg of a radical inhibitor, 3-*tert*-butyl-4-hydroxy-5-methylphenyl sulfide, was added. The desired product was removed from DMSO by several extractions with CH<sub>2</sub>Cl<sub>2</sub>. The product was purified by washing with a dilute solution of HCl and was then neutralized with a solution of NaOH. The dichloromethane solution was dried over MgSO<sub>4</sub> and evaporated. After the SOE-Br impurities had been removed under reduced pressure, 7.27 g (76%) of transparent liquid was afforded.

<sup>1</sup>H NMR (CDCl<sub>3</sub>, two diastereomers): δ(ppm) = 6.46-6.41 (dd, 1H, J<sub>trans</sub> = 16.8 Hz, J<sub>cis</sub> = 1.6 Hz, C=CH), 6.44-6.40 (dd, 1H, J<sub>trans</sub> = 17.2 Hz, J<sub>cis</sub> = 1.6 Hz, C=CH), 6.17-6.01 (m, 2H, C=CH<sub>2</sub>), 5.87-5.84 (dd, 1H, J<sub>cis</sub> = 9.6 Hz, J<sub>gem</sub> = 1.2 Hz, C=CH<sub>2</sub>), 5.86-5.83 (dd, 1H,

J<sub>cis</sub> = 10.8 Hz, J<sub>gem</sub> = 1.6 Hz, C=CH<sub>2</sub>), 4.35-3.50 (m, 1H, -O-CH-), 4.38-4.32 (m, 1H, -O-CH-), 4.38-4.01 (m, 6H, -O-CH<sub>2</sub>-), 3.96-3.89 (m, 4H, -O-CH<sub>2</sub>-), 3.84-3.77 (m, 2H, -O-CH<sub>2</sub>-), 2.16-2.10 (m, 4H, -CH<sub>2</sub>-), 2.04-1.99 (m, 4H, -CH<sub>2</sub>-).

<sup>13</sup>C NMR (CDCl<sub>3</sub>, two diastereomers): δ(ppm) = 166.04 (s, C=O), 131.73 (s, C=CH<sub>2</sub>), 129.98 (s, spiranic carbon), 128.11 (s, C=CH), 74.32 (s, -O-CH-), 73.47 (s, -O-CH-), 67.58 (s, -O-CH<sub>2</sub>-), 66.29 (s, -O-CH<sub>2</sub>-), 66.16 (s, -O-CH<sub>2</sub>-), 65.32 (s, -O-CH<sub>2</sub>-), 64.41 (s, -O-CH<sub>2</sub>-), 32.89 (s, -CH<sub>2</sub>-), 24.41 (s, -CH<sub>2</sub>-), 24.22 (s, -CH<sub>2</sub>-).

### Synthesis of SOE-P

#### Microwave Irradiation

A microwave reactor vial (10 mL) was charged in air with 0.1 g (0.46 mmol) of DOPO and 0.108g (0.50 mmol) of SOE-acrylate and a new magnetic stirring bar. The vial was purged with nitrogen.

The maximum power setting of 50 W was maintained until the desired temperature (130 °C) had been reached (160 s). The power was reduced to 11 W for the remainder of the reaction time to maintain 130 °C. After 60 min, the mixture reaction was cooled to room temperature.

The product was purified by flash chromatography with silica gel neutralized with triethylamine and using acetone with 1% triethylamine

as eluent. A yellowish viscous oil (0.184 g, 93%) was afforded.

$^1\text{H}$  NMR ( $\text{CDCl}_3$ , four diastereomers):  $\delta(\text{ppm})= 7.93\text{--}7.80$  (m, 12H, Ar-H), 7.66 (t, 4H,  $J_o = 7.6$  Hz, Ar-H), 7.47 (t, 4H,  $J_o = 7.6$  Hz, Ar-H), 7.33 (dt, 4H,  $J_o = 8.4$  Hz,  $J_m = 1.2$  Hz, Ar-H), 7.22-7.15 (m, 8H, Ar-H), 4.38 (m, 2H, -O-CH-), 4.29-4.17 (m, 4H, -O-CH-, -O-CH<sub>2</sub>-), 4.10-4.00 (m, 10H, -O-CH<sub>2</sub>-), 3.90-3.84 (m, 8H, -O-CH<sub>2</sub>-), 3.73-3.65 (m, 4H, -O-CH<sub>2</sub>-), 2.67-2.57 (m, 8H, -CH<sub>2</sub>-), 2.40-2.30 (m, 8H, -P-CH<sub>2</sub>-), 2.12-2.05 (m, 8H, -CH<sub>2</sub>-), 1.97-1.90 (m, 8H, -CH<sub>2</sub>-).

$^{13}\text{C}$  NMR ( $\text{CDCl}_3$ , four diastereomers):  $\delta(\text{ppm})= 171.29$  (d,  $J_{\text{C-P}} = 17.5$  Hz, C=O), 171.28 (d,  $J_{\text{C-P}} = 17.5$  Hz, C=O), 148.78 (d,  $J_{\text{C-P}} = 7.9$  Hz, Ar-C), 148.77 (d,  $J_{\text{C-P}} = 7.9$  Hz, Ar-C), 135.52 (d,  $J_{\text{C-P}} = 6.1$  Hz, Ar-C), 135.51 (d,  $J_{\text{C-P}} = 6.0$  Hz, Ar-C), 135.50 (d,  $J_{\text{C-P}} = 6.1$  Hz, Ar-C), 133.45 (d,  $J_{\text{C-P}} = 2.3$  Hz, Ar-CH), 133.42 (d,  $J_{\text{C-P}} = 2.2$  Hz, Ar-CH), 130.59 (s, Ar-CH), 130.60 (s, Ar-CH), 129.93 (d,  $J_{\text{C-P}} = 11.1$  Hz, Ar-CH), 129.92 (d,  $J_{\text{C-P}} = 11.1$  Hz, Ar-CH), 129.62 (s, spiranic C), 129.60 (s, spiranic C), 129.50 (s, spiranic C), 128.50 (d,  $J_{\text{C-P}} = 13.5$  Hz, Ar-CH), 128.49 (d,  $J_{\text{C-P}} = 13.4$  Hz, Ar-CH), 125.11 (s, Ar-CH), 125.10 (s, Ar-CH), 125.09 (s, Ar-CH), 125.08 (s, Ar-CH), 124.66 (s, Ar-CH), 124.64 (s, Ar-CH), 123.91 (d,  $J_{\text{C-P}} = 9.5$  Hz, Ar-CH), 123.90 (d,  $J_{\text{C-P}} = 9.5$  Hz, Ar-CH), 123.88 (d,  $J_{\text{C-P}} = 9.5$  Hz, Ar-CH), 124.10 (d,  $J_{\text{C-P}} = 121.3$  Hz, Ar-C), 124.09 (d,  $J_{\text{C-P}} = 121.2$  Hz, Ar-C), 124.08 (d,  $J_{\text{C-P}} = 121.2$

Hz, Ar-C), 124.07 (d,  $J_{\text{C-P}} = 121.3$  Hz, Ar-C), 121.88 (d,  $J_{\text{C-P}} = 11.1$  Hz, Ar-C), 121.86 (d,  $J_{\text{C-P}} = 11.1$  Hz, Ar-C), 120.19 (d,  $J_{\text{C-P}} = 6.1$  Hz, Ar-CH), 73.79 (s, -CH-) 73.77 (s, -CH-), 72.92 (s, -CH-), 67.16 (s, -O-CH<sub>2</sub>-), 67.07 (s, -O-CH<sub>2</sub>-), 65.64 (s, -O-CH<sub>2</sub>-), 65.63 (s, -O-CH<sub>2</sub>-), 65.61 (s, -O-CH<sub>2</sub>-), 65.59 (s, -O-CH<sub>2</sub>-), 65.21 (s, -O-CH<sub>2</sub>-), 65.17 (s, -O-CH<sub>2</sub>-), 64.56 (s, -O-CH<sub>2</sub>-), 64.51 (s, -O-CH<sub>2</sub>-), 32.48 (s, -CH<sub>2</sub>-), 32.45 (s, -CH<sub>2</sub>-), 26.38 (d,  $J_{\text{C-P}} = 6.1$  Hz, -CH<sub>2</sub>-), 26.37 (d,  $J_{\text{C-P}} = 6.5$  Hz, -CH<sub>2</sub>-), 26.36 (d,  $J_{\text{C-P}} = 6.1$  Hz, -CH<sub>2</sub>-), 26.35 (d,  $J_{\text{C-P}} = 6.4$  Hz, -CH<sub>2</sub>-), 24.13 (d,  $J_{\text{C-P}} = 99.1$  Hz, -CH<sub>2</sub>-), 24.05 (s, -CH<sub>2</sub>-), 24.03 (s, -CH<sub>2</sub>-), 23.88 (-CH<sub>2</sub>-), 23.85 (s, -CH<sub>2</sub>-).

$^{31}\text{P}$  NMR ( $\text{CDCl}_3$ , four diastereomers)  $\delta(\text{ppm})= 37.02$  (s), 37.01 (s), 36.93 (s), 36.90 (s).

### Conventional Heating

In a 25-mL round-bottom flask equipped with a nitrogen inlet, a condenser, and a magnetic stirrer, 0.5 g (2.31 mmol) of DOPO and drops of 5%  $\text{H}_2\text{PtCl}_6$  catalyst in isopropyl alcohol were dissolved in 2.5 mL of xylene. The flask was heated to 125 °C and then 0.5 g (2.33 mmol) SOE-acrylate with 3 mL of xylene was added slowly for 20 min. After the complete addition of SOE-acrylate, the reaction was maintained at that temperature for 150 min. After cooling to room temperature, the reaction product was filtered, washed with acetone several times, and then dried in an

oven at 120 °C for 4 h. The recovered solid was a complex mixture in which the desired product was not detected.

### Polymerization Reactions

About 10 mg of pure spiroorthoester or spiroorthoester/PGE mixture was put into an aluminium pan and the polymerization was monitored in a dynamic DSC experiment.

*Polymerization of SOE-P.* The sample was prepared by mixing SOE-P (0.1 g, 0.23 mmol) with 1 mol % of ytterbium triflate (1.45 mg, 0.00234 mmol).

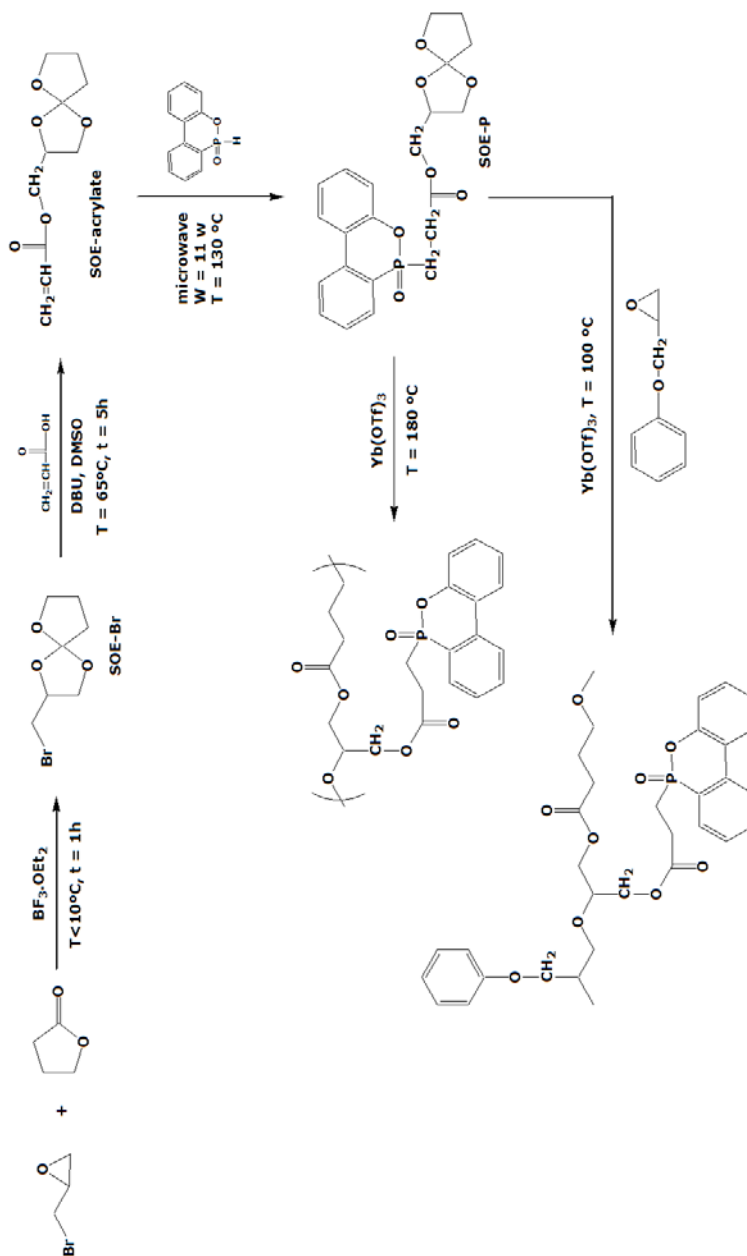
Copolymerization of SOE-P with PGE. The sample was prepared by mixing SOE-P (0.1 g, 0.23 mmol) and PGE (0.0349 g, 0.23 mmol)

with 1 mol % of ytterbium triflate (2.9 mg, 0.00468 mmol).

## RESULTS AND DISCUSSION

SOE-P was synthesized following the synthetic pathway shown in Scheme 2. First, we synthesized 2-bromomethyl-1,4,6-trioxaspiro [4,4] nonane (SOE-Br). This was prepared from epibromohydrin and  $\gamma$ -butyrolactone,<sup>9</sup> using  $\text{BF}_3 \cdot \text{OEt}_2$  as catalyst and its structure was confirmed by spectroscopic experiments. The reaction of SOE-Br with acrylic acid in the presence of DBU in DMSO, to obtain SOE-acrylate, was carried out under mild conditions. Direct ester formation from a primary halide and a carboxylic acid using DBU is a useful method that has been

38 | Synthesis of Spiroorthoesters



**Scheme 2.** Synthesis of SOE-P and its homo and copolymerization.

used by several authors.<sup>21,22</sup> This method also leads to good results in polymer modification.<sup>23-25</sup> The following synthetic step consisted in the incorporation of DOPO by means a conjugated addition reaction to the  $\alpha,\beta$ -unsaturated SOE-acrylate. When DOPO reacts with a double-bond-containing compound, the structures of double-bond-containing compounds have a significant influence on the reaction rate. For example, when DOPO reacts with benzoquinone<sup>26</sup> or maleic acid,<sup>27</sup> with two electron-withdrawing carbonyl groups next to the double bond, the reaction temperature is about 70-90 °C. However, when DOPO reacts with itaconic acid,<sup>27</sup> with only one electron-withdrawing carbonyl group next to the double bond, the reaction is very slow, even at 140 °C. Thus, the addition of the  $H_2PtCl_6$  catalyst is necessary to facilitate the reaction. The electron density of double bonds in the double-bond-containing compound is responsible for this. In the case of itaconic acid, because one carbonyl group is not next to the double bond, the double bond can only resonate with one carbonyl group, and the inductive effect of carbonyl decreases because of the considerable distance between the carbonyl group and the double bond. In our case, the SOE-acrylate should exhibit almost the same reactivity towards DOPO as itaconic acid. Thus, SOE-acrylate was reacted with DOPO at 125 °C in a xylene solution and with  $H_2PtCl_6$  as catalyst in reaction conditions that were

similar to those of DOPO-itaconic acid. However, the reaction did not lead to the desired compound but a complex mixture in which the presence of SOE-P was not detected.

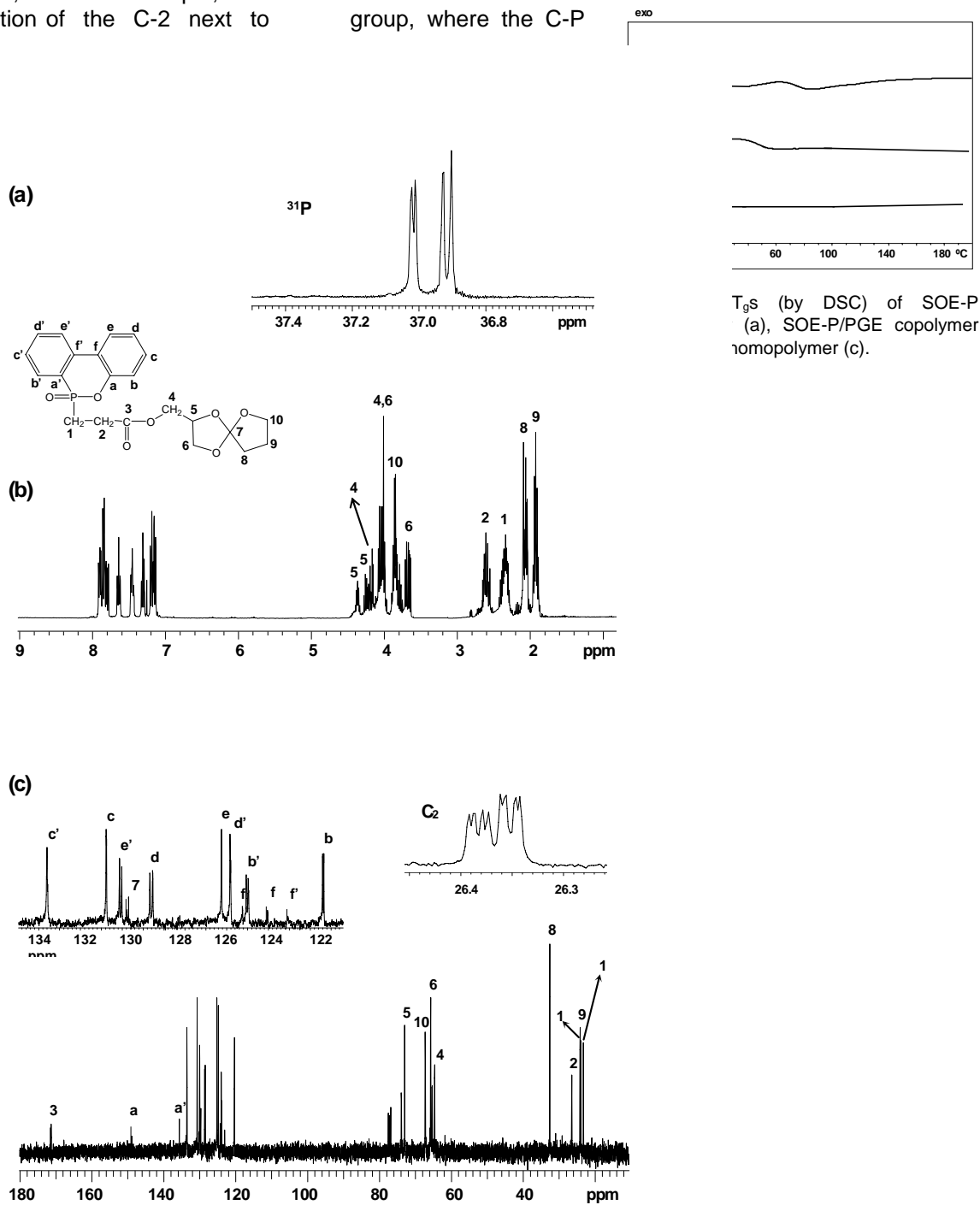
Although this addition of hydrogen phosphinate to alkenes can take place thermally, one way to avoid the undesirable transformations of the organophosphorus compounds is to reduce the reaction time. One promising way of doing this is to apply microwave energy. Microwave irradiation has a number of advantages over conventional heating, such as noncontact heating, which for many organophosphorus compounds is very important, and rapid and highly specific heating.<sup>28,29</sup> Thus, the hydrogen phosphinate was added to the unsaturated spiroortho-ester under microwave irradiation and SOE-P was obtained in a significantly short reaction time and in a good yield.<sup>30</sup>

This novel phosphorus-containing spiroorthoester was characterized by means of  $^1H$ ,  $^{13}C$ , and  $^{31}P$  NMR spectroscopy. Since the phosphorus center in DOPO is chiral and the spiroorthoester has two chiral carbons, the product of the addition reaction produced a mixture of diastereomers. Figure 1 shows the  $^{31}P$  (a),  $^1H$  (b), and  $^{13}C$  (c) NMR spectra, with all the assignments. The single  $^{31}P$  signal is split because of the presence of the four diastereomers. In  $^1H$  and  $^{13}C$  NMR spectra, some signals are

also split because of the four diastereomers. The inset in Figure 1 (c) shows, as an example, the amplification of the C-2 next to

the ester

group, where the C-P



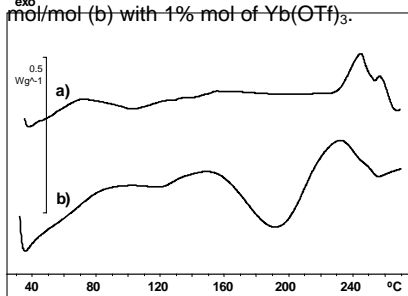
J Polym Sci Part A: Polym Chem 2006, 44, 4722

Figure 1. NMR spectra of SOE-P;  $^{31}\text{P}$  (a),  $^1\text{H}$  (b), and  $^{13}\text{C}$  (c).

coupling can also be observed. The spiroorthoester rings, aromatic proton, and carbon signals were assigned unequivocally by means of DEPT, HSQC, and COSY experiments.

As mentioned earlier, we are interested in testing the ability of the phosphorus-containing monomer SOE-P to modify epoxy resins. The polymerization of SOE-P, using 1 mol % of ytterbium triflate as cationic initiator was studied by DSC. Figure 2 (a) shows the dynamic DSC plot of this reaction in which there is a broad exotherm with a maximum at 245 °C, attributed to the polymerization. In a second scan, the  $T_g$  of the polymer at 74 °C was observed (Fig. 3a). TGA experiments in air showed that the 5% weight loss occurred at 202 °C. The derivative curve showed that the temperature of maximum rate of degradation was 390 °C and a second step was observed at 455

**Figure 2.** DSC plots of homopolymerization of SOE-P (a) and copolymerization of SOE-P/PGE 1:1 mol/mol (b) with 1% mol of  $\text{Yb}(\text{OTf})_3$ .



°C. The char yield at 750 °C was 20%.

This polymerization reaction was monitored by FTIR/ATR spectroscopy in isothermal experiment at 180 °C. This technique allowed us to monitor the evolution of the groups involved in the reaction by means of the variations in the corresponding absorptions. Figure 4 shows the FTIR spectra of SOE-P with 1 mol % of  $\text{Yb}(\text{OTf})_3$  before and after polymerization. The double ring-opening of the spiroorthoester that took place during the polymerization led to a linear poly(ether-ester) formation, so a typical band of carbonyl ester group must appear<sup>31</sup> at about 1735-1750  $\text{cm}^{-1}$ . Our acrylate derivative initially contains an ester group, which appears at 1734  $\text{cm}^{-1}$ , and therefore in this zone, only an increase in this band was observed on polymerizing.

Figure 5 shows the  $^{31}\text{P}$  and  $^{13}\text{C}$  NMR spectra of the obtained polymer. The broadness of P signal is characteristic

of polymeric compounds because of the different environment. The  $^{13}\text{C}$  NMR spectrum shows two different

carbonyl signals, attributed to the main chain and side chain ester groups, and the aromatic carbons between 150 and 120 ppm. The various aliphatic carbons appear below 80 ppm. The methylene and methine carbons attached to the oxygen atom appear between 80 and 60 ppm. The methylene group attached to the phosphorus atom appears at about 30 ppm and the other methylene

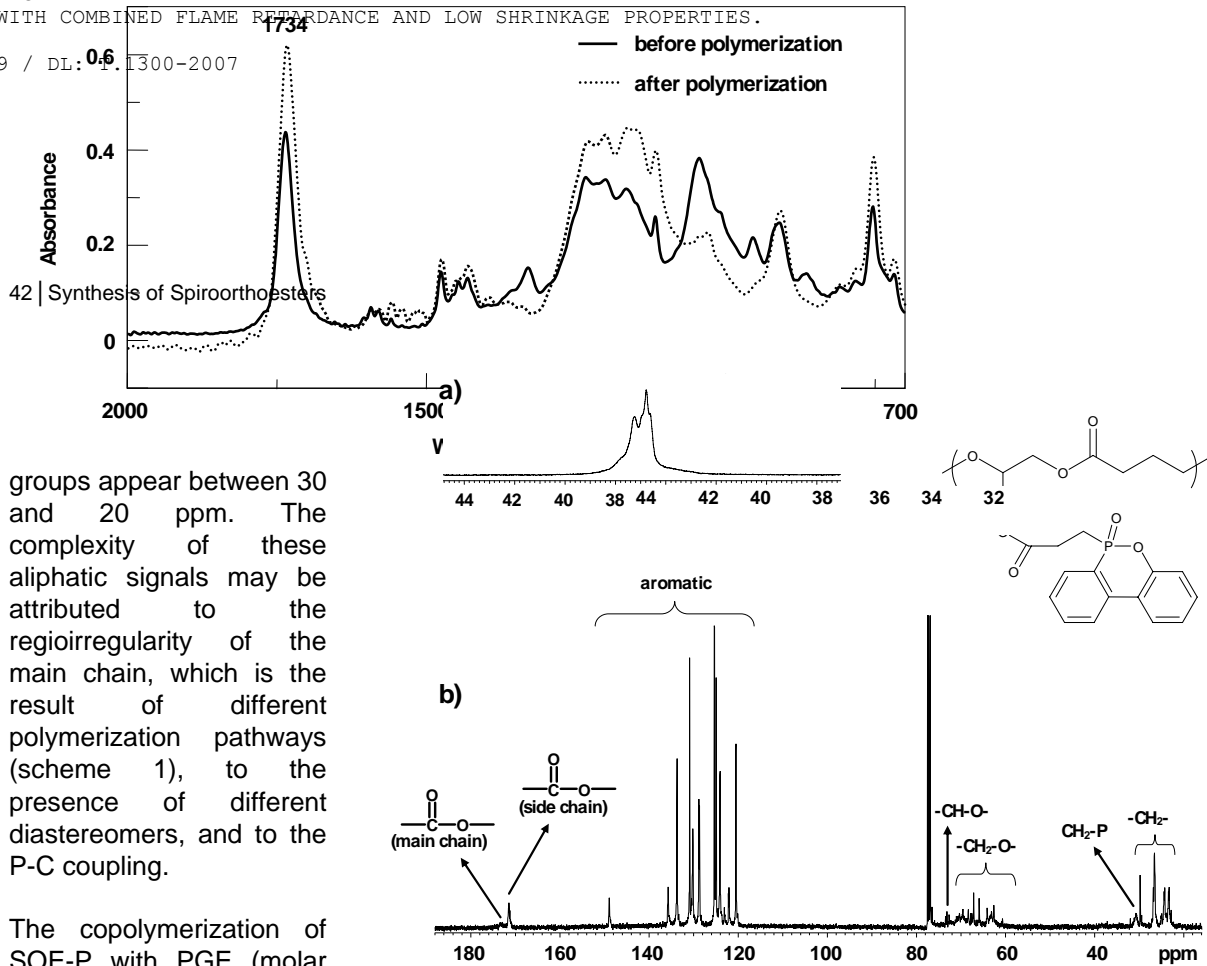


Figure 5.  $^{31}\text{P}$  (a) and  $^{13}\text{C}$  (b) NMR spectra of the polymer obtained by cationic polymerization of SOE-P.

groups appear between 30 and 20 ppm. The complexity of these aliphatic signals may be attributed to the regioirregularity of the main chain, which is the result of different polymerization pathways (scheme 1), to the presence of different diastereomers, and to the P-C coupling.

The copolymerization of SOE-P with PGE (molar ratio 1:1), using 1 mol % of ytterbium triflate as cationic initiator was studied by DSC. Figure 2 (b) shows the first broad exotherm attributed to the copolymerization of the two comonomers. The second exotherm, with a maximum at 230 °C, was attributed to the remaining spiroorthoester, which homopolymerizes in the last stage of the process. It must be noted that PGE homopolymerization exotherm, the maximum of which is at 170 °C, is not observed. Figure 3 plots the  $T_g$ s obtained in a second scan of SOE-P homopolymer (a), PGE homopolymer (c) and copolymer (b). As can be seen, the  $T_g$  value of the copolymer is between both homopolymer values, which indicates that a random

copolymer was obtained. The fact that a single  $T_g$  was observed indicates that the homopolymerization of the remaining SOE-P takes place only to a small extent.

This copolymerization reaction was monitored by FTIR/ATR spectroscopy in isothermal experiments at 100 °C. The carbonyl band was observed to increase, which indicates that the spiroorthoester opening took place. Unfortunately, the disappearance of the typical epoxy band at  $913\text{ cm}^{-1}$  could not be confirmed, because the initial spiroorthoester presented absorptions in the same zone.

The  $^{31}\text{P}$  spectrum of the copolymer showed a signal at 36.5-37.5 ppm in the same range as the homopolymer. The  $^{13}\text{C}$  NMR spectrum of the obtained copolymer showed a pattern similar to that of the SOE-P homopolymer but with a greater complexity in the aliphatic zone.

We did the flame retardant testing of the synthesized homopolymer (no test of the copolymer was made because its low  $T_g$ ), using a modified UL-94 flame test, in which the sample was suspended above cotton.<sup>32</sup> The sample was subjected to two 10-s ignitions with a calibrated methane-fueled flame in a controlled-size unit that was free of passing air currents. After the first ignition, the flame was removed and the time for the polymer to self-extinguish was recorded. The second ignition was then performed on the same sample and the self-extinguishing time/dripping characteristics were recorded. If the sample self-extinguished in less than 10 s with no dripping, we considered it to be a V-0 material, which is an industry standard for flame retardancy. According to the UL-94 test, the homopolymer sample produced a V-0 result as we expected from phosphorus-containing polymers.

## CONCLUSIONS

The microwave irradiation method was used to synthesize a phosphorylated spiroorthoester (SOE-P). This method avoids the undesirable transformations of the organophosphorus compounds that take place with conventional heating, which failed in the case of the synthesis of SOE-P. This new spiroorthoester was polymerized and copolymerized using an epoxy compound by a cationic mechanism with ytterbium triflate as initiator. Therefore, this spiroorthoester can be used to modify epoxy resins and even to form thermosets with improved properties.

*The authors thank the Comisión Interministerial de Ciencia y Tecnología, CICYT, (MAT2002-00223) (MAT2002-00291) (MAT2005-01593) (MAT2005-01806) for providing financial support for this work.*

## REFERENCES AND NOTES

1. Epoxy resins. Chemistry and Technology; May, C. A. Ed.; Marcel Dekker: New York, 1988.
2. Camino, G. In Chemistry and Technology of Polymer Additives; Al-Malaika, S.; Golovoy, A.; Wilkie, C. A., Eds.; Blackwell Science: London 1999; p.108.
3. Lu, S.-Y.; Hamerton, I. Prog Polym Sci 2002, 27, 1661.
4. Green, J. J Fire Sci 1992, 10, 470.

5. Expanding monomers, Synthesis, Characterization and Applications; Shadir, R. K.; Luck, R. M. Ed.; CRC Press: Boca Raton, 1992.
6. Hino, T.; Endo, T. *Macromolecules* 2003, 36, 5902.
7. Smith, R. E.; Pinzino, C. S.; Chappelow, C. C.; Holder, A. J.; Kostoryz, E. L.; Guthrie, J. R.; Miller, M.; Yourtee, D. M.; Eick, J. D. *J Appl Polym Sci* 2004, 92, 62.
8. Nishida, H.; Morikawa, H.; Nakahara, T.; Ogata, T.; Kusumoto, K.; Endo, T. *Polymer*, 2005, 46, 2531.
9. Bodenbenner, K.; Justus Liebigs *Ann Chem* 1959, 625, 183.
10. Fedtke, M.; Houfe, J.; Kahlert, E.; Müller, G. *Angew Makromol Chem* 1998, 255, 53.
11. Wang, C.-S.; Shieh, J.-Y. *Polymer* 1998, 39, 5819.
12. Takata, T.; Endo, T. *Prog Polym Sci* 1993, 18, 839.
13. Yoshida, K.; Sanda, F.; Endo, T. *J Polym Sci Part A: Polym Chem* 1999, 37, 2551.
14. Chikaoka, S.; Takata, T.; Endo, T. *Macromolecules* 1992, 25, 625.
15. Shimbo, M.; Ochi, M.; Inamura, T.; Inoue, M. *J Mater Sci* 1985, 20, 2965.
16. Ochi, M.; Yamazaki, K.; Shimbo, M. *J Mater Sci* 1989, 24, 3189.
17. Castell, P.; Galià, M.; Serra, A.; Salla, J. M.; Ramis, X. *Polymer* 2000, 41, 8465.
18. Mas, C.; Serra, A.; Mantecón, A.; Salla, J. M.; Ramis, X. *Macromol Chem Phys* 2001, 202, 2554.
19. Lanthanides: Chemistry and Use in Organic Synthesis; Kobayashi, S., Ed.; Springer-Verlag: Berlin, 1999. *Topics in Organometallic Chemistry*.
20. Aspinall, H. C.; Dwyer, J. L. M.; Greeves, N.; McIver, E. G.; Wooley, J. C. *Organometallics* 1998, 35, 433.
21. Nishikubo, T.; Iizawa, T.; Takahashi, A.; Shimokawa, T. *J Polym Sci Part A: Polym Chem* 1990, 28, 105.
22. Endo, T.; Kitamura, N.; Takata, T. *J Polym Sci Part A: Polym Chem* 1988, 26, 517.
23. Nishikubo, T.; Ozaki, K. *Polym J* 1990, 22, 1043.
24. Galià, M.; Mantecón, A.; Cádiz, V.; Serra, A. *J Polym Sci Part A: Polym Chem* 1994, 32, 7790.
25. Callau, L.; Reina, J. A.; Mantecón, A.; Tessier, M.; Spassky, N. *Macromolecules* 1999, 32, 829.
26. Shan, W. C.; Hsuan, L. C. *Polymer* 1999, 40, 4387.
27. Lin, C. H.; Wu, C. Y.; Wang, C. S. *J Appl Polym Sci* 2000, 78, 228.
28. Bogdal, D.; Penczek, P.; Pielchowski, J.; Prociak, A. *Adv Polym Sci* 2003, 163, 193.
29. Lidstrom, P.; Tieney, J.; Wathey, B.; Westman, J. *Tetrahedron* 2001, 57, 922.
30. Stockland, R. A. Jr.; Taylor, R. I.; Thompson, L. E.; Patel, P. B. *Org Lett* 2005, 7, 851.

31. Pretsch, E.; Clerc, T.; Seibl, J.; Simon, W. Tablas para la elucidación estructural de compuestos orgánicos por métodos espectroscópicos; Springer-Verlag Ibérica: Barcelona, 1998. Spanish Edition.
32. Standard for tests for flammability of plastic materials for parts in devices and appliances, 4th ed.; Underwriters Laboratories UL 94: Research Triangle Park, NC, 1991.

## SYNTHESIS OF A NOVEL BIS-SPIROORTHOESTER CONTAINING 9,10-DIHYDRO-9-OXA-10- PHOSPHAPHENANTRENE-10-OXIDE AS A SUBSTITUENT: HOMOPOLYMERIZATION AND COPOLYMERIZATION WITH DIGLYCIDYL ETHER OF BISPHENOL A

J. Canadell, A. Mantecón, V. Cádiz

Departament de Química Analítica i Química Orgànica. Universitat Rovira i Virgili.  
Marcel·lí Domingo s/n, 43007 Tarragona, Spain

---

### Abstract

A new bis-spiroorthoester-containing monomer, bis[(1,4,6-trioxaspiro [4,4] nonan-2-yl)-methyl] 2-[10-(9,10-dihydro-9-oxa-10-phosphaphenantrene-10-oxide-10-yl)] maleate (SOE-DOPOMA), was synthesized with good yields by an esterification reaction with a hydroxylated spiroorthoester (2-hydroxymethyl-1,4,6-trioxaspiro-[4,4]-nonane) and a phosphorus-containing diacid (2-[10-(9,10-dihydro-9-oxa-10-phosphaphenantrene-10-oxide-10-yl)] maleic acid), both of which were previously synthesized. SOE-DOPOMA was characterized with  $^1\text{H}$ ,  $^{13}\text{C}$ , and  $^{31}\text{P}$  NMR spectroscopy. This new spiroorthoester was crosslinked with ytterbium triflate as a cationic initiator. A mixture of SOE-DOPOMA and diglycidyl ether of bisphenol A was also crosslinked under the same conditions. The curing was studied with differential scanning calorimetry and monitored with Fourier transform infrared spectroscopy. The materials were characterized with differential scanning calorimetry, thermogravimetric analysis, and thermodynamomechanical analysis. The shrinkage effect on cationic crosslinking was assessed with gas pycnometry, and the flame retardant properties were determined with limiting oxygen index measurements.

**Keywords:** cationic polymerization; curing of polymers; epoxy resins; flame retardancy; ring opening

---

## INTRODUCTION

Epoxy networks are very versatile materials that can be used in a wide number of applications. Each application has some requirements that include a combination of physical, mechanical, and other specific properties. In many industrial applications such as industrial casting, coatings, and microelectronics, shrinkage during curing is a major problem because it leads to poor adhesion to the substrate, delamination, and microvoids and microcracks, which reduce the durability of the material.<sup>1</sup> Another disadvantage of epoxy resins is that they are more flammable than similar thermosets, because they have a reduced tendency to carbonize. To reduce this flammability, both halogenated and inorganic flame retardants have been used.<sup>2</sup> The generation and release of toxic, corrosive, and halogenated gases in the combustion of polymers when halogen flame retardants are used might be avoided with a halogen-free flame retardant in polymeric materials. Therefore, phosphorus-containing polymers, which have been reported to have great flame retardancy, have been widely investigated in recent years.<sup>3</sup> Polymerization with phosphorus monomers and polymer

modification with phosphorus compounds have both been used to obtain phosphorus-containing polymers, the former method having the advantages of convenience in molecular design, synthesis diversity, and polymer property modulation, which can allow the modification of various properties simultaneously.

The goal of this work is to develop a new phosphorus-containing monomer bearing spiroorthoester (SOE) groups. SOEs are considered *expanding monomers*,<sup>1</sup> a term that refers to monomers that lead to zero shrinkage or even positive expansion during polymerization. Some kinds of cyclic monomers have been reported to maintain their volume or actually expand during double ring-opening polymerization.<sup>4-6</sup> SOEs can be synthesized from epoxides and lactones<sup>7,8</sup> and undergo cationic ring-opening polymerization by Lewis acid catalysts. Moreover, SOEs can copolymerize with epoxides and therefore can be used to modify epoxy resins, reducing their shrinkage during curing, which leads to significant change in the volume.

In a previous work,<sup>9</sup> we synthesized a phosphorus-containing SOE from 9,10-dihydro-9-oxa-10-phosphaphenanthrene-10-oxide (DOPO), which was

homopolymerized and copolymerized with phenyl glycidyl ether, using as a cationic initiator ytterbium triflate, a Lewis acid, that can cure epoxy resins.<sup>10,11</sup> Lanthanide triflates are commercially available and have many advantages over  $\text{BF}_3$  derivatives and alkylating agents because they maintain their catalytic activity even in the presence of water.<sup>12</sup>

In this work, we synthesized a bis-spiroorthoester (bis-SOE) monomer from DOPO: bis[(1,4,6-trioxaspiro[4,4]-nonan-2-yl)-methyl] 2-[10-(9,10-dihydro-9-oxa-10-phosphaphenan-trene-10-oxide-10-yl)] maleate (SOE-DOPOMA). DOPO with an active hydrogen can react with electron-deficient compounds such as maleic acid<sup>13</sup> and subsequently with a hydroxylic compound bearing an SOE moiety. The incorporation of the rigid and bulky phosphorus-containing DOPO confers good flame-retardant properties to materials. This approach allows both flame retardancy and expanding properties in the bis-SOE monomer, which can be crosslinked by a double ring-opening using ytterbium triflate as cationic initiator. This bis-SOE was also copolymerized with diglycidylether of bisphenol A (DGEBA) to obtain modified epoxy resins with lower shrinkage and flame-retardant properties than conventional epoxy resins.

The curing was studied with differential scanning calorimetry

(DSC) and Fourier transform infrared (FTIR) spectroscopy. The materials were characterized with DSC, thermo-gravimetric analysis (TGA), and thermodynamomechanical analysis (DMTA). The shrinkage effects during the cationic crosslinking were assessed with gas pycnometry. The flame-retardant properties were determined with limiting oxygen index (LOI) measurements.

## EXPERIMENTAL

### Materials

Commercial DOPO was kindly supplied by Aismalibar and purified before use via heating at 130 °C in vacuo for 2 h and then gradual heating to 150 °C. The purified product was cooled to room temperature under an argon atmosphere. Maleic acid (Merck); epibromo-hydrin (Fluka); glycidol (Aldrich);  $\gamma$ -butirolactone ( $\gamma$ -BL; Aldrich), boron trifluoride diethyl etherate ( $\text{BF}_3 \cdot \text{OEt}_2$ ; Aldrich), triethylamine (Fluka), 1,8-diazabicyclo[5.4.0]-undec-7-en (DBU; Aldrich), N-(3-dimethylaminopropyl)-N'-ethyl-carbodiimide hydrochloride (EDC; Fluka), 4-(dimethylamino)pyridine (DMAP; Fluka), DGEBA (Epikote Resin 827, Shell Chemicals; epoxy equivalent = 182.08 g/equiv), ytterbium(III) trifluoromethanesulfonate [ $\text{Yb}(\text{OTf})_3$ ; Aldrich] were used as received. All solvents were purified by standard procedures.

### Instrumentation

The microwave-irradiated reaction was carried out in a 10-mL reactor vial with a CEM Discover monomodal microwave reactor and an IR temperature sensor at a maximum power of 300 W.

NMR spectra ( $^1\text{H}$ , 400 MHz;  $^{13}\text{C}$ , 100.6 MHz; and  $^{31}\text{P}$ , 161.9 MHz) were obtained with a Varian Gemini 400 spectrometer with Fourier transform,  $\text{CDCl}_3$  or DMSO as the solvent, and with tetramethylsilane or phosphoric acid as the internal standard.

Calorimetric studies (DSC) were carried out on a Mettler DSC-821e thermal analyzer in covered Al pans under  $\text{N}_2$  at scanning rates of 10  $^\circ\text{C}/\text{min}$  in the first scan and 20  $^\circ\text{C}/\text{min}$  in the second. The samples weighed approximately 8 mg.

The isothermal crosslinking process at 120  $^\circ\text{C}$  was monitored with a 680 Plus FTIR spectrophotometer with a resolution of 4  $\text{cm}^{-1}$  in the absorbance mode. An attenuated total reflection (ATR) accessory with a thermal control and a diamond crystal was used to determine the FTIR/ATR spectra.

TGAs were carried out with a Mettler TGA/SDTA 851e thermobalance. Cured samples with an approximate mass of 10 mg were degraded between 30 and 800  $^\circ\text{C}$  at a heating rate of 10  $^\circ\text{C}/\text{min}$  in an atmosphere of  $\text{N}_2$  or air.

DMTA were carried out with TA DMA 2928 working with a three-point bending clamp from 30 to 200  $^\circ\text{C}$  at a heating rate of 3  $^\circ\text{C}/\text{min}$ .

The densities of the materials were measured with a Micromeritics Accupyc 1330 TC gas pycnometer at 30  $^\circ\text{C}$ .

LOIs were measured on a Fire Testing Technology flammability unit in conformance with ASTM D 2863 on samples measuring 100 mm x 6 mm x 3 mm.

### Synthesis of 2-bromomethyl-1,4,6-trioxaspiro [4,4] nonane (SOE-Br)

Epibromohydrin (50 g, 0.36 mol) was added dropwise over a period of 15 min at a temperature below 10  $^\circ\text{C}$  in an argon atmosphere to a mixture of 180 g (2.09 mol) of  $\gamma$ -BL and 1.5 mL (11.8 mmol) of  $\text{BF}_3 \cdot \text{OEt}_2$  as a catalyst. After the addition was completed, the mixture was stirred for 60 min at the same temperature. The reaction was quenched by the addition of 1.9 mL (13.5 mmol) of triethylamine. After the solvent was removed under reduced pressure, the residue was distilled fractionally to yield 60.4 g (74 %) of a transparent, colorless liquid.

$^1\text{H}$  NMR ( $\text{CDCl}_3$ , two diastereomers):  $\delta(\text{ppm}) = 4.54\text{--}4.48$  (m, 1H, -O-CH-), 4.43-4.37 (m, 1H, -O-CH-), 4.21-4.17 (dd, 2H, -O-CH<sub>2</sub>-), 3.98-3.87 (m, 6H, -O-CH<sub>2</sub>-), 3.91-3.31 (m, 4H, Br-CH<sub>2</sub>-), 2.20-2.11

(m, 4H, -CH<sub>2</sub>-), 2.05-1.98 (m, 4H, -CH<sub>2</sub>-).

<sup>13</sup>C NMR (CDCl<sub>3</sub>, two diastereomers): δ(ppm) = 129.98 (s, spiranic C), 129.88 (s, spiranic C), 75.48 (s, -O-CH-), 74.74 (s, -O-CH-), 68.72 (s, -O-CH<sub>2</sub>-), 67.68 (s, -O-CH<sub>2</sub>-), 67.40 (s, -O-CH<sub>2</sub>-), 67.38 (s, -O-CH<sub>2</sub>-), 32.87 (s, -CH<sub>2</sub>-), 32.81 (s, -CH<sub>2</sub>-), 32.74 (s, Br-CH<sub>2</sub>-), 32.28 (s, Br-CH<sub>2</sub>-), 24.20 (s, -CH<sub>2</sub>-), 24.05 (s, -CH<sub>2</sub>-).

#### **Synthesis of 2-hydroxymethyl-1,4,6-trioxaspiro [4,4] nonane (SOE-OH)**

Glycidol (30 g, 0.40 mol) was added dropwise over a period of 15 min at a temperature below 10 °C in an argon atmosphere to a mixture of 200 g (2.3 mol) of  $\gamma$ -BL and 1.0 mL (7.9 mmol) of BF<sub>3</sub>·OEt<sub>2</sub> as a catalyst. After the addition was completed, the mixture was stirred for 60 min at the same temperature. The reaction was quenched by the addition of 1.4 mL (10 mmol) of triethylamine. After the solvent was removed under reduced pressure, the residue was distilled fractionally to yield 11.2 g (17%) of a transparent, colorless liquid.

<sup>1</sup>H NMR (CDCl<sub>3</sub>, two diastereomers): δ(ppm) = 4.41-4.32 (m, 2H, -O-CH-), 4.14-4.03 (m, 2H, -O-CH<sub>2</sub>-), 3.99-3.89 (m, 4H, -O-CH<sub>2</sub>-), 3.85-3.80 (m, 2H, -O-CH<sub>2</sub>-), 3.73-3.54 (m, 4H, -CH<sub>2</sub>-OH), 2.89 (br, 2H, OH), 2.18-2.12 (m, 4H, -CH<sub>2</sub>-), 2.05-1.97 (m, 4H, -CH<sub>2</sub>-).

<sup>13</sup>C NMR (CDCl<sub>3</sub>, two diastereomers): δ(ppm) = 129.60 (s, spiranic C), 129.32 (s, spiranic C), 75.99 (s, -O-CH-), 67.42 (s, -O-CH<sub>2</sub>-), 65.69 (s, HO-CH<sub>2</sub>-), 64.92 (s, HO-CH<sub>2</sub>-), 62.81 (s, -O-CH<sub>2</sub>-), 62.54 (s, -O-CH<sub>2</sub>-), 32.67 (s, -CH<sub>2</sub>-), 32.50 (s, -CH<sub>2</sub>-), 24.51 (s, -CH<sub>2</sub>-), 24.35 (s, -CH<sub>2</sub>-).

#### **Synthesis of 2-[10-(9,10-dihydro-9-oxa-10-phosphaphenanthrene-10-oxi-de-10-yl)] Maleic Acid (DOPOMA)**

Into a 250-mL, round-bottom flask equipped with a condenser, 20 g (92.5 mmol) of DOPO, 30 mL of xylene, and 30 mL of THF were introduced. The flask was heated to 80 °C under an argon atmosphere with vigorous stirring. After the complete dissolution of DOPO, 10.74 g (92.5 mmol) of maleic acid was added for 1 h, and the reaction mixture was maintained at that temperature for 20 h. After cooling to room temperature, the reaction product was filtered, washed with a mixture of xylene and THF (1/1) three times, and then dried in an oven at 120 °C to yield 24.7 g (80%) of a white powder (mp = 222 °C, DSC).

<sup>1</sup>H NMR (DMSO, two diastereomers): δ(ppm) = 12.63 (br, 4H, -OH), 8.24-8.15 (m, 4H, Ar-H), 8.05-7.79 (m, 4H, Ar-H), 7.65-7.59 (m, 2H, Ar-H), 7.47-7.44 (m, 2H, Ar-H), 7.34-7.24 (m, 4H, Ar-H), 3.72-3.64 (m, 1H, -CH-), 3.52-3.43 (m,

1H, -CH-), 2.92-2.82 (m, 2H, -CH<sub>2</sub>-), 2.70-2.61 (m, 2H, -CH<sub>2</sub>-).

<sup>13</sup>C NMR (DMSO, two diastereomers): δ(ppm) = 172.06 (d, J<sub>C-P</sub> = 18.3 Hz, C=O), 171.89 (d, J<sub>C-P</sub> = 18.3 Hz, C=O), 168.62 (d, J<sub>C-P</sub> = 4.6 Hz, C=O), 148.74 (d, J<sub>C-P</sub> = 8.3 Hz, Ar-C), 135.21 (d, J<sub>C-P</sub> = 6.1 Hz, Ar-C), 134.29 (s, Ar-CH), 134.12 (s, Ar-CH), 131.25 (s, Ar-CH), 131.13 (d, J<sub>C-P</sub> = 10.7 Hz, Ar-CH), 128.85 (d, J<sub>C-P</sub> = 13.9 Hz, Ar-CH), 125.93 (s, Ar-CH), 125.78 (s, Ar-CH), 125.28 (s, Ar-CH), 125.08 (s, Ar-CH), 124.42 (d, J<sub>C-P</sub> = 9.9 Hz, Ar-CH), 124.28 (d, J<sub>C-P</sub> = 9.9 Hz, Ar-CH), 122.71 (d, J<sub>C-P</sub> = 124.3 Hz, Ar-C), 122.62 (d, J<sub>C-P</sub> = 124.5 Hz, Ar-C), 121.68 (d, J<sub>C-P</sub> = 10.8 Hz, Ar-C), 121.37 (d, J<sub>C-P</sub> = 10.6 Hz, Ar-C), 120.28 (d, J<sub>C-P</sub> = 6.1 Hz, Ar-CH), 120.21 (d, J<sub>C-P</sub> = 6.1 Hz, Ar-CH), 43.82 (d, J<sub>C-P</sub> = 83.9 Hz, -CH-), 42.97 (d, J<sub>C-P</sub> = 86.2 Hz, -CH-), 30.13 (d, J<sub>C-P</sub> = 22.1 Hz, -CH<sub>2</sub>-).

<sup>31</sup>P NMR (DMSO, two diastereomers): δ(ppm) = 31.25 (s); 30.72 (s)

### Synthesis of SOE-DOPOMA

#### Way A

**Conventional Heating.** Into a three-necked, 100 mL, round-bottom flask equipped with an argon inlet, a condenser and a magnetic stirrer, 0.5 g (1.5 mmol) of DOPOMA was dissolved in 10 mL of anhydrous DMSO. After the complete dissolution, 0.45 mL (3.0 mmol) of

DBU was added. The brown solution was heated to 50 °C; then 0.67 g (3.0 mmol) of SOE-Br with 10 mL of DMSO was added slowly. After the complete addition of SOE-Br, the reaction mixture was maintained at that temperature for 12 h to ensure completion of the reaction. After it cooled at room temperature, water was added, and then the product was obtained by several extractions with CH<sub>2</sub>Cl<sub>2</sub> (4 x 30 mL). The product was purified by several washes with dilute solution of HCl and then was neutralized with a solution of NaOH. The dichloromethane solution was dried over MgSO<sub>4</sub> and the solvent was evaporated to yield a brown, viscous oil that was a complex mixture where (1,4,6-trioxaspiro[4,4]nonan-2-yl)-methyl 3-[10-(9,10-dihydro-9-oxa-9-phosphaphenanthrene-10-oxide-10-yl)]-propanoate (SOE-P) was detected.

**Microwave irradiation.** In a microwave reactor vial (10 mL) equipped with a magnetic stirring bar, 0.1 g (0.3 mmol) of DOPOMA was dissolved in 1.5 mL of anhydrous DMSO. After the complete dissolution, 90 μL (0.6 mmol) of DBU and 0.135 g (0.6 mmol) of SOE-Br were added. The vial was purged with argon.

The maximum power setting of 50 W was maintained until the desired temperature (130 °C) was reached (160 s). The power was reduced to 27 W for the remainder of the reaction time to maintain 130 °C.

After 60 min, the reaction mixture was cooled to room temperature. The purification was performed in the same way that in conventional heating to yield a yellowish, viscous oil that corresponds to SOE-P.

Other microwave assays were performed with a similar procedure at different temperatures: 100 °C (12 W), 80 °C (8 W) and 65 °C (5 W) leading in all cases to the same result.

### Way B

Under an argon atmosphere, an oven-dried 100 mL, round-bottom flask containing 20 mL of anhydrous dichloromethane was charged with 0.50 g (1.5 mmol) of DOPOMA, 0.53 g (3.3 mmol) of SOE-OH, 0.60 g (3.1 mmol) of EDC, and 0.38 g (3.1 mmol) of DMAP. The brown solution was stirred and heated at 40 °C for 4 h. After cooling to room temperature, the solution was washed with two 30-mL portions of a 10% citric acid solution, twice with 30-mL portions of a 10% sodium bicarbonate solution, and twice with brine. The organic solution was dried over anhydrous magnesium sulfate, and the solvent was removed by evaporation to give 0.66 g (71%) of a white solid (mp= 58-60 °C).

<sup>1</sup>H NMR (CDCl<sub>3</sub>, diastereomers mixture): δ(ppm) = 7.98-7.87 (m, 3H, Ar-H); 7.74 (m, 1H, Ar-H); 7.55

(m, 1H, Ar-H); 7.38 (m, 1H, Ar-H); 7.27-7.22 (m, 2H, Ar-H); 4.42-3.17 (m, 15H, -O-CH-, -COO-CH<sub>2</sub>-, -O-CH<sub>2</sub>-, -P-CH-); 2.99-2.95 (m, 2H, CH<sub>2</sub>-CO-); 2.93-1.60 (m, 8H, -CH<sub>2</sub>-).

Table 1. Compositions (wt % P), DSC Data, and Curing Conditions of the

Assay	Sample	P	$\Delta H$ (J/g) <sup>a</sup>	$\Delta H$ (KJ/ee) <sup>b</sup>	$T_{max}$ (°C) <sup>d</sup>	Tg (°C)	Curing Conditions			
							Temperature (°C)		Time (h)	
1	SOE-DOPOMA	5.0	31.1	9.7 <sup>c</sup>	207	94	180		5	
2	DGEBA/SOE-DOPOMA	2.7	141.7	106.0	165/184	103	140	160	3	2
3	DGEBA	Enthalpies per gram of mixture.			215	130	150		5	

<sup>a</sup> Enthalpies expressed by equivalent epoxy.  
<sup>b</sup> Enthalpy expressed by equivalent SOE.  
<sup>c</sup> Enthalpy expressed by equivalent SOE.  
<sup>d</sup> Temperature of the maximum heat release rate.

<sup>13</sup>C NMR (CDCl<sub>3</sub>, diastereomers mixture): δ(ppm) = 170.82 (d, J<sub>C-P</sub> = 17.68 Hz, -C=O); 170.77 (d, J<sub>C-P</sub> = 17.50 Hz, C=O), 170.48 (d, J<sub>C-P</sub> = 16.80 Hz, C=O); 170.65 (d, J<sub>C-P</sub> = 17.50 Hz, C=O); 170.60 (d, J<sub>C-P</sub> = 16.80 Hz, C=O); 170.54 (d, J<sub>C-P</sub> = 16.80 Hz, C=O); 167.29 (br, C=O); 167.00 (d, J<sub>C-P</sub> = 4.12 Hz, C=O); 166.97 (d, J<sub>C-P</sub> = 4.12 Hz, C=O), 149.06 (d, J<sub>C-P</sub> = 9.15 Hz, Ar-C); 136.11 (d, J<sub>C-P</sub> = 6.13 Hz, Ar-C); 134.19 (br, Ar-CH); 131.36 (br, Ar-CH); 131.97 (br, Ar-CH); 129.79 (s, spiranic C); 129.67 (s, spiranic C); 129.61 (s, spiranic C); 129.49 (s, spiranic C); 128.68 (d, J<sub>C-P</sub> = 13.78 Hz, Ar-CH); 125.16 (s, Ar-CH); 125.06 (s, Ar-CH); 123.81 (s, Ar-CH); 122.56 (br, Ar-CH-); 121.51 (d, J<sub>C-P</sub> = 125.07 Hz, Ar-C); 121.43 (d, J<sub>C-P</sub> = 125.67 Hz, Ar-C); 121.34 (d, J<sub>C-P</sub> = 10.70 Hz, Ar-C); 120.48 (d,

$J_{C-P} = 6.23$  Hz, Ar-CH); 120.24 (d,  $J_{C-P} = 6.33$  Hz, Ar-CH); 73.83 (s, -O-CH-); 73.17 (s, -O-CH-); 73.11 (s, -O-CH-); 73.00 (s, -O-CH-); 72.96 (s, -O-CH-); 72.48 (s, -O-CH-); 67.34 (s, -O-CH<sub>2</sub>-); 67.28 (s, -O-CH<sub>2</sub>-); 67.18 (s, -O-CH<sub>2</sub>-); 66.48 (s, -O-CH<sub>2</sub>-); 66.38 (s, -O-CH<sub>2</sub>-); 66.18 (s, -O-CH<sub>2</sub>-); 66.13 (s, -O-CH<sub>2</sub>-); 65.78 (s, -O-CH<sub>2</sub>-); 65.62 (s, -O-CH<sub>2</sub>-); 65.04 (s, -COO-CH<sub>2</sub>-); 64.89 (s, -COO-CH<sub>2</sub>-); 44.49 (d,  $J_{C-P} = 85.53$  Hz, -P-CH-); 44.45 (d,  $J_{C-P} = 85.12$  Hz, -P-CH-); 44.41 (d,  $J_{C-P} = 86.94$  Hz, -P-CH-); 43.48 (d,  $J_{C-P} = 87.04$  Hz, -P-CH-); 32.61 (s, -CH<sub>2</sub>-); 30.39 (br, -CH<sub>2</sub>-CO-); 29.85 (br, -CH<sub>2</sub>-COO-); 24.19 (s, -CH<sub>2</sub>-); 24.26 (s, -CH<sub>2</sub>-); 24.01 (s, -CH<sub>2</sub>-).

<sup>31</sup>P NMR (CDCl<sub>3</sub>, diastereomers mixture):  
 $\delta$ (ppm) = 29.68 (s); 29.66 (s); 29.53 (s); 29.50 (s); 29.48 (s); 29.47 (s); 29.43 (s); 29.41 (s); 29.35 (s); 29.31 (s); 29.28 (s); 29.26 (s); 29.23 (s); 29.18 (s); 29.12 (s); 29.01 (s).

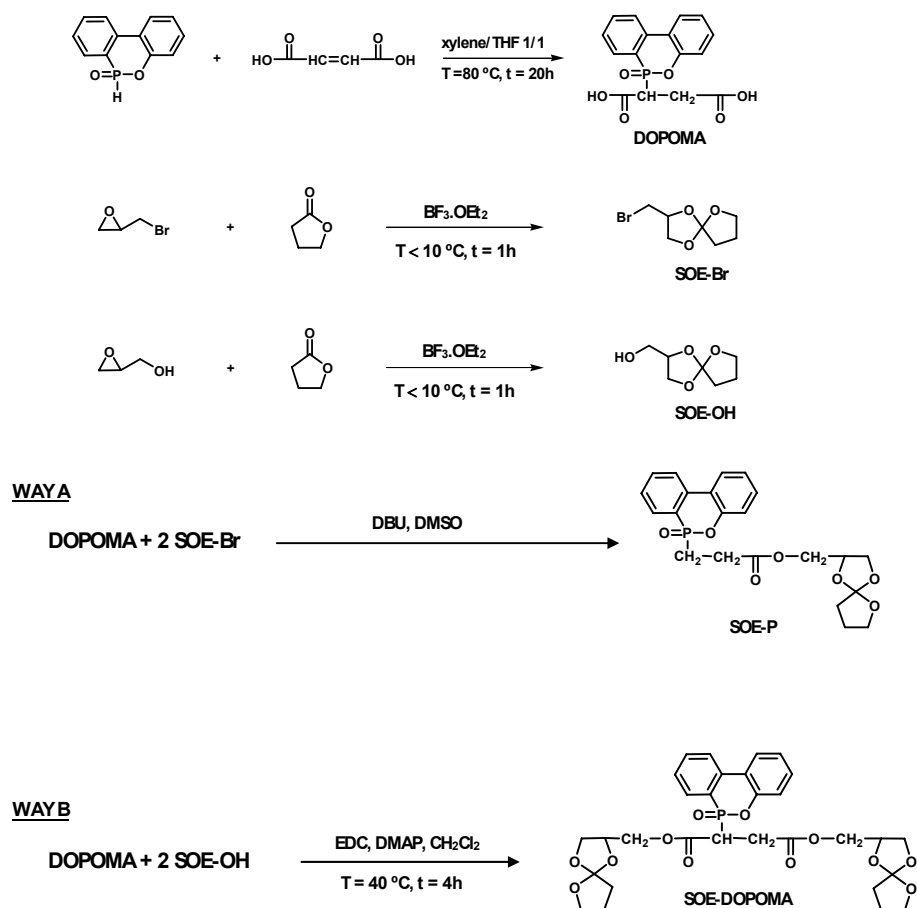
### Crosslinking Reaction

The cationic crosslinking reactions were carried out through the mixing of the corresponding monomers with 1.5 phr ytterbium triflate (1 phr = 1 part per 100 parts of

the monomer mixture weight/weight). The molar ratio used in the copolymerization of DGEBA and SOE-DOPOMA was 2:1. The sample bars used for dynamo-mechanical analysis, TGA, and burn tests were cured in aluminium molds by heating in an oven. The curing conditions were determined from DSC data and are listed in Table 1.

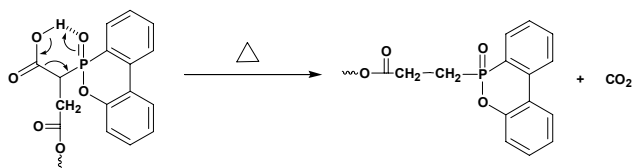
### RESULTS AND DISCUSSION

The synthesis of SOE-DOPOMA was carried out with the two



synthetic pathways shown in Scheme 1. First, we synthesized the substituted maleic acid, DOPOMA, as previously described.<sup>13</sup> This synthetic step consisted of the incorporation of DOPO by means of a conjugated addition reaction to the  $\alpha,\beta$ -unsaturated dicarboxylic acid. When DOPO reacts with a double-bond-containing compound, the structures of the double-bond-containing compounds have a significant influence on the reaction rate. For example, when DOPO reacts with a compound with only one electron-withdrawing carbonyl group next to the double bond, such as itaconic acid, the reaction is very slow, even at 140 °C,<sup>13</sup> whereas the reaction with two electron-

of DBU in DMSO at different temperatures under an argon atmosphere (way A). Direct ester formation from a primary halide and a carboxylic acid using DBU is a useful method that has been used by several authors.<sup>15,16</sup> This method also leads to good results in polymer modification.<sup>17-19</sup> However, in this case, after 12 h of reaction, we obtained a complex mixture which SOE-P was detected. The presence of this compound could be confirmed by <sup>1</sup>H, <sup>13</sup>C, and <sup>31</sup>P NMR spectra.<sup>9</sup> The formation of SOE-P can be explained by a thermal decarboxylation reaction similar to  $\beta$ -keto acid decarboxylations, as shown in Scheme 2. This decarboxylation takes place in the



Scheme 2

withdrawing carbonyl groups next to the double bond, such as maleic acid or benzoquinone,<sup>14</sup> occurs at about 70-90 °C. The second intermediate synthesized was SOE-Br. This compound was prepared from epibromohydrin and  $\gamma$ -BL<sup>15</sup> with  $\text{BF}_3 \cdot \text{OEt}_2$  as a catalyst, and its structure was confirmed by spectroscopic experiments. The reaction of SOE-Br with DOPOMA to obtain SOE-DOPOMA was initially carried out in the presence

monosubstituted compound in C-1 because the other possible product of monosubstitution (in C-4) cannot undergo thermal  $\beta$ -decarboxylation.

One way to avoid this and other undesirable transformations of the organophosphorus compounds is to reduce the reaction time. One promising approach to reducing the reaction time is the application of microwaves energy. Microwave irradiation offers a number of advantages over conventional hea-

ting, such as noncontact heating, which for many organophosphorus compounds is very important, and rapid and highly specific heating.<sup>20,21</sup>

Thus, the reaction was carried out in a microwave reactor with anhydrous DMSO as solvent and DBU as a catalyst. Initially, a power of 27 W at 130 °C was applied. After 1 h of reaction and further purification, an oil was obtained, which was identified as SOE-P by NMR spectroscopy. To avoid this undesired reaction, lower temperatures: 100 °C (12W), 80 °C

(8W) and 65 °C (5W) were tested. In this way, SOE-DOPOMA was obtained but always together with SOE-P.

To improve these results, another synthetic way was followed. Pathway B uses the esterification reaction of DOPOMA with SOE-OH in the presence of EDC and DMAP.<sup>22</sup> We use water soluble EDC as an alternative to dicyclohexylcarbodiimide because its

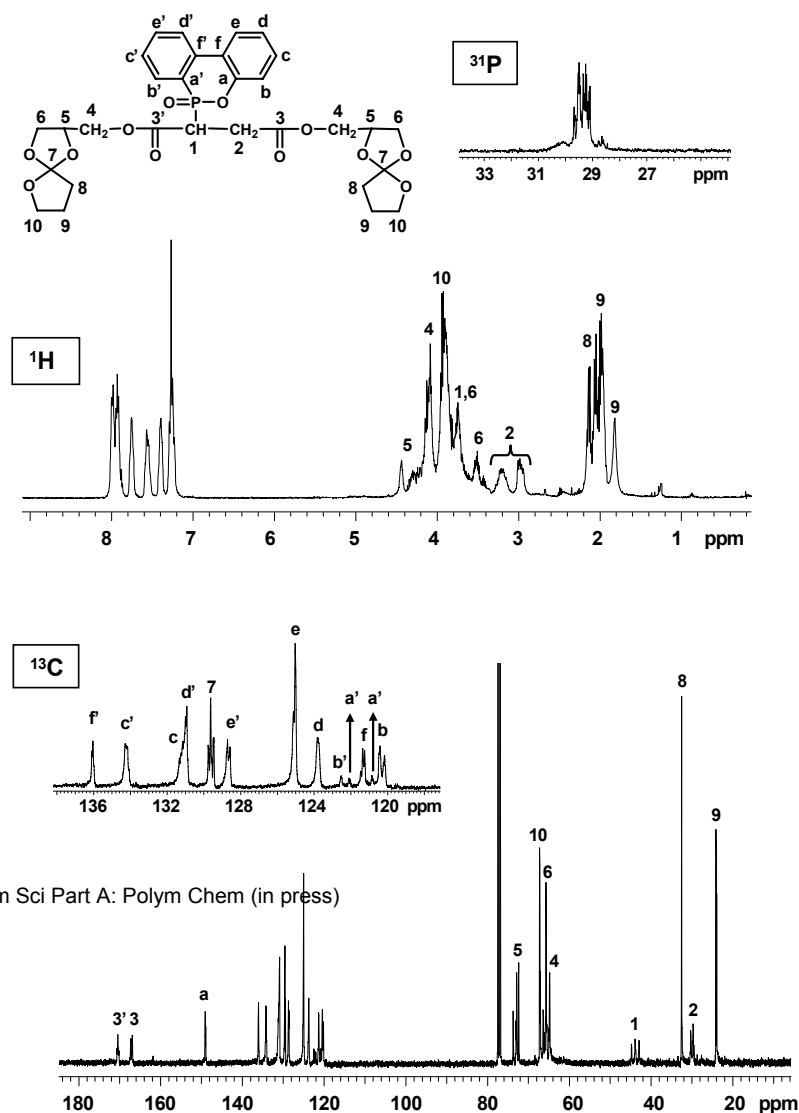


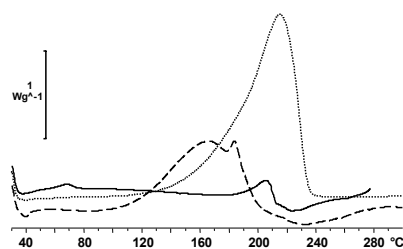
Figure 1. <sup>31</sup>P, <sup>1</sup>H, and <sup>13</sup>C NMR spectra of SOE-DOPOMA.

elimination was easier and we obtained better yields. SOE-OH was synthesized from  $\gamma$ -BL and glycidol by a procedure similar to that described by Nishida et al.<sup>6</sup> for other hydroxylic SOEs. By this procedure, a solid product was obtained with a good yield.

This novel phosphorus-containing bifunctional SOE, SOE-DOPOMA, was characterized by  $^1\text{H}$ ,  $^{13}\text{C}$ , and  $^{31}\text{P}$  NMR spectroscopy. Because of the several chiral centers in the molecule, a mixture of diastereomers was formed. Figure 1 shows the  $^{31}\text{P}$ ,  $^1\text{H}$ , and  $^{13}\text{C}$  NMR spectra, with all assignments. The single  $^{31}\text{P}$  signal is split because of the presence of the different diastereomers. In  $^1\text{H}$  and  $^{13}\text{C}$  NMR spectra, some signals are also split for the same reason. The SOE ring and aromatic protons and carbon signals could be assigned unequivocally by means of gHSQC and COSY experiments and by comparison with the DOPOMA and SOE-P spectra.<sup>9</sup> Although the two SOEs and the methylene directly attached to them are nonequivalent, their signals in both  $^1\text{H}$ ,  $^{13}\text{C}$  spectra are not different. However, carbonylic carbons appear as two different signals.

As we previously mentioned, we are interested in using this phosphorus-containing monomer to modify epoxy resins. In the cationic copolymerization of DGEBA and

SOE-DOPOMA, three simultaneous processes are expected (Scheme 3): (a) the reaction of SOE with epoxy groups, (b) the homopolymerization of SOE, and (c) the homopolymerization of epoxy groups. Processes a and b lead to the formation of linear ether-ester moieties, whereas reaction c leads only to ether linkages. The homo-polymerization of SOE-DOPOMA and its copolymerization with DGEBA were carried out with 1.5 phr ytterbium triflate as a cationic initiator. Figure 2 shows the dynamic DSC plots of these reactions. For comparison, the corresponding DGEBA curve is also included in the figure. The enthalpy of the SOE-DOPOMA homopolymerization is very low, corresponding to the ring opening of a nontensionated spiroorthoester.<sup>23</sup> The maximum of the exotherm of both homopolymerizations (SOE-DOPOMA and DGEBA) appears at a higher temperature than that of the copolymerization. However, this copolymerization shows two maxima, indicating that more than one process occurs. From these dynamic experiments, the

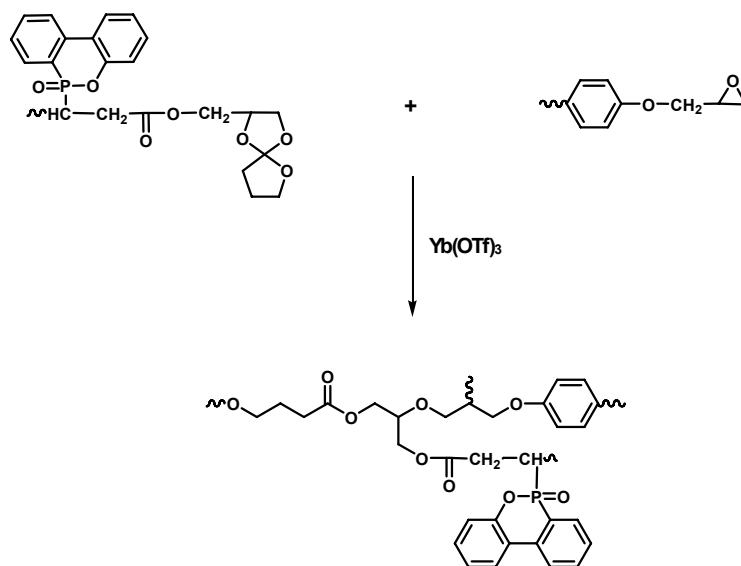


**Figure 2.** Dynamic DSC plots of (—) SOE-DOPOMA; (---) 2/1 (mol/mol) DGEBA/SOE-DOPOMA; (.....) DGEBA initiated by 1.5 phr  $\text{Yb}(\text{OTf})_3$  obtained at a 10 °C/min heating rate  
J Polym Sci Part A: Polym Chem (in press)

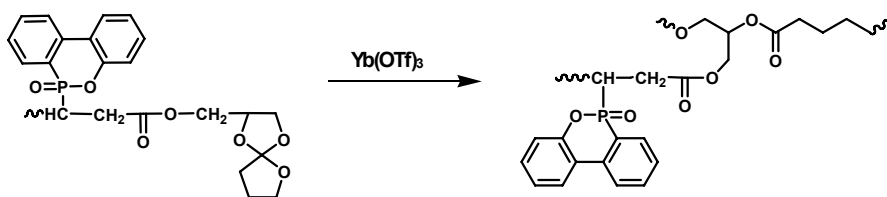
isothermal curing conditions were established. For the copolymerization of 2/1 (mol/mol) DGEBA/SOE-DOPOMA mix-ture,

the curing conditions were 140 °C for 3 h and then 160 °C for 2 h. The

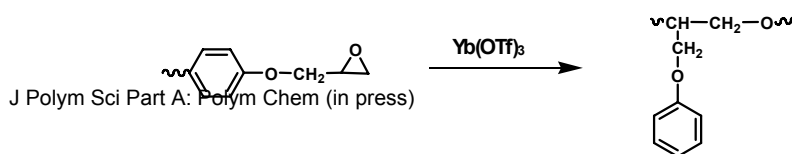
a) Reaction of SOE-DOPOMA with DGEBA



b) Homopolymerization of SOE-DOPOMA

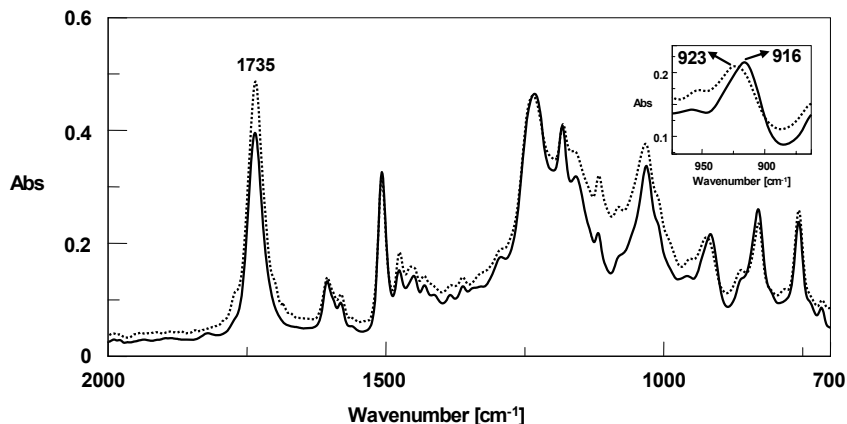


c) Homopolymerization of DGEBA



J Polym Sci Part A: Polym Chem (in press)

Scheme 3



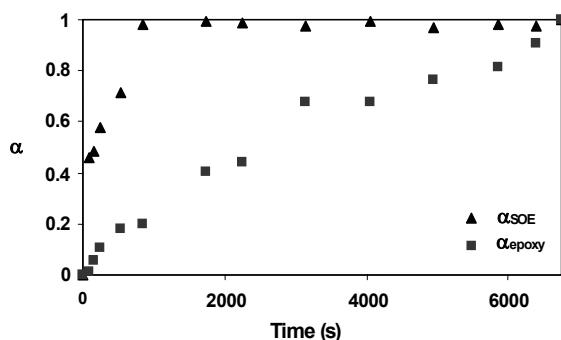
**Figure 3.** FTIR spectra of 2/1 (mol/mol) DGEBA/SOE-DOPOMA with 1.5 phr  $\text{Yb}(\text{OTf})_3$  before (—) and after (.....) polymerization at 120 °C.

enthalpy values, temperatures of the maximum of the exotherms, phosphorus contents, and curing conditions are collected in Table 1. A dynamic run for the cured samples allowed us to calculate the glass transition temperature ( $T_g$ ) values (Table 1). The copolymer  $T_g$  is between the  $T_g$  values of the two homo-polymers.

The copolymerization reaction was monitored by FTIR-ATR spectroscopy in isothermal experiments at 120 °C. This technique allowed us to follow the evolution of the groups involved in the process by means of the variations in the corresponding absorptions. Figure 3 shows the FTIR spectra of the DGEBA/SOE-DOPOMA mixture with 1.5 phr  $\text{Yb}(\text{OTf})_3$  before and after polymerization. The double ring-opening of SOE that took place during the polymerization led to a

linear poly(ether-ester) group formation; thus, a typical band of carbonyl ester group must appear<sup>24</sup> around 1735-1750  $\text{cm}^{-1}$ . SOE-DOPOMA contains ester groups that appear at 1735  $\text{cm}^{-1}$  in the initial spectrum, and therefore in this zone only an increase in this band was observed upon polymerization. Unfortunately, the disappearance of the typical epoxy band at 916  $\text{cm}^{-1}$  could not be confirmed by FTIR because the initial SOE presented absorptions in the same zone. Therefore, we confirmed the total epoxy reaction by DSC. A dynamic scan of the sample cured in FTIR did not show any residual enthalpy.

To study the different processes that occur during crosslinking, we calculated the conversion of SOE groups by calculating the increase of the band at 1735  $\text{cm}^{-1}$ . The band at 916  $\text{cm}^{-1}$



**Figure 4.**  $\alpha_{SOE}$  and  $\alpha_{epoxy}$  versus time for the 2/1 (mol/mol) DGEBA/SOE-DOPOMA reaction system with 1.5 phr  $Yb(OTf)_3$  cured in an FTIR spectrometer at 120 °C.

overlaps the band associated with the O-P-Ph moiety of SOE-DOPOMA, which appears at about  $920\text{ cm}^{-1}$ .<sup>25</sup> As the intensity of this band must not change during the reaction, the diminution observed in this zone during the crosslinking may be attributed to the reaction of the epoxy groups. Therefore, the conversion of the epoxy group was calculated by this difference. During the crosslinking the maximum of this band was shifted to  $923\text{ cm}^{-1}$ .

The absorbances were calculated in terms of the peak areas. The conversions of the epoxy and SOE groups ( $\alpha_{epoxy}$  and  $\alpha_{SOE}$ , respectively) were determined by the Lambert-Beer law from the normalized changes in the absorbance with respect to the band at  $1507\text{ cm}^{-1}$  corresponding to the phenyl group in DGEBA, and the conversions were calculated with the following equations:

$$\alpha_{SOE} = \left( \frac{\overline{A}_{1735}^t}{\overline{A}_{1735}^\infty} \right)$$

$$\overline{A}_{1735}^t = \frac{A_{1735}^t}{A_{1507}^t} - \frac{A_{1735}^0}{A_{1507}^0} \quad \overline{A}_{1735}^\infty = \frac{A_{1735}^\infty}{A_{1507}^\infty} - \frac{A_{1735}^0}{A_{1507}^0}$$

Figure 4 shows the conversions against the time. As we can see, the SOE group reacts very fast in the beginning of the process up to a conversion of about 0.5 and reaches its maximum conversion below 1000 s. On the other hand,

$$\alpha_{epoxy} = 1 - \left( \frac{\overline{A}_{916}^t}{\overline{A}_{916}^0} \right)$$

$$\overline{A}_{916}^t = \frac{A_{916}^t}{A_{1507}^t} - \frac{A_{923}^\infty}{A_{1507}^\infty} \quad \overline{A}_{916}^0 = \frac{A_{916}^0}{A_{1507}^0} - \frac{A_{923}^\infty}{A_{1507}^\infty}$$

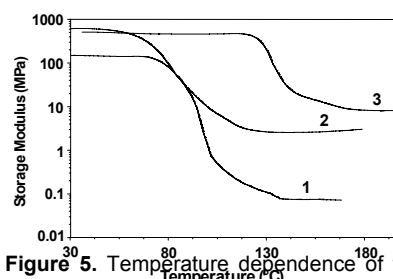
the evolution of epoxy group steadily progresses up to the complete reaction. It must be noted that the epoxy/SOE group ratio is 2:1 in the initial mixture. In the first

stages of the crosslinking, when SOE is present in the mixture reaction, processes a and b in Scheme 3 must be more significant, and then, when SOE is run out, process c predominantly occurs.

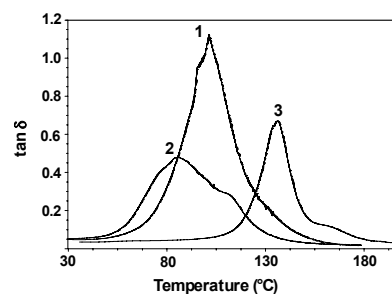
The dynamic mechanical behavior of the crosslinked materials was obtained as a function of the temperature from the glassy state to the rubbery plateau of each material. The crosslinking density of a polymer can be estimated from the plateau of the elastic modulus in the rubbery state.<sup>26</sup> However, this theory is strictly valid only for slightly crosslinked materials and is therefore used only to make qualitative comparisons of the level of crosslinking among the various polymers. As can be seen in Figure 5, the incorporation of SOEs reduces the crosslinking density. Therefore, samples 1 and 2 show a lower storage modulus in the rubbery state. This is due to the greater distance between knots produced by the linear ether-ester moieties introduced in the network by SOEs.

Figure 6 shows  $\tan \delta$  versus temperature for the crosslinked materials. The highest  $T_g$  value corresponds to the more aromatic DGEBA homo-polymer. As the height of the  $\tan \delta$  peak is associated with the crosslinking density, the lowest density of crosslinking corresponds to the SOE-homopolymer. The peak width at half-height broadens as the number of branching modes

increases, and this produces a wider distribution of structures. The copolymer shows a broad curve in which, moreover, it is possible to detect two maxima indicating the non-homogeneity of the material.



**Figure 5.** Temperature dependence of the storage modulus for the cured systems of (1) SOE-DOPOMA, (2) 2/1 (mol/mol) DGEBA/SOE-DOPOMA, and (3) DGEBA.



**Figure 6.** Temperature dependence of  $\tan \delta$  for the cured systems of (1) SOE-DOPOMA, (2) 2/1 (mol/mol) DGEBA/SOE-DOPOMA, and (3) DGEBA.

It has been reported that cationic double ring-opened SOE-based materials exhibit almost no shrinkage and that copolymers having SOE moieties will also crosslink without shrinkage.

Therefore, the volume changes ( $\Delta$ ) in the crosslinking reaction of the copolymers containing SOE moieties were evaluated by density measurements with a Micromeritics gas pycnometer before and after crosslinking (Table 2).  $\Delta$  was calculated from the following equation:

$$\Delta V (\%) = \frac{d_{\text{crosslinked polymer}} - d_{\text{initial mixture}}}{d_{\text{initial mixture}}} \times 100$$

where  $d$  is the density. Thus, negative values indicate expansion.

In SOE-containing samples 1 and 2, the observed values of  $\Delta$  were negative, and therefore the crosslinking process shows an expansion greater for sample 1, which corresponds to pure SOE. Sample 3, corresponding to pure DGEBA, shows the typical volume shrinkage that generally accompanies crosslinking reactions.<sup>27</sup> Therefore, it can be concluded that the SOE moieties are effective monomers to obtain crosslinkable copolymers that do not shrink.

**Table 2.** Volume change upon

Assay	density ( $d^{20}$ , g/cm <sup>3</sup> )		Volume Change (%) <sup>a</sup>
	Mixture	Crosslinked	
1	1.422	1.381	-2.9
2	1.294	1.282	-0.9
3	1.158	1.192	2.9

<sup>a</sup> Calculated with the following equation: Volume change (%) = [(Density of the crosslinked polymer) - (Density of initial mixture)] / (Density of initial mixture) x 100.  
 J. Polym. Sci. Part A: Polym. Chem. (in press)

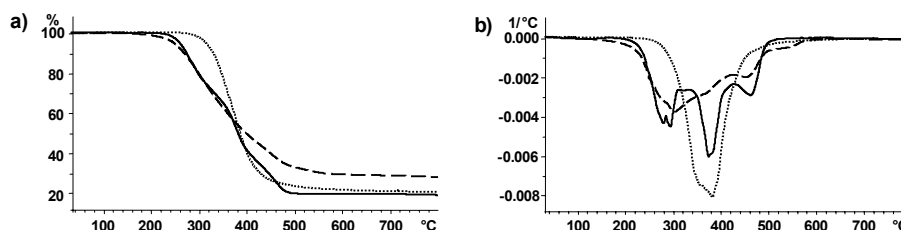
To examine the effect of the phosphorus content on the thermal stability and the decomposition behaviour, TGA data under nitrogen and air atmospheres were determined and analysed. Figures 7 and 8 show the weight loss with the temperature for the three samples as well as the derivative curves under nitrogen and air respectively. Table 3 summarizes the thermogravimetric data.

In both nitrogen and air atmospheres, only the sample of pure DGEBA has a single major break in their decomposition curve, indicating a single decomposition step. However, the other two samples show a more complex decomposition processes. The temperatures of 5% weight loss are, in both atmospheres, above 300 °C for pure DGEBA but about 250 °C for SOE-containing samples, probably due to the ester linkage break.

In air, a second stage of weight loss for sample 3, without phosphorus, corresponds to thermooxidative degradation. This behaviour is in accordance with the mechanism of improved fire performance via phosphorous modification. In this retarded-degradation phenomenon, the phosphorous groups form an insulating protective layer, which prevents the combustible gases from transferring to the surface of the materials, increases the thermal stability at higher temperatures, and improves the fire resistance.

The char yields under nitrogen is normally correlated with the polymer's

polymer's flame retardancy for the phosphorus-containing resins, were measured and are shown in Table



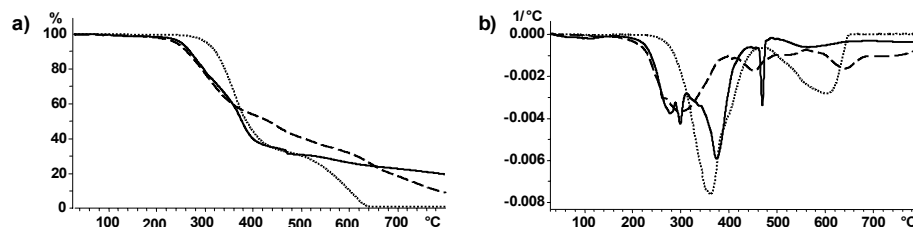
**Figure 7.** (a) TGA thermograms of (—) SOE-DOPOMA, (---) 2/1(mol/mol) DGEBA/SOE-DOPOMA, and (····) DGEBA and (b) first derivatives under N<sub>2</sub>.

flame retardance,<sup>28</sup> but it should be pointed out that, in our case, the experimental char yields of the phosphorus-containing resins and the phosphorus-free resins are not significantly different under nitrogen. However, under air, the char yield is significantly lower in sample 3 without phosphorus, and sample 1 with a higher phosphorus content has the greater char yield.

3. The presence of phosphorus slightly increases the LOI values for the phosphorus-containing samples, but no significant increase can be observed when the phosphorus content increases; this indicates that low amounts of phosphorus are sufficient to obtain improvements in the flame retardancy.

The LOI values, which can be taken as an indicator to evaluate the

## CONCLUSIONS



**Figure 8.** (a) TGA thermograms of (—) SOE-DOPOMA, (---) 2/1(mol/mol) DGEBA/SOE-DOPOMA, and (····) DGEBA and (b) first derivatives under air.

Assay	N <sub>2</sub> Atmosphere			Air Atmosphere			LOI
	T <sub>5%</sub> <sup>a</sup>	T <sub>max</sub> <sup>b</sup>	Char yield at	T <sub>5%</sub> <sup>a</sup>	T <sub>max</sub> <sup>b</sup>	Char yield at	
	(°C)	(°C)	800 °C (wt%)	(°C)	(°C)	800 °C (wt%)	
1	258	278/293/373/461	18,6	250	278/299/373/469	19,3	25.6
2	247	303/450	27,9	242	298/451/640	9,1	25.1
3	314	381	20,4	303	360/602	0,5	24.0

A new bis-SOE-containing monomer, SOE-DOPOMA, was synthesized with good yields by an esterification reaction with SOE-OH and a phosphorus-containing diacid, both of which were previously synthesized. This method avoids the undesirable decarboxylation of the diacid precursor, which leads to a mono-SOE compound. This new SOE was crosslinked with ytterbium triflate as a cationic initiator. A mixture of SOE-DOPOMA and DEGBA was also crosslinked under the same conditions. These two curing processes occurred with expansion, which was higher for pure SOE-DOPOMA. The incorporation of phosphorus into the materials produced an increase in the char yields and a slight increase in the LOI values; thus, the flame retardancy of the materials was increased.

*The authors thank the Comisión Interministerial de Ciencia y Tecnología (MAT2005-01593) and (MAT2005-01806) for providing financial support for this work.*

## REFERENCES AND NOTES

- Expanding Monomers: Synthesis, Characterization and Applications; Shadir, R. K.; Luck, R. M., Ed; CRC: Boca Raton, FL, 1992.
- Camino, G. In Chemistry and Technology of Polymer Additives; Al-Malaika, S.; Golovoy, A.; Wilkie, C. A., Eds.; Blackwell Science: London, 1999; p.108.
- Lu, S.-Y.; Hamerton, I. Prog Polym Sci 2002, 27, 1661.
- Hino, T.; Endo, T. Macromolecules 2003, 36, 5902.
- Smith, R. E.; Pinzino, C. S.; Chappelow, C. C.; Holder, A. J.; Kostoryz, E. L.; Guthrie, J. R.; Miller, M.; Yourtee, D. M.; Eick, J. D. J Appl Polym Sci 2004, 92, 62.
- Nishida, H.; Morikawa, H.; Nakahara, T.; Ogata, T.; Kusumoto, K.; Endo, T. Polymer, 2005, 46, 2531.

7. Bodenbenner, K. *Justus Liebigs Ann* 1959, 625, 183.
8. Fedtke, M.; Houfe, J.; Kahlert, E.; Müller, G. *Angew Makromol Chem* 1998, 255, 53.
9. Canadell, J.; Mantecón, A.; Cádiz, V. *J Polym Sci Part A: Polym Chem* 2006, 44, 4722.
10. Castell, P.; Galià, M.; Serra, A.; Salla, J. M.; Ramis, X. *Polymer* 2000, 41, 8465.
11. Mas, C.; Serra, A.; Mantecón, A.; Salla, J. M.; Ramis, X. *Macromol Chem Phys* 2001, 202, 2554.
12. Lanthanides: Chemistry and Use in Organic Synthesis; Kobayashi, S., Ed.; Topics in Organometallic Chemistry; Springer-Verlag: Berlin, 1999.
13. Lin, C. H.; Wu, C. Y.; Wang, C. S. *J Appl Polym Sci* 2000, 78, 228.
14. Shan, W. C.; Hsuan, L. C. *Polymer* 1999, 40, 4387.
15. Endo, T.; Kitamura, N.; Takata, T. *J Polym Sci Part A: Polym Chem* 1988, 26, 517.
16. Nishikubo, T.; Iizawa, T.; Takahashi, A.; Shimokawa, T. *J Polym Sci Part A: Polym Chem* 1990, 28, 105.
17. Nishikubo, T.; Ozaki, K. *Polym J* 1990, 22, 1043.
18. Galià, M.; Mantecón, A.; Cádiz, V.; Serra, A. *J Polym Sci Part A: Polym Chem* 1994, 32, 829.
19. Callau, L.; Reina, J. A.; Mantecón, A.; Tessier, M.; Spassky, N. *Macromolecules* 1999, 32, 7790.
20. Bogdal, D.; Penczek, P.; Pielchowski, J.; Prociak, A. *Adv Polym Sci* 2003, 163, 193.
21. Lidstrom, P.; Tieney, J.; Wathey, B.; Westman, J. *Tetrahedron* 2001, 57, 922.
22. (a) Neises, B.; Steglich, W. *Org Synth* 1990, 7, 93; (b) Neises, B.; Steglich, W. *Org Synth* 1985, 63, 183.
23. Mas, C.; Ramis, X.; Salla, J. M.; Mantecón, A.; Serra, A. *J Polym Sci Part A: Polym Chem* 2003, 41, 2794.
24. Pretsch, E.; Clerc, T.; Seibl, J.; Simon, W. *Tablas para la Elucidación Estructural de Compuestos Orgánicos por Métodos Espectroscópicos*; Springer-Verlag Ibérica: Barcelona, 1998.
25. Liu, Y.-L.; Tsai, S.-H. *Polymer* 2002, 43, 5757.
26. Tobolsky, A. V.; Carlson, D. W.; Indocor, N. J. *J Polym Sci* 1961, 54, 175.
27. Chung, K.; Takata, T.; Endo, T. *Macromolecules* 1997, 30, 2532.
28. Van Krevelen, D. W. *Polymer* 1975, 16, 615.



## NOVEL SILICON-CONTAINING SPIROORTHOESTER WITH COMBINED FLAME RETARDANCY AND LOW SHRINKAGE PROPERTIES TO MODIFY EPOXY RESINS

J. Canadell, A. Mantecón, V. Cádiz

Departament de Química Analítica i Química Orgànica. Universitat Rovira i Virgili.  
Marcel·lí Domingo s/n, 43007 Tarragona, Spain

---

### Abstract

A new silicon-containing spiroorthoester, 1,4,6-trioxaspiro[4,4]-2-nonylmethyl 3-trimethylsilyl propionate (SOE-Si), was synthesized with good yields by an esterification reaction with a previously synthesized 2-hydroxymethyl-1,4,6-trioxaspiro [4,4] nonane and trimethylsilyl propionic acid. The structure of the new SOE-Si was confirmed by  $^1\text{H}$ , and  $^{13}\text{C}$  NMR spectroscopy. The SOE-Si was homopolymerized with ytterbium triflate as a cationic initiator. A mixture of SOE-Si and diglycidyl ether of bisphenol A was also polymerized under the same conditions. The curing was studied with differential scanning calorimetry and monitored by Fourier transform infrared spectroscopy. The materials were characterized with differential scanning calorimetry, thermogravimetric analysis and thermodyna-momechanical analysis. The volume change was evaluated with a Micromeritics gas pycnometry, and the flame retardancy was tested by the limiting oxygen index measurements.

**Keywords:** cationic polymerization; epoxy resins; ring opening; flame retardance; heteroatom-containing polymers; spiroorthoester; ytterbium triflate

---

### INTRODUCTION

Epoxy resins are widely used in casting, coating, adhesion, and composite applications. They have many attractive properties: they are easy to cure and process, are resistant to moisture, solvents, and chemicals and they have good mechanical and electrical properties.<sup>1</sup> However, in some applications, epoxy resins require special functions, such as low flammability and low shrinkage.

Traditionally, halogen-containing monomers such as diglycidylether of tetrabromobisphenol A have been used to render effective flame retardant properties, although their uses are limited because of their productions of toxic and corrosive gases as well as carcinogenic chemicals during combustion. On the contrary, the halogen-free flame retardants are environmentally friendly because they generate less toxic and corrosive substances during fire. The common halogen-free flame retardants are mainly organophosphorus<sup>2-3</sup> and organosilicon<sup>4-5</sup> compounds. Both elements are described that can function in the condensed phase or vapor phase, and possibly concurrently in both phases.<sup>6</sup>

Phosphorus-containing polymers mainly act changing the chemical reactions of decomposition, in favor of reactions yielding carbonaceous char rather than CO and CO<sub>2</sub>. They form a surface layer of protective char during fire before the unburned material begins to decompose. The char

layer acts as a barrier to inhibit gaseous products from diffusing to the flame and to shield the polymer surface from heat and air.<sup>3,7,8</sup>

Silicon-containing polymers have also a flame retardant effect, arising partly from the property that such compounds dilute the more combustible gases and partly from the barrier that siliceous residues can form to an advancing flame.<sup>4,9</sup>

Another problem of the epoxy resins is their shrinkage during curing, which can lead to internal compressive stress in the material, poor adhesion of coatings to the substrate, and the appearance of microvoids and micro-cracks, which reduce the durability of materials.<sup>10</sup> One of the best solutions to solve the shrinkage is the use of monomers that show no volume shrinkage in their polymerization, such as spiroorthoesters (SOEs)<sup>11,12</sup>, spiroorthocarbonates (SOCs)<sup>13,14</sup>, and bicyclicorthoesters (BOEs).<sup>15</sup>

We recently reported the synthesis of phosphorus-containing spiroortho-esters<sup>16,17</sup> and their homopolymerization and copolymerization with epoxy resins to obtain materials with enhanced flame retardancy and with low shrinkage during curing.

The aim of the present study is to use silicon instead of phosphorus to solve the above mentioned disadvantages of epoxy resins, by

means of the cationic crosslinking of a new silicon-containing spiroorthoester with mixtures of DGEBA.

The cationic crosslinking was carried out using ytterbium triflate as a cationic initiator, which has shown to be effective to polymerize glycidyl compounds and spiroorthoesters.<sup>18</sup> This crosslinking was studied with differential scanning calorimetry (DSC) and Fourier transform infrared spectroscopy (FTIR). The materials were characterized by DSC, thermogravimetric analysis (TGA), and thermodynamomechanical analysis (DMTA). The volume change was evaluated with a Micromeritics gas pycnometry and the flame retardancy was tested by the limiting oxygen index (LOI) measurements.

## EXPERIMENTAL

### Materials

Glycidol (Aldrich),  $\gamma$ -butyrolactone ( $\gamma$ -BL; Aldrich), boron trifluoride diethyl etherate ( $\text{BF}_3 \cdot \text{OEt}_2$ ; Aldrich), triethylamine (Fluka), trimethylsilyl acetic acid (Aldrich), trimethylsilylpropionic acid (Fluorochem), N-(3-Dimethylamino-propyl)-N'-ethyl-carbodiimide hydrochloride (EDC; Fluka), 4-(dimethyl-amino)pyridine (DMAP; Fluka), DGEBA (Epikote Resin 827, Shell Chemicals; epoxy equivalent = 182.08 g/eq), ytterbium(III) trifluoromethanesulfonate [ $\text{Yb}(\text{OTf})_3$ ; Aldrich] were used

as received. All solvents were purified by standard procedures.

### Instrumentation

NMR spectra ( $^1\text{H}$  400 MHz;  $^{13}\text{C}$  100.6 MHz) were obtained with a Varian Gemini 400 spectrometer with Fourier transform,  $\text{CDCl}_3$  as the solvent.  $^{29}\text{Si}$  MAS NMR spectra were performed, with finely ground samples, on a Varian Gemini 400 MHz spectrometer at a 79 MHz resonance frequency, MAS being applied with a 20-s delay time.

Polymerization and crosslinking studies were performed on a Mettler DSC-821e thermal analyzer in covered Al pans under nitrogen at scan rates of 10  $^\circ\text{C}/\text{min}$ . The determination of glass transition temperatures ( $T_g$ 's) were carried out on a Mettler DSC-822e thermal analyzer in covered Al pans under  $\text{N}_2$  at scan rates at 20  $^\circ\text{C}/\text{min}$ . The samples weighed approximately 8 mg.

The isothermal crosslinking process at 140  $^\circ\text{C}$  was monitored with a 680 Plus FTIR spectrophotometer with a resolution of 4  $\text{cm}^{-1}$  in the absorbance mode. An attenuated total reflection (ATR) accessory with a thermal control and a diamond crystal was used to determine the FTIR/ATR spectra.

TGAs were carried out with a Mettler TGA/SDTA 851e thermobalance. Cured samples with an approximate mass of 10 mg were degraded between 30  $^\circ\text{C}$  and

800 °C at a heating rate of 10 °C/min in an atmosphere of N<sub>2</sub> or air.

DMTA were carried out with TA DMA 2928 working with a three-point bending clamp from 30 to 180 °C at a heating rate of 5 °C/min.

The molecular weight distribution of the polymers was determined with a Waters gel permeation chromatograph equipped with the Waters 510 differential refractive-index detector (RID-6A from Shimadzu). The gel permeation chromatograph was operated using three Waters Shodex columns (K80M, 5- $\mu$  mixed-D gel, and 3- $\mu$  Mixed-E gel) at a nominal flow rate of 1 mL/min and with a sample concentration of 0.1% in tetrahydrofuran as the solvent. Monodisperse polystyrene standards were purchased from Polymer Laboratories for instrument calibration.

The densities of the materials were measured with a Micromeritics Accu-pyc 1330 TC gas pycnometer at 30 °C.

LOIs were measured on a Fire Testing Technology flammability unit in conformance with ASTM D 2863 for samples measuring 100 mm x 6 mm x 3 mm.

Scanning electron microscopy (SEM) was performed on a JEOL JSM 6400 scanning electron microscope at an activation voltage of 8 kV. For the atomic mapping, an

Oxford INCA energy-dispersive X-Ray microanalyzer was used.

XRD measurements were made using a Siemens D 5000 diffractometer (Bragg-Brentano parafocusing geometry and vertical  $\theta$ - $\theta$  goniometer) fitted with a curved graphite diffracted-beam monochromator and diffracted-beam Soller slits, a 0.06° receiving slit and scintillation counter as a detector. The angular  $2\theta$  diffraction range was between 5 and 70°. Sample was tested on to a low background Si(510) sample holder. The data were collected with an angular step of 0.05° at 3 s per step and sample rotation. Cu<sub>K $\alpha$</sub>  radiation was obtained from a copper X-ray tube operated at 40 kV and 30 mA.

#### **Synthesis of 2-hydroxymethyl-1,4,6-trioxaspiro [4,4] nonane (SOE-OH)**

Glycidol (30 g, 0.40 mol) was added dropwise over a period of 15 min at a temperature below 10 °C in an argon atmosphere to a mixture of 200 g (2.3 mol) of  $\gamma$ -BL and 1.0 mL (7.9 mmol) of BF<sub>3</sub>·OEt<sub>2</sub> as a catalyst. After the addition was completed, the mixture was stirred for 60 min at the same temperature. The reaction was quenched by the addition of 1.4 mL (10 mmol) of triethylamine. After the solvent was removed under reduced pressure, the residue was distilled fractionally to yield 11.2 g (17%) of a transparent, colorless liquid.

$^1\text{H}$  NMR ( $\text{CDCl}_3$ , two diastereomers):  $\delta(\text{ppm}) = 4.41\text{--}4.32$  (m, 2H, -O-CH-), 4.14-4.03 (m, 2H, -O-CH<sub>2</sub>-), 3.99-3.89 (m, 4H, -O-CH<sub>2</sub>-), 3.85-3.80 (m, 2H, -O-CH<sub>2</sub>-), 3.73-3.54 (m, 4H, -CH<sub>2</sub>-OH), 2.89 (br, 2H, OH), 2.18-2.12 (m, 4H, -CH<sub>2</sub>-), 2.05-1.97 (m, 4H, -CH<sub>2</sub>-).

$^{13}\text{C}$  NMR ( $\text{CDCl}_3$ , two diastereomers):  $\delta(\text{ppm}) = 129.60$  (s, spiranic C), 129.32 (s, spiranic C), 75.99 (s, -O-CH-), 67.42 (s, -O-CH<sub>2</sub>-), 65.69 (s, HO-CH<sub>2</sub>-), 64.92 (s, OH-CH<sub>2</sub>-), 62.81 (s, -O-CH<sub>2</sub>-), 62.54 (s, -O-CH<sub>2</sub>-), 32.67 (s, -CH<sub>2</sub>-), 32.50 (s, -CH<sub>2</sub>-), 24.51 (s, -CH<sub>2</sub>-), 24.35 (s, -CH<sub>2</sub>-).

#### Reaction of trimethylsilyl acetic acid with SOE-OH

Under an argon atmosphere, an oven-dried 100 mL round-bottom flask containing 20 mL of anhydrous dichloromethane was charged with 1.0 g (7.5 mmol) of trimethylsilyl acetic acid, 1.20 g (7.5 mmol) of SOE-OH, 1.59 g (8.3 mmol) of EDC, and 1.01 g (8.3 mmol) of DMAP. The solution was stirred and heated at 40 °C for 2 h. After cooling to room temperature, the solution was washed with two 30-mL portions of a 10% citric acid solution, twice with 30-mL portions of a 10% sodium bicarbonate solution, and twice with brine. The organic solution was dried over anhydrous magnesium sulfate, and the solvent was removed by evaporation to give 1.04 g of transparent colorless liquid, which

corresponds to a mixture of 1,4,6-trioxaspiro [4,4]-2-nonylmethyl acetate (SOE-Ac) and 1,4,6-trioxaspiro [4,4]-2-nonylmethyl trimethylsilyl ether (SOE-OSi). The mixture of SOEs was separated by flash chromatography with a silica gel neutralized with triethylamine and ethyl acetate/hexane (8:2) containing 1% of triethylamine as eluent.

#### SOE-Ac.

$^1\text{H}$  NMR ( $\text{CDCl}_3$ , two diastereomers):  $\delta(\text{ppm}) = 4.49\text{--}4.42$  (m, 1H, -O-CH-), 4.35-4.28 (m, 1H, -O-CH-), 4.25-4.19 (m, 2H, -O-CH<sub>2</sub>-), 4.16-4.03 (m, 4H, -O-CH<sub>2</sub>-), 3.94-3.81 (m, 4H, -O-CH<sub>2</sub>-), 3.77-3.70 (m, 2H, -O-CH<sub>2</sub>-), 2.16- 2.09 (m, 4H, -CH<sub>2</sub>-), 2.15-2.12 (d, 6H, -CH<sub>3</sub>), 2.10-1.94 (m, 4H, -CH<sub>2</sub>-).

$^{13}\text{C}$  NMR ( $\text{CDCl}_3$ , two diastereomers):  $\delta(\text{ppm}) = 170.84$  (s, -COO-), 129.82 (s, spiranic C), 74.28 (s, -O-CH-), 73.40 (s, -O-CH-), 67.47 (s, -O-CH<sub>2</sub>-), 67.40 (s, -O-CH<sub>2</sub>-), 66.13 (s, -O-CH<sub>2</sub>-), 66.05 (s, -COO-CH<sub>2</sub>-), 65.20 (s, -O-CH<sub>2</sub>-), 64.30 (s, -COO-CH<sub>2</sub>-), 32.78 (s, -CH<sub>2</sub>-), 24.32 (s, -CH<sub>2</sub>-), 24.14 (s, -CH<sub>2</sub>-), 20.97 (s, -CH<sub>3</sub>), 20.76 (s, -CH<sub>3</sub>).

#### SOE-OSi.

$^1\text{H}$  NMR ( $\text{CDCl}_3$ , two diastereomers):  $\delta(\text{ppm}) = 4.29\text{--}4.26$  (m, 1H, -O-CH-), 4.17-4.09 (m, 1H, -O-CH-), 4.08-4.03 (m, 2H, -O-CH<sub>2</sub>-), 3.91-3.84 (m, 4H, -O-CH<sub>2</sub>-), 3.77-3.73 (m, 2H, -O-CH<sub>2</sub>-), 3.66-3.47

(br, 4H, -O-CH<sub>2</sub>-), 2.11-2.05 (m, 4H, -CH<sub>2</sub>-), 1.99-1.92 (m, 4H, -CH<sub>2</sub>-), 0.06 (d, 18H, -CH<sub>3</sub>).

<sup>13</sup>C NMR (CDCl<sub>3</sub>, two diastereomers): δ(ppm) = 129.78 (s, spiranic C), 129.60 (s, spiranic C), 76.79 (s, -O-CH-), 75.90 (s, -O-CH-), 67.38 (s, -O-CH<sub>2</sub>-), 67.26 (s, -O-CH<sub>2</sub>-), 66.39 (s, -O-CH<sub>2</sub>-), 64.41 (s, -O-CH<sub>2</sub>-), 63.03 (s, -O-CH<sub>2</sub>-), 33.02 (s, -CH<sub>2</sub>-), 32.80 (s, -CH<sub>2</sub>-), 24.36 (s, -CH<sub>2</sub>-), 24.29 (s, -CH<sub>2</sub>-), 1.11 (s, -CH<sub>3</sub>), -0.46 (s, -CH<sub>3</sub>).

### Synthesis of 1,4,6-trioxaspiro[4,4]-2-nonylmethyl 3-trimethylsilyl propio-nate (SOE-Si)

Under an argon atmosphere, an oven-dried 100 mL round-bottom flask containing 20 mL of anhydrous dichloromethane was charged with 1.0 g (6.8 mmol) of trimethylsilyl propionic acid, 1.09 g (6.8 mmol) of SOE-OH, 1.44 g (7.5 mmol) of EDC, and 0.91 g (7.5 mmol) of DMAP. The solution was stirred and heated at 40 °C for 3 h. After cooling to room temperature, the solution was washed with two 30-mL portions of a 10% citric acid solution, twice with 30-mL portions of 10% sodium bicarbonate solution, and twice with brine. The organic solution was dried over anhydrous magnesium sulfate, and the solvent was removed by evaporation to give 1.97 g (90%) of a transparent, colorless liquid.

<sup>1</sup>H NMR (CDCl<sub>3</sub>, two diastereomers): δ(ppm) = 4.37-4.34 (m, 1H, -O-CH-), 4.24-4.21 (m, 1H, -O-CH-), 4.15-4.13 (m, 2H, -O-CH<sub>2</sub>-), 4.12-3.96 (m, 4H, -CH<sub>2</sub>-OCO-), 3.86-3.75 (m, 4H, -O-CH<sub>2</sub>-), 3.69-3.64 (m, 2H, -O-CH<sub>2</sub>-), 3.63-2.14 (m, 4H, -CH<sub>2</sub>-COO-), 2.08-1.99 (m, 4H, -CH<sub>2</sub>-), 1.91-1.85 (m, 4H, -CH<sub>2</sub>-), 1.19-0.69 (m, 4H, -Si-CH<sub>2</sub>-), -0.08 (s, 8H, -CH<sub>3</sub>).

<sup>13</sup>C NMR (CDCl<sub>3</sub>, two diastereomers): δ(ppm) = 174.63 (s, -COO-), 129.69 (s, spiranic C), 129.61 (s, spiranic C), 74.20 (s, -O-CH-), 73.32 (s, -O-CH-), 67.21 (s, -O-CH<sub>2</sub>-), 67.14 (s, -O-CH<sub>2</sub>-), 65.99 (s, -O-CH<sub>2</sub>-), 65.89 (s, -CH<sub>2</sub>-OCO-), 64.95 (s, -CH<sub>2</sub>-O-), 64.05 (s, -O-CH<sub>2</sub>-), 32.61 (s, -CH<sub>2</sub>-), 28.56 (s, -CH<sub>2</sub>-COO-), 24.17 (s, -CH<sub>2</sub>-), 23.98 (s, -CH<sub>2</sub>-), 11.47 (s, -Si-CH<sub>2</sub>-), -2.03 (s, -CH<sub>3</sub>).

### Polymerization of SOE-Si

A mixture of 0.5 g of SOE-Si with 1 phr (1 part per 100 of monomer mixture weight/weight) of ytterbium triflate was heated in an oven for 4 h at 180 °C to obtain SOE-Si homopolymer (SOE-Si hom)

### Crosslinking reactions

The cationic crosslinking reaction was carried out through the mixing DGEBA/SOE-Si in (mol/mol) ratio 2:1, with 1 phr of ytterbium triflate. The sample bars used for dynamo-mechanical and thermogravimetric

analysis and burn tests were cured in aluminum molds by heating in an oven. The curing conditions were determined from DSC.

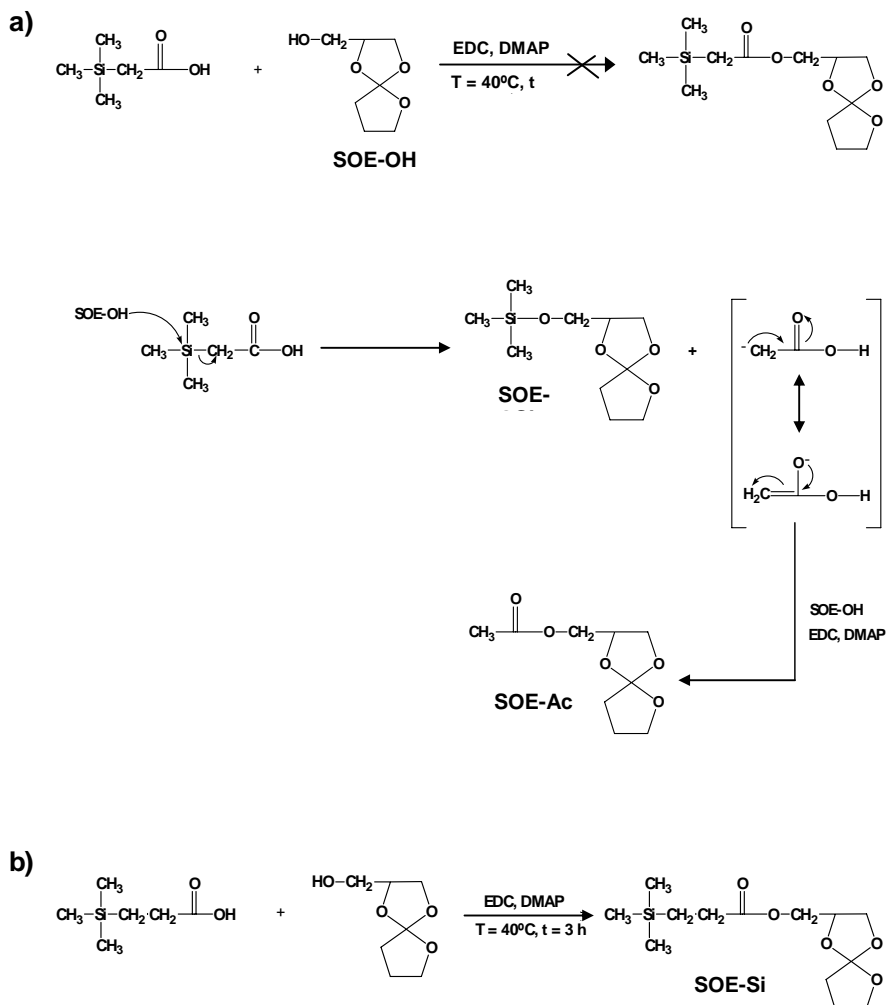
## RESULTS AND DISCUSSION

The synthesis of a silicon-containing spiroorthoester was assayed with two different substrates. The synthetic pathway consisted in the esterification reaction of two commercially available silicon-containing acids and a hydroxyl-containing spiroorthoester (SOE-OH) in presence of EDC and DMAP. Direct ester formation from acids and alcohols or phenols using a carbodiimide coupling agent is a useful method which has been utilized by several authors.<sup>19,20</sup> In a

previous work we synthesized a phosphorus-containing spiroorthoester using this synthetic method<sup>17</sup> but with the water soluble EDC as alternative to dicyclohexylcarbo-diimide (DCC) because its elimination result easier and we obtained better yields. The SOE-OH was synthesized, as previously described,<sup>17</sup> from glycidol and  $\gamma$ -BL.

First, the esterification of the trimethylsilyl acetic acid with SOE-OH [scheme 1(a)] was assayed, not obtaining the desired product but yielding a mixture of two products: SOE-OSi and SOE-Ac. The formation of these compounds could be confirmed with <sup>1</sup>H and <sup>13</sup>C NMR spectroscopy.

76 | Synthesis of Spiroorthoesters



Scheme 1

The formation of SOE-OSi could be explained by a nucleophilic attack of SOE-OH to silicon centre. Different factors facilitate this process: a) the unique nature of silicon in comparison to carbon that arises from the longer bond between silicon and carbon (Si-C = 1.89 Å) in

comparison to the corresponding system involving only carbon (C-C = 1.54 Å) and the vacant d-orbitals of silicon which facilitates nucleophilic attacks<sup>21,22</sup> and b) the enolate leaving group is stabilized by resonance. The formation of SOE-Ac could be explained for the further

esterification of the acetate with 7 H<sub>SOE-Ac</sub>). This SOE-OSi was not

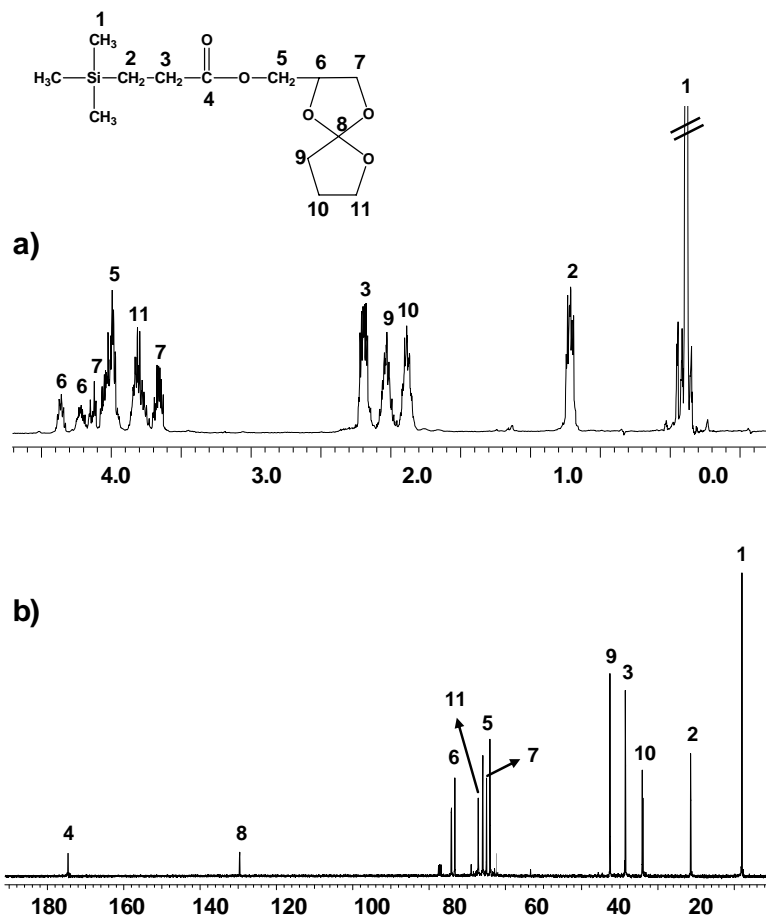


Figure 1. NMR spectra of SOE-Si; <sup>1</sup>H (a) and <sup>13</sup>C (b).

SOE-OH in presence of EDC/DMAP.

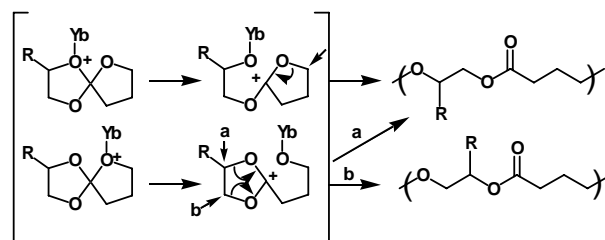
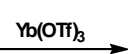
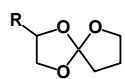
The ratio 68%:32% for SOE-OSi/SOE-Ac was determined by means of <sup>1</sup>H NMR, by the integration ratios of the following signals of <sup>1</sup>H NMR spectra: 0 ppm (9 H<sub>SOE-OSi</sub>) and 2.2-1.8 (4 H<sub>SOE-OSi</sub> +

tested as monomer because its tedious work-up and the low yield reached in its formation.

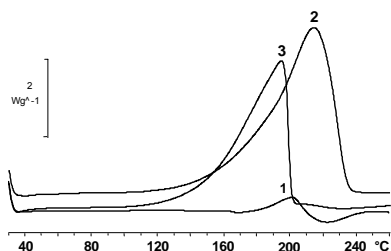
We assayed the synthesis of another silicon-containing acid without a possible leaving group. Thus, the esterification of trimethylsilyl propionic acid with

78 | Synthesis of Spiroorthoesters

SOE-OH [(scheme 1(b))] allows a silicon-containing spiro-orthoester (SOE-Si) to be obtained with a good



Scheme 2



**Figure 2.** Dynamic DSC plots of (1) SOE-Si; (2) DGEBA and; (3) 2/1 (mol/mol) DGEBA/SOE-Si initiated by 1 phr  $\text{Yb}(\text{OTf})_3$  obtained at 10 °C/min heating rate.

yield (90 %). This novel SOE-Si was characterized by means of  $^1\text{H}$ ,  $^{13}\text{C}$ , COSY, and HSQC experiments. Figure 1 shows the  $^1\text{H}$  (a), and  $^{13}\text{C}$  (b) NMR spectra, with all the assignments. Because the spiroortho-ester has two chiral carbons, the presence of two diastereomers was detected through some split signals in  $^1\text{H}$  and  $^{13}\text{C}$  NMR spectra.

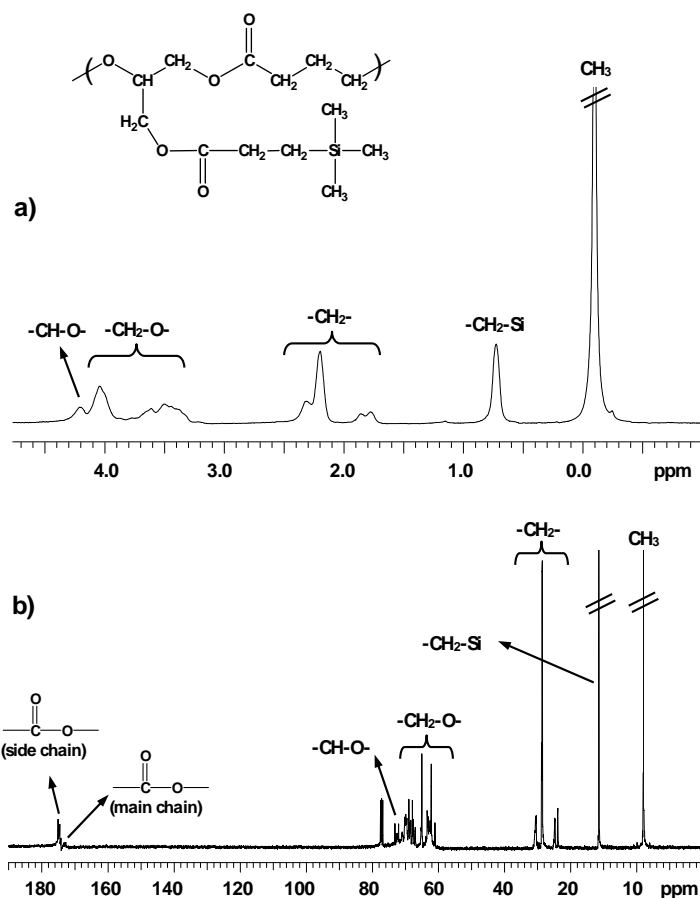
The homopolymerization of SOE-Si with ytterbium triflate as a cationic initiator was first studied by DSC. Scheme 2 summarizes the different ring-opening polymerization pathways to form linear poly(ether-ester) structures. The dynamic DSC plot of this reaction (Figure 2, curve 1) shows a small exotherm with a maximum at 202 °C. The enthalpy of this SOE-Si homopolymerization is very low ( $\Delta H$

= 10.5 KJ/SOE equiv.) as observed for ring opening of a non-tensionated spiroorthoester.<sup>18</sup> In a second scan, the  $T_g$  of the polymer at -51 °C was observed.

Figure 3 shows the  $^1\text{H}$  (a) and  $^{13}\text{C}$  (b) spectra of the poly(ether-ester), obtained after heating at 180 °C for 4 h in an oven. In the  $^1\text{H}$  NMR spectrum, the broadness of protons signals is characteristic of polymeric compounds due to the different environment. The methylene and methyl attached to the silicon atom appears at 0.8 ppm and -0.1 ppm respectively. In the  $^{13}\text{C}$  NMR spectrum the spiranic carbon does not appear, which indicates the successful polymerization of the SOE yielding a poly(ether-ester). Moreover, two different carbonyl signals appear, attributed to the main chain and side chain ester groups. The various aliphatic carbons appear below 80 ppm. The

**Figure 3.** NMR spectra of homopolymer SOE-Si obtained by cationic polymerization;  $^1\text{H}$  (a) and  $^{13}\text{C}$  (b)

methylene and methine carbons attached to the oxygen atom appear between 80 and 60 ppm. The methylene and methyl groups attached to the silicon atom appear at about 16 ppm and 0.8 ppm, respectively. The complexity of



these signals could be attributed to the regioirregularity of the main chain, which are the result of different polymerization pathways and the presence of diastereomers.

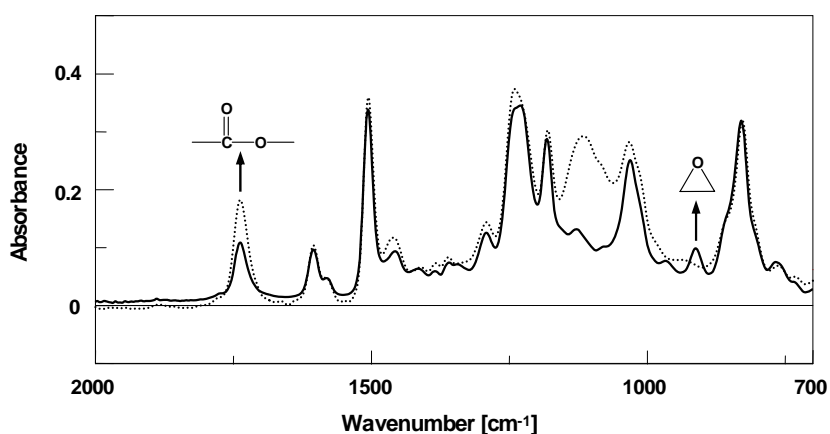
The molecular weight of the homopolymer, determined by size exclusion chromatography, was about  $3 \times 10^3$  g/mol and a polydispersity of 2.5. The unimodal but broad curve of the polymer denotes the different path-ways of polymerization.

As earlier mentioned, our first interest is focused on the modification of epoxy resins with this silicon-containing SOE monomer. In the cationic copolymerization of epoxy resins with spiroorthoesters three simultaneous processes are expected (Scheme 3): a) reaction of SOE with epoxy groups, b) homopolymerization of SOE and c) homopolymerization of epoxy groups. Both a) and b) processes lead to the formation of linear ether

ester moieties, whereas c) reaction only lead to ether linkages. The copolymerization of DGEBA with SOE-Si (molar ratio 2:1) was monitored by FTIR/ATR spectroscopy in isothermal experiments at 140 °C. This technique allowed us to follow the evolution of the groups involved in the process by means of the variations in the corresponding absorptions. Figure 4 shows the FTIR spectra of the DGEBA/SOE-Si mixture with 1 phr of  $\text{Yb}(\text{OTf})_3$  before and after polymerization. The ring opening of spiroorthoester that takes place during the polymerization led to a linear poly(ether-ester) moieties, thus a typical band of carbonyl ester group must appear about 1735-1750  $\text{cm}^{-1}$ .<sup>1,23</sup> SOE-Si contains ester groups which appear at 1737  $\text{cm}^{-1}$  in the initial spectrum, and therefore in this zone only an increase in this band was observed on polymerizing. We

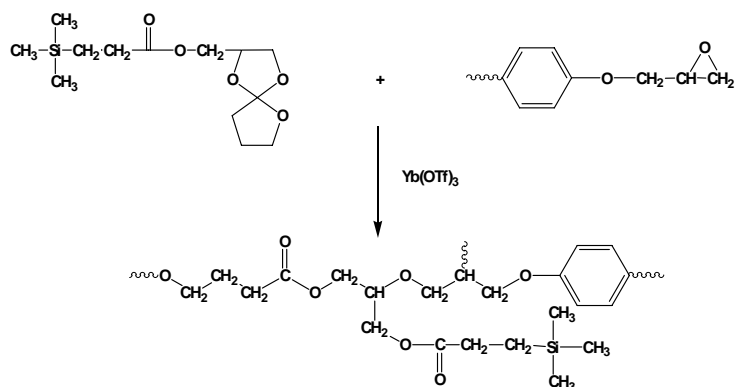
can see the disappearance of the absorption at 912  $\text{cm}^{-1}$  due to the oxirane ring, thus confirming that the glycidic compound has completely reacted. The Si-C absorption, seen in the SOE-Si homopolymer spectrum at 829  $\text{cm}^{-1}$ , in this case appears overlapped with the aromatic CH absorption of DGEBA.

Figure 2 shows the dynamic DSC plot corresponding to this copolymerization of DGEBA/SOE-Si (curve 3) with an exotherm at 195 °C. To compare, the corresponding DGEBA polymerization curve is also included in the same figure (curve 2). The maximum of the exotherm of both homopolymerizations (SOE-Si and DGEBA) appears at higher temperature than that of the copolymerization. From these dynamic experiments the isothermal

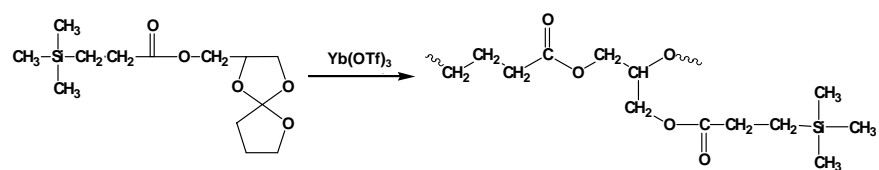


**Figure 4.** FTIR spectra of 2/1 (mol/mol) DGEBA/SOE-Si with 1 phr of  $\text{Yb}(\text{OTf})_3$  before (—) and after (.....) polymerization at 140 °C.

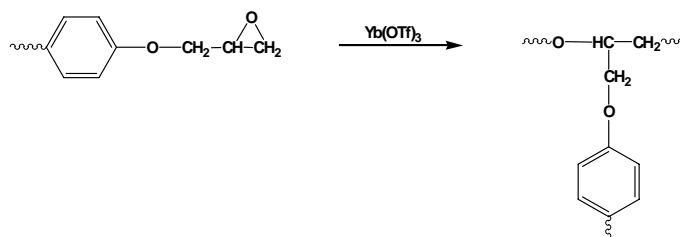
a) Copolymerization of DGEBA with SOE-Si



b) Homopolymerization of SOE-Si



c) Homopolymerization of DGEBA

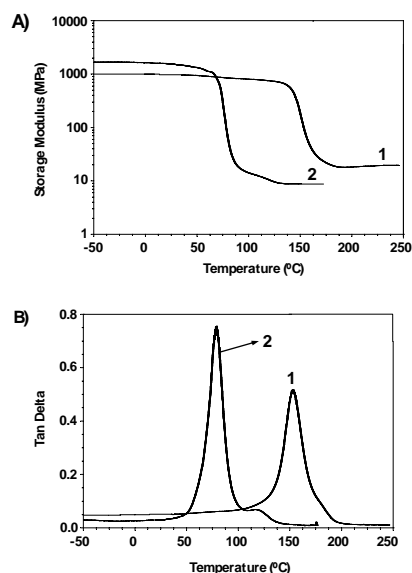


Scheme 3

curing conditions were established.

For the copolymerization of DGEBA/SOE-Si the curing conditions were: 150 °C for 3 h and then 175 °C for 3 h. The enthalpy values of DGEBA and DGEBA/SOE-Si polymerizations are very similar, 98.1 and 94.8 KJ/epoxy equiv respectively. A dynamic run for cured samples allows the calculation of  $T_g$  values, which are 139 °C for DGEBA and 73 °C for DGEBA/SOE-Si copolymer. The  $T_g$  of copolymer is between the  $T_g$  values of the two homopolymers.

The dynamic mechanical behaviour of the silicon-modified epoxy resin was obtained as a function of the temperature beginning in the glassy state to the rubbery plateau.<sup>24</sup> Figure 5 (a) shows the storage modulus plots versus the temperature for the DGEBA/SOE-Si copolymer, and the DGEBA homopolymer plot is also included for comparison. The dynamic mechanical properties for the SOE-Si homopolymer, due to its low  $T_g$ , was not tested. The crosslinking density of a polymer can be estimated from the plateau of the elastic modulus in the rubbery state. This theory is strictly valid only for lightly crosslinked materials and was therefore used to make qualitative comparisons of the crosslinking density among the two polymers. As can be seen, the incorporation of SOE reduces the crosslinking density. This is due to the greater distance between knots



**Figure 5.** Temperature dependence of (a) Storage Modulus and, (b) Tan Delta for the cured systems of: (1) DGEBA; and (2) 2/1 (mol/mol) DGEBA/SOE-Si.

produced by the linear ether-ester moieties introduced into the network by the SOE.

The plots of loss factor versus temperature show the  $\alpha$  relaxation peak, which is associated with the  $T_g$  of the material. Figure 5 (b) shows the  $\text{Tan } \delta$  versus temperature for the crosslinked materials. The highest  $T_g$  value corresponds to the more aromatic DGEBA homopolymer. As the height of the  $\text{Tan } \delta$  peak is associated with the crosslinking density, the plots show a lower crosslinking density for the copo-

lymer. Moreover, the analysis of the width of the  $\text{Tan } \delta$  shows trends in the network homogeneities, and because there are not significant differences among the homopolymer and the copolymer, the branching distribution for the two samples must be similar.

It has been reported that cationic double ring opened SOE based materials exhibit almost no shrinkage and that copolymers having SOE moieties will also crosslink without shrinkage. The volume changes ( $\Delta$ ) in the crosslinking reaction of the copolymers containing SOE moieties were evaluated by density measurements with a Micromeritics gas pycnometer before and after crosslinking (Table 1).  $\Delta$  was calculated from the following equation:

$$\Delta V (\%) = \frac{d_{\text{crosslinked polymer}} - d_{\text{initial mixture}}}{d_{\text{initial mixture}}} \times 100$$

where  $d$  is the density. Thus, negative values indicate expansion.

In SOE-Si sample, the observed value was negative and therefore the polymerization process shows an expansion. The copolymerization

of SOE-Si with DGEBA show a positive value, but SOE-Si is much lower than those observed in the crosslinking of pure DGEBA, which shows the typical volume shrinkage that generally accompanied the

**Table 1.** Volume Change on Crosslinking.

Assay	Density ( $d^{30}$ , g/cm <sup>3</sup> )		Volum Chang (%)
	Mixture	Crosslinked	
SOE-Si	1.005	0.976	-3
DGEBA/SOE-Si	1.186	1.197	0.9
DGEBA	1.158	1.193	3

crosslinking reactions.<sup>25</sup> Therefore, it can be concluded that the SOE moieties are effective monomers to obtain crosslinkable copolymers which do not shrink.

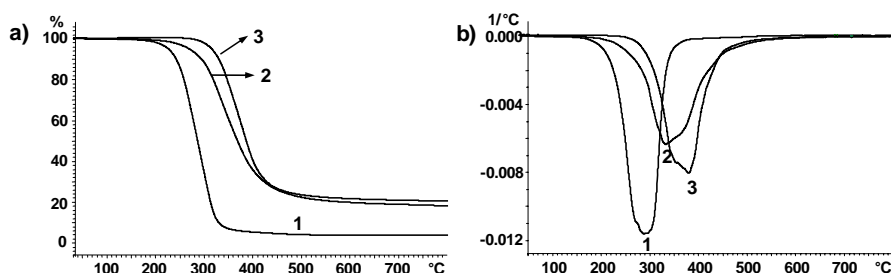
To examine the effect of silicon content on the thermal stability and decomposition behaviour, TGA data under nitrogen and air atmospheres were determined and analyzed. Figure 6 and 7 show the weight loss with the temperature and the derivative curves under N<sub>2</sub> and air respectively. Table 2 summarizes the thermogravimetric data.

**Table 2.** Thermogravimetric Data in N<sub>2</sub> and Air and LOIs of the Polymers.

Assay	Temperature of 5% Weight Loss (°C)		T <sub>max</sub> <sup>a</sup> (°C)		Char yield at 800 °C (% wt)		LOI
	N <sub>2</sub>	Air	N <sub>2</sub>	Air	N <sub>2</sub>	Air	
SOE-Si	224	222	288	290	3.6	0.0	—
DGEBA/SOE-Si	266	260	332	321/635	18.0	0.0	20.9
DGEBA	314	314	381	360/602	20.4	0.5	20.0

<sup>a</sup> Temperature of the maximum weight loss rate.

J Polym Sci Part A: Polym Chem (submitted)

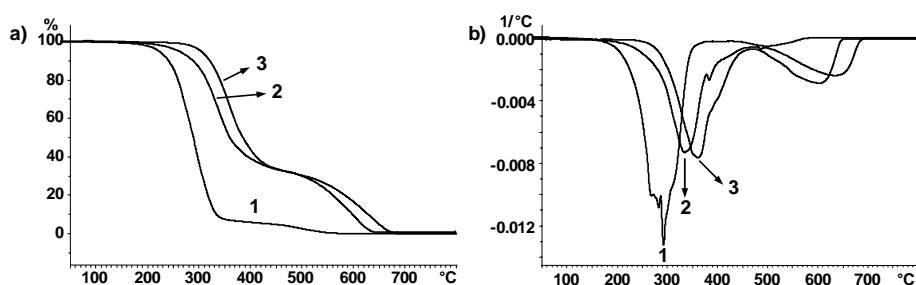


**Figure 6.** (a) TGA thermograms and (b) first derivative of: (1) SOE-Si homopolymer; (2) DGEBA/SOE-Si copolymer; and (3) DGEBA homopolymer under N<sub>2</sub> atmosphere.

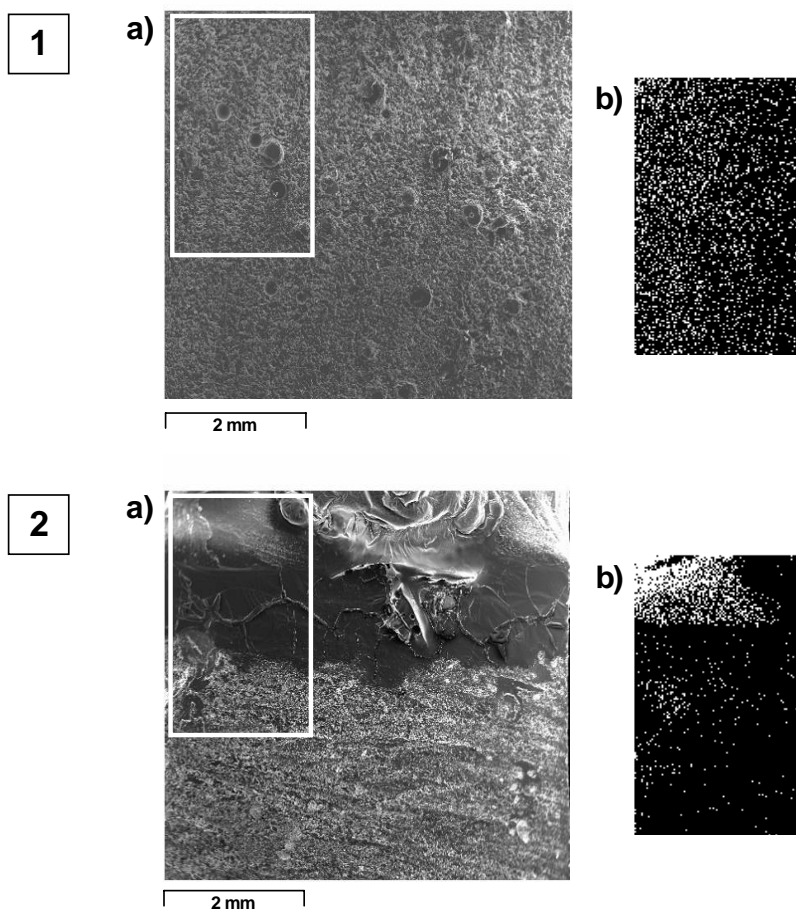
In nitrogen, only one-stage degradation was observed for the three materials. The polymers with SOE-Si degrade at lower temperatures than pure DGEBA, due to the presence of ester moieties in the structure. Under air, the polymers exhibited similar weight loss behaviour as they did under nitrogen atmosphere at temperatures below 400 °C. A second weight loss at temperatures above 500 °C occurs in the crosslinked materials. This second stage takes place at higher temperatures when silicon is incorporated into the epoxy resin. This behaviour indicates that the

introduction of silicon has slightly improved the thermal stability of the char formed in the first degradation stage. It has been reported that silicon-containing thermosets exhibit significant char formation on heating under air.<sup>5</sup> In this case, the DGEBA/SOE-Si copolymer does not form char residue at temperatures above 700 °C, what could be explained by its low silicon content (2.75 wt %).<sup>26</sup>

The LOI values, which can be taken as indicators to evaluate the polymer's flame retardancy for the silicon-containing resins, were measured and are shown in Table



**Figure 7.** (a) TGA thermograms and (b) first derivative of: (1) SOE-Si homopolymer; (2) DGEBA/SOE-Si copolymer; and (3) DGEBA homopolymer under air atmosphere.



**Figure 8.** SEM (a) and SEM-EDX Si mapping (b) micrographs of DGEBA/SOE-Si copolymer before (1) and after (2) LOI test.

2. The SOE-Si homopolymer could not be determined because its low  $T_g$ . The presence of silicon only slightly increases the LOI value, indicating that a higher silicon content is necessary to achieve a significant flame retardancy. However, in this case, an increase of SOE-Si in the final materials

should lead to materials with poor mechanical properties.

To better understand the role of silicon in the flame retardant properties of the polymer, the element mapping was performed with energy-dispersive X-ray spectroscopy (EDX) on the surfaces of the initial sample and the sample

after the LOI test. The Si mapping of the initial sample of the DGEBA/SOE-Si copolymer indicated a homogeneous distribution of this element, as can be observed in the micrograph of Figure 8 (1b). The white points in the figure denote Si atoms. Figure 8 (2a) shows the SEM micrograph of the top surface view of the sample after the LOI test. The burned zone has the appearance of a black and charred material. The Si distribution, in Figure 8 (2b), shows that the silicon density increased toward the top burned surface and that a silicon-rich layer formed. This result could be explained to the low surface energy of silicon renders it to migrate to the surface of the material and to form a protective layer. Incorporating silicon into the polymers enhanced flame retardancy because it produced a continuous layer of silica that retarded the oxidation of the char.<sup>27</sup>

The solid-state <sup>29</sup>Si MAS NMR allowed to detect the presence of the SiO<sub>2</sub>, at -71 ppm, in the char produced in the LOI test of DGEBA/SOE-Si copolymer. A pure SiO<sub>2</sub> spectrum was recorded in the same conditions to confirm this signal assignation. By Ray-X diffraction a crystalline fraction was observed, which can be attributed to the presence of SiO<sub>2</sub>.

## CONCLUSIONS

A new silicon-containing spiroorthoester, SOE-Si, was synthesized with

good yield by an esterification reaction with a previously synthesized SOE-OH and the commercially available trimethylsilyl propionic acid. This new SOE and a mixture of DGEBA/SOE-Si were polymerized with ytterbium triflate as a cationic initiator. The homopolymerization occurred with expansion and the copolymerization occurred with slight shrinkage which is lower than that observed in conventional epoxy resins. The incorporation of silicon into the epoxy resin improved the thermal stability of the formed char but only slightly increased the LOI values.

*The authors thank the Comisión Interministerial de Ciencia y Tecnología, CICYT, (MAT2005-01593 and MAT2005-01806) for providing financial support for this work.*

## REFERENCES AND NOTES

1. Epoxy Resins: Chemistry and Technology; May, C. A. Ed.; Marcel Dekker, New York, 1988.
2. Jain, P.; Choudhary, V.; Varma, I. K. *J Macromol Sci Polym Rev* 2002, C42(2), 139.
3. Lu, S-Y.; Hamerton, I. *Prog Polym Sci* 2002, 27, 1661.
4. Hsue, G-H.; Wang, W-J.; Chang, F-C. *J Appl Polym Sci* 1999, 73, 1231.
5. Wang, W-J.; Perng, L. H.; Hsue, G-H.; Chang, F-C. *Polymer* 2000, 41, 6113.

6. Levchik, S.; Weil, E. *Polym Int* 2004, 53, 1901.
7. Liu, Y. L. *Polymer* 2001, 42, 3445.
8. Ebdon, J. R.; Jones, M. S. In *Polymeric Materials Encyclopedia*; J.C. Salomone, Ed., CRC Press, Boca Raton, FL, 1996.
9. Hsue, G-H.; Liu, Y-L.; Tsiao, J. *J Appl Polym Sci* 2000, 78, 1.
10. Expanding monomers: Synthesis, Characterization and Applications; Shadir, R. K.; Luck, R. M. Ed.; CRC Press: Boca Raton, FL, 1992.
11. Nishida, H.; Morikawa, H.; Nakahara, T.; Ogata, T.; Kusumoto, K.; Endo, T. *Polymer* 2005, 46, 2531.
12. Kume, M.; Hirano, T.; Ochiai, B., Endo, T. *J Polym Sci Part A: Polym Chem* 2006, 44, 3666.
13. Kume, M.; Maki, Y, Ochiai, B, Endo, T. *J Polym Sci Part A: Polym Chem* 2006, 44, 7040.
14. Zhou, Z.; Jin, B.; He, P. *J Appl Polym Sci* 2002, 84, 1457.
15. Saigo, K.; Bailey, W. J.; Ento, T.; Okawara, M. *J Polym Sci Part A: Polym Chem* 1983, 21, 1435.
16. Canadell, J.; Mantecón, A.; Cádiz, V. *J Polym Sci Part A: Polym Chem* 2006, 44, 4722.
17. Canadell, J.; Mantecón, A.; Cádiz, V. *J Polym Sci Part A: Polym Chem* (in press).
18. Mas, C.; Ramis, X.; Salla, J. M.; Mantecón, A.; Serra, A. *J Polym Sci Part A: Polym Chem* 2003, 41, 2794.
19. Bringmann, G.; Breuning, M.; Henschel, P.; Hinrichs, J. *Org Synt Coll* 2002, 79, 72.
20. Neises, B.; Steglich, W. *Org Synt Coll* 1990, 7, 93.
21. *Organic Synthesis: The Roles of Boron and Silicon*. Thomas, S.E. Oxford University Press, 1992.
22. *Silicon Reagents in Organic Chemistry*. Colvin, E.W. Academic Press Limited, 1988.
23. Pretsch, E.; Clerc, T.; Seibl, J.; Simon, W. *Tablas para la elucidación estructural de compuestos orgánicos por métodos espectroscópicos*. Spanish Edition, Springer-Verlag Ibérica, Barcelona, 1998.
24. Tobolsky, A. V.; Carlson, D. W.; Indictor, N. J. *J Polym Sci* 1961, 54, 175.
25. Chung, K.; Takata, T.; Endo, T. *Macromolecules* 1997, 30, 2532.
26. Liu, Y-L.; Chiu, Y-C.; Wu, C-S. *J Polym Sci Part A: Polym Chem* 2003, 41, 404.
27. Kambour, R. P.; Lignon, W. V.; Russell, R. R. *J Polym Sci Part C: Polym Lett* 1978, 16, 327.



## COPOLYMERIZATION OF A SILICON-CONTAINING SPIROORTHOESTER WITH A PHOSPHORUS-CONTAINING DIGLYCIDYL COMPOUND. INFLUENCE IN FLAME RETARDANCE AND SHRINKAGE

J. Canadell, A. Mantecón, V. Cádiz

Departament de Química Analítica i Química Orgànica. Universitat Rovira i Virgili.  
Marcel·lí Domingo s/n, 43007 Tarragona, Spain

---

### Abstract

The cationic copolymerization of spiroorthoesters with diglycidyl compounds to introduce silicon and phosphorus has been carried out with ytterbium triflate as an initiator. The curing process was studied by Differential Scanning Calorimetry and monitored by Fourier Transform Infrared Spectroscopy. The thermomechanical and thermogravimetric properties were evaluated. The incorporation of phosphorus or silicon into the network increased the limiting oxygen index values, thus improving the flame retardance of the materials. The shrinkage during crosslinking for all mixtures was lower than that observed in conventional epoxy resins.

**Keywords:** cationic polymerization; heteroatom-containing polymer; flame retardance; crosslinking; spiroorthoester

---

### INTRODUCTION

In recent modern industry, epoxy resins play an important role due to their excellent characteristics of great versatility, toughness, good

moisture resistance, solvent and chemical resistance, outstanding adhesion, and superior electrical and mechanical properties. So, they are

widely applied in surface coating, adhesives, painting, composites, laminates, en-capsulants for semiconductor and insulating materials for electrical devices, etc.<sup>1,2</sup> However, epoxy resins have two main disadvantages: one is their flammability and the other is the shrinkage on curing. Up to now, research efforts on improving the properties of epoxy resins are under progress for meeting the requirements from the versatile and advanced applications. For epoxy resins used in electronics, superior thermal stability, electrical properties, and halogen-free in flame retardation were specially focused. The halogen-free flame retardants are environmentally friendly because they generate less toxic and corrosive substances during fire. The common halogen-free flame retardants are mainly organophosphorus<sup>3,4</sup> and organosilicon<sup>5,6</sup> compounds. Both elements are described that can function in the condensed phase or vapor phase, and possibly concurrently in both phases.<sup>7</sup>

Phosphorus-containing polymers confer fire resistance mainly by modifying the thermal decomposition of the polymers, in favor of reactions yielding carbonaceous char rather than CO and CO<sub>2</sub>. They form a surface layer of protective char during fire before the unburned material begins to decompose. The char layer acts as a barrier to inhibit gaseous products from diffusing to the flame and to shield the

polymer surface from heat and air.<sup>4,8,9</sup> However, oxidation of phosphorus char is observed at temperatures higher than 600 °C.<sup>10,11</sup> The efficiency of flame retardation of phosphorus basically depends on the amount of char formation; thus, by improving the thermal stability of phosphorus char at high temperatures could be improved the flame-retardancy efficiency. Silicon-containing polymers are described that can degrade forming thermally stable silica, which have the tendency to migrate to the char surface serving as a protection layer to prevent further degradation of char at high temperatures.<sup>5,12</sup>

Although, phosphorus or silicon compounds could be used alone as flame retardants, recently, when the flame retardants simultaneously contained both elements some synergistic effect has been described.<sup>12-14</sup> The reason for this synergistic effect is that phosphorus offers the tendency of char formation and silicon provides the thermal stability of the forming char during fire.<sup>6,14-16</sup>

Another problem of the epoxy resins is their shrinkage during curing, because the monomer molecules are located at a van der Waals distance from one another, while in the corresponding polymer the monomeric units move to a covalent distance of each other. Thus, the atoms are much closer to one another in the polymer than

they were in the original monomer. This shrinkage can lead to internal compressive stress in the material, poor adhesion of coatings to the substrate, and the appearance of microvoids and microcracks, which reduce the durability of materials.<sup>17</sup> One of the best solutions to solve the shrinkage is the use of monomers that show no volume shrinkage in their polymerization, such as spiroorthoesters (SOEs),<sup>18,19</sup> spiroor-thocarbonates (SOCs)<sup>20,21</sup> and bicy-clicorthoesters (BOEs).<sup>22</sup>

The aim of the present study is to reduce together the above mentioned disadvantages of epoxy resins by means of the cationic crosslinking of a new silicon-containing spiro-orthoester with mixtures of DGEBA and a phosphorus-containing glycidyl derivative. Also, the aim of this study is to investigate the possible synergistic effect of phosphorus-silicon on flame retardancy.

The cationic crosslinking was carried out with ytterbium triflate as initiator, which has shown to be effective to polymerize glycidyl compounds and spiroorthoesters.<sup>23</sup> This crosslinking was studied with differential scanning calorimetry (DSC) and Fourier transform infrared spectroscopy (FTIR). The materials were characterized by DSC, thermogravimetric analysis (TGA), and thermodynamomechanical analysis (DMTA). The volume change was evaluated with a Micromeritics gas

pycnometry and the flame retardancy was tested by the limiting oxygen index (LOI) measurements.

## EXPERIMENTAL

### Materials

Glycidol (Aldrich), glycidyl isopropyl ether (Aldrich),  $\gamma$ -butirolactone ( $\gamma$ -BL; Aldrich), boron trifluoride diethyl etherate ( $\text{BF}_3 \cdot \text{OEt}_2$ ; Aldrich), triethylamine (Fluka), trimethylsilylpropionic acid (Fluorochem), N-(3-Dimethyl-amino-propyl)-N'-ethyl-carbodiimide hydrochloride (EDC; Fluka), 4-(dimethylamino)pyridine (DMAP; Fluka), 1,4-benzoquinone (Aldrich), epichlorohydrin (EPC; Fluka), benzyl-trimethylammonium chloride (BTMA; Fluka), DGEBA (Epikote Resin 827, Shell Chemicals; epoxy equivalent = 182.08), ytterbium(III) trifluoromethanesulfonate [ $\text{Yb}(\text{OTf})_3$ ; Aldrich] were used as received. Commercial DOPO was kindly supplied by Aismalibar and it was purified before use by heating at 130 °C under vacuum for 2 h and then gradually heated to 150 °C. The purified product was cooled to room temperature under argon atmosphere. All solvents were purified by standard procedures.

### Instrumentation

NMR spectra ( $^1\text{H}$ , 400 MHz;  $^{13}\text{C}$  100.6 MHz) were obtained with a Varian Gemini 400 spectrometer

with Fourier transform, and  $\text{CDCl}_3$  as the solvent.

Crosslinking studies were performed on a Mettler DSC-821e thermal analyzer in covered Al pans under nitrogen at scan rates of  $10\text{ }^\circ\text{C}/\text{min}$ . The determination of glass transition temperatures ( $T_g$ 's) were carried out on a Mettler DSC-822e thermal analyzer in covered Al pans under  $\text{N}_2$  at scan rates of  $20\text{ }^\circ\text{C}/\text{min}$ . The samples weighed approximately 8 mg.

The IR spectrums were recorder with a 680 Plus FTIR spectrophotometer with a resolution of  $4\text{ cm}^{-1}$  in the absorbance mode. TGAs were carried out with a Mettler TGA/SDTA 851e thermobalance. Cured samples with an approximate mass of 10 mg were degraded between  $30\text{ }^\circ\text{C}$  and  $800\text{ }^\circ\text{C}$  at a heating rate of  $10\text{ }^\circ\text{C}/\text{min}$  in atmosphere of  $\text{N}_2$  or air.

Thermodynamomechanical analysis (DMTA) were carried out with a TA DMA 2928 thermal analyzer, working with three point bending clamp from  $-50\text{ }^\circ\text{C}$  to  $200\text{ }^\circ\text{C}$  with a heating rate of  $5\text{ }^\circ\text{C}/\text{min}$  and at fixed frequency of 1 Hz.

The densities of the materials were measured with a Micromeritics Accu-pyc 1330 TC gas pycnometer at  $30\text{ }^\circ\text{C}$ .

Limiting oxygen indices were measured on a Fire Testing Technology flammability unit in conformance with ASTM D 2863 for

samples measuring  $100\text{ mm} \times 6\text{ mm} \times 3\text{ mm}$ .

### **Synthesis of 2-hydroxymethyl-1,4,6-trioxaspiro [4,4] nonane (SOE-OH)**

Glycidol (30 g, 0.40 mol) was added dropwise over a period of 15 min at a temperature below  $10\text{ }^\circ\text{C}$  in an argon atmosphere to a mixture of 200 g (2.3 mol) of  $\gamma$ -BL and 1.0 mL (7.9 mmol) of  $\text{BF}_3 \cdot \text{OEt}_2$  as a catalyst. After the addition was completed, the mixture was stirred for 60 min at the same temperature. The reaction was quenched by the addition of 1.4 mL (10 mmol) of triethylamine. After the solvent was removed under reduced pressure, the residue was distilled fractionally to yield 11.2 g (17%) of a transparent, colorless liquid.

$^1\text{H}$  NMR ( $\text{CDCl}_3$ , two diastereomers):  $\delta(\text{ppm}) = 4.41\text{--}4.32$  (m, 2H, -O-CH-),  $4.14\text{--}4.03$  (m, 2H, -O-CH<sub>2</sub>-),  $3.99\text{--}3.89$  (m, 4H, -O-CH<sub>2</sub>-),  $3.85\text{--}3.80$  (m, 2H, -O-CH<sub>2</sub>-),  $3.73\text{--}3.54$  (m, 4H, -CH<sub>2</sub>-OH), 2.89 (br, 2H, OH),  $2.18\text{--}2.12$  (m, 4H, -CH<sub>2</sub>-),  $2.05\text{--}1.97$  (m, 4H, -CH<sub>2</sub>-).

$^{13}\text{C}$  NMR ( $\text{CDCl}_3$ , two diastereomers):  $\delta(\text{ppm}) = 129.60$  (s, spiranic C),  $129.32$  (s, spiranic C),  $75.99$  (s, -O-CH-),  $67.42$  (s, -O-CH<sub>2</sub>-),  $65.69$  (s, HO-CH<sub>2</sub>-),  $64.92$  (s, OH-CH<sub>2</sub>-),  $62.81$  (s, -O-CH<sub>2</sub>-),  $62.54$  (s, -O-CH<sub>2</sub>-),  $32.67$  (s, -CH<sub>2</sub>-),  $32.50$  (s, -CH<sub>2</sub>-),  $24.51$  (s, -CH<sub>2</sub>-),  $24.35$  (s, -CH<sub>2</sub>-).

**Synthesis of 1,4,6-trioxaspiro[4,4]-2-nonylmethyl 3-trimethylsilyl propionate (SOE-Si)**

Under an argon atmosphere, an oven-dried 100 mL round-bottom flask containing 20 mL of anhydrous dichloromethane was charged with 1.0 g (6.8 mmol) of trimethylsilyl propionic acid, 1.09 g (6.8 mmol) of SOE-OH, 1.44 g (7.5 mmol) of EDC, and 0.91 g (7.5 mmol) of DMAP. The solution was stirred and heated at 40 °C for 3 h. After cooling to room temperature, the solution was washed with two 30-mL portions of a 10% citric acid solution, twice with 30-mL portions of 10% sodium bicarbonate solution, and twice with brine. The organic solution was dried over anhydrous magnesium sulfate, and the solvent was removed by evaporation to give 1.97 g (90%) of a transparent, colorless liquid.

$^1\text{H}$  NMR ( $\text{CDCl}_3$ , two diastereomers):  $\delta(\text{ppm}) = 4.37\text{-}4.34$  (m, 1H, -O-CH-), 4.24-4.21 (m, 1H, -O-CH-), 4.15-4.13 (m, 2H, -O-CH<sub>2</sub>-), 4.12-3.96 (m, 4H, -CH<sub>2</sub>-OCO-), 3.86-3.75 (m, 4H, -O-CH<sub>2</sub>-), 3.69-3.64 (m, 2H, -O-CH<sub>2</sub>-), 3.63-2.14 (m, 4H, -CH<sub>2</sub>-COO-), 2.08-1.99 (m, 4H, -CH<sub>2</sub>-), 1.91-1.85 (m, 4H, -CH<sub>2</sub>-), 1.19-0.69 (m, 4H, -Si-CH<sub>2</sub>-), -0.08 (s, 8H, -CH<sub>3</sub>).

$^{13}\text{C}$  NMR ( $\text{CDCl}_3$ , two diastereomers):  $\delta(\text{ppm}) = 174.63$  (s, -COO-), 129.69 (s, spiranic C), 129.61 (s, spiranic C), 74.20 (s, -O-CH-), 73.32 (s, -O-CH-), 67.21 (s, -

O-CH<sub>2</sub>-), 67.14 (s, -O-CH<sub>2</sub>-), 65.99 (s, -O-CH<sub>2</sub>-), 65.89 (s, -CH<sub>2</sub>-OCO-), 64.95 (s, -CH<sub>2</sub>-O-), 64.05 (s, -O-CH<sub>2</sub>-), 32.61 (s, -CH<sub>2</sub>-), 28.56 (s, -CH<sub>2</sub>-COO-), 24.17 (s, -CH<sub>2</sub>-), 23.98 (s, -CH<sub>2</sub>-), 11.47 (s, -Si-CH<sub>2</sub>-), -2.03 (s, -CH<sub>3</sub>).

**Synthesis of 2-(isopropoxymethyl)-1,4,6-trioxaspiro [4,4]-2-nonane (SOE-iso)**

Glycidyl isopropyl ether (25 g, 0.2 mol) was added dropwise over a period of 20 min at a temperature below 10 °C in an argon atmosphere to a mixture of 55 g (0.6 mol) of  $\gamma$ -BL and 0.52 mL (4.1 mmol) of  $\text{BF}_3 \cdot \text{OEt}_2$  as a catalyst. After the addition was completed, the mixture was stirred for 2 h at the same temperature. The reaction was quenched by the addition of 1.0 mL (7.2 mmol) of triethylamine. After the solvent was removed under reduced pressure, the residue was distilled fractionally to yield 12.1 g (28 %) of a transparent, colorless liquid.

$^1\text{H}$  NMR ( $\text{CDCl}_3$ , two diastereomers):  $\delta(\text{ppm}) = 4.38\text{-}4.31$  (m, 1H, -O-CH-), 4.24-4.20 (m, 1H, -O-CH-), 4.12-4.07 (m, 2H, -O-CH<sub>2</sub>-), 3.91-3.87 (m, 2H, -O-CH<sub>2</sub>-), 3.78-3.76 (m, 4H, -O-CH<sub>2</sub>-), 3.66-3.32 (br, 6H, -O-CH<sub>2</sub>-, -CH<sub>3</sub>-CH-), 2.12-2.10 (m, 4H, -CH<sub>2</sub>-), 2.01-1.94 (m, 4H, -CH<sub>2</sub>-), 1.12 (s, 12H, -CH<sub>3</sub>).

$^{13}\text{C}$  NMR ( $\text{CDCl}_3$ , two diastereomers):  $\delta(\text{ppm}) = 129.60$  (s,

spiranic C), 75.58 (s, -O-CH-), 74.69 (s, -O-CH-), 72.44 (s, -CH<sub>3</sub>-CH-), 69.82 (s, -O-CH<sub>2</sub>-), 68.58 (s, -O-CH<sub>2</sub>-), 67.51 (s, -O-CH<sub>2</sub>-), 67.34 (s, -O-CH<sub>2</sub>-), 67.86 (s, -O-CH<sub>2</sub>-), 33.00 (s, -CH<sub>2</sub>-), 32.89 (s, -CH<sub>2</sub>-), 24.39 (s, -CH<sub>2</sub>-), 24.28 (s, -CH<sub>2</sub>-), 22.01 (s, CH<sub>3</sub>).

**Synthesis of 10-(2',5'-bis(glycidyl-oxy)phenyl)-9, 10-dihydro-9-oxa-10-phosphaphenanthrene-10-oxide (DOPO-BQ-Gly)**

DOPO-BQ-Gly was synthesized from DOPO and benzoquinone in a first step reaction, and this was followed by the reaction of the two phenolic groups with EPC and BTMA as a catalyst, as is described in the literature.<sup>24,26</sup>

**Crosslinking reactions**

The cationic crosslinking reactions were carried out by mixing the corresponding monomers in a molar ratio diglycidyl/SOE 2:1 with 1 phr of ytterbium triflate (1 phr = 1 part per 100 parts of the monomer mixture weight/weight). The composition of the mixtures is listed in Table 1. The sample bars used for dynamo-mechanical and thermogravimetric analysis and burn tests were cured in aluminium molds by heating in an



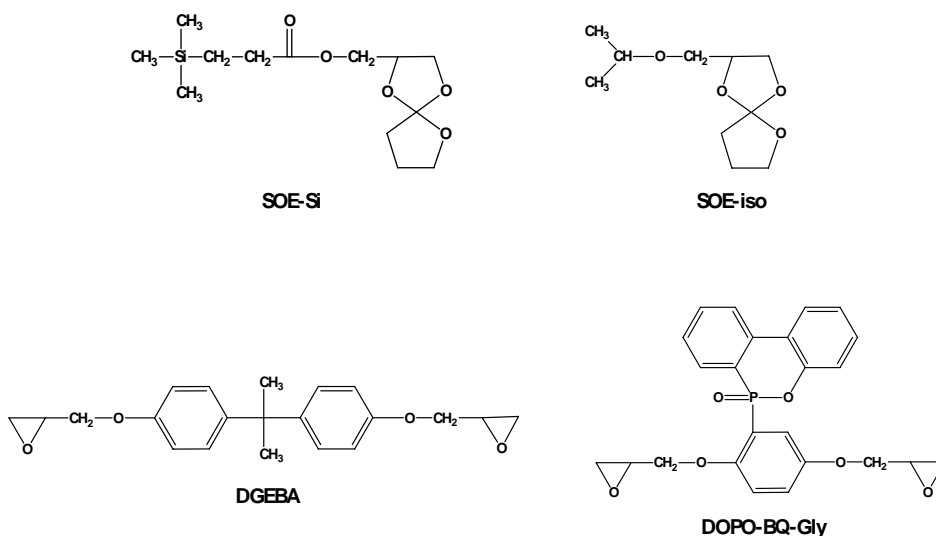
oven. The curing conditions were established by Dynamic Differential Scanning Calorimetry and are also listed in Table 1.

## RESULTS AND DISCUSSION

First, we synthesized the starting spiroorthoesters: SOE-Si and SOE-iso, one of them containing silicon in its structure, and the phosphorus-containing glycidyl compound (DOPO-BQ-Gly) (Scheme 1). SOE-Si was synthesized as previously described<sup>26</sup> by an esterification reaction between a commercially trimethylsilylpropionic acid and a previously synthesized hydroxyl-containing spiroorthoester (SOE-OH) under mild conditions using EDC and DMAP. The intermediate SOE-OH and the SOE-iso monomers were synthesized by a

cyclization reaction between  $\gamma$ -BL and a glycidyl compound: glycidol or glycidyl iso-propyl ether respectively. The phosphorus-containing glycidyl monomer (DOPO-BQ-Gly) was synthesized by a two steps reaction. First, DOPO was reacted with benzoquinone,<sup>24</sup> followed by the reaction of the two phenolic groups with EPC in excess and BTMA as a catalyst.<sup>25</sup>

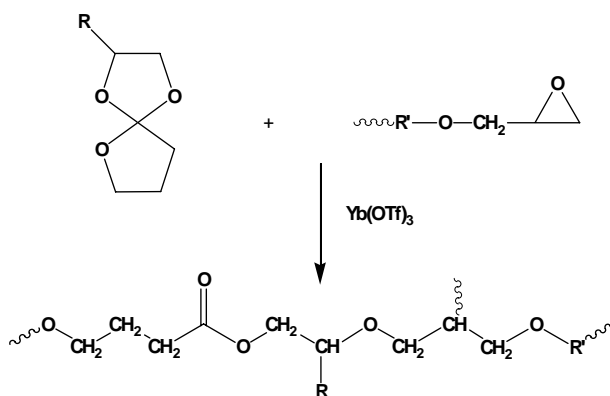
Silicon and phosphorus were introduced into the network from a silicon-containing spiroorthoester and a phosphorus-containing diglycidyl compound. To introduce different phosphorus and silicon contents in the mixtures, commercial DGEBA and an aliphatic spiroorthoester, SOE-iso, were also used. In all cases, the ratio of diglycidyl compounds:SOEs was 2/1 (mol/mol).



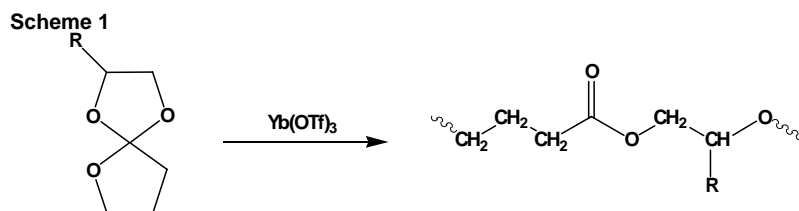
Scheme 1

In the cationic copolymerization of epoxy resins with spiroorthoesters three different processes are expected

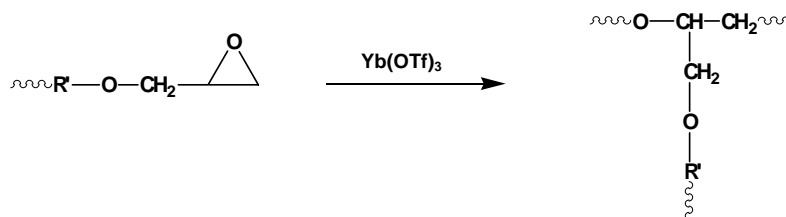
a) Copolymerization of glycidyl compounds with SOE



b) Homopolymerization of SOEs



c) Homopolymerization of glycidyl units



Scheme 2

ted (Scheme 2): a) reaction of SOE

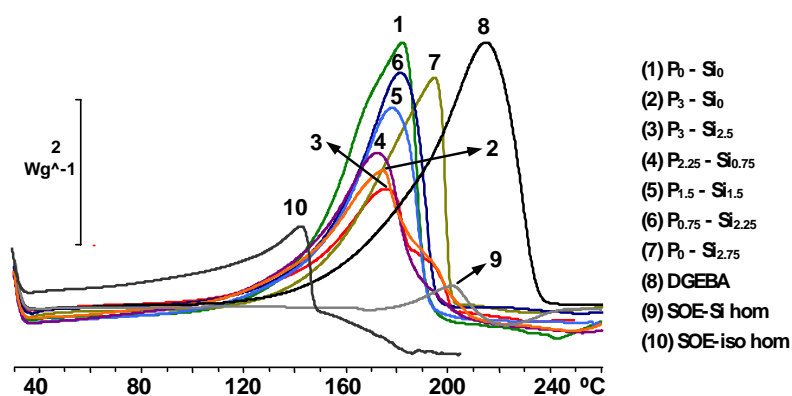
with epoxy groups, b) homopolymer-rization of SOE and c) homopolymer-rization of epoxy groups. Both processes a) and b) lead to the formation of linear ether-ester moieties whereas reaction c) only leads to ether linkages.

To study the combined effect of introducing silicon and phosphorus together we have prepared samples with different compositions which are listed in Table 1.

The crosslinking was studied by dynamic DSC. Figure 1 shows the calorimetric curves for the curing of different mixtures. In the same figure is indicated the P and Si content by means of subscripts (% weight). The crosslinking exotherms of DGEBA, SOE-Si and SOE-iso has been included for the purpose of comparison. As can be seen both SOEs have a low enthalpy as is reported in previous works,<sup>27,28</sup> but their reactivity is different, as show their crosslinking exotherms, being more reactive the silicon-free SOE. The crosslinking exotherms of the mixtures shift to higher

temperatures as silicon content increases probably due to the higher reaction temperature of SOE-Si. In Table 1 the temperatures of the maximum of the exotherms and the enthalpies are collected. As can be seen the enthalpies per epoxy equivalent decreases as the phos-phorus content increases. This could be attributed to the incomplete reaction of diglycidyl compounds, especially in the case of DOPO-BQ-Gly which must melts (about 150 °C) before reacting, whereas DGEBA is liquid and facilitates the reaction with SOEs at lower temperatures.

To confirm the reaction of SOEs and glycidyl compounds we recorded the FTIR spectra before and after crosslinking. On polymerizing, a new band of carbonyl of linear ester group formed must appear at 1735-1750  $\text{cm}^{-1}$ , but in the mixtures that contains SOE-Si a band at 1737  $\text{cm}^{-1}$ , due to its ester group, overlaps with the band of linear ester moieties, and therefore only an increase of this band was

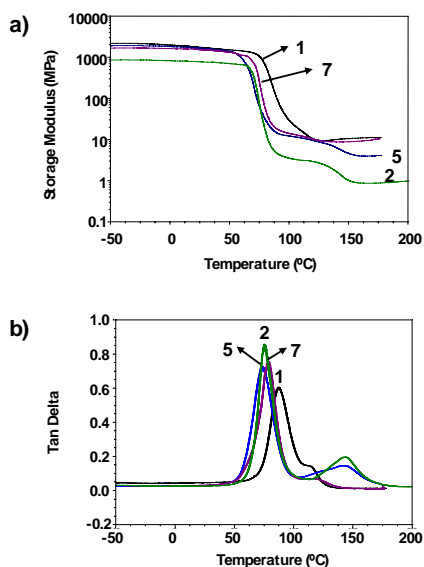


**Figure 1.** Dynamic DSC plots of different composition mixtures of 2:1 (mol:mol) (DGEBA/DOPO-BQ-Gly):(SOE-Si/SOE-iso), DGEBA and, SOEs initiated by 1 phr of  $\text{Yb}(\text{OTf})_3$  obtained at 10  $^\circ\text{C}/\text{min}$  heating rate. (submitted)

**Table 2.** DMA results of Cured Polymers and Volume Changes upon Crosslinking.

Entry	Tg <sup>a</sup> (°C)	E' max (°C)	Tan δ (°C)	Density (g/cm <sup>3</sup> )		Volume Change (%)
				Mixture	Crosslinked	
1	76	79	87	1.186	1.197	0.9
2	111	69/135	75/143	1.199	1.208	0.7
3	77	67/140	82/149	1.198	1.207	0.7
4	72	69/148	76/153	1.196	1.202	0.5
5	71	64/135	73/143	1.194	1.201	0.6
6	66	61	72	1.186	1.196	0.8
7	73	70	78	1.186	1.197	0.9
8	139	144	152	1.158	1.193	3

<sup>a</sup> Obtained by DSC.



**Figure 2.** Temperature dependence of Storage Modulus (a), and Tan Delta (b) for 1, 2, 5, 7 cured samples.

absorption at 916 cm<sup>-1</sup> due to oxirane ring normally confirms the complete crosslinking reaction, but in this case is difficult to confirm this disappearance because it partially overlaps with the band associated to the O-P-Ph moiety of DOPO-BQ-Gly, which appears about 920 cm<sup>-1</sup>.

The dynamic mechanical behavior of the crosslinked materials was obtained as a function of the temperature beginning in the glassy state to the rubbery plateau of each material. Figure 2 depicts the storage modulus (a) and Tan δ (b) of some representative samples: 1, without P and Si, 2, with only P, 5, with P and Si, and 7, with only Si. All samples showed a degree of non-homogeneity, but it is significant only for P-containing samples which show two maxima in Tan δ and two steps in the storage

observed. The disappearance of the

modulus. Table 2 collects  $\tan \delta$  and loss modulus values and the  $T_g$  values obtained by DSC are also included. All samples have similar  $T_g$ s but lower than pure DEGBA what agrees with the higher distance between knots as consequence of the linear ether-ester moieties introduced by the double ring-opening of SOEs. In the phosphorus-containing samples, the two maxima of  $\tan \delta$  appear clearly separated. The maximum at lower temperature can be associated to the SOE reaction, alone or with epoxy. The second maximum which corresponds to a more densely crosslinked material, can be associated to the homopolymerization of epoxy, mainly the phosphorus-containing DOPO-BQ-Gly, which needs to reach its melting point before

reacting.

The volume changes in the cross-linking reaction of all reactive mixtures were evaluated by density measurements with a Micromeritics gas pycnometer before and after crosslinking (Table 2). The volume change ( $\Delta$ ) was calculated from the following equation:

$$\Delta V (\%) = \frac{d_{\text{crosslinked polymer}} - d_{\text{initial mixture}}}{d_{\text{initial mixture}}} \times 100$$

where  $d$  is the density.

Sample 8, corresponding to pure DGEBA, show the typical volume shrinkage that generally accompanied the crosslinking reactions.<sup>30</sup>

<sup>a</sup> Temperature of 5% weight loss.

<sup>b</sup> Temperature of the maximum rate of degradation.

**Table 3.** TGA and LOI results for the Cured Polymers.

Entry	$T_{5\%}^a$ (°C)		$T_{\max}^b$ (°C)		Char yield at 800°C (wt%)		LOI
	N <sub>2</sub>	Air	N <sub>2</sub>	Air	N <sub>2</sub>	Air	
1	271	264	332	334/633	20.4	0.0	19.7
2	262	253	307/404	305/683	17.5	7.0	24.0
3	264	257	326/415	307/639	23.5	10.0	25.4
4	262	261	311/402	315/680	20.9	6.1	23.4
5	265	264	319	314/640	22.1	5.5	22.1
6	276	271	330	330/644	20.5	2.6	21.6
7	266	260	332	321/635	18.0	0.0	20.9
8	314	303	381	360/602	20.4	0.5	20.0

The SOE-containing samples 1-7 show a lower shrinkage (0.5-0.9%). Therefore, it can be concluded that the SOE moieties are effective monomers to obtain crosslinkable copolymers which do not shrink.

at similar temperatures, being slightly lower in air. The introduction of SOEs (sample 1) reduces the stability in comparison to pure DGEBA (sample 8). The

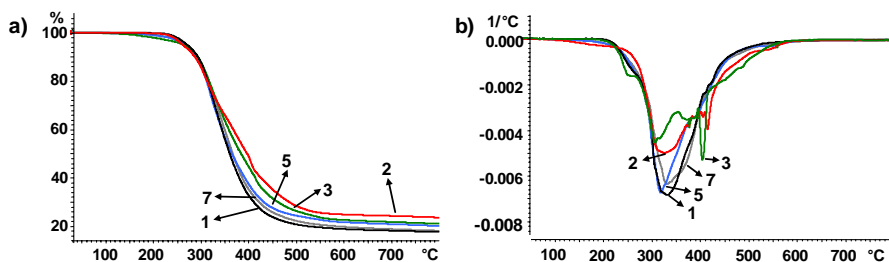


Figure 3. (a) TGA thermograms of samples: 1, 2, 3, 5, and 7 and (b) first derivative under

Thermogravimetric analysis (TGA) is one of the commonly used techniques for rapid evaluation of the thermal stability of different materials. Figure 3 and 4 show the TGA thermograms and DTG curves of some obtained thermosets, from room temperature to 800 °C, in nitrogen and air atmosphere respectively. Three parameters: temperatures for 5% weight loss, temperatures of the maximum loss rate and char residue at 800 °C, have been used to compare the thermal properties of the cured resins. The values of these parameters are tabulated in Table 3.

introduction of Si or P into the reactive mixtures does not decrease the thermal stability respect to the material 1. Thus, the stability diminution must be attributed to the ester groups in the network and not to the presence of Si or P.

Independent on the atmosphere, all the thermosets start the degradation

In N<sub>2</sub>, one or two-stage degradation was observed depending on the composition of the material. Two-stage degradation was detected for the samples that contain higher amount of phosphorus (3 and 2.25 P %wt), what seems to indicate that the second-stage degradation, which does not appear under air, corresponds to the phosphorus-containing compound. The char yields slightly increase with the presence of heteroatoms, mainly with P.

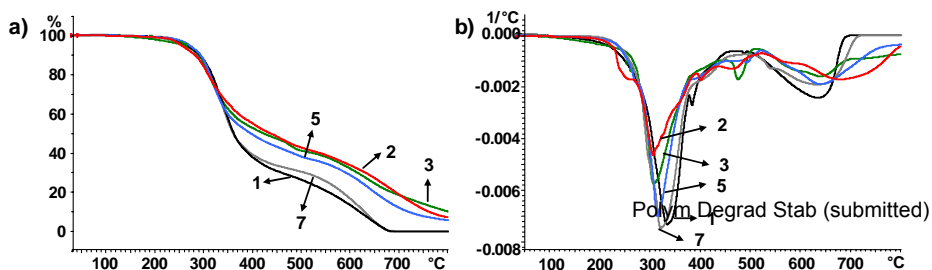


Figure 4. (a) TGA thermograms of samples: 1, 2, 3, 5, and 7 and (b) first derivative under

In air, the degradation initiates at slightly lower temperatures. Moreover, all the samples show at temperatures above 600 °C the typical stage of weight loss, arising from oxidative-degradation. In Figure 4 a) curves 1 (without Si and P) and 7 (with only Si) indicate that the presence of Si slightly increases the stability. By comparison of curves 2 (with only 3% of P) and 3 (with 3% of P and 2.5% of Si) we can observe a higher char yield for 3. The char yield increases with the P content and when Si is also present (sample 3) this increase is greater. Thus, it can be said that phosphorus provided a tendency of char formation and silicon favorably provides thermal stability of char as is previously reported.<sup>12</sup>

The LOI values, which can be taken as indicators to evaluate the polymer's flame retardancy for the materials, were measured and are shown in Table 3. From samples 1 (without Si and P) and 7 (with Si) we observe a slight increase of LOI value for the second. Sample 2 (with P) has a higher LOI value. Thus, based on the similar weight percent, it is noteworthy that phosphorus exhibits a relatively higher flame retardant efficiency than silicon. Whereas small amounts of P are sufficient to increase the LOI value<sup>4,31</sup> it seems that higher amount of silicon are needed to reach a similar effect.<sup>14,32</sup> Sample 3 shows the highest LOI value, as a consequence of both P and Si effect.

Polym Degrad Stab (submitted)

## CONCLUSIONS

The copolymerization of SOEs and diglycidyl compounds to introduce silicon and phosphorus has been carried out with ytterbium triflate as an initiator. The thermal stability of the materials increases with the introduction of both heteroatoms mainly with phosphorus. Silicon favourably provides thermal stability of char promoted by phosphorus. Small amounts of phosphorus are sufficient to increase the LOI values, but similar amount of silicon only slightly increase the LOI values. The crosslinking of all mixtures take place with low shrinkage, lower than those observed in conventional epoxy resins.

*The authors thank the Comisión Interministerial de Ciencia y Tecnología, CICYT, (MAT2005-01593 and MAT2005-01806) for providing financial support for this work.*

## REFERENCES AND NOTES

1. Epoxy Resins: Chemistry and Technology; May, C. A. Ed.; Marcel Dekker, New York, 1988.
2. Kinjo, N.; Ogata, M.; Nishi, K.; Kaneda, A. *Adv Polym Sci* 1989, 88, 1.

3. Jain, P.; Choudhary, V.; Varma, I. K. *J Macromol Sci Polym Rev* 2002, C42(2), 139.
4. Lu, S-Y.; Hamerton, I. *Prog Polym Sci* 2002, 27, 1661.
5. Hsue, G-H.; Wang, W-J.; Chang, F-C. *J Appl Polym Sci* 1999, 73, 1231.
6. Wang, W-J.; Perng, L. H.; Hsue, G-H.; Chang, F-C. *Polymer* 2000, 41, 6113.
7. Levchik, S.; Weil, E. *Polym Int* 2004, 53, 1901.
8. Liu, Y. L. *Polymer* 2001, 42, 3445.
9. Ebdon, J. R.; Jones, M. S. In *Polymeric Materials Encyclopedia*; J.C. Salomone, Ed., CRC Press, Boca Raton, FL, 1996.
10. Liu, Y. L.; Hsue, G. H.; Lan, C. W.; Chiu, Y. S. *J Polym Degrad Stab*, 1997, 56, 291.
11. Banerjee, S.; Palit, S. K.; Maiti, S. *J Polym Sci Polym Chem* 1994, 32, 219.
12. Hsue, G-H.; Liu, Y-L.; Tsiao, J. *J Appl Polym Sci* 2000, 78, 1.
13. Hsue, G-H.; Liu, Y-L.; Liao, H-H. *J Polym Sci Part A: Polym Chem* 2001, 39, 986.
14. Wu, C. S.; Liu, Y-L.; Chiu, Y-S. *Polymer* 2002, 43, 4277.
15. Ebdon, J. R.; Hunt, B. J.; Jones, M. S.; Thorpe, F. G. *Polym Degrad Stab* 1996, 54, 395.
16. Liu, Y-L.; Chou, C-I. *Polym Degrad Stab* 2005, 90, 515.
17. Expanding monomers: Synthesis, Characterization and Applications; Shadir, R. K.; Luck, R. M. Ed.; CRC Press: Boca Raton, FL, 1992.
18. Nishida, H.; Morikawa, H.; Nakahara, T.; Ogata, T.; Kusumoto, K.; Endo, T. *Polymer* 2005, 46, 2531.
19. Kume, M.; Hirano, T.; Ochiai, B., Endo, T. *J Polym Sci Part A: Polym Chem* 2006, 44, 3666.
20. Kume, M.; Maki, Y, Ochiai, B, Endo, T. *J Polym Sci Part A: Polym Chem* 2006, 44, 7040.
21. Nagai, D.; Nishida, M.; Nagasawa, T.; Ochiai, B.; Miyazaki, K.; Endo, T. *Macromol Rapid Commun* 2006, 27, 921.
22. Saigo, K.; Bailey, W. J.; Ento, T.; Okawara, M. *J Polym Sci Part A: Polym Chem* 1983, 21, 1435.
23. Mas, C.; Ramis, X.; Salla, J. M.; Mantecón, A.; Serra, A. *J Polym Sci Part A: Polym Chem* 2003, 41, 2794.
24. Cho C-S.; Chen L-W.; Chiu Y-S.; *Polymer Bull* 1998, 41, 45.
25. Serra, A.; Cádiz, V.; Mantecón, A.; Martínez, P.A. *Tetrahedron* 1985, 41, 763.
26. Canadell, J.; Mantecón, A.; Cádiz, V. *J Polym Sci Part A: Polym Chem* (Submitted).
27. Canadell, J.; Hunt, B. J.; Cook, A. G.; Mantecón, A.; Cádiz, V. *J Polym Sci Part A: Polym Chem* 2006, 44, 6728
28. Canadell, J.; Mantecón, A.; Cádiz, V. *J Polym Sci Part A: Polym Chem* (in press).
29. Liu, Y-L.; Tsai, S-H. *Polymer* 2002, 43, 5757.
30. Chung, K.; Takata, T.; Endo, T. *Macromolecules* 1997, 30, 2532.

31. Ebdon, J. R.; Jones, M. S. In *Polymeric Materials Encyclopedia*; J.C. Salomone, Ed., CRC Press, Boca Raton, FL, 1996, vol. 4, p. 2397.
32. Liu, Y-L.; Chiu, Y-C.; Wu, C-S. *J Polym Sci Part A: Polym Chem* 2003, 41, 404.

## PHOSPHORYLATED COPOLYMERS CONTAINING PENDANT, CROSSLINKABLE SPIROORTHOESTER MOIETIES

J. Canadell<sup>1</sup>, B. J. Hunt<sup>2</sup>, A. G. Cook<sup>2</sup>, A. Mantecón<sup>1</sup>, V. Cádiz<sup>1</sup>

<sup>1</sup> Departament de Química Analítica i Química Orgànica. Universitat Rovira i Virgili.  
Marcel·lí Domingo s/n, 43007 Tarragona, Spain

<sup>2</sup> Polymer Centre, Department of Chemistry, University of Sheffield, Sheffield S3 7HF,  
United Kingdom

---

### Abstract

The synthesis of a novel spiroorthoester containing monomer, 1,4,6-trioxaspiro[4,4]-2-nonylmethyl acrylate, is presented. This monomer was polymerized via a free-radical system to yield the homopolymer and a series of copolymers with phosphorus-containing comonomers. Diethyl vinyl phosphonate, allyldiphenyl phosphine oxide, and diethyl(methacryloyloxymethyl)phosphonate were used in various feed ratios to produce copolymers with different phosphorus concentrations containing crosslinkable spiroorthoester side-chain units. The crosslinking of the polymers was performed cationically with ytterbium triflate, and in all cases, the expansion of the polymer was observed. Moreover, the incorporation of phosphorus into the copolymers increases the limiting oxygen indices, regardless of the percentage of phosphorus used.

**Keywords:** cationic polymerization; copolymerization; crosslinking; flame retardance; heteroatom-containing polymers; radical copolymerization; spiroorthoesters; ytterbium triflate

---

### INTRODUCTION

A major concern for the production of polymeric materials is shrinkage upon crosslinking or curing. This is a particular problem in the coating, casting, molding and microelectronics industries. It can cause poor adhesion to a substrate, delamination, microvoids, and microcracks, which in turn can reduce the durability of a product. A number of different techniques have been employed to reduce shrinkage, such as the addition of fillers and curing at lower temperatures. However, these methods are not totally efficient as the shrinkage is due to the crosslinking reaction rather than as a consequence of production methods.

The most effective method of solving this problem is to use monomers with groups that undergo polymerization with nearly zero shrinkage or expansion. A number of cyclic monomers have been reported that appear to maintain their volume or actually expand during the double ring-opening polymerization.<sup>1-5</sup> Among these are the spiroorthoesters (SOEs); these materials are easily prepared from epoxides and lactones and exhibit a wide variety of structures.<sup>6-8</sup> The addition of a vinyl or acrylate for radical polymerization allows the SOE moiety to be carried into the polymeric system for later crosslinking.<sup>9</sup> Copolymers containing SOE moieties can be crosslinked, without significant shrinkage, by cationic double ring-opening polymerization by Lewis acid catalysts.

The flammability of organic polymers has become a major research interest in recent years because of the increasing use of polymeric materials in both domestic and public environments. Although halogen-containing flame retardants are exceptionally efficient, they have clear disadvantages, as they generate toxic and corrosive gases during thermal degradation. In recent times, developments in the chemistry of halogen-free flame-retardant polymers have involved the incorporation of a number of heteroelements such as P, Si, B, and N, and other miscellaneous elements.<sup>10</sup> For years, phosphorylation has been considered one of the most efficient means of conferring flame retardancy on synthetic polymer materials.<sup>11-13</sup>

In this article, the radical copolymerization of SOE and a phosphorus-containing comonomer is presented. The shrinkage effects of the copolymer during cationic cross-linking reactions are assessed by gas pycnometry. The flame-retardant properties of the polymers are determined by limiting oxygen index (LOI) measurements.

## EXPERIMENTAL

### Materials

Epibromohydrin (Fluka),  $\gamma$ -butyrolactone ( $\gamma$ -BL; Aldrich), boron trifluoride diethyl etherate ( $\text{BF}_3 \cdot \text{OEt}_2$ ; Aldrich),

triethylamine (Fluka), acrylic acid (Aldrich), 1,8-diazabicyclo[5.4.0]-undec-7-ene (DBU; Aldrich), 3-*tert*-butyl-4-hydroxy-5-methylphenyl sulfide (Aldrich), diethyl vinyl phosphonate (DEVP; Aldrich), allyldiphenylphosphine oxide (ADPPO; Aldrich), methacryloyl chloride (Aldrich), diethylhydroxymethylphosphonate (Aldrich), ytterbium (III) trifluoromethanesulfonate [Yb(OTf)<sub>3</sub>; Aldrich] were used as received. 2,2'-Azobisisobutyronitrile (AIBN; Aldrich) which was recrystallized from methanol before use. All solvents were purified with standard procedures.

### Instrumentation

<sup>1</sup>H NMR (400 MHz), <sup>13</sup>C NMR (100.6 MHz), and <sup>31</sup>P NMR (161.9 MHz) spectra were obtained with a Varian Gemini 400-MHz Fourier transform spectrometer with CDCl<sub>3</sub> as the solvent and tetramethylsilane or phosphoric acid as the internal standard.

Crosslinking studies were performed on a Mettler DSC-821e thermal analyzer in covered Al pans under N<sub>2</sub> at a scanning rate of 10 °C/min. The determination of the glass transition temperatures (T<sub>g</sub>'s) was carried out on a Mettler DSC-822e thermal analyzer in covered Al pans under N<sub>2</sub> at scanning rate of 20 °C/min.

The isothermal polymerization process at 80 °C was monitored with

an FTIR-680 Plus spectrophotometer with a resolution of 4 cm<sup>-1</sup> in the absorbance mode. An attenuated-total-reflection accessory with thermal control and a diamond crystal was used to obtain Fourier transform infrared/attenuated total reflection (FTIR-ATR) spectra.

Thermogravimetric analyses (TGAs) were performed with a Mettler TGA/SDTA 851e thermobalance. Cured samples with an approximate mass of 8 mg were degraded between 30 and 800 °C at a heating rate of 10 °C/min under nitrogen and air atmospheres.

The molecular weight distribution of the polymers was determined with a Waters gel permeation chromatograph equipped with a Waters 510 differential refractive-index detector (RID-6A from Shimadzu). The gel permeation chromatograph was operated using three Waters Shodex columns (K80M, 5-μ mixed-D gel, and 3-μ mixed-E gel) at a nominal flow rate of 1 mL/min and with a sample concentration of 0.1% in tetrahydrofuran as the solvent. Monodispersed polystyrene standards were purchased from Polymer Laboratories for instrument calibration.

The densities of the materials were measured with a Micromeritics Accu-pyc 1330 TC gas pycnometer at 30 °C.

LOIs were measured on a Fire Testing Technology flammability unit in conformance with ASTM D 2863 for samples measuring 100 mm x 6 mm x 3 mm and supported on glass fibers.

### Monomer Synthesis

#### Synthesis of 2-Bromomethyl-1,4,6-trioxaspiro [4,4] nonane (SOE-Br)<sup>6</sup>

Epibromohydrin (50 g, 0.36 mol) was added dropwise over a period of 15 min at a temperature below 10 °C in an argon atmosphere to a mixture of 180 g (2.09 mol) of  $\gamma$ -BL and 1.5 mL (11.8 mmol) of  $\text{BF}_3 \cdot \text{OEt}_2$  as a catalyst. After the addition was completed, the mixture was stirred for 60 min at the same temperature. The reaction was quenched by the addition of 1.9 mL (13.5 mmol) of triethylamine. The solvent was removed under reduced pressure, and the residue was fractionally distilled to yield 60.4 g (74 %) of a transparent, colorless liquid.

<sup>1</sup>H NMR ( $\text{CDCl}_3$ , two diastereomers):  $\delta$ (ppm) = 4.54-4.48 (m, 1H, -O-CH-), 4.43-4.37 (m, 1H, -O-CH-), 4.21-4.17 (dd, 2H, -O-CH<sub>2</sub>-), 3.98-3.87 (m, 6H, -O-CH<sub>2</sub>-), 3.91-3.31 (m, 4H, Br-CH<sub>2</sub>-), 2.20-2.11 (m, 4H, -CH<sub>2</sub>-), 2.05-1.98 (m, 4H, -CH<sub>2</sub>-).

<sup>13</sup>C NMR ( $\text{CDCl}_3$ , two diastereomers):  $\delta$ (ppm) = 129.98 (s, spiranic C), 129.88 (s, spiranic C), 75.48 (s, -O-CH-), 74.74 (s, -O-CH-

), 68.72 (s, -O-CH<sub>2</sub>-), 67.68 (s, -O-CH<sub>2</sub>-), 67.40 (s, -O-CH<sub>2</sub>-), 67.38 (s, -O-CH<sub>2</sub>-), 32.87 (s, -CH<sub>2</sub>-), 32.81 (s, -CH<sub>2</sub>-), 32.74 (s, Br-CH<sub>2</sub>-), 32.28 (s, Br-CH<sub>2</sub>-), 24.20 (s, -CH<sub>2</sub>-), 24.05 (s, -CH<sub>2</sub>-).

#### Synthesis of 1,4,6-Trioxaspiro [4,4]-2-nonylmethyl Acrylate (SOE-AC)<sup>14</sup>

SOE-Br (10 g, 45.0 mmol) in 10 mL of anhydrous dimethyl sulfoxide (DMSO) was added slowly to a mixture of 3.24 g (45.0 mmol) of acrylic acid and 6.84 g (45.0 mmol) of DBU in 20 mL of anhydrous DMSO and stored under an argon atmosphere in a three-necked flask in a bath at 65 °C. This mixture was stirred vigorously for a period of 30 min during the addition. After the addition was complete, the mixture was stirred for an additional 5 h at the same temperature. The radical inhibitor, 3-*tert*-butyl-4-hydroxy-5-methylphenyl sulfide (8 mg), was added when the reaction had reached completion. The desired product was taken out of DMSO with several extractions with  $\text{CH}_2\text{Cl}_2$  (4 x 30 mL). The product was purified through washing with a dilute solution of HCl and was then neutralized with a solution of NaOH. The dichloromethane solution was dried over  $\text{MgSO}_4$  and evaporated. After the removal of the SOE-Br impurities under reduced pressure, 7.27 g (76%) of a transparent liquid was yielded.

$^1\text{H}$  NMR ( $\text{CDCl}_3$ , two diastereomers):  $\delta(\text{ppm}) = 6.46\text{--}6.41$  (dd, 1H,  $J_{\text{trans}} = 16.8$  Hz,  $J_{\text{cis}} = 1.6$  Hz, C=CH),  $6.44\text{--}6.40$  (dd, 1H,  $J_{\text{trans}} = 17.2$  Hz,  $J_{\text{cis}} = 1.6$  Hz, C=CH),  $6.17\text{--}6.01$  (m, 2H, C=CH<sub>2</sub>),  $5.87\text{--}5.84$  (dd, 1H,  $J_{\text{cis}} = 9.6$  Hz,  $J_{\text{gem}} = 1.2$  Hz, C=CH<sub>2</sub>),  $5.86\text{--}5.83$  (dd, 1H,  $J_{\text{cis}} = 10.8$  Hz,  $J_{\text{gem}} = 1.6$  Hz, C=CH<sub>2</sub>),  $4.35\text{--}3.50$  (m, 1H, -O-CH-),  $4.38\text{--}4.32$  (m, 1H, -O-CH-),  $4.38\text{--}4.01$  (m, 6H, -O-CH<sub>2</sub>-),  $3.96\text{--}3.89$  (m, 4H, -O-CH<sub>2</sub>-),  $3.84\text{--}3.77$  (m, 2H, -O-CH<sub>2</sub>-),  $2.16\text{--}2.10$  (m, 4H, -CH<sub>2</sub>-),  $2.04\text{--}1.99$  (m, 4H, -CH<sub>2</sub>-).

$^{13}\text{C}$  NMR ( $\text{CDCl}_3$ , two diastereomers):  $\delta(\text{ppm}) = 166.04$  (s, C=O),  $131.73$  (s, C=CH<sub>2</sub>),  $129.98$  (s, spiranic carbon),  $128.11$  (s, C=CH),  $74.32$  (s, -O-CH-),  $73.47$  (s, -O-CH-),  $67.58$  (s, -O-CH<sub>2</sub>-),  $66.29$  (s, -O-CH<sub>2</sub>-),  $66.16$  (s, -O-CH<sub>2</sub>-),  $65.32$  (s, -O-CH<sub>2</sub>-),  $64.41$  (s, -O-CH<sub>2</sub>-),  $32.89$  (s, -CH<sub>2</sub>-),  $24.41$  (s, -CH<sub>2</sub>-),  $24.22$  (s, -CH<sub>2</sub>-).

**Synthesis of Diethyl(methacryloyloxymethyl)phosphonate (DEMMP)**<sup>15,16</sup>

A mixture of 16.8 g (0.10 mol) of diethyl (hydroxymethyl)phosphonate and 12 g (0.12 mol) of triethylamine was dissolved in anhydrous dichloro-methane (100 mL), cooled in an iced bath, and purged with argon. To this solution was added, dropwise with stirring, an argon-purged solution of 11.5 g (0.11 mol) of methacryloyl chloride in anhydrous dichloro-methane (30

mL). The mixture was then warmed to room temperature and stirred for 18 h more. The precipitated triethylamine hydrochloride was removed by filtration. The solution was then evaporated to remove the solvent, cooled overnight in a freezer, filtered again, and washed with deionised water to leave yield a brown oil. 3-*tert*-Butyl-4-hydroxy-5-methylphenyl sulphide (8 mg) was added to serve as polymerization inhibitor, and the oil was distilled under reduced pressure to yield 16.9 g (72%) of a colorless, viscous liquid (bp = 109 °C at 0.6 mmHg).

$^1\text{H}$  NMR ( $\text{CDCl}_3$ ):  $\delta(\text{ppm}) = 6.23$  (d, 1H, vinyl),  $5.72$  (d, 1H, vinyl),  $4.51$  (d, 2H, -O-CH<sub>2</sub>-P),  $4.23$  (m, 4H, P-O-CH<sub>2</sub>-),  $2.04$  (s, 3H, =C-CH<sub>3</sub>),  $1.45$  (t, 6H, -CH<sub>3</sub>).

$^{13}\text{C}$  NMR ( $\text{CDCl}_3$ ):  $\delta(\text{ppm}) = 166.41$  (d, C=O,  $J_{\text{C-P}} = 8.4$  Hz),  $135.40$  (s, C=),  $127.14$  (s, =CH<sub>2</sub>),  $62.91$  (d, -O-CH<sub>2</sub>-P,  $J_{\text{C-P}} = 6.1$  Hz),  $57.13$  (d, -O-CH<sub>2</sub>-P,  $J_{\text{C-P}} = 169.4$  Hz),  $18.48$  (s,  $\alpha$ -CH<sub>3</sub>),  $16.55$  (d, CH<sub>3</sub>,  $J_{\text{C-P}} = 5.3$  Hz).

$^{31}\text{P}$  NMR ( $\text{CDCl}_3$ ):  $\delta(\text{ppm}) = 19.7$ .

## Polymer Synthesis

### Homopolymerization of SOE-AC

A solution of 3 g (14.0 mmol) of SOE-AC and 69.1 mg (0.42 mmol) of AIBN in benzene (20 mL) in a sealed ampule was heated in a water bath at 65 °C for 40 h. The reaction mixture was added

dropwise into *n*-hexane to precipitate the polymer as a white powder. The polymer was further purified by reprecipitation of the dissolved polymer from dry dichloromethane into *n*-hexane. The yield was 2.0 g (66%).

<sup>1</sup>H NMR (CDCl<sub>3</sub>, two diastereomers): δ(ppm) 4.45 (br, -O-CH-), 4.31 (br, -O-CH-), 4.12 (br, -O-CH<sub>2</sub>-), 3.93 (br, -O-CH<sub>2</sub>-), 3.74 (br, -O-CH<sub>2</sub>-), 2.30 (br, main chain -CH-), 2.10 (br, -CH<sub>2</sub>-), 1.97 (br, -CH<sub>2</sub>-), 1.64 (br, main chain -CH<sub>2</sub>-).

<sup>13</sup>C NMR (CDCl<sub>3</sub>, two diastereomers): δ(ppm) 174.33 (s, C=O), 129.98 (s, spiranic C), 129.86 (s, spiranic C), 74.07 (s, -O-CH-), 73.28 (s, -O-CH-), 67.46 (s, -O-CH<sub>2</sub>-), 67.40 (s, -O-CH<sub>2</sub>-), 66.60 (s, -O-CH<sub>2</sub>-), 66.21 (s, -O-CH<sub>2</sub>-), 65.76 (s, -O-CH<sub>2</sub>-), 64.64 (s, -O-CH<sub>2</sub>-), 41.45 (s, main chain -CH<sub>2</sub>-), 35.28 (s, main chain -CH-), 32.87 (s, -CH<sub>2</sub>-), 24.47 (s, -CH<sub>2</sub>-), 24.28 (s, -CH<sub>2</sub>-).

#### Copolymerization of SOE-AC with Phosphorus-Containing Monomers

Copolymerizations of the phosphorus-containing monomers with SOE-AC were carried out in benzene with a procedure similar to that for the homopolymerization of SOE-AC. The initiator used was AIBN, and the reaction was performed at 65 °C. The initiator concentrations were 3 mol % in all cases. All the copolymers were

recovered by precipitation in *n*-hexane. The purification of DEVP- and DEMMP-based copolymers was carried out by the reprecipitation of the dissolved polymer from dry dichloromethane into *n*-hexane. The purification of ADPPO-based copolymers was performed as follows: the polymer was washed twice with methanol (to remove any unreacted ADPPO), and then the dissolved polymer was reprecipitated from dry dichloromethane into *n*-hexane.

#### SOE-AC/DEVP.

<sup>1</sup>H NMR (CDCl<sub>3</sub>, two diastereomers): δ(ppm)= 4.45 (br, -O-CH-), 4.32 (br, -O-CH-), 4.14 (br, -O-CH<sub>2</sub>-, -P-O-CH<sub>2</sub>-), 3.89 (br, -O-CH<sub>2</sub>-), 3.78 (br, -O-CH<sub>2</sub>-), 3.62 (br, main chain -CH-P-), 2.37 (br, main chain -CH-), 2.12 (br, -CH<sub>2</sub>-), 1.96 (br, -CH<sub>2</sub>-), 1.86 (br, -CH<sub>2</sub>-), 1.83 (br, main chain -CH<sub>2</sub>-), 1.64 (br, main chain -CH<sub>2</sub>-), 1.27 (br, -CH<sub>3</sub>-).

<sup>31</sup>P NMR (CDCl<sub>3</sub>): δ(ppm)= 31.3 (br).

#### SOE-AC/ADPPO.

<sup>1</sup>H NMR (CDCl<sub>3</sub>, two diastereomers): δ(ppm) 7.74 (br, Ar-H), 7.50 (br, Ar-H), 4.51 (br, -O-CH-), 4.39 (br, -O-CH-), 4.12 (br, -O-CH<sub>2</sub>-), 3.90 (br, -O-CH<sub>2</sub>-), 3.79 (br, -O-CH<sub>2</sub>-), 3.52 (br, -P-CH<sub>2</sub>-), 2.40 (br, main chain -CH-), 2.15 (br, -CH<sub>2</sub>-), 2.01 (br, -CH<sub>2</sub>-), 1.89 (br, main chain -CH<sub>2</sub>-), 1.71 (br, main chain -CH<sub>2</sub>-).

$^{31}\text{P}$  NMR ( $\text{CDCl}_3$ ):  $\delta(\text{ppm})$  32.1 (br).

SOE-AC/DEMMP.

$^1\text{H}$  NMR ( $\text{CDCl}_3$ , two diastereomers):  $\delta(\text{ppm})$  = 4.49 (br, -O-CH), 4.38 (br, -O-CH-), 4.21 (br, -O-CH<sub>2</sub>-, -P-O-CH<sub>2</sub>-), 3.98 (br, -O-CH<sub>2</sub>-), 3.84 (br, -O-CH<sub>2</sub>-), 3.67 (br, -O-CH<sub>2</sub>-P-), 2.42 (br, main chain -CH-), 2.17 (br, -CH<sub>2</sub>-), 2.02 (br, -CH<sub>2</sub>-), 1.91 (br, main chain -CH<sub>2</sub>-), 1.71 (br, main chain -CH<sub>2</sub>-), 1.38 (br, -CH<sub>3</sub>), 1.21 (br, -C-CH<sub>3</sub>).

$^{31}\text{P}$  NMR ( $\text{CDCl}_3$ ):  $\delta(\text{ppm})$  20.5 (br)

### Crosslinking Reactions

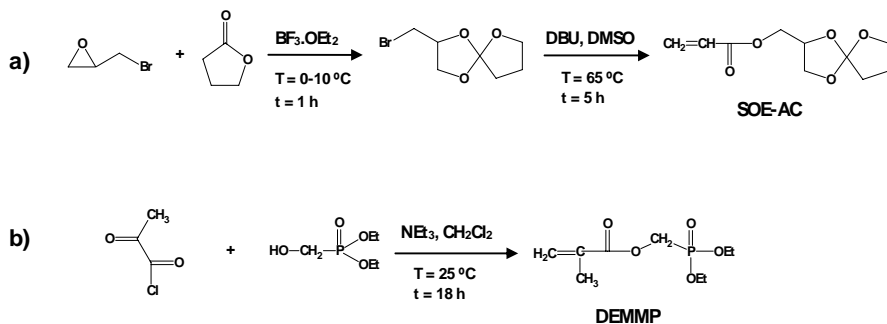
The cationic crosslinking reactions of SOE-containing copolymers were carried out via the mixing of the corresponding copolymer with 1phr ytterbium triflate, and after suitable

homogeneization, the mixture was heated at 80 °C for 5 h.

## RESULTS AND DISCUSSION

A novel SOE-containing monomer, SOE-AC, was synthesized via the reported procedure for the ester synthesis by direct C-O bond formation between carboxylic acids and halides in the presence of a strong base such as DBU.<sup>17</sup> SOE-AC was prepared by the reaction of SOE-Br with acrylic acid in the presence of DBU under mild conditions [(Scheme 1(a)]. SOE-Br was obtained from epibromohydrin and  $\gamma$ -BL in a  $\text{BF}_3 \cdot \text{OEt}_2$  catalyzed reaction.<sup>6</sup>

122 | Crosslinking through Spiroorthoesters

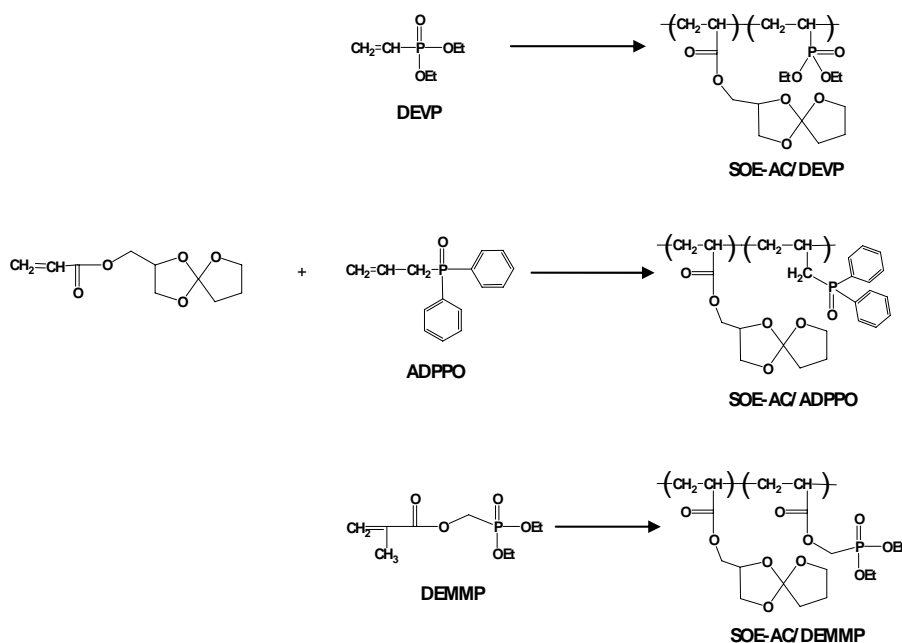


Scheme 1

A series of phosphorus-containing, unsaturated comonomers were used: DEVP; ADPPO and DEMMP (Scheme 2). DEVP and ADPPO are commercial materials, whereas DEMMP was synthesized by the esterification of methacryloyl

chloride and diethylhydroxymethyl phosphonate as shown in Scheme 1(b).

The homopolymerization of SOE-AC and the copolymerization of SOE-AC with the phosphorus-



Scheme 2

<sup>a</sup> Estimated by <sup>1</sup>H NMR

<sup>b</sup> Weight-average molecular weight estimated by GPC (based on polystyrene standards).

Polymer	Monomer Feed Ratio (mol %) SOE: monomer P (wt% P)	Copolymer Composition (mol %) SOE: monomer P (wt% P) <sup>a</sup>	Yield (%)	M <sub>w</sub> × 10 <sup>4</sup> <sub>b</sub>	T <sub>g</sub> (°C)
SOE-AC	100:0 (0%)	100:0 (0%)	66	2.5	32
SOEAC/DEV	80:20 (3%)	80:20 (3.1%)	54	2.9	24
	62:38 (6%)	63:37 (5.8%)	47	2.1	22
SOE-	79:21 (3%)	81:19 (2.7%)	41	1.0	47
AC/ADPPO	56:44 (6%)	77:23 (3.2%)	35	1.3	48
SOE-	79:21 (3%)	72:28 (3.9%)	61	2.9	25
AC/DEMMP	57:43 (6%)	52:48 (6.6%)	53	0.9	20

containing un-saturated comonomers, via a radical polymerization using AIBN as the initiator, were carried out in sealed tubes at 65 °C in benzene for 36-44 h (Scheme 2). In all cases, two different ratios of the comonomers were used to obtain phosphorus content of either 3 or 6% (Table 1). The unimodal, but broad gel permeation chromatography (GPC) curves of the obtained copolymers supported the successful copolymerizations. The structures of the polymers were confirmed with <sup>1</sup>H, <sup>13</sup>C, and <sup>31</sup>P NMR and IR spectroscopy. The composition of the copolymers was determined by the integration ratios of the following signals in <sup>1</sup>H NMR: for SOE-AC/DEV, 4.6-3.7 ppm (7 H<sub>SOE</sub> + 4H<sub>DEV</sub>) and 1.4-1.2 ppm (6H<sub>DEV</sub>); for SOE-AC/ADPPO, 8-7.3 ppm (10H<sub>ADPPO</sub>) and 4.6-3.4 ppm (7H<sub>SOE</sub> + 2H<sub>ADPPO</sub>); and for SOE-AC/DEMMP, 4.6-3.5 ppm (7H<sub>SOE</sub> +

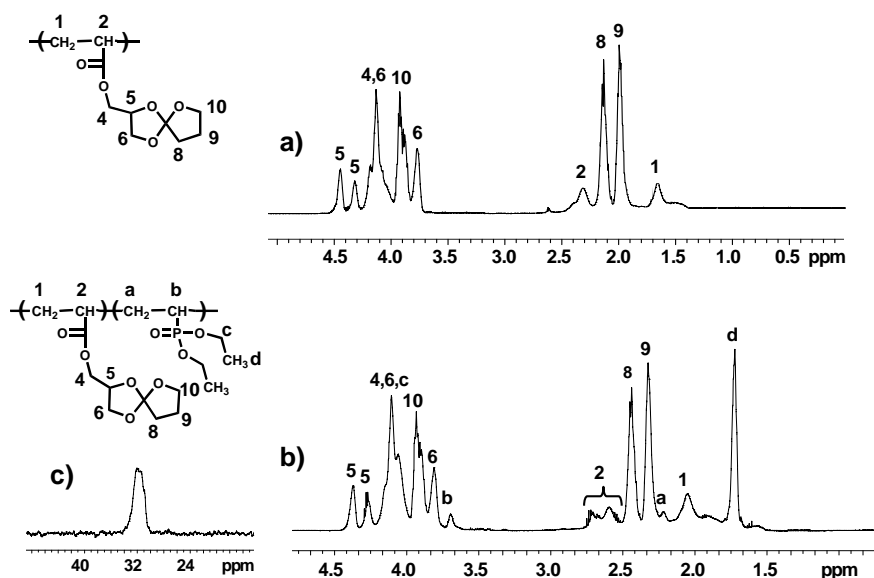
6H<sub>DEMMP</sub>) and 1.5-1.3 ppm (6H<sub>DEMMP</sub>).

In Figure 1, the <sup>1</sup>H NMR spectrum of the homopolymer and <sup>1</sup>H and <sup>31</sup>P NMR spectra of the SOE-AC/DEV copolymer are shown. In the <sup>1</sup>H NMR spectrum of SOE-AC/DEV [Fig.1(b)] the signals corresponding to the phosphorus-containing comonomer are clearly identifiable. The <sup>31</sup>P NMR spectrum is shown [Fig.1(c)]; the single <sup>31</sup>P signal is split due to the presence of different diastereomers and the sequential distribution of the comonomers. For the same reason, in the <sup>1</sup>H NMR spectra, some signals are also split.

The IR spectra of the copolymers show absorption bands in the region 1200-1000 cm<sup>-1</sup> assignable to the SOE moieties, as well as absorptions at 1732 cm<sup>-1</sup> due to the carbonyl ester group and at 1242

and  $1163\text{ cm}^{-1}$  due to  $\text{P}=\text{O}$  absorption and corresponding to the phosphonate and phosphine oxide moieties, respectively.

weights, determined by size exclusion chromatography are shown in Table 1 within a range of  $0.9 \times 10^4$  to  $2.9 \times 10^4$  g/mol. The  $T_g$  values of the copolymers are also



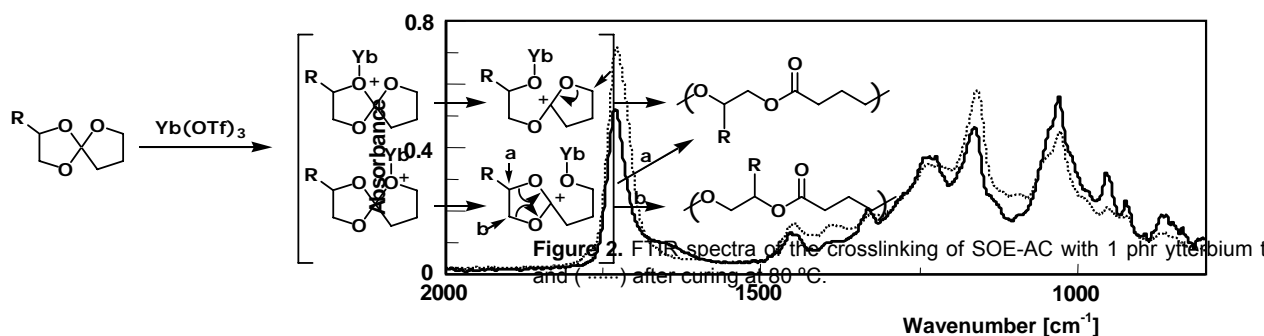
**Figure 1.** (a)  $^1\text{H}$  NMR spectrum of homopolymer SOE-AC, (b)  $^1\text{H}$  NMR spectrum of copolymer SOE-AC/DEVP (80/20), and (c)  $^{31}\text{P}$  NMR spectrum of copolymer SOE-AC/DEVP (80/20).

In the copolymerizations, the initial feed ratios and the copolymer compositions observed were in excellent agreement for SOE-AC/DEVP and SOE-AC/DEMMP. However, the SOE-AC/ADPPO copolymers showed a lower than expected incorporation of the phosphorus-containing comonomer, with a more pronounced decreased incorporation at higher phosphorus feed ratio (Table 1). These results seem to indicate that the ADPPO monomer is less reactive than the other comonomers. The molecular

shown in Table 1.  $T_g$  in the DEVP and DEMMP copolymers decreased as the amount of the phosphorus-containing monomer increased. This was probably due to a decrease in the bulky and rigid SOE moieties. Upon the addition of the DEVP and DEMMP comonomers to SOE, there was an apparent decrease in  $T_g$ . This decrease may have been due to the ethylene units from the comonomer breaking up the stacking of the SOE. This was supported by the observation of reduced  $T_g$  values as the concentration of the phosphorus-

containing comonomers was further increased. When the comonomer ADPPO was added, an increase in  $T_g$  appeared. This may have been due to the aromatic units stabilizing the SOE stacking. However, upon further addition of ADPPO comonomer, there appears to be little additional effect.

The crosslinking reaction was monitored by FTIR/ATR spectroscopy in isothermal experiments at 80 °C. This technique allowed us to monitor the evolution of the groups involved in the reaction by means of the variations in the corresponding absorptions. Figure 2 shows the FTIR spectra of the SOE-AC



Scheme 3

The cationic crosslinking of all the synthesized polymers was performed with ytterbium triflate as the cationic initiator. This reaction occurs through the double ring-opening of pendant SOEs moieties, the mechanism of which has previously been reported.<sup>18-20</sup> This process occurs through an intermediate carbocation, stabilized by the adjacent oxygens, which gives rise to a poly(ether-ester) chain (Scheme 3). In the case of the SOE used in this paper, the reaction yielded crosslinking materials that were insoluble in common organic solvents.

homopolymer before and after isothermal crosslinking with 1 phr Yb(OTf)<sub>3</sub>. The double ring opening of the SOE gave rise to the formation of a linear poly(ether-ester) moiety, which exhibit a typical carbonyl ester band<sup>21</sup> at about 1735-1750 cm<sup>-1</sup>. The acrylate derivatives used in this article contained an ester group that had a carbonyl band at 1732 cm<sup>-1</sup> and therefore overlapped the band observed during crosslinking. Therefore, only an increase in the intensity of this band could be observed during polymerization.

**Table 2.**  $T_g$  Values, Thermogravimetric Data in  $N_2$  and Air, and LOIs of the Crosslinked

Polymer	$T_g$ (°C)	$T_{5\%}^a$ (°C)		$T_{max}^b$ (°C)		Char Yield at 800°C (wt%)		LOI
		$N_2$	Air	$N_2$	Air	$N_2$	Air	
<b>SOE-AC</b>	-12	185	144	219/384	212/380/555	13.3	0	23.5
<b>SOE-AC/DEVP</b>								
<b>80/20</b>	-13	185	210	231/365	266/362	25.0	5.2	26.7
<b>63/37</b>	-12	196	178	215/229/344	221/232/341	21.0	2.7	26.9
<b>SOE-</b>								
<b>AC/ADPPO</b>	4	199	222	251/399	310/400	11.5	3.7	26.7
<b>81/19</b>	4	210	228	244/400	295/398	10.6	5.3	26.8
<b>77/23</b>								
<b>SOE-</b>								
<b>AC/DEMMP</b>	-13	190	175	211/323	250/400	27.5	3.4	28.6
<b>72/28</b>	-14	170	158	203/301	202/297	27.6	6.3	28.9

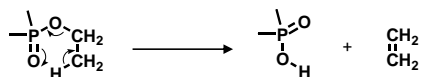
<sup>a</sup> Temperature of 5% weight loss

<sup>b</sup> Temperature of the maximum rate of degradation

The crosslinking of all linear copolymers was studied by differential scanning calorimetry (DSC). In the initial experiment performed, only a weak and broad exotherm was observed in all cases, and this did not allow an accurate determination of the reaction enthalpies. These low enthalpy values were in accordance with the low ring tension of SOEs and were in agreement with other reported data.<sup>22</sup> Further DSC experiments were performed to evaluate  $T_g$  for the crosslinked copolymers (Table 2). The  $T_g$ 's of the crosslinking materials were lower than those of the linear precursors. This is an

unusual behaviour and can be explained if we take into account that, in the crosslinking, the bulky and rigid ring SOE becomes an aliphatic, linear chain and the decrease can be attributed to the highly flexible nature of the subsequent network.

The decomposition behaviour of the copolymers was studied with TGA under nitrogen and air atmospheres (Table 2). In the presence of a nitrogen atmosphere, the degradation of all the copolymers occurred at similar temperatures. However, in air, the degradation of SOE-AC/ADPPO started at a



Scheme 4

slightly higher temperature. It has been reported<sup>16,23</sup> that polymers with alkyl phosphonate moieties can undergo an elimination of alkene, and a phosphorus acid derivative is produced, as shown in scheme 4. This phosphorus acid ester, or similar derivative, is capable of thermally decomposing at relatively low temperatures to give intermediates that can modify the degradation mechanism, such as transesterifications, anhydride group formation, and other reactions, to finally lead to a carbonaceous char. Thus, the DEVP and DEMMP copolymers could follow this mechanism. However, this was not the case for the phenyl-containing ADPPO copolymers. In addition, these materials showed several degradation steps at higher temperatures, and this was indicative of a more complex mechanism. The derivatives of the thermogravimetric plots showed various maxima (Table 2) that could be attributed to different degradation processes.

For the phosphorus-free resin, thermooxidative degradation took place at temperatures higher than 500 °C, whereas for the phosphorus-containing resins, it does not take place. This behaviour

is in accordance with the mechanism of actuation of phosphorus for improving fire resistance, in which the phosphorus forms an insulating, protective layer.

The LOI values, which can be taken as indicators for evaluating the flame retardancy of the phosphorus-modified polymers, were also measured and are shown in Table 2. The value for the SOE-AC homopolymer without phosphorus was the lowest, and the incorporation of phosphorus in the copolymers increased the LOI values; this was indicative of an improvement in the flame retardancy of the materials. However, the percentage of phosphorus used seemed to have little effect on any further increase in the LOI value, and this seems to indicate that the lowest phosphorus contents are enough to confer the flammability improvement.

Conventional wisdom in flame retardancy is when more char is produced upon burning, the flame-retardancy effect will be better. Because LOI value is an empirical measure of flame retardancy, we can expect there to be a strong correlation between the LOI and the char yield. However, in this case, the difference in the LOI values does not correspond to the char yields. Similar behaviour has been reported for other phosphorus-containing acrylates.

It has been reported that cationically double ring opened SOE-based materials exhibit almost no shrinkage and that copolymers having SOE moieties will also crosslink without shrinkage. Therefore, the volume changes in the crosslinking reaction of the copolymers containing SOE moieties were evaluated by density measurements with a Micromeritics gas pycnometer before and after

polymer. Thus, negative values indicate expansion.

In all cases, the observed values of the volume change were negative, and therefore the crosslinking process shows an expansion, although typical crosslinking reactions are generally accompanied by significant volume shrinkage.<sup>24</sup> In Table 3, it can be seen that the greater the SOE ratio

**Table 3.** Densities of the Copolymers before and after Crosslinking and Volume Changes upon Crosslinking.

Polymer	Density ( $d^{30}$ , g/cm <sup>3</sup> )		Volume Change (%)
	Linear	Crosslinked	
<b>SOE-AC</b>	1.145	1.110	-3
<b>SOE-AC/DEVP</b>			
<b>80/20</b>	1.122	1.098	-2.1
<b>63/37</b>	1.119	1.097	-1.9
<b>SOE-AC/ADPPO</b>			
<b>81/19</b>	1.121	1.092	-2.6
<b>77/23</b>	1.120	1.092	-2.5
<b>SOEAC-DEMMP</b>			
<b>72/28</b>	1.128	1.098	-2.6
<b>52/48</b>	1.115	1.096	-1.7

crosslinking (Table 3). The volume change ( $\Delta$ ) was calculated from the following equation:

$$\Delta V (\%) = \frac{d_{\text{crosslinked polymer}} - d_{\text{linear polymer}}}{d_{\text{linear polymer}}} \times 100$$

where  $d_{\text{crosslinked polymer}}$  is the density of the crosslinked polymer and  $d_{\text{linear polymer}}$  is the density of the linear

polymer. The greater the expansion coefficient is. Therefore, it can be concluded that the SOEs moieties used here proved to be effective monomers for obtaining crosslinkable copolymers that do not shrink, regardless of the copolymer composition.

## CONCLUSIONS

An SOE-containing monomer, SOE-AC, was radically homopolymerized and copolymerized with three phosphorus-containing monomers in various ratios. With ytterbium triflate as the cationic initiator, the crosslinking of the SOE moieties was achieved. SOE-AC/ADPPO, the only phosphorus-containing copolymer without alkyl phosphonate units, degraded at higher temperatures than the copolymers with alkyl phosphonate moieties. This indicated that the degradation followed a different mechanism. The incorporation of phosphorus into the copolymers increased the LOI values, thus improving the flame retardancy of the materials, regardless of the percentage of phosphorus used. All the crosslinked polymers showed expansion after crosslinking, regardless of their composition.

*The authors thank the Comisión Interministerial de Ciencia y Tecnología (MAT2005-01593) and (MAT2005-01806) for providing financial support for this work.*

## REFERENCES AND NOTES

1. Expanding Monomers: Synthesis, Characterization and Applications; Shadir, R. K.; Luck, R. M., Ed; CRC: Boca Raton, FL, 1992.
2. Bailey, W. J.; Sun, R. L.; Katsuki, H.; Endo, T.; Iwama, H.; Tsushima, R.; Saigo, K.; Bitritto, M. M. In Ring-Opening Polymerization; Saegussa, T.; Goethals, E., Eds.; ACS Symposium Series; American Chemical Society: Washington, DC, 1977.
3. Hino, T.; Endo, T. *Macromolecules* 2003, 36, 5902.
4. Smith, R. E.; Pinzino, C. S.; Chappelow, C. C.; Holder, A. J.; Kostoryz, E. L.; Guthrie, J. R.; Miller, M.; Yourtee, D. M.; Eick, J. D. *J Appl Polym Sci* 2004, 92, 62.
5. Nishida, H.; Morikawa, H.; Nakahara, T.; Ogata, T.; Kusumoto, K.; Endo, T. *Polymer*, 2005, 46, 2531.
6. Bodenbenner, K. *Justus Liebigs Ann* 1959, 625, 183.
7. Fedtke, M.; Houfe, J.; Kahlert, E.; Müller, G. *Angew Makromol Chem* 1998, 255, 53.
8. Endo, T.; Bailey, W. J. *J Polym Sci Part C: Polym Lett Ed* 1980, 18, 25.
9. Kume, M.; Hirano, A.; Ochiai, B.; Endo, T. *J Polym Sci Part A: Polym Chem* 2006, 44, 3666.
10. Lu, S.-Y.; Hamerton, I. *Prog Polym Sci* 2002, 27, 1661.
11. Ebdon, J. R.; Jones, M. S. In *Polymeric Materials Encyclopedia*; Salomone, J. C., Ed.; CRC: Boca Raton, FL, 1996.
12. Jain, P.; Choudhary, V.; Varma, I. K. *J Macromol Sci. Polym Rev* 2002, 42, 139.
13. Levchik, S. V.; Weil, E. D. *Polym Int* 2004, 53, 1901.

14. Canadell, J.; Mantecón, A.; Cádiz, V. J Polym Sci Part A: Polym Chem 2006, 44, 4722.
15. Liepins, R.; Surles, J. R.; Morosoff, N.; Stannet, V.; Duffy, J. J.; Day, F. H. J Appl Polym Sci 1978, 22, 2403.
16. Ebdon, J. R.; Hunt, B. J.; Joseph, P.; Konkel, C. S.; Price, D.; Pyrah, K.; Hull, T. R.; Milnes, G. J.; Hill, S. B.; Lindsay, C. I.; McCluskey, J.; Robinson, I. Polym Degrad Stab 2000, 70, 425.
17. Isobe, N.; Nishikubo, T.; Tagoshi, H.; Endo, T. Makromol Chem 1988, 189, 287.
18. Bailey, W. J. Macromol Sci Chem 1975, 9, 849.
19. Tagoshi, H.; Endo, T. J Polym Sci Part C: Polym Lett 198, 28, 77.
20. Nishida, H.; Sanda, T.; Endo, T.; Nakahara, T.; Ogata, T.; Kusu-moto, K. J Polym Sci Part A: Polym Chem 1999, 37, 4502.
21. Pretsch, E.; Clerc, T.; Seibl, J.; Simon, W. Tablas para la Elucidación Estructural de Compuestos Orgánicos por Métodos Espectroscópicos; Springer-Verlag Ibérica: Barcelona, 1998.
22. Mas, C.; Ramis, X.; Salla, J. M.; Mantecón, A.; Serra, A. J Polym Sci Part A: Polym Chem 2003, 41, 2794.
23. Ebdon, J. R.; Price, D.; Hunt, B. J.; Joseph, P.; Gao, F.; Milnes, G. J.; Cunliffe, L. K. Polym Degrad Stab 2000, 69, 267.
24. Chung, K.; Takata, T.; Endo, T. Macromolecules 1997, 30, 2532.

## FLAME RETARDANCE AND SHRINKAGE REDUCTION OF POLYSTYRENE MODIFIED WITH ACRYLATE CONTAINING- PHOSPHORUS AND CROSSLINKABLE SPIROORTHOESTER MOIETIES

J. Canadell<sup>1</sup>, B. J. Hunt<sup>2</sup>, A. G. Cook<sup>2</sup>, A. Mantecón<sup>1</sup>, V. Cádiz<sup>1</sup>

<sup>1</sup> Departament de Química Analítica i Química Orgànica. Universitat Rovira i Virgili.  
Marcel·lí Domingo s/n, 43007 Tarragona, Spain

<sup>2</sup> Polymer Centre, Department of Chemistry, University of Sheffield, Sheffield S3 7HF,  
United Kingdom

---

### Abstract

Styrene was radically copolymerized with a spiroorthoester with an acrylate group (SOE-AC), and terpolymerized with SOE-AC and diethyl(methacryloyloxymethyl)-phosphonate (DEMMP). This was done for several different feed ratios, to obtain polymers with spiroorthoesters moieties in the side chain. These polymers were then crosslinked with ytterbium triflate, as cationic initiator, via the double ring-opening polymerization. The thermal stability and fire retardance properties of these materials were evaluated by TGA and LOI. The DEMMP-containing polymers give materials which were significantly more flame retarded than the non phosphorus-containing materials, as indicated by the LOI measurements. The volume changes measured upon crosslinking of the polymers were evaluated by density measurements with a gas pycnometry. In all the cases, expansion was observed. This indicates that SOE-AC is an effective monomer for crosslinkable polymers without volume changes.

**Keywords:** radical copolymerization; cationic crosslinking; flame retardance; heteroatom containing polymers; spiroorthoesters; styrene; ytterbium triflate

---

## INTRODUCTION

Typical polymerizations of vinyl and monocyclic monomers (e.g., styrene, methyl methacrylate, and epoxy resins) and curing of materials are accompanied by some degree of shrinkage, which can lead to internal compressive stress in the material producing poor adhesion of coatings to the substrate, delamination, and the appearance of microvoids and microcracks, which reduce the durability of the materials.<sup>1</sup> The most common way of reducing this shrinkage is to use inert fillers. In some applications such as encapsulating, potting, and impregnating this is not possible due to the significant increase of the viscosity, which restricts material flow, and mold filling properties. Another problem inherent to the use of fillers is their tendency to settle out, giving rise to inhomogeneous systems.<sup>2</sup>

The most effective method of solving this problem is to use so-called "expanding monomers", which can polymerize without shrinkage or even show some expansion. A number of spirobicyclic monomers have been reported as an effective way of reducing shrinkage during the double ring-opening polymerization.<sup>1,3,4</sup> Amongst these are the spiroortho-esters (SOEs),

which can be prepared from epoxides and lactones and exhibit a wide variety of structures.<sup>5</sup> The introduction of vinyl or acrylate functionalities into the SOE structure allows the free-radical polymerization to yield soluble polymer with intact spiroorthoester functionality. These can be crosslinked, without significant shrinkage, by cationic double ring-opening polymerization using a Lewis acid initiators.<sup>6-8</sup>

Considerable attention has been made in the last decade to controlling the inherent flammability of organic polymers by the physical incorporation of fire retardant additives. However, the incorporation of additives has several disadvantages. These additives are often required in high loadings to be effective, leading to concomitant undesirable changes in physical and mechanical properties. Also, additives may leach from the polymer through normal service and ageing. An alternative approach is the chemical incorporation into the structure of the polymer via copolymerization or some chemical modifications. Fire retardant polymers generally contain heteroelements such as halogen, phosphorus, silicon or boron. Although halogen-containing flame-

retardants are exceptionally efficient, they have clear disadvantages, as they generate toxic and corrosive gases during thermal degradation. In recent years, phosphorylation has been considered to be one of the most efficient means of conferring flame retardancy on synthetic polymer materials.<sup>9-11</sup>

In a previous work<sup>6</sup> we studied the free-radical copolymerization of a SOE-containing monomer, 1,4,6-trioxaspiro[4,4]-2-nonylmethyl acrylate (SOE-AC), with different phosphorus-containing comonomers, yielding linear polymers with spiro-orthoester moieties as side pendant groups and phosphorus in their structure. These polymers were crosslinked cationically with ytterbium triflate as initiator. In all cases, expansion was observed and the incorporation of phosphorus increased LOI values improving the flame retardancy of materials. However, they presented glass transition ( $T_g$ s) below room temperature limiting the applications of these materials.

Encouraged by these findings, we have embarked on improving  $T_g$ s of these crosslinked polymers without detriment of flame retardancy and expansion, by introducing rigid structures into the polymer. Thus, this work presents the radical terpolymerization of styrene, SOE-AC and diethyl (methacryloyloxymethyl)-phosphonate (DEMMP). The volume change observed during the

cationic crosslinking was calculated by gas pycnometry. Finally, flame retardancy properties of the polymers were investigated by limiting oxygen index (LOI) measurements.

## EXPERIMENTAL

### Materials

Styrene (ST; Aldrich) was freshly distilled before use. Ytterbium (III) trifluoromethanesulfonate [ $\text{Yb}(\text{OTf})_3$ ; Aldrich] was used as received. 2,2'-azobisisobutyronitrile (AIBN; Aldrich) was recrystallized from methanol before use. All solvents were purified by standard procedures.

### Instrumentation

$^1\text{H}$  NMR (400 MHz),  $^{13}\text{C}$  NMR (100.6 MHz), and  $^{31}\text{P}$  NMR (161.9 MHz) spectra were obtained with a Varian Gemini 400-MHz Fourier transform spectrometer with tetrachloroethane- $d_2$  or  $\text{CDCl}_3$  as the solvent and tetramethylsilane and phosphoric acid as internal standards.

Crosslinking studies were performed on a Mettler DSC-821e thermal analyzer in covered Al pans under  $\text{N}_2$  at a scanning rate of 10 °C/min. The determination of the glass transition temperatures ( $T_g$ 's) was carried out on a Mettler DSC-822e thermal analyzer in covered Al

pans under N<sub>2</sub> at scanning rate of 20 °C/min.

The isothermal polymerization process at 80 °C was monitored with an FTIR-680 Plus spectrophotometer with a resolution of 4 cm<sup>-1</sup> in the absorbance mode. An attenuated-total-reflection accessory with thermal control and a diamond crystal was used to obtain Fourier transform infrared/attenuated total reflection (FTIR-ATR) spectra.

Thermogravimetric analyses (TGAs) were performed with a Mettler TGA/SDTA 851e thermobalance. Cured samples with an approximate mass of 8 mg were degraded between 30 and 800 °C at a heating rate of 10 °C/min under nitrogen and air atmospheres.

The molecular weight distribution of the polymers was determined with a Waters gel permeation chromatograph equipped with a Waters 510 differential refractive-index detector (RID-6A from Shimadzu). The gel permeation chromatograph was operated using three Waters Shodex columns (K80M, 5-μ mixed-D gel, and 3-μ mixed-E gel) at a nominal flow rate of 1 mL/min and with a sample concentration of 0.1% in tetrahydro-furan as the solvent. Monodispersed polystyrene standards were purchased from Polymer Laboratories for instrument calibration.

The densities of the materials were measured with a Micromeritics

Accu-pyc 1330 TC helium pycnometer at 30 °C.

LOIs were measured on a Fire Testing Technology flammability unit in conformance with ASTM D 2863 for samples measuring 100 mm x 6 mm x 3 mm and supported on glass fibers.

### Monomer Synthesis

#### Synthesis of 2-bromomethyl-1,4,6-trioxaspiro [4,4] nonane (SOE-Br)<sup>5</sup>

Epibromohydrin (Fluka), γ-butirolactone (γ-BL; Aldrich), boron trifluoride diethyl etherate (BF<sub>3</sub>.OEt<sub>2</sub>; Aldrich), triethylamine (Fluka).

#### Synthesis of 1,4,6-trioxaspiro[4,4]-2-nonylmethyl acrylate (SOE-AC)<sup>12</sup>

Acrylic acid (Aldrich), SOE-Br, 1,8-diazabicyclo[5.4.0]-undec-7-ene (DBU; Aldrich), 3-*tert*-butyl-4-hydroxy-5-methylphenyl sulfide (Aldrich).

#### Synthesis of Diethyl(methacryloyloxymethyl)phosphonate (DEMMP)<sup>13,14</sup>

Methacryloyl chloride (Aldrich), diethylhydroxymethylphosphonate (Aldrich), triethylamine (Fluka).

All these materials were used as received.

## Polymer Synthesis

### Copolymerization of ST with SOE-AC (ST/SOE-AC)

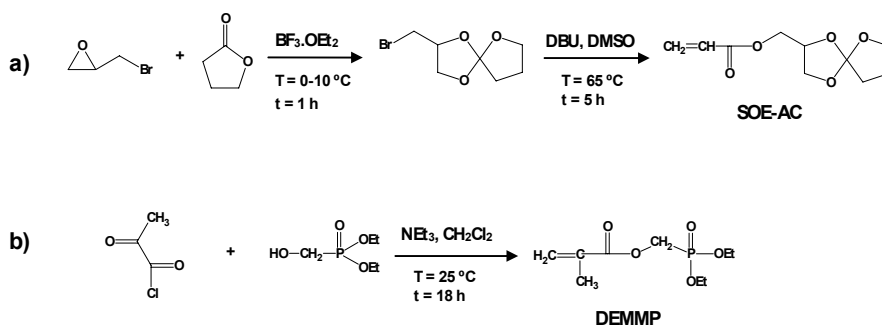
In a typical procedure, a solution of 0.99 g (9.5 mmol) of ST, 2.05 g (9.5 mmol) of SOE-AC, and 93 mg (0.56 mmol) of AIBN in benzene (20 mL) in a sealed ampoule was heated in a water bath at 65 °C for 40 h. The reaction mixture was added dropwise into n-hexane to precipitate the polymer as a white powder. The polymer was further purified by reprecipitation of the dissolved polymer from dry dichloromethane into n-hexane.

$^1\text{H}$  NMR (tetrachloroethane- $d_2$ ):  
 $\delta(\text{ppm}) = 7.4\text{--}6.2$  (br, Ar-H),  $4.2\text{--}3.2$  (br, -O-CH $_2$ -, -O-CH-),  $2.4\text{--}1.2$  (br, -CH $_2$ -, main chain -CH-, main chain -CH $_2$ -).

Terpolymers containing ST, SOE-AC, and DEMMP were obtained in benzene by a similar procedure described before. The initiator used was AIBN and the reaction was performed at 65 °C. The initiator concentration was 3% molar in all cases. All the terpolymers were recovered by precipitation in n-hexane and the purification was carried out by the reprecipitation of the dissolved polymer from dry dichloromethane into n-hexane.

$^1\text{H}$  NMR (tetrachloroethane- $d_2$ ):  
 $\delta(\text{ppm}) = 7.6\text{--}6.4$  (br, Ar-H),  $4.4\text{--}3.7$  (br, -O-CH $_2$ -, -O-CH-, -O-CH $_2$ -P-),  $3.7\text{--}3.4$  (br, -P-O-CH $_2$ -),  $2.4\text{--}2.2$  (br, -C-CH $_3$ ),  $2.0\text{--}1.7$  (br, -CH $_2$ -, main chain -CH-, main chain -CH $_2$ -),  $1.4\text{--}1.0$  (br, -CH $_3$ ).

$^{31}\text{P}$  NMR (tetrachloroethane- $d_2$ ):  
 $\delta(\text{ppm}) = 20.3$  (br).



Scheme 1

### Terpolymerization of ST with SOE-AC and DEMMP (ST/SOE-AC/DEMMP)

### Crosslinking Reactions

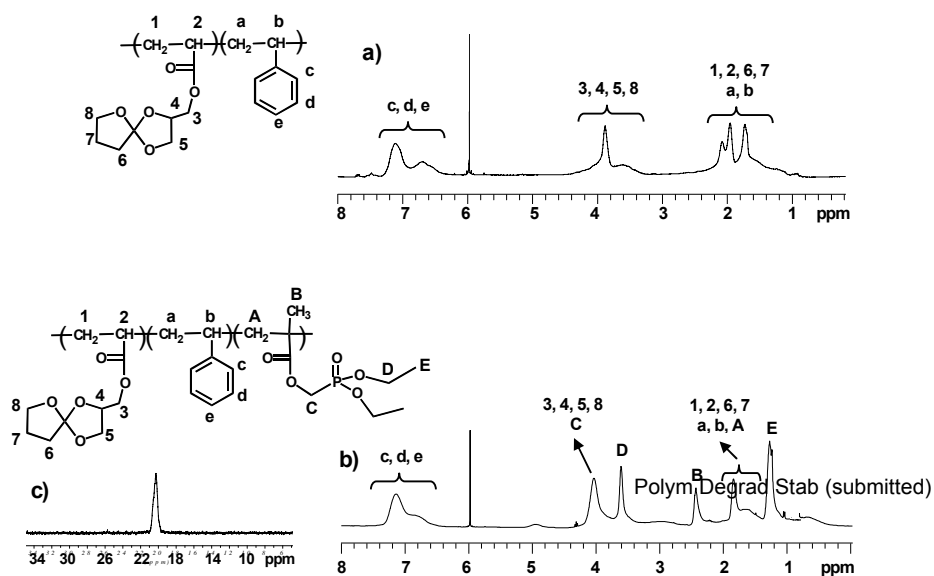


ST/SOE-AC/DEMMP: 7.6-6.2 (5  $H_{ST}$ ), 4.4-3.5 (7  $H_{SOE-AC}$  + 6  $H_{DEMMP}$ ), and 1.2-1.0 (6  $H_{DEMMP}$ ); 3) ST/DEMMP: 7.6-6.2 (5  $H_{ST}$ ) and 4.4-3.8 (6  $H_{DEMMP}$ ); 4) SOE-AC/DEMMP: 4.6-3.5 ppm (7 $H_{SOE-AC}$  + 6 $H_{DEMMP}$ ) and 1.5-1.3 ppm (6 $H_{DEMMP}$ ). These two last signals correspond to the spectra of the copolymers ST/DEMMP and SOE-AC/DEMMP, not shown in the figures. For the copolymer ST/SOE-AC system, signals of the five aromatic protons of the styrene units appear at 7.6-6.4 ppm. The signals at 4.2-3.2 ppm correspond to the  $-O-CH_2-$  and  $-O-CH-$  of SOE unit. Between 2.4-1.2 ppm the rest of SOE and main chain protons appear. In Figure (1b) the signals corresponding to the phosphorus-containing comonomer are clearly identifiable. In Figure (1c) the single  $^{31}P$  signal is broad due to the presence of different diastereomers and the sequential distribution of the comonomers. For the same reason, in the  $^1H$  NMR spectra some signals are split.

The IR spectra of the copolymers show characteristic bands of the

carbonyl ester group at  $1731\text{ cm}^{-1}$ , aromatic ring of styrene unit at  $1493\text{ cm}^{-1}$  and between  $1200$  and  $1000\text{ cm}^{-1}$  C-O-C vibrations assignable to the SOE moieties. Moreover, in the terpolymer, absorptions at  $1247\text{ cm}^{-1}$  corresponding to  $P=O$  of phosphonate moieties appear.

In the copolymerizations of ST/SOE-AC the initial feed ratios and the copolymer compositions are in close agreement with the initial feed ratios. Unfortunately, the phosphorus-containing terpolymers showed a lower incorporation of SOE-AC. When the initial feed ratio of SOE-AC was 22% molar, no incorporation of SOE-AC into the structure of the copolymer was detected (table 1). These results would seem to indicate that the DEMMP monomer is more reactive than the other monomers, especially the SOE-AC. Table 1 shows the molecular weights, determined by SEC, which are moderate, for these materials and range between  $0.9 \times 10^4$  and  $2.9 \times 10^4\text{ g/mol}$ . The  $T_g$ s values, obtained from DSC measurements, are also presented in Table 1 and



**Figure 1.** a)  $^1H$  NMR of copolymer ST/SOE-AC: 56/44, b)  $^1H$  NMR of terpolymer ST/SOE-AC/DEMMP: 42/18/40, c)  $^{31}P$  NMR of terpolymer ST/SOE-AC/DEMMP: 42/18/40.

range, between 19 and 98 °C. Figure 2 shows the DSC curves of polystyrene (1), SOE-AC homopolymer (5) and the ST/SOE-AC copolymers (2-4). As can be seen, the  $T_g$ s values of the copolymers are between those of both homopolymers, which would indicate that random copolymers were obtained. The fact that a single  $T_g$  was observed indicates that block polymerization does not

using ytterbium triflate as a cationic initiator (Scheme 3). This reaction takes place by a double ring-opening of the pendant SOEs moieties to yield a poly(ether-ester) chain.<sup>16-18</sup> In the case of the SOE used in this work, the reaction yielded crosslinking materials which were insoluble in common organic solvents.

**Table 1.** Radical copolymerization of ST with SOE-AC and radical terpolymerization of ST with SOE-AC and DEMMP.

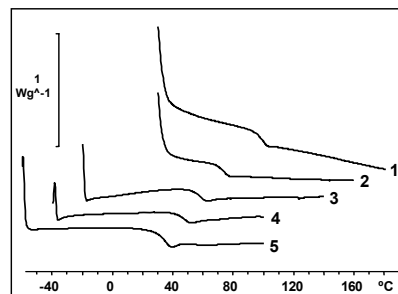
Entry	Polymer	Monomer Feed Ratio (mol %) ST : SOE-AC : DEMMP (wt% P)	Copolymer Composition (mol %) ST : SOE-AC : DEMMP (wt% P) <sup>a</sup>	Yield (%)	Mw x 10 <sup>4</sup> (g/mol) <sup>b</sup>	T <sub>g</sub> (°C)
1	SOE-AC	0 : 100 : 0 (0)	0 : 100 : 0 (0)	66	2.5	32
2	ST/SOE-AC	75 : 25 : 0 (0)	77 : 23 : 0 (0)	53	1.0	73
3		50 : 50 : 0 (0)	56 : 44 : 0 (0)	61	1.1	57
4		25 : 75 : 0 (0)	39 : 61 : 0 (0)	54	1.4	47
5	ST	100 : 0 : 0 (0)	100 : 0 : 0 (0)	82	0.9	98
6	SOE- AC/DEMMP	0 : 79 : 21 (3)	0 : 72 : 28 (3.9)	61	2.9	25
7	ST/SOE- AC/DEMMP	64 : 22 : 14 (3)	66 : 0 : 34 (7.0)	38	1.4	40
8		42 : 42 : 16 (3)	42 : 18 : 40 (8.9)	51	1.2	27
9		20 : 61 : 19 (3)	26 : 46 : 28 (6.3)	48	1.3	19
10	ST/DEMMP	88 : 0 : 11 (3)	90 : 0 : 10 (2.6)	73	0.9	75

<sup>a</sup> Estimated by <sup>1</sup>H NMR

<sup>b</sup> Weight-average molecular weight estimated by GPC (based on polystyrene standards)

occur. As expected, an increase in amount of styrene in the copolymers increases the  $T_g$  of the materials, due to the rigid and bulky phenyl groups.

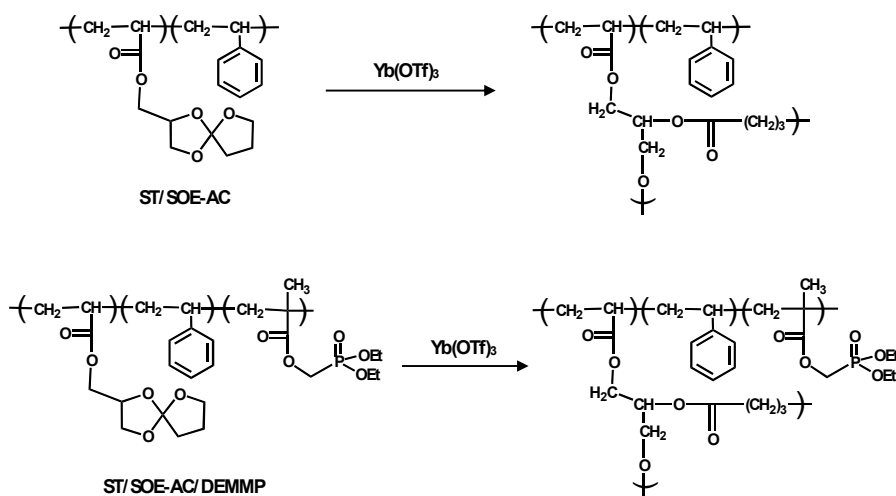
The cationic crosslinking of all SOE-containing polymers was performed



**Figure 2.**  $T_g$ s of polystyrene (1), copolymers ST/SOE-AC: 77/23 (2); 56/44 (3); 39/61 (4); and SOE-AC homopolymer (5).

polymers were studied by DSC. The experiments showed a weak and broad exotherm, which does not allow an accurate determination of the reaction enthalpies to be made. These low enthalpy values can be associated to the low ring tension of SOEs and are in agreement with

assessed by dynamic thermogravimetric analysis (TGA) under nitrogen and in air atmosphere (Table 2). The TGA curves and derivative TGA curves are given in Figures 3 and 4. Under both atmospheres, the temperature for 5% weight loss ( $T_{5\%}$ ) of the



Scheme 3

other reported data.<sup>19</sup> A second scan was performed to evaluate the  $T_g$  of the crosslinked polymers (Table 2). As can be seen,  $T_g$ s for the crosslinked polymers are lower than the linear precursors. This unusual result can be rationalized in terms of differing flexibility of the chain. The rigid and bulky ring SOE becomes an aliphatic and more flexible linear chain in the network, decreasing the  $T_g$  of materials.

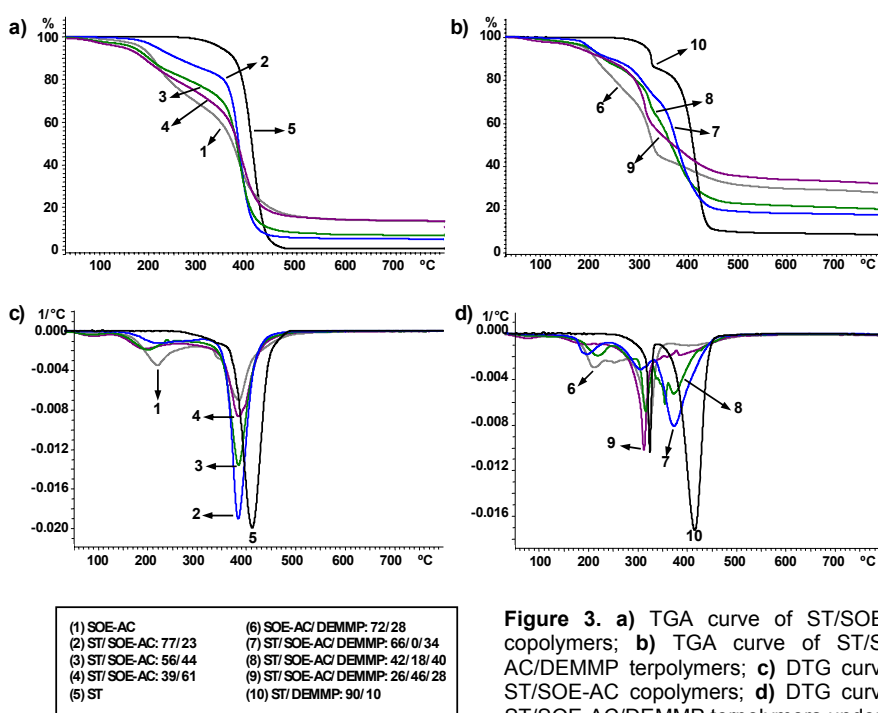
The thermal degradation behaviours of the crosslinked polymers were

copolymers lay between those the homopolymers and decreases as the SOE content increases. Under nitrogen, the presence of styrene into a copolymer with SOE-AC has a dramatic effect on char formation, with a drop from 14 to 0.7% char being observed on increasing the styrene content from 0 mol% to 100 mol% (Table 2 and Figure 3a). This can be rationalized in terms of the differing degradation mechanisms of the two base polymers: Polystyrene proceeds by a chain scissoring mechanism followed by a

depolymerization and the formation of volatiles, styrene monomer and oligomers,<sup>20-22</sup> whereas crosslinked SOE-AC does not depolymerize and promotes carbonaceous char. Similarly, under air atmosphere the char formation at 500 °C decreases as styrene content increases (Table 2 and Figure 4a).

In all cases, the char yield under air at 800 °C is zero.

It can be seen from Table 2 and Figure 3a, that the thermal degradation of the copolymers starts at lower temperatures with increasing SOE-AC content, due to the labile linear ester groups in the network. Also, we observe from derivatives of



**Figure 3.** a) TGA curve of ST/SOE-AC copolymers; b) TGA curve of ST/SOE-AC/DEMMP terpolymers; c) DTG curve of ST/SOE-AC copolymers; d) DTG curve of ST/SOE-AC/DEMMP terpolymers under N<sub>2</sub>.

However, the char yield of SOE-AC homopolymer is lower than some ST/SOE-AC copolymers. This result suggests a barrier effect of the SOE-AC, so the radicals which are produced through chain scission of polystyrene have more opportunity to undergo recombination reactions.

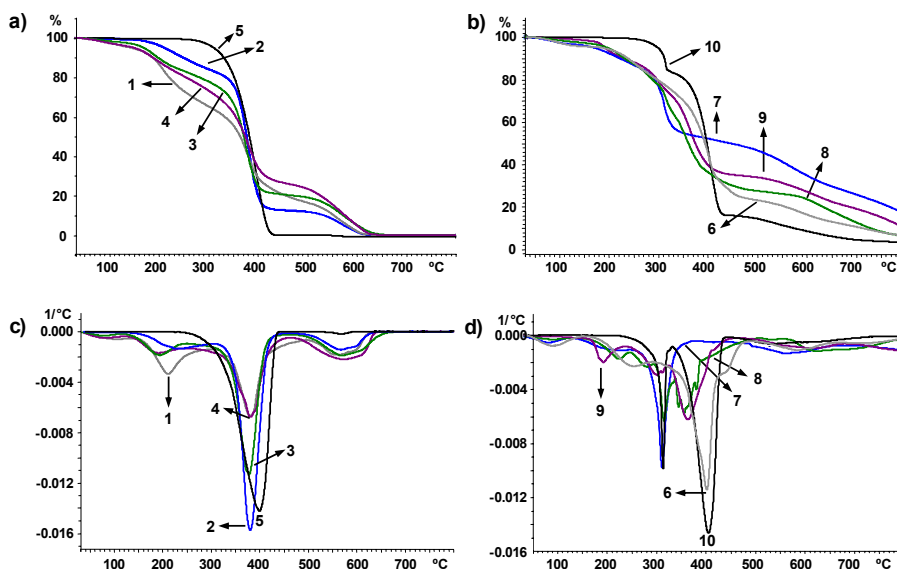
the thermogravimetric plots (Figure 3c and Figure 4c) that the mechanism of thermal degradation of copolymers is not affected by replacing nitrogen by an oxidative atmosphere with the exception of the oxidation of the char, that takes

PHYSICAL PROPERTIES.	
(1) ST/SOE-AC: 77/23	(6) SOE-AC/DEMMP: 72/28
(2) ST/SOE-AC: 56/44	(7) ST/SOE-AC/DEMMP: 66/0/34
(3) ST/SOE-AC: 39/61	(8) ST/SOE-AC/DEMMP: 42/18/40
(4) ST	(9) ST/SOE-AC/DEMMP: 26/46/28
	(10) ST/DEMMP: 90/10

place at temperatures higher than 500 °C.

The TGA char yields of DEMMP-containing terpolymers presented in Table 2 show an increase in the percentages of residual material at 800 °C under nitrogen and seems to be independent of phosphorus content. For example, the copolymer 8 that contains 8.9 % of phosphorus, presents lower char than copolymer

the phosphorus-unmodified copolymers, independently of the atmosphere. However, the derivate curves of the thermogravimetric plots (Fig. 3d) showed a new maximum that appears close to 310 °C, under nitrogen atmosphere. This maximum could be attributed to DEMMP degradation. A small peak, at around



**Figure 4.** a) TGA curve of ST/SOE-AC copolymers; b) TGA curve of ST/SOE-AC/DEMMP terpolymers; c) DTG curve of ST/SOE-AC copolymers; d) DTG curve of ST/SOE-AC/DEMMP terpolymers under air.

9, which contains 6.3 % of phosphorus. This can be attributed to the effect of increasing SOE-AC content, which also promotes char formation. Similarly results were observed under an air atmosphere.

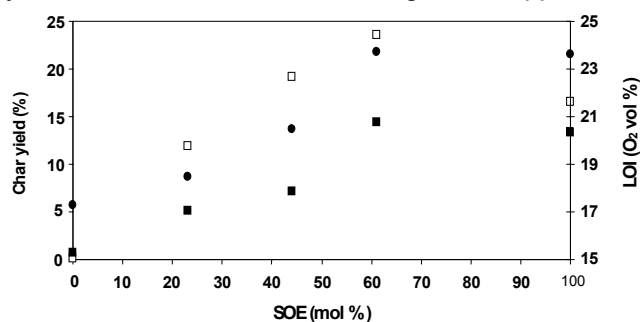
The terpolymers started the pyrolysis at similar temperatures to

200 °C, could be assigned to the degradation of SOE-AC, as it does not appear in either the polystyrene or styrene/DEMMP polymers. At higher temperatures, between 370 and 380 °C another peak appears, associated with the styrene and the SOE-AC degradations. In addition,

for the phosphorus-free resin, thermooxidative degradation takes place at temperatures higher than 500 °C, while for the phosphorus containing resins it does not take place. This behavior may be in accordance with the mechanism of activation of phosphorus in improving fire resistance, in which the phosphorus forms an insulating protective layer.

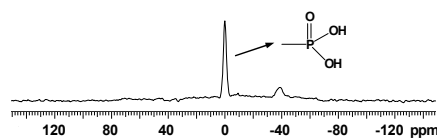
flame retardancy of the materials. However, only the % of phosphorus no justify these results and seems to be that SOE-AC content also contributes to LOI values.

The char produced in the LOI test of DEMMP-containing polymers was characterized by solid-state  $^{31}\text{P}$  MAS NMR (Figure 6). The sharp signal at 0 ppm corresponds to the



**Figure 5.** Char Yields (wt%) under nitrogen at 800 °C, under air at 500 °C and LOIs (O<sub>2</sub> vol %) for ST/SOE-AC varying levels of SOE-AC. Left abscissa: Char Yields (■) under N<sub>2</sub> and (□) under air; right abscissa: LOI (●)

The limiting oxygen index (LOI) values, which can be taken as indicators for evaluating the flame retardancy of the phosphorus-modified polymers, were also measured and are shown in Table 2. The LOI values of copolymers SOE-AC/ST increase with the SOE-AC content. Char yield is correlated to the polymer's flame retardancy.<sup>23</sup> In Figure 5 we can observe a good correlation between the amount of SOE-AC in the copolymer and the char yields and LOI values. All phosphorus-containing terpolymers showed higher LOI values, indicative of an improvement in the



**Figure 6.** Solid-state  $^{31}\text{P}$  NMR spectra of char residue (from the LOI test) of ST/SOE-AC/DEMMP : 26/46/28 terpolymer.

known monophosphoric acid.<sup>20</sup>

It has been reported that cationic double ring-opening of SOEs takes place without shrinkage or even with expansion.<sup>1,24</sup> Therefore, the volume changes in the crosslinking reaction of the polymers containing SOE moieties were evaluated by

density measurements with a Micromeritics helium pycnometer at 30 °C before and after crosslinking (Table 3). The volume change was calculated with the following equation:

$$\Delta V (\%) = \frac{d_{\text{crosslinked polymer}} - d_{\text{initial mixture}}}{d_{\text{initial mixture}}} \times 100$$

where  $d_{\text{crosslinked polymer}}$  is the density of the crosslinked polymer and  $d_{\text{linear}}$

Polymer	Density at 30 °C (g/cm <sup>3</sup> )		ΔV (%)
	Linear	Crosslinked	
SOE-AC	1.145	1.110	-3
ST/SOE-AC			
77 : 23	1.112	1.105	-0.6
56 : 44	1.127	1.111	-1.4
39 : 61	1.135	1.108	-2.3
SOE-AC/DEMMP	1.128	1.098	-2.6
ST/SOE- AC/DEMMP			
42 : 18 : 40	1.110	1.105	-0.45
26 : 46 : 28	1.123	1.106	-1.5

$d_{\text{polymer}}$  is the density of the linear polymer. Thus, negative values indicate expansion.

Although typical crosslinking reactions are generally observed significant volume shrinkage,<sup>25</sup> in all cases, negative values of the volume change were observed, and therefore the crosslinking process is accompanied by expansion. It can be seen that increasing the amount of SOE-AC gives rise to a greater expansion of the materials.

Therefore, it can be concluded that the SOE moieties used here proved to be effective mo-nomers for obtaining crosslinkable materials.

## CONCLUSIONS

Styrene was copolymerized radically with a SOE-containing monomer, SOE-AC, previously synthesized, and terpolymerized with both SOE-AC and diethyl(methacryloyloxymethyl)phos-phonate. The structure of linear polymers was confirmed by <sup>1</sup>H and <sup>31</sup>P NMR and as well as IR spectroscopy. These polymers were crosslinked through the SOE moieties to yield a poly(ether-ester) network using ytterbium triflate as cationic initiator. A correlation of SOE-AC content in ST/SOE-AC copolymers with LOI values and char yields was detected. Furthermore, phosphorus-containing polymers showed higher LOI and char yields values compared with free-phosphorus polymers, indicating an improvement in the flame retardancy of the materials. All the polymers undergo expansion during crosslinking, increasing with SOE-AC content.

*The authors thank the Comisión Interministerial de Ciencia y Tecnología (MAT2005-01593) and (MAT2005-01806) for providing financial support for this work.*

## REFERENCES AND NOTES

1. Expanding Monomers: Synthesis, Characterization and Applications; Shadir, R. K.; Luck, R. M., Ed; CRC: Boca Raton, FL, 1992.
2. Handbook of Epoxy Resins, Lee, H.; Neville, K.; Eds. McGraw-Hill: New York, 1982.
3. Hino, T.; Endo, T. *Macromolecules* 2003, 36, 5902.
4. Takata, T.; Endo, T. *Prog Polym Sci* 1993, 18, 839
5. Bodenbenner, K. *Justus Liebig Ann* 1955, 625, 183.
6. Canadell, J.; Hunt, B. J.; Cook, A.; Mantecón, A.; Cádiz, V. *J Polym Sci Part A: Polym Chem* 2006, 44, 6728.
7. Kitamura, N.; Takata, T.; Endo, T.; Nishikubo, T. *J Polym Sci Part A: Polym Chem* 1991, 29, 1151.
8. Kume, M.; Hirano, A.; Ochiai, B.; Endo, T. *J Polym Sci Part A: Polym Chem* 2006, 44, 3666.
9. Ebdon, J. R.; Jones, M. S. in *Polymeric Materials Encyclopedia*, Eds. J. C. Salomone, CRC Press, 1996.
10. Jain, P.; Choudhary, V.; Varma, I. K. *J Macromol Sci. Polym Rev* 2002, 42, 139.
11. Liaw, D. J. *J Polym Sci Part A: Polym Chem* 1997, 35, 2365.
12. Canadell, J.; Mantecón, A.; Cádiz, V. *J Polym Sci Part A: Polym Chem* 2006, 44, 4722.
13. Liepins, R.; Surles, J. R.; Morosoff, N.; Stannet, V.; Duffy, J. J.; Day, F. H. *J Appl Polym Sci* 1978, 22, 2403.
14. Ebdon, J. R.; Hunt, B. J.; Joseph, P.; Konkell, C. S.; Price, D.; Pyrah, K.; Hull, T. R.; Milnes, G. J.; Hill, S. B.; Lindsay, C. I.; McCluskey, J.; Robinson, I. *Polym Degrad Stab* 2000, 70, 425.
15. Isobe, N.; Nishikubo, T.; Tagoshi, H.; Endo, T. *Makromol Chem* 1988, 189, 287.
16. Bailey, W. J. *J Macromol Sci Chem* 1975, A9(5), 849.
17. Matyjaszewski, K. *J Polym Sci Part A: Polym Chem* 1984, 22, 29.
18. Nishida, H.; Sanda, T.; Endo, T.; Nakahara, T.; Ogata, T.; Kusumoto, K. *J Polym Sci Part A Polym Chem* 1999, 37, 4502.
19. Mas, C.; Ramis, X.; Salla, J. M.; Mantecón, A.; Serra, A. *J Polym Sci Part A Polym Chem* 2003, 41, 2794.
20. Wyman, P.; Crook, V.; Ebdon, J. R.; Hunt, B. J.; Joseph, P. *Polym Intern* 2006, 55, 764.
21. Jang, B. N.; Wilkie, C. *Polymer* 2005, 46, 2933.
22. Faravelli, T.; Pincioli, M.; Pisano, F.; Bozzano, M.; Dente, M.; E. Ranzi. *J. Anal Appl Pyrol* 2001, 60, 103.
23. Van Krevelen, D. W. *Polymer* 1975, 16, 615.
24. Bailey, W. J.; Iwama, H.; Tsushima, R. *J Polym Sci: Symposium* 1976, 56, 117.
25. Chung, K.; Takata, T.; Endo, T. *Macromolecules* 1997, 30, 2532.

## CROSSLINKING OF A POLYACRYLATE BEARING A SPIROORTHOESTER PENDANT GROUP WITH MIXTURES OF DIGLYCIDYL ETHER OF BISPHENOL A AND PHOSPHORUS-CONTAINING GLYCIDYL DERIVATIVES

J. Canadell, A. Mantecón, V. Cádiz  
Departament de Química Analítica i Química Orgànica. Universitat Rovira i Virgili.  
Marcel·lí Domingo s/n, 43007 Tarragona, Spain

---

### Abstract

The cationic crosslinking of a polyacrylate bearing a spiroorthoester pendant group with mixtures of diglycidyl ether of bisphenol A and three phosphorus-containing glycidyl derivatives was carried out with ytterbium triflate as an initiator. The curing process was monitored by Fourier transform infrared spectroscopy. The thermomechanical and thermogravimetric properties were evaluated. The glass transition temperatures of the obtained materials were, in general, above 100 °C. The incorporation of phosphorus into the network increased the limiting oxygen index values, thus improving the flame retardancy of the materials. During crosslinking, all the crosslinked polymers showed slight shrinkage that was much lower than that observed in conventional epoxy resins.

**Keywords:** cationic polymerization; crosslinking; flame retardance; heteroatom-containing polymers; spiroorthoester; ytterbium triflate

---

### INTRODUCTION

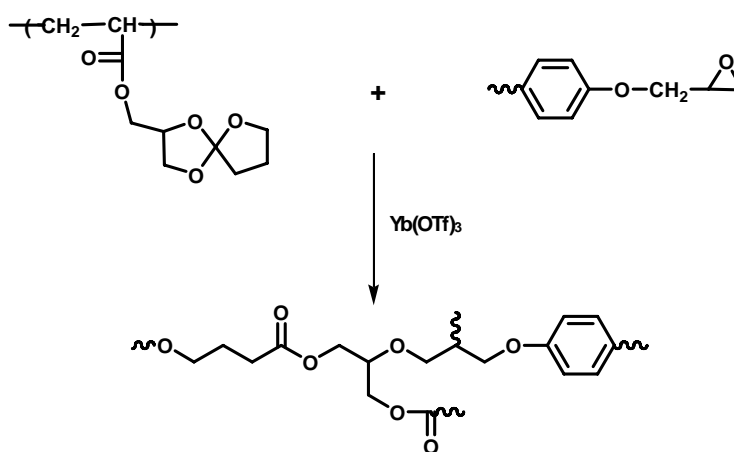
Polymeric networks are extremely versatile materials than can be used

in a wide number of applications. Each application has some require-

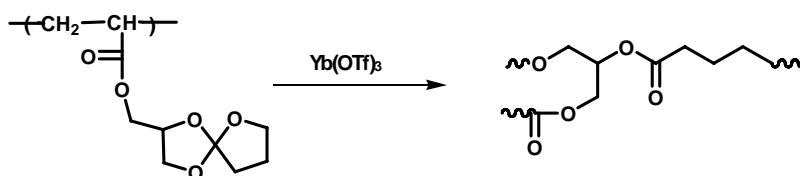
ments that include a combination of physical, mechanical, and other specific properties. Polymer properties depend on the structure of the comonomers, the polymerization mecha-

ners, the polymerization mecha-

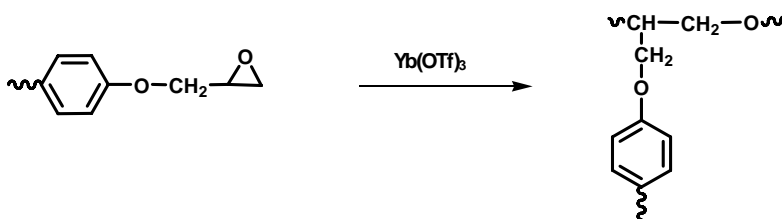
**a) Reaction of SOE-AChom with DGEBA**



**b) Homopolymerization of SOE-AChom**



**c) Homopolymerization of DGEBA**



**Scheme 1**

nism, and the catalyst used, among others.

In the production of industrial materials, a significant property is the absence of shrinkage upon cross-linking or curing. This shrinkage is a major problem in many industrial applications such as industrial castings, coatings, mold replication, and microelectronics because it leads to poor adhesion to the substrate, delamination, and microvoids and microcracks, which reduce the durability of the materials. Thus, many efforts have been made to reduce the shrinkage. A versatile method for solving this problem is the use of monomers with groups that undergo polymerization with nearly zero shrinkage or even expansion. Some kinds of cyclic monomers have been reported to maintain their volume or actually expand during the double ring-opening polymerization.<sup>1-5</sup> Among them, spiroorthoesters (SOEs) have a wide variety of structures because they can be prepared from epoxides and lactones.<sup>6-8</sup> The polymerization of SOEs bearing a vinyl or acrylate group for radical polymerization has been developed to obtain polymers carrying SOE moieties.<sup>9,10</sup> Other authors have followed a different strategy and have described the synthesis of polymers carrying SOEs by polymerizing lactone-containing acrylic monomers and the further reaction of the pendant lactones with epoxy compounds.<sup>11</sup> The polymers bearing SOEs moieties can be crosslinked, without

significant shrinkage, by cationic double ring-opening polymerization by Lewis acid catalysts.

It has been reported<sup>12-15</sup> that in the cationic copolymerization of lactones with glycidyl compounds, an inter-mediate SOE is formed that further polymerizes either itself or with epoxides to form poly(ether-ester) (Scheme 1).

Another problem inherent to organic polymers is their flammability. Improving the flame retardancy of organic polymers is a matter of mounting concern and importance given the fact that they are increasingly being used in materials in both domestic and public environments. The flammability of common epoxy systems is a disadvantage in their applications. The epoxy resins in use are mainly the diglycidyl ether of bisphenol A (DGEBA) and tetrabromobisphenol A. However, the bromine-containing epoxy resins release hydrogen bromide, dibenzo-*p*-dioxin, and dibenzofuran during combustion, which cause corrosion and toxicity. Organophosphorus compounds have demonstrated better ability than halogen-containing compounds as flame retardants for polymeric materials by forming a carbonaceous char, which acts as a physical barrier to heat transfer from the flame to the polymer and diffusion of combustible gas and smoke.<sup>16-19</sup>

Various phosphorus-containing diglycidyl ether compounds have

been synthesized from phosphoric, phosphonic, or phosphinic acids; therefore, they contain less stable P-O-C bonds.<sup>20</sup> In recent years, some diglycidyl compounds have been synthesized from bulky and rigid, phosphorus-containing, reactive 9,10-dihydro-9-oxa-10-phosphaphenan-trene-10-oxide (DOPO).<sup>21-24</sup> All these aryl phosphinate compounds contain P-O-C bonds but show unusually high thermal stability. This stability has been attributed to the O=P-O group being protected by phenylene groups. In a previous work,<sup>25</sup> we synthesized a novel glycidyl phosphinate, 9-(9,10-dihydro-9-oxa-10-phosphaphenan-threne-10-oxide)-2,3-epoxy propyl (DOPO-Gly), in which the glycidyl group was directly attached to the P atom. In our search for new phosphorus-containing glycidyls with high thermal and chemical stability without P-O bonds, we also considered phosphine oxides. The nature of this group improves the flammability properties in thermosets, whereas the polarity of the bond increases the hydrogen-bonding ability of the resulting material, possibly improving network adhesion to various substrates.<sup>26,27</sup> Therefore, we also synthesized isobutyl bis(glycidyl propyl ether) phosphine oxide (IHPO-Gly).<sup>28</sup>

The aim of this work was to reduce together the aforementioned disadvantages by means of the cationic crosslinking of a polyacrylate bearing an SOE pendant group

[poly(1,4,6-trioxaspiro[4,4]-2-nonylmethyl acrylate) (SOE-AChom) with mixtures of DGEBA and three phosphorus-containing glycidyl derivatives.

The cationic crosslinking was carried out with ytterbium triflate as an initiator, which has been shown to be effective at polymerizing glycidyl compounds and SOEs.<sup>29</sup> This crosslinking was studied with differential scanning calorimetry (DSC) and Fourier transform infrared (FTIR) spectroscopy. The materials were characterized with DSC and thermo-gravimetric analysis (TGA). The volume change was evaluated with a Micromeritics gas pycnometer, and the flame retardancy was tested by limiting oxygen index (LOI) measurements.

## EXPERIMENTAL

### Materials

#### SOE-AChom<sup>9</sup>

Epibromohydrin (Fluka),  $\gamma$ -butirolactone (Aldrich), boron trifluoride diethyl etherate (Aldrich), triethylamine (Fluka), acrylic acid (Aldrich), 1,8-diazabicyclo[5.4.0]-undec-7-ene (DBU) (Aldrich), and 3-*tert*-butyl-4-hidroxy-5-methylphenyl sulfide (Aldrich) were used as received. 2,2'-Azobisisobutyronitrile (AIBN; Aldrich) was recrystallized from methanol before use.

#### DOPO-Gly<sup>25</sup>

**Table 1.** Compositions (mol %) of the SOE-AChom/Epoxy monomers and curing cycles

Commercial DOPO was donated by Aismalibar. m-Chloroperbenzoic acid (MCPBA; Fluka), allyl bromide (Aldrich), epichlorohydrin (EPC;

phate (Aldrich) were used as received.

DGEBA (Epikote resin 827) was acquired from Shell Chemicals

Assay	Composition	Monomer Feed Ratio (mol %) SOE-AChom/DGEBA/Monomer P (wt% P)	Cured		Postcured	
			T (°C)	t (h)	T (°C)	t (h)
1	SOE-AChom/DGEBA	33/67/0 (0%)	100	2	140	5
2	SOE-AChom/DGEBA/DOPO-Gly	33/39.5/27.5 (3%)	100	2	140	5
3	SOE-AChom/DGEBA/DOPO-BQ-Gly	33/34/33 (3%)	100	2	140	4
4	SOE-AChom/DGEBA/IHPO-Gly	33/38/29 (3%)	100	2	160	6

Fluka), potassium carbonate (Panreac), and benzyltrimethylammonium chloride (BTMA; Fluka) were used as received.

**10-(2',5'-Bis(glycidyoxy)phenyl)-9,10-dihydro - 9 - oxa-10-phosphaphenanthrene-10-oxide (DOPO-BQ-Gly)<sup>30</sup>**

DOPO, 1,4-benzoquinone (Aldrich), EPC (Fluka), and BTMA (Fluka) were used as received.

**IHPO-Gly<sup>28</sup>**

Isobutyl bis(hydroxypropyl) phosphine oxide (IHPO) was kindly supplied by Cytec Canada, Inc. (trade name Cygard RF1243); EPC (Fluka) and tetrabutylammonium hydrogen sul-

(epoxy equivalent = 182.08). Ytterbium (III) trifluoromethanesulfonate [Yb(OTf)<sub>3</sub>; Aldrich] was used as received.

All solvents were purified by standard procedures.

**Crosslinking Reaction**

The epoxy monomers and SOE-AChom in a molar ratio 2:1 were polymerized with 1 phr ytterbium triflate (1 phr = 1 part per 100 parts of mixture weight/weight). Sample bars for dynamomechanical analysis, thermogravimetric analysis, and burn testing were cured in aluminium molds by heating. The prepared epoxy monomers/SOE-AChom mixtures and the curing cycles determined from DSC data, are listed in Table 1.

## Instrumentation

The molecular weight distribution of the polymer was determined with a Waters gel permeation chromatograph equipped with a Waters 510 differential RI detector (RID-6A from Shimadzu). The gel permeation chromatograph was operated with three Waters Shodex columns (K80M, Gel 5- $\mu$  Mixed-D, Gel 3- $\mu$  Mixed-E) at a nominal flow rate of 1 mL/min and a sample concentration of 0.1% in THF as the solvent. Monodisperse polystyrene standards were purchased from Polymer Laboratories for instrument calibration.

Crosslinked studies were carried out on a Mettler DSC-821e thermal analyzer in covered Al pans under N<sub>2</sub> at a scanning rate of 10 °C/min. The determination of the glass transition temperatures (T<sub>g</sub>'s) were carried out on a Mettler DSC-822e thermal analyzer in covered Al pans under N<sub>2</sub> at scanning rates of 20 °C/min.

The isothermal polymerization process was monitored with a FTIR-680 Plus spectrophotometer with a resolution of 4 cm<sup>-1</sup> in the absorbance mode. An attenuated total reflection (ATR) accessory with thermal control and a diamond crystal was used to determine FTIR/ATR spectra.

TGA was carried out with a Mettler TGA/SDTA 851e thermobalance. Cured samples with an approximate mass of 8 mg were degraded

between 30 and 800 °C at a heating rate of 10 °C/min under nitrogen and under air.

The mechanical properties were measured with a dynamic mechanical thermal analyzer (TA DMA 2928). Samples with dimensions of 3 mm x 5 mm x 10 mm were tested in a three-point-bending clamp from -30°C to 190 °C with a heating rate of 3 °C/min and at a fixed frequency of 1 Hz.

The densities of the materials were measured with a Micrometrics Accu-*pyc* 1330 TC gas pycnometer at 30 °C.

LOIs were measured on a Fire Testing Technology flammability unit in conformance with ASTM D 2863 on samples measuring 100 mm x 6 mm x 3 mm.

Scanning electron microscopy (SEM) was performed on a JEOL JSM 6400 scanning electron microscope at an activation voltage of 8 kV. For the atomic mapping, an Oxford INCA energy-dispersive X-Ray microanalyzer was used.

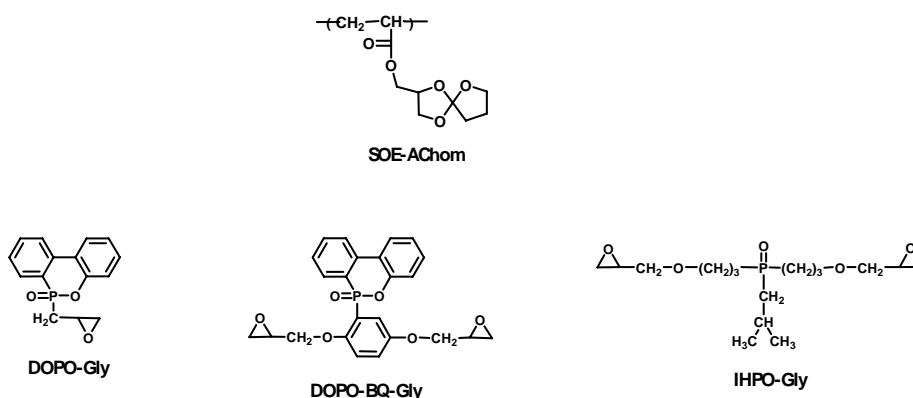
## RESULTS AND DISCUSSION

First, we synthesized the starting polyacrylate bearing a SOE (SOE-AChom) with an M<sub>w</sub> of 25.000 and the phosphorus-containing glycidyl compounds (Scheme 2). SOE-AChom was synthesized as

previously described<sup>6</sup> from the corresponding acrylic monomer SOE-AC in benzene using AIBN as a radical initiator, and as phosphorus-containing monomers, we used the three glycidyl compounds shown in scheme 2.

mixture of sodium hydroxide and EPC with tetrabutylammonium hydrogen sulfate as catalyst.<sup>28</sup>

The cationic crosslinking of SOE-AChom with mixtures of DGEBA and phosphorus-containing glycidyl derivatives was initiated by



Scheme 2

The synthesis of these glycidyl compounds was carried out in different ways. In the case of DOPO-Gly, the glycidyl phosphinate was obtained from DOPO and allyl bromide and further epoxidation of the double bond with MCPBA because the direct reaction of EPC with the active hydrogen atom of DOPO led to an allylic alcohol through an isomerization reaction.<sup>25</sup> For DOPO-BQ-Gly, the first step was the reaction of benzoquinone with DOPO,<sup>30</sup> and this was followed by the reaction of the two phenolic groups with EPC in excess and BTMA as a catalyst.<sup>31</sup> The third monomer, IHPO-Gly, was synthesized from commercial IHPO in a

ytterbium triflate. Because of the cationic character of ytterbium triflate, which is similar to boron trifluoride mono ethylamine, in addition to the reaction of SOE with epoxy groups [Scheme 1(a)], other simultaneous processes are expected: the homopolymerization of SOE [Scheme 1(b)], and the homopolymerization of epoxy group [Scheme 1(c)]. The two first reactions give linear poly(ether-ester) structures, and the third lead to polyether chains.<sup>29</sup>

To obtain the final thermosets containing about 3% phosphorous, mixtures of DGEBA with each phosphorus-containing glycidyl mo-

nomer and 1 phr ytterbium triflate were prepared and used to crosslink SOE-AChom. In this type of copolymerization, the diglycidyl mo-nomers are tetrafunctional, whereas SOE is bifunctional. Therefore, a higher proportion of the former leads to a more densely crosslinked network, whereas a higher proportion of SOE leads to a longer linear chain between crosslinks. The compositions of the samples and the cured and postcured conditions are summarized in Table 1. In all samples, the epoxy/SOE molar ratio was 2/1 to introduce aromatic moieties capable of increasing the  $T_g$  values. For comparison, the crosslinking of SOE-AChom/DGEBA was also carried out, and it is included in the same table. After isothermal curing in an oven, a DSC run showed complete cross-

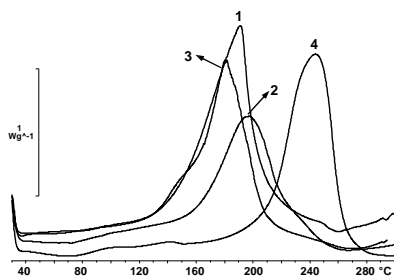
linking because no residual enthalpy was detected.

Figure 1 shows the dynamic DSC plots of all mixtures. As can be seen from the crosslinking exotherms, the temperatures of the maximum, about 190 °C, are similar for samples 1, 2 and 3, but for the sample 4, the maximum of the exotherm appears at a higher temperature, indicating its lower reactivity. The DSC data are listed in Table 2. The enthalpies per epoxy equivalent were calculated because the enthalpy evolved in the SOE ring opening is much lower than for the oxirane ring opening.<sup>29</sup> These values were similar for all the samples, though slightly higher for those with phosphorus. The  $T_g$  values were calculated after complete curing, by means of a second scan, as the temperature of

**Table 2.** Calorimetric Data for the Different 1/2 (mol/mol) SOE-AChom/Epoxy Mixtures Initiated by 1 phr Ytterbium Triflate

Assay	$\Delta H$ (J/g)	$\Delta H$ (KJ/ee)	$T_{max}$ (°C) <sup>a</sup>	$T_g$ (°C)	$E'_{max}$ (°C) <sup>b</sup>	Tan $\delta$ (°C)
1	374.7	89.1	191	106	102	113
2	350.7	96.3	197	104	76	89
3	362.4	92.6	182	132	109	135

<sup>a</sup> Temperature of the maximum heat release rate.  
<sup>b</sup> Maximum loss modulus.



J Polym Sci Part A: Polym Chem (in press)  
**Figure 1.** DSC plots of the different 1/2 (mol/mol) SOE-AChom/epoxy mixtures containing 1 phr ytterbium triflate over the temperature range of 30-300 °C at heating rate of 10 °C/min.

the half-way point of the jump in the heat capacity when the material changed from the glassy state to the rubbery state, and they are also collected in Table 2. The lowest  $T_g$

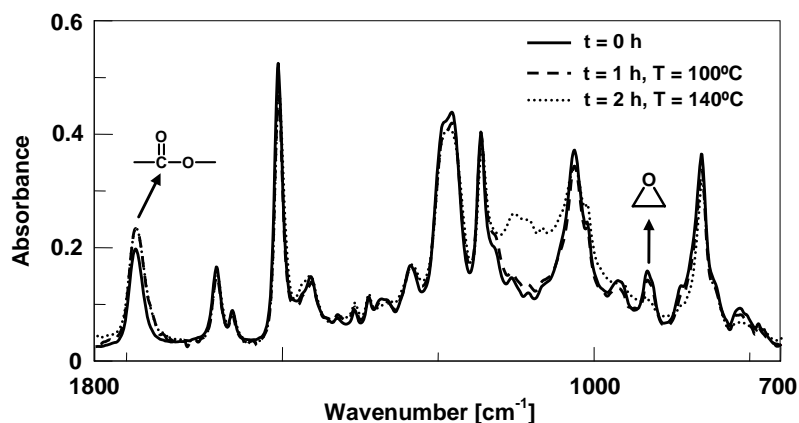
value of sample 4 can be related to the aliphatic structure of IHPO-Gly derivative, which confers a greater flexibility to the network.

FTIR spectroscopy allowed to follow the variation of the groups involved in the crosslinking process. Figure 2 depicts the spectra of the initial mixture, after 1 h at 100 °C, and the final material. We can see the disappearance of the absorption at 915 cm<sup>-1</sup> due to oxirane ring, thus confirming that the glycidyl compounds have reacted. A SOE reaction can be observed by the appearance of carbonyl absorption of double ring-opening. In our case,

To study the different processes that occur during crosslinking, we calculated the conversion of epoxy and SOE groups by means the evolution of the bands at 915 cm<sup>-1</sup> and 1735 cm<sup>-1</sup>, respectively. The absorbances were calculated in terms of the peak areas. The conversions of the epoxy and SOE groups were determined by the Lambert-Beer law from the normalized changes in the absorbance with respect to the band at 1606 cm<sup>-1</sup> corresponding to the phenyl group in DGEBA, and

$$\alpha_{SOE} = \left( \frac{\overline{A}_{1735}^t}{\overline{A}_{1735}^0} \right)$$

$$\overline{A}_{1735}^t = \frac{A_{1735}^t}{A_{1606}^t} - \frac{A_{1735}^0}{A_{1606}^0} \quad \overline{A}_{1735}^0 = \frac{A_{1735}^0}{A_{1606}^0} - \frac{A_{1735}^0}{A_{1606}^0}$$

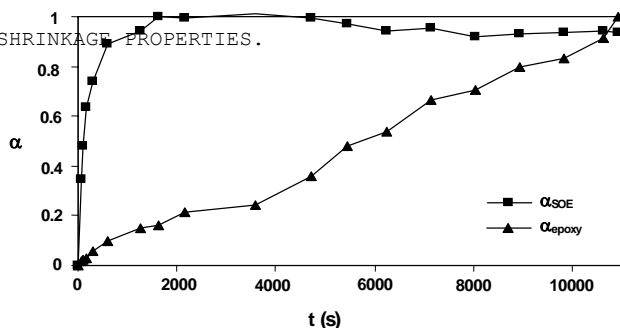


**Figure 2.** FTIR spectra of a 1/2 (mol/mol) SOE-AChom/DGEBA mixture with 1 phr of ytterbium triflate before heating, after 1 h at 100 °C, and after 2 h at 140 °C.

as the initial polymer has an ester group, this band appears in the initial spectrum, but an increase of this band was observed during crosslinking. This increase is related to the SOE polymerization.

$$\alpha_{epoxy} = 1 - \left( \frac{\overline{A}_{915}^t}{\overline{A}_{915}^0} \right)$$

$$\overline{A}_{915}^t = \frac{A_{915}^t}{A_{1606}^t} \quad \overline{A}_{915}^0 = \frac{A_{915}^0}{A_{1606}^0}$$



160 | Crosslinking through Spiroorthoesters

the conversions were calculated with the following equations:

where  $\alpha_{\text{epoxy}}$  is the epoxy conversion and  $\alpha_{\text{SOE}}$  is the SOE conversion.

Figure 3 shows the conversions versus the time. The SOE group reacts very fast at the beginning of the process up to a conversion of about 0.7 and reaches a total conversion below 2000 s at 100 °C. After 1 h, the temperature rises to 140 °C, and a decrease in the carbonyl band at 1735  $\text{cm}^{-1}$  indicates a slight disappearance of the linear ester that could be related to a depolymerization process or to the beginning of the ester breaking which can initiate the sun-ray crosslinking reactions. On the other hand, the evolution of the epoxy group steadily progresses up to the complete reaction. In the first stages of the crosslinking, when SOE is present in the mixture reaction, process a in Scheme 1 must be the more significant, and then, when SOE is run out, predominantly process c occurs. Process b should occur at the end of the reaction because in previous studies we have observed that this is the process less favored.<sup>29</sup>

Assay	Density ( $d^{30}$ , $\text{g/cm}^3$ )		Volume Change (%)
	Mixture	Crosslinked	
1	1.1886	1.1950	0.5
2	1.2147	1.2214	0.6
3	1.2153	1.2172	0.2
4	1.1942	1.2030	0.7

The dynamic mechanical behavior of the crosslinked material was obtained as a function of the temperature from the glassy state of each composition to the rubbery plateau of each material (Figure 4). The crosslinking density of a polymer can be estimated from the plateau of the elastic modulus in the rubbery state.<sup>32</sup> However, this theory is strictly valid only for lightly crosslinked materials and is therefore used only to make qualitative comparisons of the level of crosslinking among the various polymers. As can be seen, the incorporation of phosphorus-containing glycidyl compounds into the feed mixture reduces the

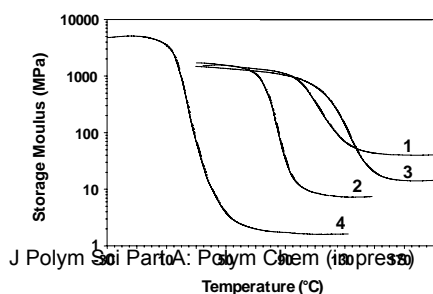


Figure 4. Storage modulus as a function of the temperature of the different thermosets obtained by the copolymerization of 1/2 (mol/mol) SOE-AChom/epoxy mixtures initiated by 1 phr ytterbium triflate.

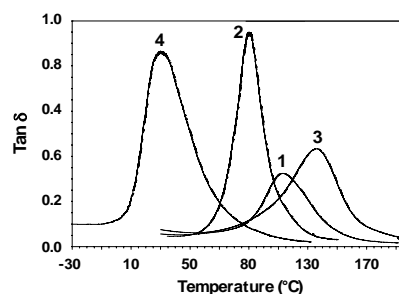


Figure 5.  $\text{Tan } \delta$  as a function of the temperature for the different thermosets obtained by the copolymerization of 1/2 (mol/mol) SOE-AChom/epoxy mixtures initiated by 1 phr ytterbium triflate.

crosslinking density, especially in the case of aliphatic IHPO-Gly (curve 4), which enlarges the distance between knots and leads to looser networks. Sample 2 shows a lower crosslinking density than sample 3, and this may be due to the presence of a lower ratio of epoxy groups because DOPO-Gly contains only an epoxy group per mole.

The  $T_g$ 's of the crosslinked materials can be detected as the maxima of the loss modulus ( $E''$ ) and loss factor ( $\tan \delta$ ). Figure 5 shows the plots of the  $\tan \delta$  versus the temperature, and Table 2 shows the values of both measurements. The lowest  $T_g$  corresponds to sample 4, which contains the more aliphatic moieties. Sample 2 shows a lower  $T_g$  value than samples 1 and 3, and this may be due to its lower crosslinking density. Moreover, the analysis of the height and width of the  $\tan \delta$  shows trends in the crosslinking densities and network homogeneities as the composition of the material changes. The height of the  $\tan \delta$  peak is associated with the crosslinking density. Because  $\tan \delta$  is the ratio of viscous components to elastic components, it can be assumed that the decreasing height is associated with lower segmental mobility and fewer relaxing species and therefore indicates that the networks for the DGEBA-rich samples are tighter. The peak width

at half-height broadens as the number of branching modes increases, and this produces a wider distribution of structures. The range of temperatures at which the different network segments gain mobility therefore increases. In our case, there were no significant differences among the samples, and this showed similar branching distributions for all of them. Moreover, all the samples showed unimodal curves indicating their homogeneity.

It has been reported that cationic-double ring-opened SOE-based materials exhibit almost no shrinkage and that copolymers having SOE moieties will also crosslink without shrinkage.

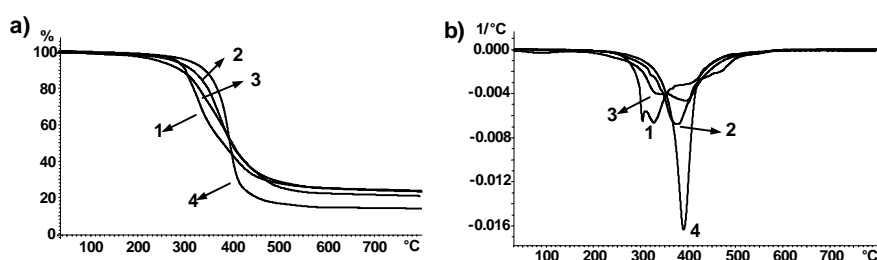


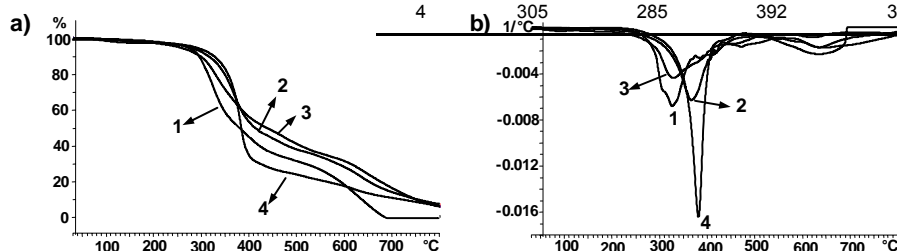
Figure 6. (a) TGA thermograms and (b) first derivatives of the different thermosets obtained by copolymerization of 1/2 (mol/mol) SOE-AChom/epoxy mixtures under  $N_2$ .

Therefore, the volume changes ( $\Delta$ ) in the crosslinking reaction of the copolymers containing SOE moieties were evaluated by density measurements with a Micro-meritics gas pycnometer before and after crosslinking (Table 3).  $\Delta$  was calculated from the following equation:

$$\Delta V (\%) = \frac{d_{\text{crosslinked polymer}} - d_{\text{linear polymer}}}{d_{\text{linear polymer}}} \times 100$$

where  $d_{\text{crosslinked polymer}}$  is the density of the crosslinked polymer and  $d_{\text{linear polymer}}$  is the density of the linear polymer. Thus, negative values indicate expansion.

Although typical crosslinking of epoxy resins is generally accompanied by significant



**Figure 7.** (a) TGA thermograms and (b) first derivatives of the different thermostets obtained by copolymerization of 1/2 (mol/mol) SOE-AChom/epoxy mixtures under air.

volume shrinkage (>3%, depending on the crosslinking mechanism),<sup>2,33</sup> in all studied mixtures of glycidyl compounds with SOEs, the observed positive values of  $\Delta$ , between 0.2 and 0.7, are much lower than those observed in the crosslinking of pure DGEBA with ytterbium triflate (ca. 3%).<sup>29,34</sup> This lower shrinkage on curing must be attributed to the expanding character of SOE moieties. In a previous work,<sup>9</sup> the crosslinking of the SOE-AC homopolymer initiated by ytterbium triflate was carried out, and it took place with expansion ( $\Delta = -3$ ), but the obtained material

presented a low  $T_g$ . The introduction of glycidyl compound in the network increases the  $T_g$  values but reduces the expansion produced by SOEs because the homopolymerization of epoxy groups takes place with

Assay	Temperature of 5% Weight Loss (°C)		$T_{\text{max}}$ (°C) <sup>a</sup>		Char Yield at 800°C (wt %)		LOI
	N <sub>2</sub>	Air	N <sub>2</sub>	Air	N <sub>2</sub>	Air	
1	279	278	302/326	325/632	23.0	0.3	22.5
2	285	273	373	364	21.4	7.3	24.0
3	240	250	331/394	331	23.5	5.8	25.4
4	305	285	392	380	13.7	6.0	24.1

shrinkage.

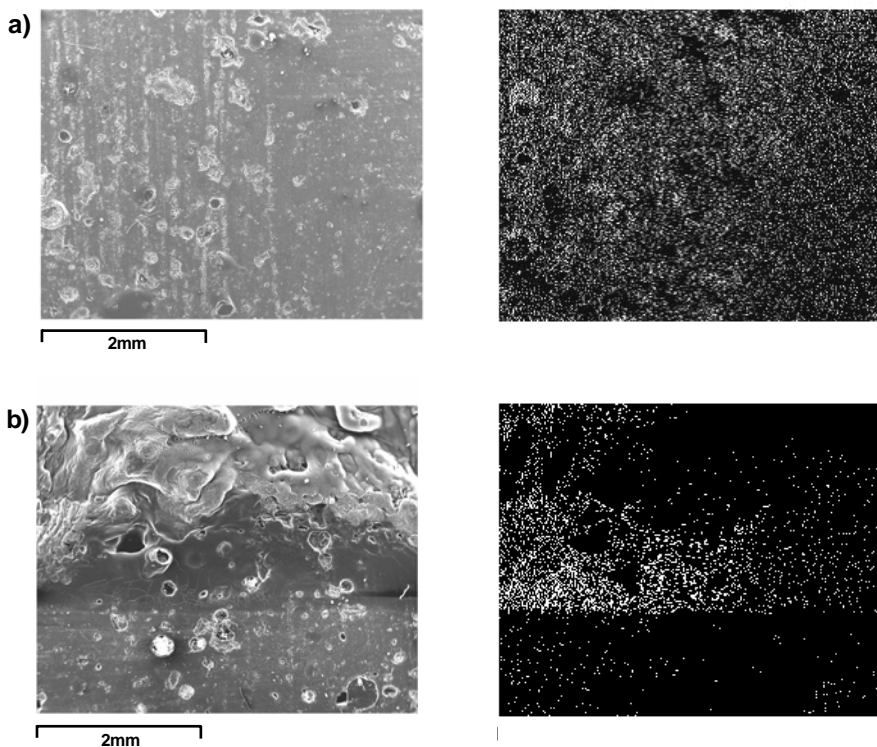
To examine the effect of phosphorous content on thermal stability and the decomposition behaviour, TGA data under nitrogen and air atmospheres were determined and analyzed. Figures 6 and 7 show the weight loss with the temperature for the epoxy compositions as well as the derivative curves under nitrogen and air, respectively. Table 4 summarizes the thermogravimetric data.

In both nitrogen and air atmospheres, only sample 4 has a

single major break in its decomposition curve, which indicates a single decomposition step. However, the other three samples show a more complex decomposition processes. The temperatures of 5% weight loss are about 300 °C, except for sample 3, which begins its degradation at a lower temperature.

In air, a second stage of weight loss for the sample 1, without phosphorus, corresponds to thermooxidative degradation. Under an air atmosphere, a polymeric material at high temperatures loss weight because the char forms is oxidized. This behaviour is in accordance with the mechanism of improved fire performance via phosphorous modification. In this retarded-degradation phenomenon, the phosphorous groups form an insulating protective layer, which prevents the combustible gases from transferring to the surface of the materials, increases the thermal stability at higher temperatures, and improves the fire resistance.

The char yield under nitrogen is correlated to the polymer's flame retardancy,<sup>35</sup> but it should be pointed out that, in our case, the experimental char yields of the



phosphorus-containing resins and the phosphorus-free resins are not significantly different under nitrogen. However, under air, the char yield is significantly lower in sample 1 without phosphorus.

The LOI values, which can be taken as indicator to evaluate the polymer's flame retardancy for the phosphorus-containing resins, were measured and are shown in Table 4. The presence of phosphorus increases the LOI values even though the phosphorus content is

**Figure 8.** SEM and SEM-EDX P mapping micrographs of sample 3 (a) before and (b) after the

164 | Crosslinking through Spiroorthoesters

low (ca. 3%), and no significant differences can be observed among the different phosphorus-containing samples.

To better understand the role of phosphorous in the flame retardant properties of the polymer, the element mapping was performed with energy-dispersive X-ray spectroscopy (EDX) on the surfaces of the initial sample and the sample after the LOI test. P mapping of the initial sample 3 indicated a homogeneous distribution of this element, as can be observed in the micrograph on the right of Figure 8(a). The white points in the figure denote P atoms. Figure 8(b) shows the SEM micrograph of the top surface view of the sample after the LOI test. The burned zone has the appearance of a black, charred material with small cavities. The P distribution, on the right of Figure 8(b), shows that the phosphorus density increased towards the top burned surface and that a phosphorus-rich layer formed.

## CONCLUSIONS

A polyacrylate bearing a SOE pendant group was crosslinked with mixtures of DGEBA and different phosphorus-containing glycidyl compounds. The  $T_g$  values of the obtained materials were above 100 °C, except for the more aliphatic diglycidyl compound. The incorporation of phosphorus into the network increased the LOI values, thus improving the flame retardance

of materials. After crosslinking, all the crosslinked polymers showed slight shrinkage that was much lower than that observed in conventional epoxy resins.

*The authors thank the Comisión Interministerial de Ciencia y Tecnología, CICYT, (MAT2005-01593 and MAT2005-01806) for providing financial support for this work.*

## REFERENCES AND NOTES

1. Expanding monomers: Synthesis, Characterization and Applications; Shadir, R. K.; Luck, R. M. Ed.; CRC Press: Boca Raton, FL, 1992.
2. Bailey, W. J.; Sun, R. L.; Katsuki, H.; Endo, T.; Iwama, H.; Tsushima, R.; Saigo, K.; Bitritto, M. M. In Ring-Opening Polymerization; Saegusa, T.; Goethals, E., Eds.; ACS Symposium Series; n° 59. American Chemical Society: Washington, DC, 1977.
3. Hino, T.; Endo, T. *Macromolecules* 2003, 36, 5902.
4. Smith, R. E.; Pinzino, C. S.; Chappelow, C. C.; Holder, A. J.; Kostoryz, E. L.; Guthrie, J. R.; Miller, M.; Yourtee, D. M.; Eick, J. D. *J Appl Polym Sci* 2004, 92, 62.
5. Nishida, H.; Morikawa, H.; Nakahara, T.; Ogata, T.; Kusumoto, K.; Endo, T. *Polymer* 2005, 46, 2531.

6. Bodenbenner, K. *Justus Liebigs Ann* 1959, 625, 183.
7. Fedtke, M.; Houfe, J.; Kahlert, E.; Müller, G. *Angew Makromol Chem* 1998, 255, 53.
8. Endo, T.; Bailey, W. J. *J Polym Sci Part C: Polym Lett* 1980, 18, 25.
9. Canadell, J.; Hunt, B. J.; Cook, A. G.; Mantecón, A.; Cádiz, V. *J Polym Sci Part A: Polym Chem* 2006, 44, 6728.
10. Kume, M.; Hirano, A.; Ochiai, B.; Endo, T. *J Polym Sci Part A: Polym Chem* 2006, 44, 3666.
11. Zamzow, M.; Höcker, H. *Macromol Chem Phys* 1994, 195, 2381.
12. Chabanne, P.; Tighzert, L.; Pascault, J. *J Appl Polym Sci* 1994, 53, 787.
13. Matejta, L.; Chabanne, P.; Tighzert, L.; Pascault, J. *J Polym Sci Part A: Polym Chem* 1994, 32, 1447.
14. Mas, C.; Mantecón, A.; Serra, A.; Ramis, X.; Salla, J. M. *J Polym Sci Part A: Polym Chem* 2005, 43, 2337.
15. Fernández, X.; Salla, J. M.; Mantecón, A.; Serra, A.; Ramis, X. *J Polym Sci Part A: Polym Chem* 2005, 43, 3421.
16. Lu, S.-Y.; Hammerton, I. *Prog Polym Sci* 2002, 27, 1661.
17. Ebdon, J. R.; Jones, M. S. In *Polymeric Materials Encyclopedia*; Salomone, J. C., Eds.; CRC: Boca Raton, FL, 1996.
18. Jain, P.; Choudhary, V.; Varma, I. K. *J Macromol Sci. Polym Rev* 2002, 42, 139.
19. Levchik, S. V.; Weil, E. D. *Polym Int* 2004, 53, 1901.
20. Weil, E. D. *Encyclopedia of Polymer Science and Engineering*; Wiley: New York, 1988; Vol. 11.
21. Cho, C. S.; Chen, L. V.; Fu, S. C.; Wu, T. R. *J Polym Res* 1998, 5, 59.
22. Wang, C. S.; Shieh, J. Y. *J Appl Polym Sci* 1999, 73, 353.
23. Liu, Y. L. *J Appl Polym Sci* 2002, 83, 1697.
24. Liu, Y. L. *J Polym Sci Part A: Polym Chem* 2002, 40, 359.
25. Alcón, M. J.; Espinosa, M. A.; Galià, M.; Cádiz, V. *Macromol Rapid Commun* 2001, 22, 1265.
26. Wang, S.; Zhuang, H.; Shobha, H. K.; Glass, T. E.; Shankarapandian, M.; Shultz, A. R.; McGrath, J. E. *Macromolecules* 2001, 34, 1265.
27. Shobha, H. K.; Johnson, H.; Shankarapandian, M.; Kim, Y. S.; Rangarajan, P.; Baird, D. G.; McGrath, J. E. *J Polym Sci Part A: Polym Chem* 2001, 39, 2904.
28. Alcón, M. J.; Ribera, G.; Galià, M.; Cádiz, V. *Polymer* 2003, 44, 7291.
29. Mas, C.; Ramis, X.; Salla, J. M.; Mantecón, A.; Serra, A. *J Polym Sci Part A: Polym Chem* 2003, 41, 2794.
30. Cho, C.-S.; Chen, L.-W.; Chiu, Y.-S. *Polym Bull* 1998, 41, 45.
31. Serra, A.; Cádiz, V.; Mantecón, A.; Martínez, P. A. *Tetrahedron* 1985, 41, 763.
32. Tobolsky, A. V.; Carlson, D. W.; Indictor, N. J. *J Polym Sci* 1961, 54, 175.

166 | Crosslinking through Spiroorthoesters

33. Chung, K.; Takata, T.; Endo, T. *Macromolecules* 1997, 30, 2532.
34. Cervellera, R.; Ramis, X.; Salla, J. M.; Serra, A.; Mantecón, A. *Polymer* 2005, 46, 6878.
35. Van Krevelen, D. W. *Polymer* 1975, 16, 615.



## MICROWAVE ACCELERATE POLYMERIZATION OF 2-PHENOXYMETHYL-1,4,6-TRIOXASPIRO [4,4] NONANE WITH DIGLYCIDYL ETHER OF BISPHENOL A

J. Canadell, A. Mantecón, V. Cádiz

Departament de Química Analítica i Química Orgànica. Universitat Rovira i Virgili.  
Marcel·lí Domingo s/n, 43007 Tarragona, Spain

---

### Abstract

We studied for the first time the cationic copolymerization of the SOE: 2-phenoxyethyl-1,4,6-trioxaspiro [4,4] nonane with diglycidyl ether of Bisphenol A (DGEBA) under microwave irradiation using ytterbium and lanthanum triflates as initiators. A comparison with thermal heating showed a great enhancement in the reaction rates and a higher SOE incorporation in the network. The double ring-opening of SOE reduces the usual shrinkage of epoxy resins on curing, and it was lower under microwave irradiation. Moreover, the ytterbium triflate initiator leads to a higher incorporation of linear ester moieties in the network than lanthanum triflate.

**Keywords:** cationic polymerization; crosslinking; microwave; spiroorthoester; epoxy resins; lanthanide triflate

---

### INTRODUCTION

The curing of thermoset polymers such as epoxy resins has become increasingly important, arising from their application as coatings, adhesives and encapsulants in

microelec-tronic applications. In particular, the requirement for higher performing systems has also led to unacceptably long cure times

become the bottleneck of the whole production process.

The incentive for using alternative non thermal curing methods is typically to accelerate the curing process and thus reduce the time of cure. These include the use of ultraviolet (UV) light, gamma rays and electron beams. UV and electron beam curing have limited application due to their poor penetration ability and limited dose rate. Gamma rays have enormous radiation hazards and environmental issues. In many cases, the use of microwave irradiation appears to be a more selective and much faster approach to the synthesis and also leads to higher yields for a number of organic and polymer reactions compared to classical thermal heating.<sup>1-3</sup> Micro-wave curing has been also found to be a viable alternative method for the curing of thermoset polymers, with a significant increase in the rate of reaction.<sup>4-6</sup>

Another disadvantage that epoxy resins present is their shrinkage during curing that can cause poor adhesion to a substrate, delamination, microvoids and micro-cracks, which in turn can reduce the durability of the materials. A number of different techniques have been employed to reduce shrinkage, such as the addition of fillers and also curing at lower temperatures. However, these methods are not totally efficient as the shrinkage is due to the crosslinking reaction

rather than as a consequence of production methods. One way of solving this problem is to copolymerize the epoxy resins with the so-called “expanding monomers”,<sup>7</sup> which are monomers that lead to zero shrinkage or even positive expansion during polymerization. Some kinds of bicyclic monomers such as spiroorthoesters (SOEs), spiroorthocarbonates (SOCs), and bicycloorthoesters (BOEs) have been reported to maintain their volume or actually expand during the double ring-opening polymerization.<sup>7-10</sup> SOEs can be readily synthesized from epoxides and lactones<sup>11,12</sup> and undergo cationic ring-opening polymerization by Lewis acid catalysts.

This work focuses on the first reported copolymerization of the SOE: 2-phenoxyethyl-1,4,6-trioxaspiro [4,4] nonane with diglycidyl ether of Bisphenol A (DGEBA) under micro-wave conditions and a comparison is made with conventional thermal conditions. Furthermore, we depict the influence of SOE incorporation in the network on shrinkage during curing.

## EXPERIMENTAL

### Materials

Diglycidyl ether of bisphenol A (Epikote Resin 827, Shell Chemicals; epoxy equiv. = 182.08 g/equiv), phenyl glycidyl ether (PGE; Aldrich) and  $\gamma$ -butyrolactone

( $\gamma$ -BL; Aldrich) were used as received. Ytterbium (III) and lanthanum (III) trifluoromethanesulfonates (Aldrich) and boron trifluoride diethyl etherate ( $\text{BF}_3 \cdot \text{OEt}_2$ ; Aldrich) were used without purification.

### Instrumentation

Microwave irradiation was performed in a CEM microwave, model Discover, with IR temperature sensor and power control.

The FTIR analysis was monitored with a FTIR-680PLUS spectrophotometer with a resolution of  $4 \text{ cm}^{-1}$  in the absorbance mode.

Calorimetric studies (DSC) were carried out on a Mettler DSC-821e thermal analyzer in covered Al pans under  $\text{N}_2$  at scan rate of  $10 \text{ }^\circ\text{C}/\text{min}$  to determine the degree of conversion ( $\alpha$ ) and at a heating rate of  $20 \text{ }^\circ\text{C}/\text{min}$  to determine the glass transition temperatures ( $T_g$ 's).

TGAs were carried out with a Mettler TGA/SDTA 851e thermobalance. Cured samples with an approximate mass of 10 mg were degraded between  $30 \text{ }^\circ\text{C}$  and  $800 \text{ }^\circ\text{C}$  at a heating rate of  $10 \text{ }^\circ\text{C}/\text{min}$  in atmosphere of  $\text{N}_2$  or air.

Thermodynamomechanical analysis (DMTA) were carried out with a TA DMA 2928, working with a three point bending clamp from  $30 \text{ }^\circ\text{C}$  to

$150 \text{ }^\circ\text{C}$  with heating rate of  $3 \text{ }^\circ\text{C}/\text{min}$ .

**Table 1.** Curing and Postcuring conditions for DGEBA/SOE-PGE system Yb(OTf)<sub>3</sub> and La(OTf)<sub>3</sub> under microwave and thermal conditions.

Assay	Curing Conditions		Postcuring Conditions	
	Temperature (°C)	Time (min)	Temperature (°C)	Time (min)
Yb-MW	60	6	100	8
Yb-OVEN	120	60	140	90
La-MW	60	8	100	10
La-OVEN	120	100	140	140

The densities of materials were measured with a Micromeritics Accu-pyc 1330 TC gas pycnometer at  $30 \text{ }^\circ\text{C}$ .

### Preparation of the curing mixtures

The mixtures were prepared by mixing 2 g (5.4 mmol) of DGEBA and 0.64 g (2.7 mmol) of SOE-PGE with 1 phr (1 part per 100 of mixture weight/weight) of the selected triflate.

### Curing procedure

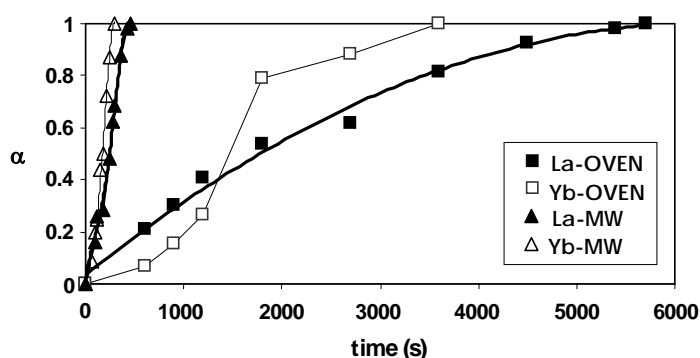
The sample was placed into a 5 mm (internal diameter) glass tube inside the microwave reactor vial (10 mL) and subjected to MW irradiation using a power of 50 W. Overheating of reaction mixtures was avoided by cooling with compressed air. The reaction mixtures without

microwave irradiation were heated in a standard oven. The curing conditions are listed in table 1.

The determination of the extent of polymerization was as follows: after a time of heating the sample under mi-

as catalyst. Mixtures of SOE-PGE and DGEBA reacted using lanthanide triflates as initiator.

We found that the reaction of SOE-PGE and DGEBA with lanthanide triflates as initiators takes place under microwave irradiation and thermo-sets can be obtained in a



**Figure 1.** Plot of the conversion against the cure time for the DGEBA/SOE-PGE system initiated by Yb(OTf)<sub>3</sub> and La(OTf)<sub>3</sub> for microwave and thermal curing.

crowave or thermal conditions, it was quickly cooled by liquid nitrogen quench to stop the polymerization. The extent of polymerization was determined by DSC and the conversion of the reactive species was determined by FTIR measurements.

## RESULTS AND DISCUSSION

The synthesis of 2-phenoxyethyl-1,4,6-trioxaspiro [4,4] nonane (SOE-PGE) was carried out by a previously described procedure<sup>11</sup> from PGE and  $\gamma$ -BL using BF<sub>3</sub>·OEt<sub>2</sub>

significantly shorter reaction time in comparison to conventional heating. Figure 1 shows the reaction conversion against curing times. After curing at different times the residual enthalpy ( $\Delta H_{residual}$ ) was calculated by dynamic DSC. The degree of conversions were calculated by the following equation:

$$\alpha_t = \frac{\Delta H_{total} - \Delta H_{residual}}{\Delta H_{total}}$$

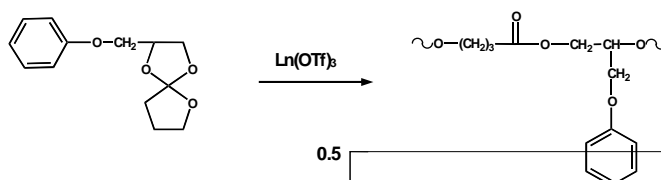
where  $\Delta H_{total}$  is the heat of reaction obtained in a dynamic DSC of the initial mixture. As can be seen,

thermal and microwave initiated reactions with ytterbium triflate are faster. However, the most significant difference lies in the reaction conditions, that is, the reaction under microwave irradiation is much faster than conventional thermal heating with both initiators. Thus, only 250-

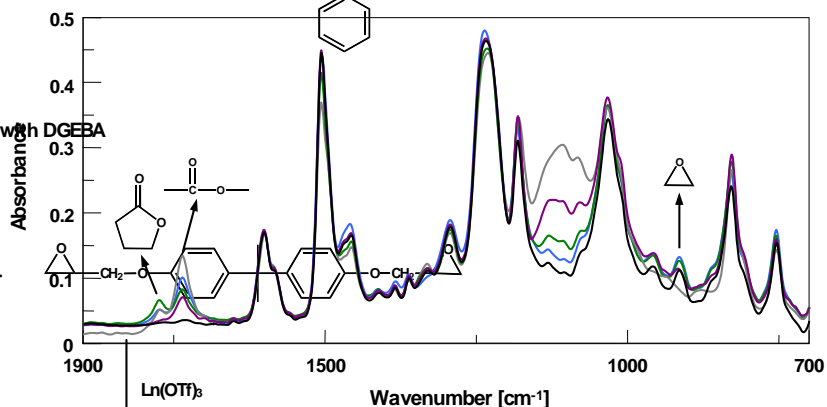
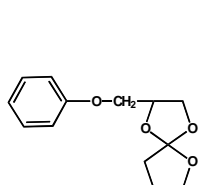
300 seconds are necessary to reach the total conversion under microwave irradiation against 3600-5700 seconds under thermal conditions.

In Scheme 1 are represented the

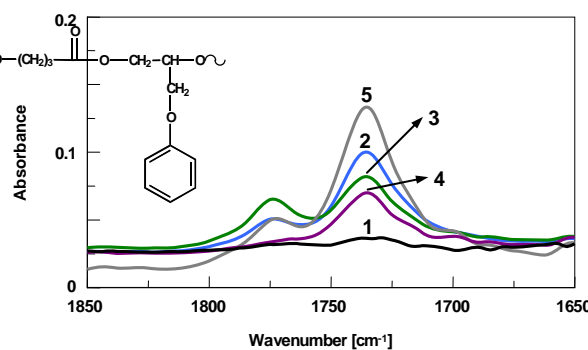
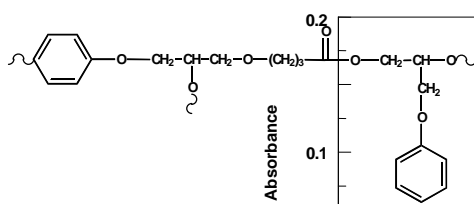
a) Homopolymerization of SOE-PGE



b) Copolymerization of SOE-PGE with DGEBA



c) Homopolymerization of DGEBA



**Figure 2.** FTIR spectra of the initial mixture without initiator (1), just after add 1phr of Yb(OTf)<sub>3</sub> (2), after 300 s reaction (3), after 2100 s reaction (4), and at the end of curing (5) of DGEBA/SOE-PGE : 2/1 (mol/mol) under thermal conditions.  
 Macromol Chem Phys (Submitted)

Scheme 1

different processes for the cationic copolymerization of DGEBA/SOE-PGE, which are usually expected: a) homopolymerization of SOE-PGE; b) copolymerization of SOE-PGE and DGEBA; and c) homopolymerization of DGEBA.

To follow the evolution of the different reactive species the FTIR was used. Figure 2 shows the FTIR spectra of the 2/1 (mol/mol) DGEBA/SOE-PGE mixture initiated by 1 phr of  $\text{Yb}(\text{OTf})_3$  at different times of reaction under thermal conditions: without initiator (1); just after addition the initiator (2); at two intermediate curing times, 300 sec (3) and 2100 sec (4); and after completely curing (5).

As can be seen, the initial mixture (spectrum 1) shows an oxirane band at  $914\text{ cm}^{-1}$ , due to the ring deformation, and does not show any carbonyl signals. Just after addition of the initiator (spectrum 2) two carbonyl signals appear, one at  $1734\text{ cm}^{-1}$  attributable to the linear ester moieties formed in the double ring-opening of the SOE, and another at  $1770\text{ cm}^{-1}$ . This later band corresponds to the carbonyl group of  $\gamma$ -lactones<sup>13</sup> which could be formed by the reversion of SOE to a  $\gamma$ -butirolactone ( $\gamma$ -BL) and epoxide (Scheme 2). The reversibility of SOEs was previously reported in the literature.<sup>14</sup> The appearance of these two carbonyl bands implies that the SOE-PGE is very reactive at ambient temperature. After 300 sec (spectrum 3) a decrease of the band of linear ester and an increase

of the band of  $\gamma$ -BL is observed. This could be explained by a back biting process.<sup>15</sup> The band of the  $\gamma$ -BL decreases in the next steps of the reaction, arising to zero at 2100 sec (spectrum 4), indicating that  $\gamma$ -BL completely reacts with glycidyl to form SOE groups. These SOE groups must homo-polymerize or copolymerize with DGEBA because an increase of the linear ester band was observed in the following steps. At the end of the curing (spectrum 5), the glycidyl band disappears indicating that the epoxide completely polymerizes. Furthermore, the band of  $\gamma$ -BL is newly formed, which seems to indicate that some degree of depolymerization by back biting takes place at the last steps of the curing, giving  $\gamma$ -BL which now cannot react with epoxy groups because they are not present, and  $\gamma$ -BL does not homopolymerize by thermodynamical reasons.<sup>16,17</sup>

The evolution of these three species, SOE, lactone and epoxy, was followed by recording the FTIR spectrum of the samples after different curing times. The conversion of SOE groups was calculated from the variation of the carbonyl linear ester band at  $1734\text{ cm}^{-1}$ , the conversion of  $\gamma$ -BL from the variation of the carbonyl band at  $1770\text{ cm}^{-1}$ , and the conversion of epoxides from the decrease of the band at  $914\text{ cm}^{-1}$ .

The absorbances were calculated in terms of peak areas. The

$$\alpha_{epoxy} = 1 - \left( \frac{\overline{A}_{914}^t}{\overline{A}_{914}^0} \right)$$

$$\overline{A}_{914}^t = \frac{A_{914}^t}{A_{1603}^t} = \left( \frac{\overline{A}_{1734}^t}{\overline{A}_{1734}^0} \right) = \frac{A_{914}^0}{A_{1603}^0}$$

$$\overline{A}_{1734}^t = \frac{A_{1734}^t}{A_{1603}^t} \quad \overline{A}_{1734}^\infty = \frac{A_{1734}^\infty}{A_{1603}^\infty}$$

conversions were determined by the Lambert-Beer Law from the normalized changes in absorbance respect to the band at  $1603\text{ cm}^{-1}$  corresponding to the phenyl group in DGEBA and using the following equations:

$$\alpha_{\gamma\text{-BL}} = \left( \frac{\overline{A}_{1770}^t}{\overline{A}_{1770}^\infty} \right)$$

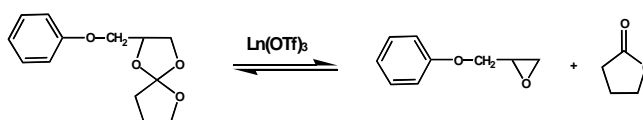
$$\overline{A}_{1770}^t = \frac{A_{1770}^t}{A_{1603}^t} \quad \overline{A}_{1770}^\infty = \frac{A_{1770}^\infty}{A_{1603}^\infty}$$

where:

$\overline{A}_{1734}^\infty = \frac{A_{1734}^\infty}{A_{1603}^\infty}$  : is the highest value obtained for all the systems.

$\overline{A}_{1770}^\infty = \frac{A_{1770}^\infty}{A_{1603}^\infty}$  : is the highest value obtained for all the systems.

different evolution in function of the reaction conditions and the initiator used. With ytterbium triflate, initially the linear ester content decreases, being higher under microwave conditions. This diminution of the ester band and a similar increase in the conversion of  $\gamma$ -BL could be associated to the back biting process, which forms  $\gamma$ -BL and diminishes the proportion of linear ester groups. When lanthanum triflate was used some differences were observed. A decrease of ester band also occurred in the first reaction stages, being more pronounced under thermal conditions. However, with this initiator, the higher amount of formed  $\gamma$ -BL could not be only explained by the back biting process above mentioned. Thus, other factors have been considered. An explanation could be the reversion of SOE groups to yield an epoxide and a lactone, therefore the epoxide absorption should increase in a similar proportion than the lactone band. However, this fact was not observed, maybe because of the homo-polymerization of



Scheme 2

Figures 3 and 4 show the conversion of SOE and  $\gamma$ -BL, respectively against time. As we can see, the two species follow a

epoxide reduces the proportion of the epoxy groups formed in this reversion reaction. Another possibility that could contribute to

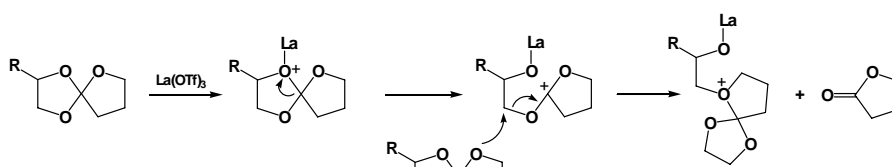
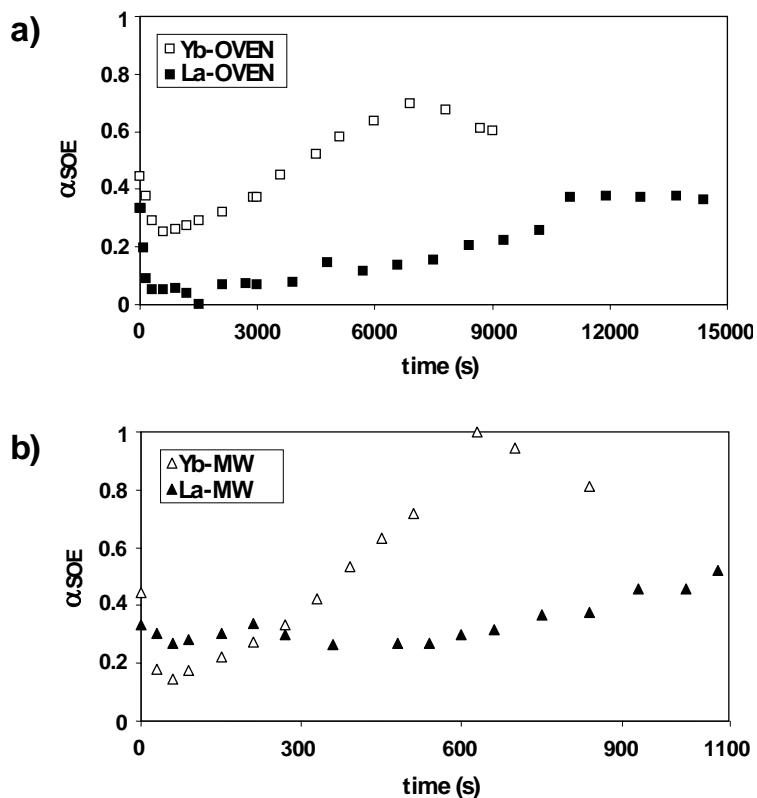
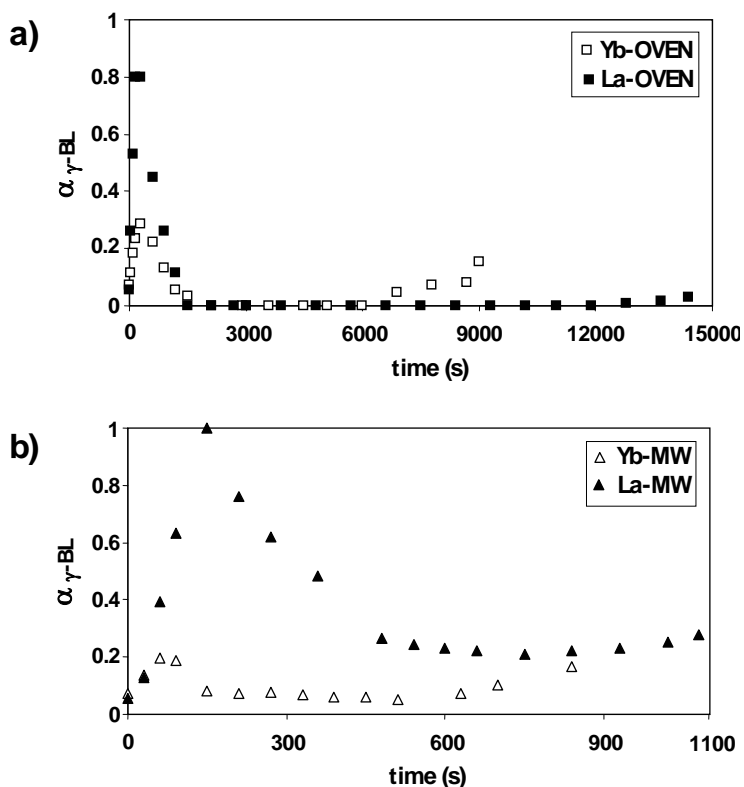


Figure 3. Plot of SOE conversion against the cure time for the DGEBA/SOE-PGE system initiated by Yb(OTf)<sub>3</sub> and La(OTf)<sub>3</sub> under thermal (a) and microwave (b) conditions.



the  $\gamma$ -BL formation lies in a different mechanism pathway in the ring-opening of SOEs (Scheme 3). The ring-opening of SOEs has been described<sup>7</sup> that starts by a coordination of the Lewis acid to the ether oxygen of the SOE to form an oxonium cation, followed by isomerization into a carbonium cation stabilized by the two adjacent oxygen atoms. The propagation reaction is a nucleophilic attack by another monomer. Different pathways are possible in the ring-

opening of SOEs,<sup>18</sup> leading some of them to the formation of  $\gamma$ -BL, being the most probable of these pathways represented in Scheme 3. The  $\gamma$ -BL generated in this reaction may in turn reacts with epoxy to get a new SOE group, what agrees with the decrease of the  $\gamma$ -BL conversion observed for all the systems studied. Some differences were observed related to curing conditions. Under conventional heating, the conversion of  $\gamma$ -BL beco-

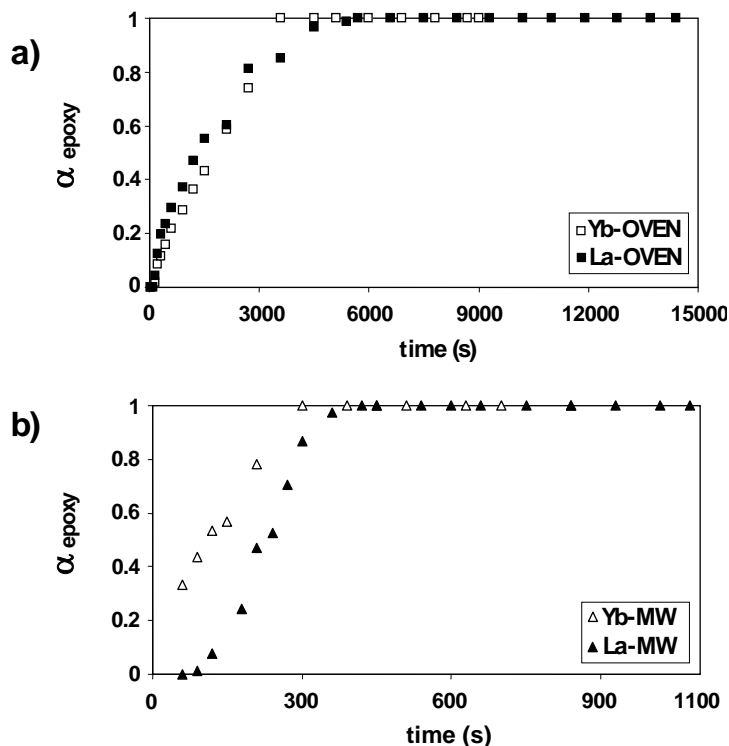


**Figure 4.** Plot of  $\gamma$ -BL conversion against the cure time for the DGEBA/SOE-PGE system initiated by  $\text{Yb}(\text{OTf})_3$  and  $\text{La}(\text{OTf})_3$  under thermal (a) and microwave (b) conditions.

mes to zero with both initiators at similar times. However, under microwave irradiation some amount of  $\gamma$ -BL remains unreacted. This difference could be explained by the faster reaction, which not allows the complete formation of SOE groups. The initial SOE and the SOE formed from  $\gamma$ -BL and epoxides can homopolymerize or copolymerize with DGEBA, thus, an increase of the conversion of SOE was observed.

At longer reaction times, clear differences between the two initiators and curing conditions were observed. With  $\text{Yb}(\text{OTf})_3$  the incorporation of SOE to yield a poly(ether-ester) is higher than with  $\text{La}(\text{OTf})_3$ , what can be attributed to the higher Lewis acidity of  $\text{Yb}(\text{OTf})_3$  which favours the reaction. We also observed that the conversion is higher under microwave conditions than in thermal conditions for both initiators.

SOEs takes place without shrinkage



**Figure 5.** Plot of epoxy conversion against the cure time for the DGEBA/SOE-PGE system initiated by Yb(OTf)<sub>3</sub> and La(OTf)<sub>3</sub> under thermal (a) and microwave (b) conditions.

At the end of the curing process, a low diminution of the ester band was detected, being higher with Yb(OTf)<sub>3</sub> and under microwave irradiation, which indicates that the depolymerization process takes place in a higher extent.

Figure 5 depicts the conversion of epoxy groups, which in all cases is complete at relatively short times.

It has been reported that the cationic double ring-opening of

or even with expansion.<sup>19,20</sup> Therefore, the volume changes in the crosslinking reaction of the mixtures DGEBA/SOE-PGE were evaluated by density measurements with a Micromeritics helium pycnometer at 30 °C before and after crosslinking (Table 2). The volume change was calculated with the following equation:

$$\Delta V (\%) = \frac{d_{\text{crosslinked polymer}} - d_{\text{initial mixture}}}{d_{\text{initial mixture}}} \times 100$$

where  $d_{\text{crosslinked network}}$  is the density of the crosslinked material and  $d_{\text{initial}}$

is also observed under conventional heating.

**Table 2.**  $T_g$ s of crosslinked polymers and densities before and after crosslinking and volume change upon crosslinking.

ASSAY	$T_g$ (°C) <sup>a</sup>	Tan Delta (°C)	Density at 30 °C (g/cm <sup>3</sup> )		Volume Change (%)
			Initial mixture	Crosslinked	
<b>Yb-MW</b>	70	79	1.178	1.192	1.1
<b>Yb-OVEN</b>	71	80	1.178	1.204	2.2
<b>La-MW</b>	64	77	1.178	1.197	1.6
<b>La-OVEN</b>	67	80	1.178	1.209	2.6

$d_{\text{mixture}}$  is the density of the initial mixture of comonomers.

Although typical crosslinking of epoxy resins are generally accompanied by a significant volume shrinkage (above 3%, depending on the crosslinking mechanism),<sup>21,22</sup> in all mixtures of glycidyl compounds with SOEs studied, the observed positive values, between 1.1-2.6, are lower than those observed in the crosslinking of pure DGEBA with lanthanide triflates (about 3%).<sup>23,24</sup> This lower shrinkage on curing must be attributed to the expanding character of SOE moieties. Moreover, we observed a lower shrinkage under microwave irradiation than under conventional heating and it is lower with ytterbium triflate than with lanthanum triflate. This can be attributed to the higher SOE conversion at the end of the curing with Yb(OTf)<sub>3</sub>. This later behaviour

The same table 2 collects the  $T_g$  values of the crosslinked materials obtained by DSC and Tan  $\delta$ .  $T_g$ s as well as Tan  $\delta$  are similar for all the samples. The materials obtained with ytterbium triflate, under both microwave and thermal conditions and lanthanum triflate under conventional heating showed similar shape of Tan  $\delta$  plots, whereas the Tan  $\delta$  plot of the material obtained with lanthanum triflate by microwave irradiation is broader, indicating a higher number of branching modes which produces a wider distribution of structures.

By TGA experiments we observed that the materials obtained under microwave conditions initiate the degradation at lower temperatures. Thus, the weight loss of 5% under nitrogen, was observed at 232 °C (with ytterbium triflate) and 238 °C (with lanthanum triflate). The thermally obtained materials start the degradation at 271 °C and 273

°C with ytterbium triflate and lanthanum triflate respectively. This higher de-gradability can be associated to a higher ester content in the network. In air, the degradations start at slightly lower temperatures. The temperature of the maximum rate degradation was similar for all materials, about 360° C under nitrogen atmosphere, and about 350° C under air.

## CONCLUSIONS

It can be concluded from the above-described results that in all cases, the curing time was considerably shortened by microwave irradiation. Under these reaction conditions materials with a higher content of ester groups in the network, from SOE incorporation, were obtained and showed a lower shrinkage than conventional epoxy resins. Moreover, the ytterbium triflate initiator led to a higher incorporation of linear ester moieties in the network than lanthanum triflate.

*The authors thank the Comisión Interministerial de Ciencia y Tecnología, CICYT, (MAT2005-01593 and MAT2005-01806) for providing financial support for this work.*

## REFERENCES AND NOTES

1. F. Wiesbrock, R. Hoogenboom, U.S. Schubert, *Macromol. Rapid Commun.* **2004**, *25*, 1739.
2. S. Sinnwell, H. Ritter, *Macromol. Rapid Commun.* **2005**, *26*, 160.
3. S. Sinnwell, H. Ritter, *Macromol. Rapid Commun.* **2006**, *27*, 1335.
4. E. Marand, K. R. Baker, J. D. Graybeal, *Macromolecules* **1992**, *25*, 2243.
5. F. Y. C. Boey, B. H. Yap, L. Chia, *Polym. Test.* **1999**, *18*, 93.
6. D. Zhang, J. V. Crivello, J. O. Stoffer, *J. Polym. Sci. Part B: Polym. Phys.* **2004**, *42*, 4230.
7. R. K. Shadir, R. M. Luck Eds., "Expanding monomers, Synthesis, Characterization and Applications". CRC Press: Boca Raton, FL, **1992**.
8. T. Hino, T. Endo, *Macromolecules* **2003**, *36*, 5902.
9. R. E. Smith, C. S. Pinzino, C. C. Chappelow, A. J. Holder, E. L. Kostoryz, J. R. Guthrie, M. Miller, D. M. Yourtee, J. D. Eick, *J. Appl. Polym. Sci.* **2004**, *92*, 62.
10. H. Nishida, H. Morikawa, T. Nakahara, T. Ogata, K. Kusumoto, T. Endo, *Polymer*, **2005**, *46*, 2531.
11. K. Bodenbenner, *Justus Liebig Ann.* **1959**, *625*, 183.
12. M. Fedtke, J. Houfe, E. Kahlert, G. Müller, *Angew. Makromol. Chem.* **1998**, *255*, 53.
13. E. Pretsch, T. Clerc, J. Seibl, W. Simon, "Tablas para la elucidación estructural de compuestos orgánicos por

- métodos espectroscópicos". Spanish Edition, Springer-Verlag Ibérica, Barcelona, **1998**.
14. H. J. Both, in "Expanding monomers: Synthesis, Characterization and Applications". R. K. Sadhir, M. R. Luck, Eds.; CRC Press: Boca Raton, FL, **1992**, p. 208.
  15. M. Szwarc, M. Van Beylen, "Ionic Polymerization and Living Polymers", Chapman and Hall, New York, **1993**, p.334.
  16. C. W. Lee, R. Urakawa, Y. Kimura, *Eur. Polym. J.* **1998**, *34*, 117.
  17. W. Saiyosombat, R. Molloy, T. M. Nicholson, A. F. Johnson, I. M. Ward, S. Poshychinda, *Polymer* **1998**, *39*, 5581.
  18. H. Nishida, F. Sanda, T. Endo, T. Nakahara, T. Ogata, K. Kusumoto, *J. Polym. Sci. Part A: Polym. Chem.* **1999**, *37*, 4502.
  19. W. J. Bailey, *J. Macromol. Sci.-Chem.* **1975**, *A9(5)*, 849.
  20. W. J. Bailey, H. Iwama, R. Tsushima, *J. Polym. Sci. Symposium*, **1976**, *56*, 117.
  21. K. Chung, T. Takata, T. Endo, *Macromolecules*, **1997**, *30*, 2532.
  22. W. J. Bailey, R. L. Sun, H. Katsuki, T. Endo, H. Iwama, R. Tsushima, K. Saigo, M. M. Bitritto, in "Ring-Opening Polymerization"; T. Saegusa, E. Goethals, Eds. ACS Symposium Series; American Chemical Society: Washington, DC, **1977**.
  23. R. Cervellera, X. Ramis, J. M. Salla, A. Serra, A. Mantecón, *Polymer* **2005**, *46*, 6878.
  24. C. Mas, X. Ramis, J. M. Salla, A. Mantecón, A. Serra, *J. Polym. Sci. Part A: Polym. Chem.* **2003**, *41*, 2794.